

# **Synthesis and Host-Guest Chemistry of Organic Polycations**

A thesis presented to the University of London in partial fulfilment of the  
requirements for the degree of Doctor of Philosophy

by

Ashley James Ibbett

UCL Chemistry Department  
Christopher Ingold Laboratories  
20 Gordon Street  
London WC1H 0AJ

April 1997

ProQuest Number: 10045850

All rights reserved

INFORMATION TO ALL USERS

The quality of this reproduction is dependent upon the quality of the copy submitted.

In the unlikely event that the author did not send a complete manuscript and there are missing pages, these will be noted. Also, if material had to be removed, a note will indicate the deletion.



ProQuest 10045850

Published by ProQuest LLC(2016). Copyright of the Dissertation is held by the Author.

All rights reserved.

This work is protected against unauthorized copying under Title 17, United States Code.  
Microform Edition © ProQuest LLC.

ProQuest LLC  
789 East Eisenhower Parkway  
P.O. Box 1346  
Ann Arbor, MI 48106-1346

*To My Parents*

## Abstract

The field of host-guest chemistry has received much attention in recent years. The design of anion receptors is anticipated to provide materials with interesting biological applications. This thesis describes the synthesis and host-guest properties of some potential anion receptors.

The synthesis of a variety of polycationic materials using simple nucleophilic substitution methodology is described. The reactions of 1,4-diazabicyclo[2.2.2]octane and related compounds with tri- and hexasubstituted benzenes is reported. These reactions give rise to a series of compounds containing three formal positive charges. A strategy employing the reaction of monocationic derivatives of 1,4-diazabicyclo[2.2.2]octane with tri- and hexasubstituted benzenes was employed in the synthesis of hexacationic materials. Characterisation and purification of the tri- and hexacationic materials is discussed. The synthesis of an optically active tricationic compound is reported.

A variety of techniques have been employed in the investigation of the anion complexing properties of the polycationic materials synthesised. Specific recognition of ferricyanide over ferrocyanide was observed with one tricationic compound. A crystal structure analysis performed on the material thus formed revealed interesting information regarding the conformation adopted by the tricationic compound. Nuclear magnetic resonance techniques were extensively utilised to investigate the behaviour of the polycationic materials with simple anionic guests. NMR titration curves were analysed using non-linear regression and association constants derived. The stoichiometries of the complexes were determined using the method of continuous variation. The strength of association with anionic guests of differing charge was examined.

The use of isothermal titration calorimetry in the determination of enthalpies of complexation and association constants is reported. The technique revealed aspects of complexation behaviour that could not be observed using NMR techniques. The association constants determined using calorimetric techniques differed from those obtained using NMR experiments.

## Acknowledgements

First and foremost I wish to thank Professor Peter Garratt for giving me the opportunity to undertake this project and for the constant support, encouragement and advice he has provided throughout its duration.

I would also like to thank past and present members of the Garratt group for their friendship, including Najeeb, Yiu-Fai, Letitia, Maria, Rob and Stefan.

To all my friends in the department especially Kit, Nicola, Tiz, Rodney, Alvin, Simon and Ellen who have made the whole experience much more enjoyable. Thanks too to Mark, Thomas, Chris and Anne-Marie.

Thanks to the UCL Chemistry Department staff, especially John Hill and Steve Corker for mass spec., Jill Maxwell for NMR, Peter Leighton for constantly making me feel guilty, and Dick Waymark and Seamus Stewart for fixing my cordless phone!

I am very grateful to John Ladbury and Ronan O'Brien of UCL Biochemistry Department for performing the microcalorimetry experiments, to Drs K.M.A. Malik and M.B. Hursthouse at the SERC Crystallography Service in Cardiff for the crystal structure analysis, to Dr Andrea Sella and Professor John Ridd for invaluable discussions and to Dr Roger Wrigglesworth for his useful advice and for making sure I got up early on Friday mornings.

Finally, I owe a great debt of gratitude to my parents for their love and support and to Annie and John for lending me the computer that allowed me to write up. And for ringing during the afternoons!

# Contents

Abstract	3
Acknowledgements	4
Contents	5
Glossary	8
1 Introduction	9
1.1 Electrostatics	9
1.1.1 Debye-Hückel Theory	9
1.1.2 Theory of Ionic Association	10
1.1.3 Electrostatic Effects in Dicarboxylic Acids	11
1.1.4 The Kirkwood Model	13
1.1.5 Electrostatic Effects in Proteins	14
1.1.6 Electrostatic Interactions Between Organic Ions	15
1.2 Host-Guest Chemistry	16
1.2.1 Conventions in Host-Guest Chemistry	18
1.2.2 Factors Determining Strength of Association	21
1.2.3 Design of Anion Receptors	25
1.2.4 Guanidinium Receptors	25
1.2.5 Polyammonium Macrocycles	27
1.2.6 Derivatives of Polyammonium Macrocycles	31
1.2.7 Non-Macrocyclic Anion Receptors	37
1.2.8 Template Synthesis	38
1.3 Aim of Project	39
2 Synthesis of Polycationic Compounds	40
2.1 Introduction	40
2.2 Routes to 1,3,5-Tris(bromomethyl)benzene	43

2.3 Synthesis of 2,4,6-Tris(bromomethyl)mesitylene	45
2.4 DABCO-based Trications	46
2.5 DABCO-based Hexacations	49
2.5.1 Divergent Strategy	49
2.5.2 Convergent Strategy	51
2.5.3 Monocationic DABCO intermediates	51
2.5.4 Synthesis of DABCO-based Hexacations	54
2.6 Other Trications	58
2.7 Conclusion	62
 3 Host-Guest Chemistry of Organic Polycations	 63
3.1 Introduction	63
3.2 Selective Crystallisation	68
3.2.1 Solid State $^{13}\text{C}$ NMR Spectroscopy	72
3.3 Nuclear Magnetic Resonance Techniques	73
3.3.1 Theory of NMR Titration	73
3.3.2 Method of Continuous Variations	75
3.4 Binding Studies	76
3.4.1 NMR Titration of Tricationic Compounds	76
3.4.2 Job Plots - Trications	87
3.4.3 NMR Titration of Hexacationic Compounds	89
3.4.4 Job Plots - Hexacations	95
3.5 Microcalorimetry	96
3.5.1 Introduction	96
3.5.2 Calorimetric Analysis of Polycationic Materials	98
3.5.3 Comparison of Results from $^1\text{H}$ NMR Titrations and ITC	103
3.6 Future Perspectives	103
3.7 Conclusion	104

4 Experimental	106
4.1 Synthesis	106
4.2 Starting Materials	107
4.3 Monocations	111
4.4 Trications	116
4.5 Hexacations	126
4.6 NMR Titrations and Job Plots	140
4.7 Isothermal Titration Calorimetry	175
References	176
Appendix 1 - Program Used for the Determination of Association Constants	182
Appendix 2 - Selected NMR Spectra	183
Appendix 3 - Crystal Structure Analysis for <b>185</b>	193



## Glossary

AMP	adenosine monophosphate
ADP	adenosine diphosphate
ATP	adenosine triphosphate
br	broad
d	doublet
$\text{CDCl}_3$	deuterated chloroform
$(\text{CD}_3)_2\text{CO}$	deuterated acetone
DABCO	1,4-diazabicyclo[2.2.2]octane. Dabco is a registered trademark of Air Products & Chemicals Inc.
DMSO	dimethylsulfoxide
$d_6$ -DMSO	deuterated dimethylsulfoxide
$\text{D}_2\text{O}$	deuterium oxide
EI	electron impact
FAB	fast atom bombardment
IR	infra-red
ITC	isothermal titration calorimetry
J	coupling constant
m (IR)	medium absorption
m (NMR)	multiplet
NMR	nuclear magnetic resonance
q	quartet
s (IR)	strong absorption
s (NMR)	singlet
t	triplet
w (IR)	weak absorption

# 1 Introduction

## 1.1 Electrostatics

Electrostatic effects have a profound effect on the behaviour of molecules, both in the case of small organic systems and in macromolecules such as proteins. The theory of electrostatic interactions between point charges in a vacuum is well understood, but the behaviour of ions in solution is somewhat different from their behaviour in a vacuum and is less well understood. Relatively simple theories, such as that of Debye-Hückel, describing the expected behaviour of electrolyte solutions have been developed but most cases show marked deviations from ideal behaviour. This has led to the development of further models to account for these differences. These models are described qualitatively in the following sections. Electrostatic interactions in host-guest chemistry and biology are believed to be important in controlling the structure and function of complexes<sup>1,2</sup> and the application of molecular electrostatics to such systems has been discussed.<sup>3</sup>

### 1.1.1 Debye-Hückel Theory

A general description of the electrostatic force between two charges  $Q_1$  and  $Q_2$  separated by a distance  $r$  in a vacuum of permittivity  $\epsilon_0$  is given by Coulomb's Law, the magnitude of the force being given by Equation 1.<sup>4</sup>

$$F = \frac{Q_1 Q_2}{4\pi\epsilon_0 r^2} \quad (1)$$

Electrostatic forces between ions in solution differ from those in a vacuum and models have been developed in order to predict their behaviour. The theory of Debye and Hückel is based on the assumption that strong electrolytes are completely dissociated into ions.<sup>5</sup> Observed deviations from real behaviour are then ascribed to electrostatic interactions between ions. To obtain theoretically the equilibrium properties of ionic solutions, it is necessary to calculate the extra free energy arising from these electrostatic interactions.

If the ions were completely distributed at random, the chances of finding either a positive or a negative ion in the neighbourhood of a given ion would be identical. Such a random distribution would have no electrostatic energy, since on average attractive interactions would be balanced by repulsive ones. It is evident that this cannot be the physical situation, since in the immediate neighbourhood of a positive ion, a negative ion is more likely to be found than another positive ion. Indeed, were it not for the fact that ions are continually undergoing molecular collisions, an ionic solution might acquire a structure similar to that of an ionic crystal. The thermal motions effectively prevent any complete ordering, but the final situation is a dynamic compromise between the electrostatic interactions tending to produce ordered configurations and the kinetic

---

collisions tending to destroy them. Calculating the average electric potential of a given ion in solution arising from interactions with all the other ions allows the work that must be expended to charge the ions reversibly to this potential to be determined, this work being the free energy due to electrostatic interactions. Extra electric free energy is directly related to the ionic activity coefficients, since both are a measure of the deviation from ideality. Electrostatics is based on an abstract model for natural phenomena and it is necessary finally to combine the calculated quantities in such a way as to provide a predicted value of some measurable quantity.

In aqueous solution, the Debye-Hückel limiting law is given by Equation 2.

$$\log \gamma_{\pm} = -0.509 |z_+ z_-| I^{1/2} \quad (2)$$

In this equation  $\gamma_{\pm}$  is the mean activity coefficient of the ions,  $z_+$  and  $z_-$  are the ionic charges, and  $I$  is the ionic strength of the solution. The Debye-Hückel model suffers from several basic flaws. Firstly, it uses a macroscopic dielectric constant. Dipolar solvent molecules in the immediate neighbourhood of an ion, however, will not be able to orient themselves freely in an external electric field, and consequently the effective dielectric constant may be much lower than the value for the bulk solvent. Secondly, the derivation of the model assumes that the solution is so dilute that ions will rarely be close together. This means that the interionic potential energy is usually small, and much less than the average thermal energy. In the neighbourhood of a central ion this assumption is only true when separation is about equal to the diameter of one water molecule, and at higher concentrations it is likely that the electrostatic energy is greater than the thermal energy. At low concentrations, however, the Debye-Hückel theory has been found to be well substantiated.<sup>6</sup>

Although the Debye-Hückel theory is interesting in many ways, it is of little quantitative use in calculating the properties of solutions except in the limit of extreme dilution. Some of the inaccuracy and inconsistencies have been removed by the theory of ionic association.

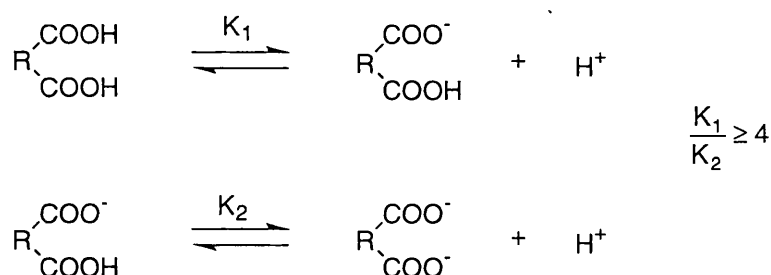
### 1.1.2 Theory of Ionic Association

One of the real difficulties in many electrochemical theories is to obtain an answer to the question, "What is the degree of dissociation of an electrolyte in solution?" In the dissociation of a gas such as  $\text{N}_2\text{O}_4$  into two  $\text{NO}_2$  molecules, the  $\text{NO}_2$  will, on average, exist for a considerable time before recombining with another  $\text{NO}_2$  molecule and during the time it is dissociated it travels freely through the gas undergoing collisions. Most of the time it will be either definitely dissociated or definitely associated and any measurements made on the gas give the same value for the degree of dissociation.

In the case of a molecule such as  $\text{HNO}_3$  in water, however, the situation is different in two respects. Firstly, the dissociation of the molecule to give  $\text{H}^+$  and  $\text{NO}_3^-$  requires separation of oppositely charged ions. The electrostatic attraction between these two ions decreases relatively slowly as they separate, so that some kind of association still exists even when they are several molecular diameters apart. Secondly, the rates of dissociation and reformation of molecules or complexes from ions in solution are very high, the mean lifetime of a dissociated ion perhaps being only of the order of  $10^{-10}$  s as opposed to 1 s in a gas. In this short time, few ions can become really free and the most likely step after dissociation is an almost immediate reassociation. Since the boundary in solution between completely free ions and those which are associated is not clear, one experimental technique may view two ions as associated whilst another records ions at the same distance apart as being dissociated. As a consequence different experimental techniques may yield differing values for the degree of dissociation. The ionic association theory for more concentrated solutions was developed by Bjerrum and considers that definite, although transient, ion pairs are brought together by electrostatic attraction. The formation of pairs will be greater in solvents of lower dielectric constant and where the ionic radii are small, both of these factors tending to increase the electrostatic attractions. Evidence of ionic association is shown by the low conductivity of dilute solutions of salts of multivalent ions such as magnesium sulfate.

### 1.1.3 Electrostatic Effects in Dicarboxylic Acids

The dicarboxylic acids were the earliest group of compounds in which electrostatic effects were studied. In symmetrically disubstituted carboxylic acids the ratio of the first to the second dissociation constant of a dibasic organic acid was found to be always greater than four, and approached four as the length of the acid was increased.



In the ionisation of an acid, a proton is removed against the electrostatic force created by the incipient negative charge that is then left behind on the anion. When a second proton is removed from a symmetrical polybasic acid, the second proton must be removed not only against a similar force, but also against the additional force created by the negative charge left over from the first ionisation. The ionisation of the second proton that is removed, for example in the ionisation in water of the monoanion of glutaric acid (Figure 1.1), takes place in the presence of a residual

negative charge. Because of the extra electrostatic work required to remove a proton from this anionic residue, the second ionisation constant is less than the first.

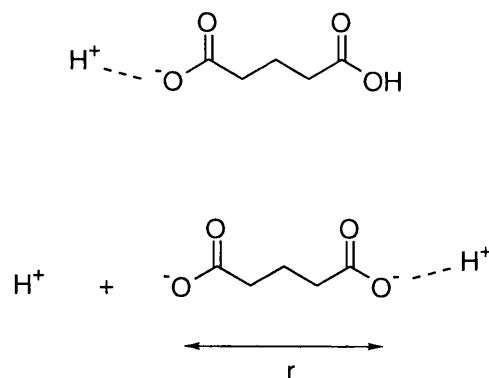


**Figure 1.1**

In 1923 Bjerrum<sup>7</sup> suggested that the ratio of dissociation constants could be accounted for by the combination of a statistical factor of four and the electrostatic effect of the negative charge of the acid-ion on the dissociation of the second hydrogen. Bjerrum's theory viewed these effects as through-space interactions. Whilst the model worked fairly well for the longer chain dicarboxylic acids it was found to be very poor in the case of small molecules such as phosphoric acid, grossly underestimating the electrostatic effects.

Gane and Ingold<sup>8-11</sup> suggested that Bjerrum's theory was too simple to warrant the expectation of quantitative accuracy. The theory is concerned with the propagation of electrical influences from an ionic centre to a focus of reaction situated elsewhere in the same molecule. Two important points are ignored however. Firstly, polar transmission through the molecule itself is neglected. Secondly although account is taken of the propagation of the polar field through the medium, local variations in the properties of the medium are overlooked.

The first of these problems is the less serious since it is less general. Gane and Ingold concluded that internally transmitted polar effects become negligibly small after propagation through two, or at most three, saturated carbon atoms.

A number of problems are associated with the medium. One of these relates to the interionic effect caused by the influence of dissolved ions. To deal with the interionic influences an empirical method was employed in which a series of potentiometric titration curves were determined for each acid at varying concentrations. Above a certain dilution, the equilibrium constants were found to vary slowly and linearly with the concentration. Using linear extrapolation, values for the association constants which should pertain to conditions under which the interionic

effects were negligible were determined. Gane and Ingold found that this technique gave moderately good agreement with values obtained by conductivity methods.

The problem presented by the attraction between the solvent molecules and the ions and the consequential change in the properties of the solvent near ions could not be easily solved using an empirical method, such as that employed in connection with the interionic effects, and mathematical methods were used instead. Using these methods the mutual potential energy of ions at any distance from each other could be calculated.

A further consideration taken into account by Gane and Ingold was the nature of the molecule itself, in particular whether a rigid or flexible model should be adopted. The dimension calculated from the ratio of dissociation constants represented the distance between ionic centres (the points at which net ionic charges may be supposed to be concentrated) in a dipolar ion. A pliable model implies that non-ionic resistance to conformational flexibility is negligible in comparison with ionic resistance, whilst a rigid model implies non-ionic resistance to flexibility dominates. Upon investigation they concluded that the non-ionic sources of potential energy within the molecule dominated those of the ionic sources and that the rigid model was a more appropriate description of the problem.

Whilst the model put forward by Gane and Ingold gave good correlation with the longer chain dicarboxylic acids, it still gave very poor estimations for short chain dibasic acids. A model developed by Kirkwood and Westheimer was shown to give much more accurate results.

#### 1.1.4 The Kirkwood Model

Kirkwood and Westheimer<sup>12,13</sup> introduced a model in which the charges or dipoles were contained in a sphere or prolate ellipsoid of low dielectric constant, representing the molecule, surrounded by a solvent, water, of dielectric constant 80 (Figure 1.2). Using classical physics they then worked out the electrostatics.

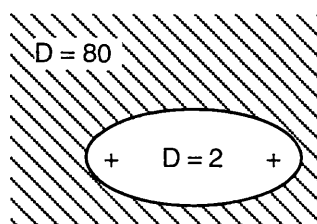


Figure 1.2

Though the model was obviously simplified, it was less crude than placing the charges directly in water as Bjerrum had done and it was found to work remarkably well, having the advantage of

consistency for both charge and dipoles.<sup>14</sup> The equations took the same form as those of Bjerrum but with an effective dielectric constant substituted for the dielectric constant in those equations. The mathematical complexity of the model related to the calculation of the effective dielectric constant. Barton noted, however, that the use of the model of Kirkwood and Westheimer was generally too complex and unreliable to be applied by the organic chemist in the elucidation of molecular structure.<sup>15</sup>

More recently, electrostatic interactions in aliphatic dicarboxylic acids<sup>16</sup> and other small molecules<sup>17</sup> have been predicted from computational methods utilising a finite-difference Poisson-Boltzmann methodology and have been found to be in good agreement with experiment.

### 1.1.5 Electrostatic Effects in Proteins

The importance of electrostatic effects in proteins has been discussed by Perutz.<sup>2</sup> Electrostatic effects dominate many aspects of protein behaviour, having an often decisive influence on the structure, assembly, and hydration of proteins, and on the catalytic power of enzymes. In essence, the challenge faced by those who had sought to apply Debye-Hückel theory to polyelectrolytes of undefined structure has been reversed. Whilst the structures of many of the active sites of enzymes are known in detail, the theoretical knowledge to understand their mechanism is often lacking.

The apparent density of proteins in water is greater than their dry density in organic solvents. This increase is due to the electrostriction of bound water. Some of these water molecules are usually involved in a network of hydrogen bonding of the protein structure but there are others which are less strongly bound. Salt bridges between oppositely charged functional groups of residues in amino acid sequences also account for structure and behaviour in proteins such as haemoglobin.<sup>18-20</sup> Perutz comments that electrostatic effects dominate the activities and properties of many proteins, though the general distribution of charges on their surface is of little importance compared to the microscopic interaction between ionisable groups selected for some specific purpose such as subunit assembly, substrate binding and activation, cooperativity or thermal stability.

Many proteins have an amino acid side chain with an abnormally high or low dissociation constant. These shifts are attributed to the presence of nearby charged groups or a low-polarity microenvironment. Such shifts in association constants are often associated with an enzyme's catalytic activity. Mehler *et al.*<sup>21</sup> presented a simple electrostatic approach for estimating the changes in association constants. This method was a further elaboration of the theory of Kirkwood and Westheimer discussed previously but differed in an important respect. In the Kirkwood model the ion of interest was assumed to have a spherical or elliptical shape with an

---

internal dielectric permittivity dependent on the molecular makeup of the ion and with the solvent's permittivity for the external region, whereas active sites are often far from spherical or elliptical and water molecules and ions are often found in these regions. In order to account for the shielding effect of the dielectric medium, they proposed an empirical dielectric permittivity function of charge separation. The functional form and parametrisation are based on dielectric permittivity data obtained from experimental and theoretical studies of the ratio of the first to the second dissociation constant of bifunctional organic acids and bases. The results of experiments led to the conclusion that in solvent-accessible regions attenuation of electrostatic effects by the environment was often greater than commonly assumed - these regions are not similar to nonpolar regions of the protein interior.

An alternative technique to that adopted by Mehler is to use a finite difference approach to solve the Poisson-Boltzmann equation (Equation 3) using numerical methods.<sup>22</sup>

$$\nabla \cdot [\epsilon(\mathbf{r}) \nabla \phi(\mathbf{r})] = -4\pi\rho(\mathbf{r}) \quad (3)$$

In this equation  $\epsilon(\mathbf{r})$  is the dielectric constant as a function of position,  $\phi(\mathbf{r})$  is the electrostatic potential and  $\rho(\mathbf{r})$  is the charge density. This method has been applied by Gilson and Honig<sup>23</sup> who concluded that the continuum solvent model they used in their calculations reproduced the essential features of the interaction. A more complex technique has been used by Fersht and co-workers to predict the electrostatic effects in the protein subtilisin.<sup>24</sup>

Mehler and Solmajer<sup>25</sup> compared the results of these two differing approaches to predicting the electrostatic effects in proteins where the charged sites are separated by 3-12 Å. They concluded that the simpler method, in which a screened Coulomb potential was used, gave results at least as accurate as those using the more complex techniques based on the Poisson-Boltzmann equation. They also noted that the simpler model gave substantially better results in cases where the separation was in the distance range 3-5 Å. This difference is attributed to the involvement of nonelectrostatic interactions such as charge-transfer effects. These effects tend to increase the apparent dielectric permittivity value. The arbitrarily low value of the dielectric constant assigned to the protein in techniques where the Poisson-Boltzmann equation is solved means that such nonelectrostatic interactions are not accounted for.

### 1.1.6 Electrostatic Interactions Between Organic Ions

Most organic reactions are studied in non-aqueous media and interactions between oppositely charged organic molecules in water have only received limited attention. In a biochemical environment these interactions are overwhelmingly important as most small organic molecules in biology are present in aqueous solution and carry charges. Electrostatic competition between organic ions and the considerable quantities of inorganic ions which are also present in these



biological solutions must also occur. Lemieux has discussed the importance of water to molecular recognition in biological associations.<sup>26</sup> Tam and Williams<sup>27</sup> have studied the association constants of organic cations and anions with different charge separations, rigidity and shapes and compared them with the association constants of inorganic ions.

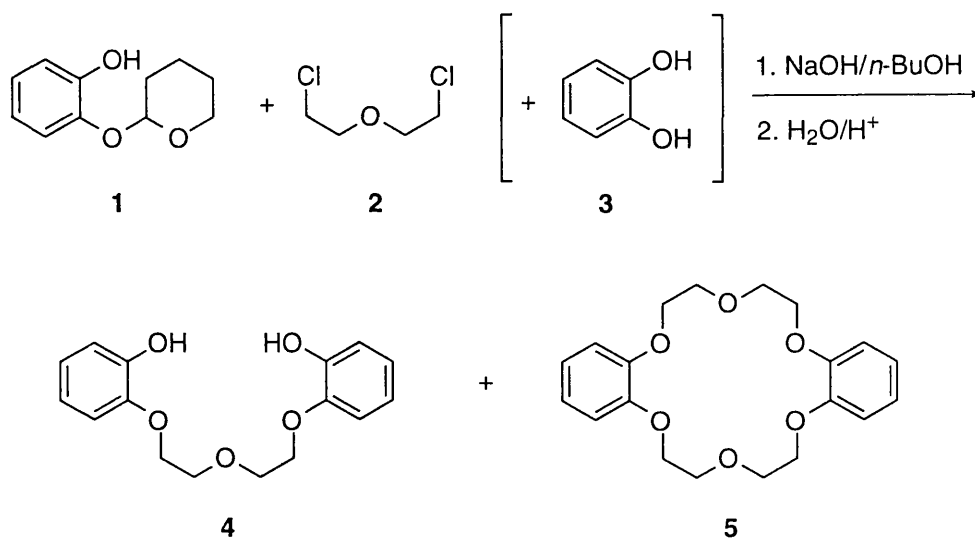
The quantitative description devised by Bjerrum of the binding between ions of symmetrical charge distribution was based on electrostatic interaction energy and the Boltzmann distribution. Two important assumptions were made, namely a macroscopic dielectric constant and a point-charge model for the ions. In general, experimental data for binding between inorganic ions shows good agreement with Bjerrum's prediction. The binding of inorganic cations with organic anions follows the model less well as size-matching effects become more important. Binding between organic cations and organic anions introduces anisotropy into both components and charge matching becomes a major feature though complications arise from configurational entropy in flexible ions.

Tam and Williams draw several conclusions from their studies concerning the factors which govern electrostatic interactions between organic ions in an aqueous medium. Charge and size are the most pertinent but a spherically symmetrical model of the ions is inappropriate in many cases. Selectivity can result from spatial charge matching between oppositely charged ions but steric and hydrophobic factors are also relevant, as are entropy terms. The importance of charge and shape matching has also been observed by Lehn and co-workers.<sup>28</sup>

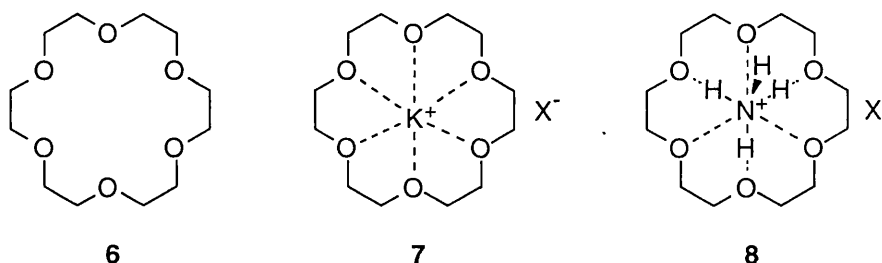
## 1.2 Host-Guest Chemistry

The remarkable abilities of enzymes to catalyse organic reactions and regulate their occurrence challenges the chemist to devise simpler organic compounds that will perform similar functions. Complexation is a crucial factor in enzyme catalysis since complexation and decomplexation are the first and last steps in an enzymatic reaction.

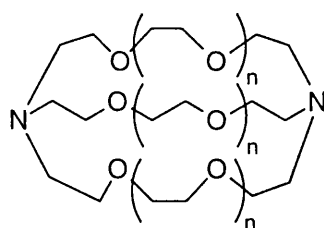
In 1967 Pedersen<sup>29,30</sup> published his discovery of the crown ethers and their complexing power with metal cations. The first crown ether was a chance discovery. Pedersen wanted to prepare bis-phenol **4** from mono-protected catechol **1** and ether **2**. As a slightly impure sample of **1** was used which contained some unprotected catechol **3**, a very small amount of hexaether **5** was also obtained.



Pedersen's interest was aroused by the good crystallisability of hexaether **5** and its unusual solubility properties. The compound was only slightly soluble in methanol but on addition of sodium salts it dissolved surprisingly easily. Coupled with the fact that with potassium permanganate compound **5** could be dissolved in benzene or chloroform Pedersen was led to postulate that sodium or potassium ions occupied the centre of the molecule giving a complex. Pedersen termed the family of oligo-ethylene glycol ethers related to **5** 'crown-compounds'. The prototype crown ether is 18-crown-6 **6** which readily forms complexes **7** and **8** with potassium and ammonium salts.



This early work provided the starting point for much of the field of host-guest chemistry. A wide variety of crown compounds have been synthesised and their complexation properties studied. In 1969 Dietrich *et al.*<sup>31,32</sup> presented papers on the design, synthesis and binding properties of cryptands such as **9** and **10** which further demonstrated the attractions and opportunities of complexation chemistry.



9  $n=1$   
10  $n=2$

In general the host-guest studies undertaken so far have involved studying complexation between species and attempting to determine the critical factors affecting the process. Cram<sup>1</sup> stated that a host molecule must "recognise" by complexing best those guest molecules that contain the array of binding sites and steric features that best complement those of the host. Since two objects cannot occupy the same space at the same time, the host and guest must be compatible with respect to shape if they are to complex. The simple attraction of positive and negative charges accounts for much of the binding between host and guest molecules.

### 1.2.1 Conventions in Host-Guest Chemistry

The concepts and terms relating to hosts, guests, complexes, and their binding forces were defined by Cram and co-workers<sup>33</sup> in 1977 and have since gained broad international acceptance. Complexes are composed of two or more molecules or ions held together in unique structural relationships by electrostatic forces other than those of full covalent bonds. Molecular complexes are usually held together by hydrogen bonding, by ion-pairing, by  $\pi$ -acid to  $\pi$ -base interactions, by metal to ligand binding, by van der Waals attractive forces, by solvent reorganising, and by partially made and broken covalent bonds (transition states). High structural organisation is usually produced only through multiple binding sites and a highly structured molecular complex is composed of at least one host and one guest component. A host-guest relationship involves a complementary stereoelectronic arrangement of binding sites in host and guest. In host-guest chemistry, the host component is defined as an organic molecule or ion whose binding sites converge in the complex, whilst the guest component is defined as any molecule or ion whose binding sites diverge in the complex.

Many different types of host molecule have been designed and synthesised, containing a wide variety of structural features and binding sites. Each host, however, can be envisaged as belonging to one of three generic classes of molecule (Figure 1.3).

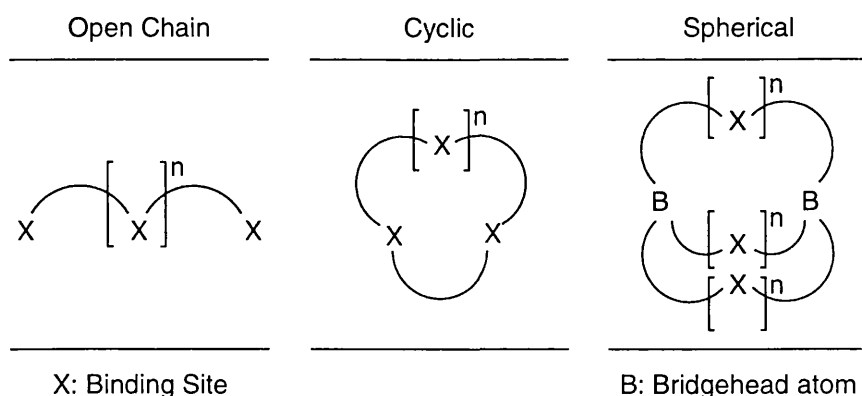
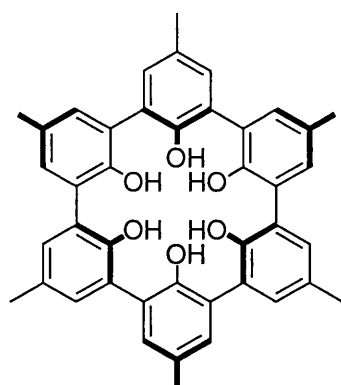
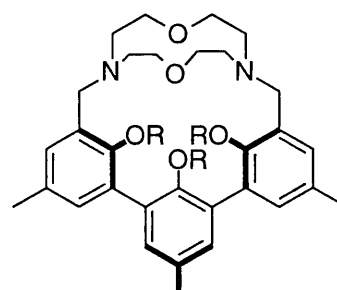


Figure 1.3

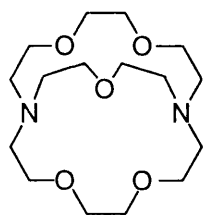
Cram<sup>34</sup> has further subdivided these generic groups to give smaller families of host compounds. These families are exemplified by spherand **11**, cryptaspherand **12**, cryptand **13**, hemispherand **14**, corand **15** and podand **16**. In spherands, the donor centres are parts of the intraannular substituents which point into the interior of a rigid ring. Cryptands were first introduced by Lehn<sup>35</sup> in the 1970's and have a three-dimensional cavity, whose size changes as the length of the bridges are varied. Corands are monocyclic compounds which can have many different types of symmetry. Corands which contain ether oxygens exclusively are referred to as crown ethers. Cryptaspherands are a hybrid of spherand and cryptand, whilst hemispherands are a hybrid of spherand and corand. In contrast to the other host molecules described, podand refers to an acyclic host. Podands are distinguished by their notable lack of ring and bridge systems. In principle, this type of compound has been known for a long time. However, it was the crown ether chemistry that led to the synthesis of specific podands, especially those with terminal functionalities or pronounced lipophilicity.

**11**

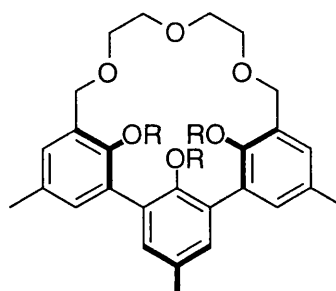
Spherand

**12** R=Me

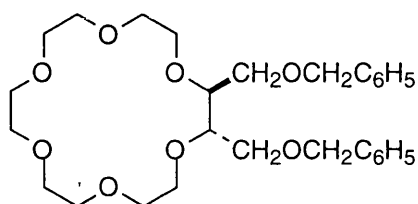
Cryptaspherand



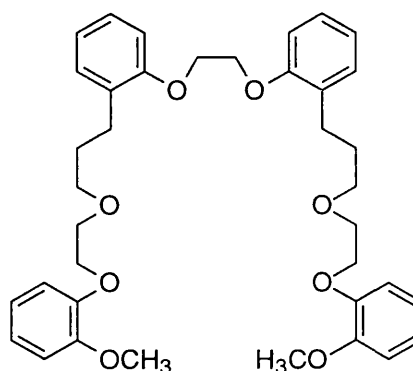
**13**  
Cryptand



**14** R=Me  
Hemispherand

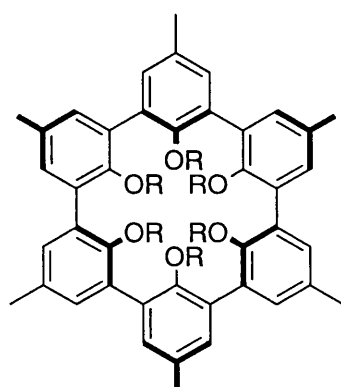


**15**  
Corand

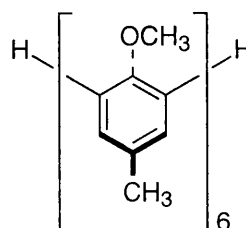


**16**  
Podand

Cram has compared podand **17** and spherand **18**. The podand differs constitutionally from the spherand only in the sense that the podand contains two hydrogen atoms in place of one covalent bond in the spherand. The two hosts differ radically in their conformational structures and states of solvation. The spherand possesses a single conformation ideally arranged for binding lithium and sodium ions. Its oxygens are deeply buried within a hydrocarbon shell and the orbitals of their unshared electron pairs are in a microenvironment whose dielectric properties are between those of a vacuum and a hydrocarbon. No solvent can approach these six oxygens, which remain unsolvated. Thus the spherand is preorganised for binding. The podand, however, can in principle exist in over 1000 conformations, only two of which can bind the metal octahedrally. The free energy for organising the podand into a binding conformation and desolvating its six oxygens must come out of its complexation free energy. The podand is not preorganised for binding, but is randomised to maximise the entropy of mixing of its conformers, and to maximise the attractions between solvent and molecular parts.



17 R=Me



18

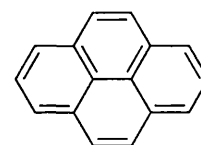
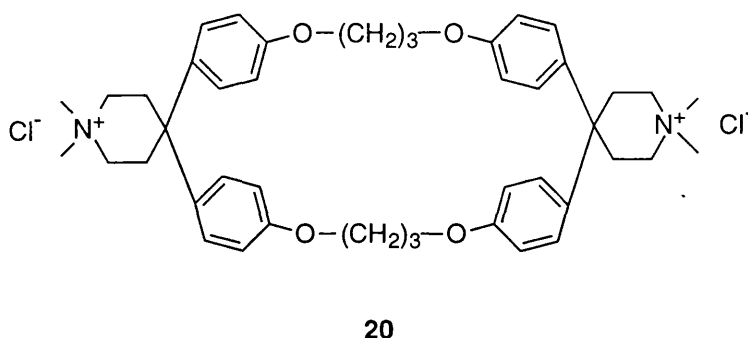
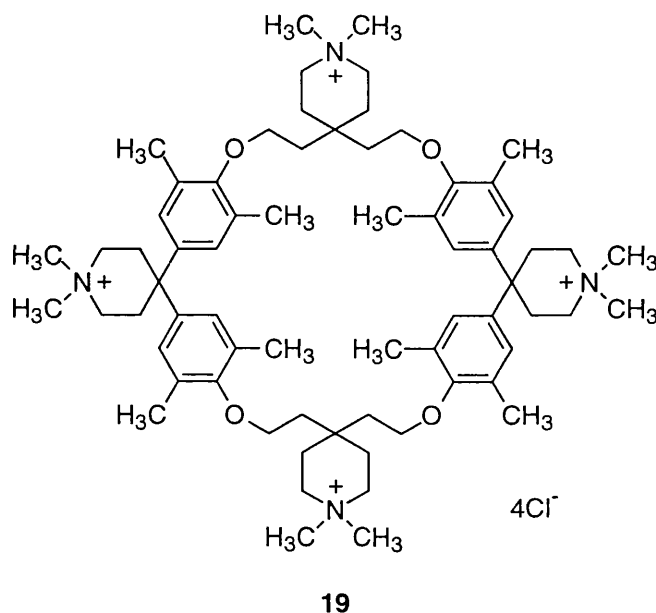
The difference in free energy values for spherand **17** and podand **18** binding a lithium ion corresponds to a difference in association constants of  $>10^{12}$ . In general, spherands bind their most complementary guests the strongest, followed (in order) by cryptaspherands, cryptands, hemispherands, corands and podands. Cram concluded that preorganisation was a central determinant of binding power.

### 1.2.2 Factors Determining Strength of Association

In the complexation of organic molecules, the intermolecular interactions that lead to binding are essentially weaker than those in the complexation of metal ions. The requirements in terms of the steric and functional complementarity and spatial preorganisation of the host compounds are correspondingly high. In addition, suitable binding niches or cavities have to be considerably larger than in ligands for metal complexes.

In the molecular recognition of organic molecules with polar or protic functional groups, the formation of hydrogen bonds between the host and the guest is most often the driving force of complex formation. Rebek<sup>36</sup> has reported a family of hosts which have different functional groups forming hydrogen bonds whilst the molecular tweezers of Wilcox<sup>37</sup> similarly bind *via* hydrogen bonds. The binding forces that occur in the complexing of nonpolar organic molecules by nonpolar binding sites of corresponding host compounds are weaker. Binding forces in this case include van der Waal's interactions, arene stacking, cation- $\pi$  interactions, dipole-induced-dipole interactions and electron-donor-acceptor interactions. One of the greatest influences in complexation, however, is the effect of the solvent.<sup>38</sup> Where water is the solvent this is referred to as the "hydrophobic effect". Hildebrand<sup>39</sup> has studied the interactions between alkanes and water and suggested that the use of the term "hydrophobic" is misleading. He states that rather than the existence of hydrophobia between water and alkanes, there is simply not enough hydrophilia to pry apart the hydrogen bonds of water so that alkanes can go into solution without assistance from attached polar groups.

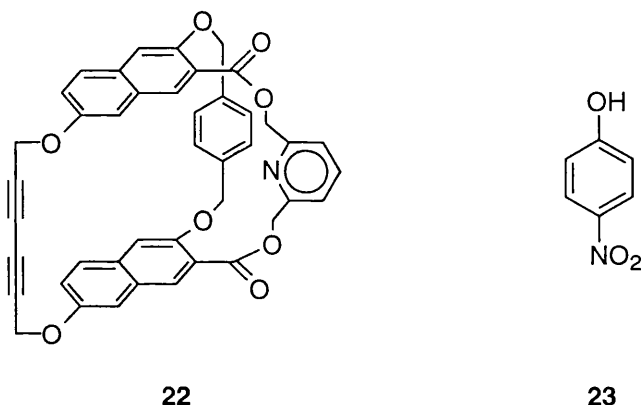
Diederich and co-workers<sup>40-44</sup> have investigated the solvent dependence of the binding strength in the complexation of aromatic guest molecules in studies involving water-soluble cyclophane hosts such as **19** and **20** with hydrophobic cavities. Aromatic guests, for example pyrene **21**, can be complexed even in a nonpolar solvent such as carbon disulfide and also in aromatic solvents.



The complex formation constants were found to be particularly large in water, as well as in ethylene glycol and decrease in the transition from polar protic solvents to dipolar aprotic solvents, being weakest in nonpolar solvents. The empirical factor of solvent polarity is related to the macroscopic properties such as the dielectric constant, dipole moment, cohesion, and polarisability.<sup>45</sup> Since the shape of the complex is unchanged in the different solvents,<sup>46</sup> the difference in binding constants must be related to solvation. Where it is energetically favourable for the solvent to solvate the host and guest, then association of the binding partners becomes less favourable, whilst with weak solvation of the host and guest species, complex formation is promoted. If a solvent such as water is considered, the solvation of nonpolar molecular surfaces and cavities is unfavourable enthalpically as the solvent molecules on the surface can participate

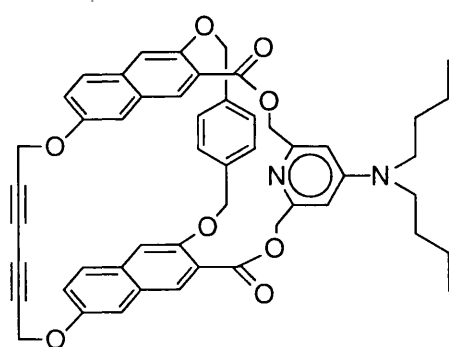
in fewer hydrogen bonds than those in the bulk and consequently are higher in energy. If two nonpolar surfaces become associated, for example in the inclusion of aromatic molecules in molecular cavities, the surface solvent molecules are released into the bulk and their energy content is lowered, promoting complex formation. This is entropically favoured also since the ordered solvent cage surrounding the host and guest species is destroyed at the binding sites. Lipophilic solvents such as chloroform or benzene have favourable interactions with both nonpolar host and guest species and could be considered as only weak competitors for the host receptor site, but due to their large excess they effectively compete with the host molecules. In contrast, water is the most favourable medium for the complexation of nonpolar compounds.

Whitlock *et al.*<sup>47</sup> reported the synthesis and binding properties of cyclophane host **22** in organic solvents such as chloroform with *p*-nitrophenol **23**.

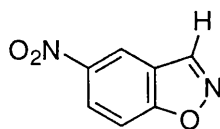


The complexation of neutral guests in organic solvents means that hydrophobic forces become less important whilst structural features in the host have added significance. Whitlock suggest that for strong binding, a rigid cavity is required to immobilise the guest relative to the coordinate frame of the host. Stronger complexation will occur for a tight fitting host-guest pair. A functional group in the host which can protrude into the internal cavity can act as a binding force to the guest species. Face-to-face and face-to-edge interactions between aromatic groups may also be fruitfully employed in the design of hosts accepting aromatic guests. Related host **24** has been shown to catalyse the base-promoted decomposition of 5-nitrobenzisoxazole **25** to cyanophenol **26** via complex **27**.<sup>48</sup>

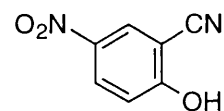




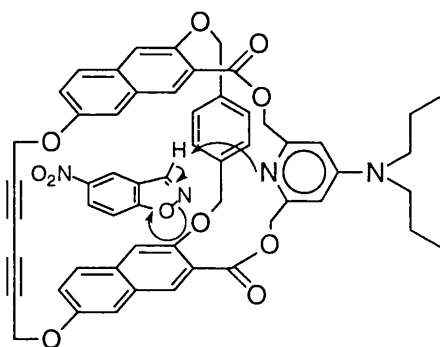
24



25

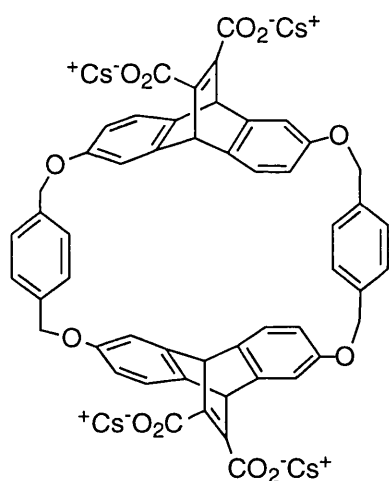


26

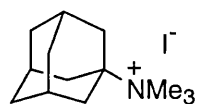


27

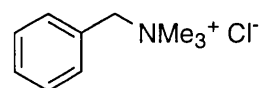
Dougherty and co-workers have investigated the forces driving molecular recognition between host **28** and various guests in aqueous solution using circular dichroism and NMR methods.<sup>49-54</sup> Host **28** acts as a general receptor for positively charged ammonium and immonium guests such as **29-32**. Much lower association constants are obtained with neutral guests.



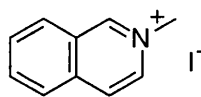
28



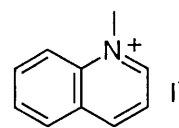
29



30



31



32

Along with the hydrophobic interaction and electrostatic effects, Dougherty suggests that donor-acceptor  $\pi$ -stacking interactions and ion-dipole attractions can also contribute significantly to aqueous binding.<sup>49-51</sup> More specifically, the electron rich  $\pi$ -system of host **28** acts to stabilise an electron deficient guest, an effect referred to as a cation- $\pi$  interaction. Significant heat-capacity effects have been observed in the association of host **28** with guests **29-32**,<sup>52</sup> although the origin of the cation- $\pi$  interaction is predominantly enthalpic. The magnitude of these heat-capacity effects depends on the nature of the solvent as well as on the electronic and structural properties of the guests. Bromination of host **28** greatly enhances its binding ability in a general fashion, primarily as a result of hydrophobic interactions.<sup>53</sup> Circular dichroism experiments<sup>54</sup> have provided evidence of binding orientations and revealed a preference of guests to rotate in the host cavity to better fill space. Data suggests a preference of the cation- $\pi$  interaction for certain orientations of bound guests with a significant hydrophobic contribution to the binding. Strong binding of ammonium compounds by water soluble polyphenolates has been reported by Schneider *et al.*<sup>55</sup>

The results of these studies indicate that even for systems that are designed to be extremely simple, with minimal degrees of freedom and relatively well defined interactions, noncovalent binding interactions are extremely complicated phenomena. The affinity of any individual guest for a particular host is determined by a delicate interplay of hydrophobic, electrostatic, conformational and solvation effects.

### 1.2.3 Design of Anion Receptors

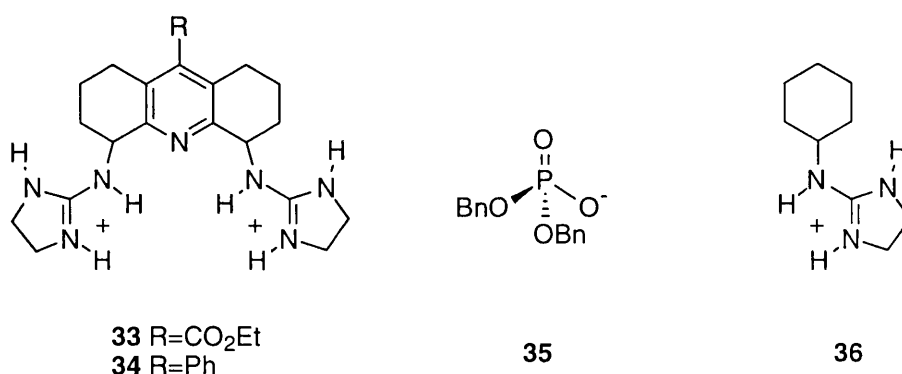
Although anionic species play a very important role in chemistry and in biology, their complexation chemistry went unrecognised as a specific field of research, while the complexation of metal ions and, more recently, cationic molecules was extensively studied. The synthesis of anion receptors may yield host species with a variety of interesting chemical and biological properties and research into anion receptors has been increasingly active.<sup>56-58</sup> Examples of possible applications for anion receptors include the extraction and transport of anions, the construction of sensors and molecular catalysis as well as potential biological applications.

Positively charged or neutral electron-deficient groups may serve as interaction sites for anion binding. Ammonium and guanidinium units have mainly been used, but neutral polar hydrogen bonds, electron-deficient centres, or metal-ion centres in complexes also interact with anions.

### 1.2.4 Guanidinium Receptors

Anslyn and co-workers<sup>59</sup> have investigated bis(alkylguanidinium) hosts, such as **33** and **34**, as artificial enzymes which can bind phosphodiester.

---



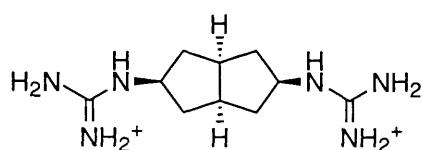
Both a *meso* form, in which both guanidinium substituents lie on the same side of the spacer, and a *d,l* form, in which they lie on opposite sides, of these hosts are possible. Each guanidinium moiety in receptors **33** and **34** can form two hydrogen bonds with phosphate guest **35**, giving four hydrogen bonds in total with little reorganisation of the host structure. A mixture of dimethylsulfoxide and water was used as the solvent system. From <sup>1</sup>H and <sup>31</sup>P NMR titrations, either 1:1 or 2:1 phosphate to host complex formation was observed, depending on the solvent composition. For systems with a low percentage water content, 2:1 binding was observed but as the percentage of water was increased, the 2:1 binding vanished and only 1:1 binding was observed. The association constants decreased with increasing concentrations of water. Dimethylsulfoxide is a strong hydrogen-bond acceptor and competes with the phosphodiester for hydrogen bonding to the host. Water is able to solvate both the host and guest by hydrogen bond accepting and donating respectively, whilst in addition the higher dielectric constant of water tends to shield the electrostatic attraction of the host and guest better than dimethylsulfoxide.

Investigations were also carried out into the effect of host cavity size and counterions for hosts **33** and **34**. With tetraphenylborate as the guanidinium counterion, in pure dimethylsulfoxide the *meso* forms of the hosts were found to be the best receptors. This suggests cooperativity between the two guanidinium moieties where both groups are positioned on the same side of the spacer. Receptor **33** showed stronger binding than **34**, the authors attributing this difference to **33** possessing a more complementary cavity, possible due to it having increased flexibility. The guanidinium moieties in the *d,l* form of **34** were found to behave somewhat independently with 2:1 phosphate to host binding equally as likely as 1:1 binding. This indicates that the complexing groups cannot be appropriately positioned to act cooperatively to bind the phosphodiester. In contrast, 1:1 complex formation was preferred by the *d,l* form of **33**, again possibly due to increased flexibility in the host. Further support for cooperativity between the two guanidinium groups was shown by comparison with the binding constant of dibenzyl phosphate to the monoguanidinium species **36**, which was found to be much less than that of the bis(guanidinium) receptors. It is important to note that cooperativity refers to an enhanced binding of

phosphoesters by **33** and **34** in comparison with host **36**, and not that the binding is over twice that of the monoguanidinium species.

The chloride salts of the bis(guanidinium) receptors behaved differently from their tetraphenylborate counterparts. Overall, the association constants are typically larger than with tetraphenylborate. Here, however, whilst *meso*-**34** still binds more strongly than *d,l*-**34**, it is the *d,l* form of **33** which binds phosphoester **35** more strongly. The noncoordinating tetraphenylborates had been expected to bind more strongly since the counterion should present no competition in coordinating to the guanidinium. The chloride counterion, however, appears to be intimately associated with the 1:1 host to guest complex and is probably involved in some form of coordination to a guanidinium for charge neutrality.

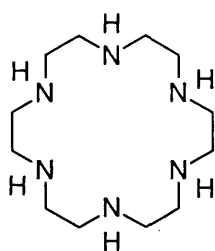
Recently, Hamilton and co-workers<sup>60</sup> have reported that the guanidinium receptor **37** binds selectively to closely spaced aspartate pairs in helical peptides.



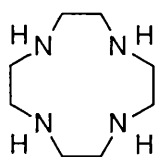
**37**

### 1.2.5 Polyammonium Macrocycles

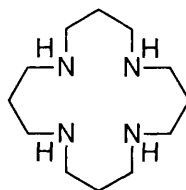
Polyammonium macrocycles and macropolycycles have been studied most extensively as anion receptor molecules. They bind a variety of anionic species (inorganic anions, carboxylates, phosphates, etc.) with stabilities and selectivities resulting from both electrostatic and structural effects.



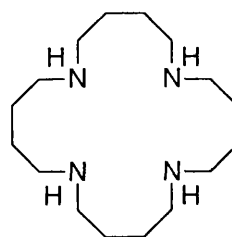
**38**



**39**



**40**



**41**

The 18-azacrown-6 **38**, also called hexacyclen, has been extensively studied in aqueous solution and shown to complex a large variety of anions in its tri- and tetraprotonated forms. Polycarboxylate anions such as succinate, citrate and malonate have been found to form

complexes with **38** in its triprotonated form.<sup>61</sup> Inorganic anions such as chloride, nitrate, bromide, chlorate and iodate have been found to form weak to moderate complexes with **38** in its tetraprotonated form.<sup>62</sup> In general 1:1 host to guest complexes are formed but some exceptions have been observed. For example, with iodate anion a 1:2 host to guest complex has been observed,<sup>63</sup> whilst with sulfate anion evidence exists for the formation of both 1:1 and 1:2 host to guest stoichiometries.<sup>64</sup> From an analysis of thermodynamic data it appears that the driving force for complexation between hexacyclen and anionic guests is due to water loss from both the hexacyclen and sulfate solvation spheres. Molecular mechanics calculations have shown that several conformations of **38** exist which have a similarly low energy and that there is a reasonable enthalpy of complexation associated with the formation of hydrogen bonds between protonated ammonium groups in the host and oxygen atoms in the guests.<sup>65</sup>

The complexation ability of a large variety of polyamines in their protonated forms has been studied and formation of complexes of phosphate anions such as inorganic phosphates and biologically relevant phosphates has been observed. Studies involving polyamines **39-41** have illustrated some important points regarding the number of protons a polyamine can support at neutral pH. These symmetric amines have two, three or four methylene groups between two successive nitrogen atoms. Whilst the first and second association constants show little difference between the polyamines, the third and fourth association constants vary considerably (Table 1.1).<sup>61,66</sup>

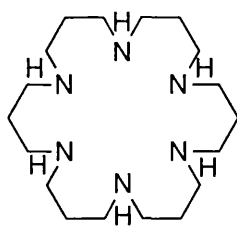
	pK <sub>1</sub>	pK <sub>2</sub>	pK <sub>3</sub>	pK <sub>4</sub>
<b>39</b>	10.7	9.7	1.7	<1
<b>40</b>	10.8	9.6	6.9	5.4
<b>41</b>	11.8	11.4	10.6	8.9

pK<sub>n</sub> refers to the pK<sub>a</sub> for the nth association constant

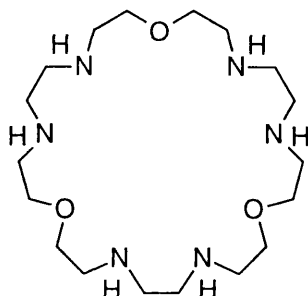
**Table 1.1**

At physiological pH, **39** can only be diprotonated whilst **41** is fully protonated. The correct spacing of successive nitrogens is thus of primary importance in the design of anion receptors based on polyamine macrocycles, since in order to achieve strong complexation highly charged ligands are required. Strong complexation has been observed between **41** and fluoride ion.<sup>66</sup>

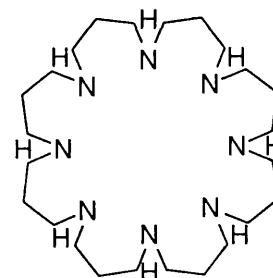
Lehn and co-workers have synthesised a variety of polyamines containing six or more nitrogens with the aim of obtaining highly charged receptors.<sup>67,68</sup> Hosts **42** and **43** in their hexaprotonated forms complex a variety of di-, tri- and tetraanions, the stability constants of the complexes increasing as the charge on the anion increases.



42

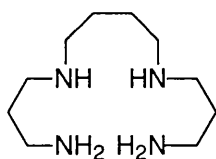


43

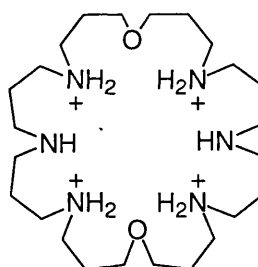


44

Nucleotide phosphate polyanions form complexes of much higher stability with the macrocyclic polyammonium structures than with the acyclic tetraammonium ligand spermine **45**.<sup>69</sup> This enhanced stability is attributed to a macrocyclic effect on binding with respect to acyclic ligands. Electrostatic interactions play a major role in both strength and selectivity of binding. Thus, for a given receptor, the anions most strongly complexed are usually the smallest and most highly charged i.e. those of highest charge density. In general larger anions are bound more strongly by larger macrocycles such as **44**, which contains eight nitrogen atoms, though there are exceptions. It has also been found that whilst the protonated forms of macrocycles such as **42** and **43** form 1:1 complexes with AMP, ADP, and ATP nucleotides,<sup>69</sup> the larger macrocycle **44** binds two nucleotides.<sup>70</sup> At pH 7, macrocycle **44** is found in its octaprotonated form.



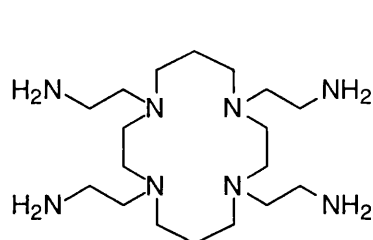
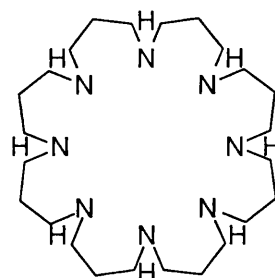
45



46

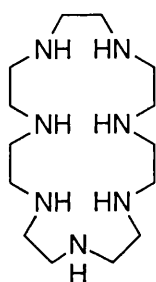
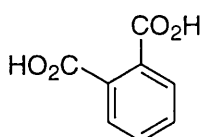
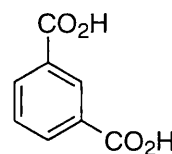
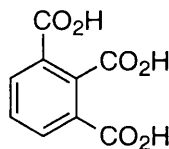
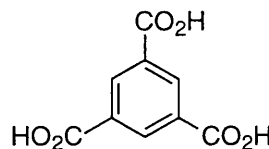
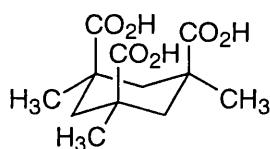
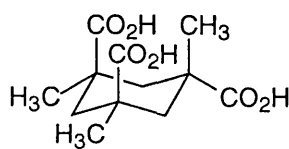
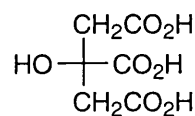
Mertes<sup>71</sup> has drawn analogies between simple monomacrocyclic polyaza molecules such as **46**<sup>67</sup> and phosphoryl-transfer enzymes. A number of enzyme characteristics are shown by the macrocycle. Its reactions proceed in neutral aqueous media, anionic bonding occurs by electrostatic and hydrogen bonding, metal-ion catalysis and regulation are observed, the reaction is dependent on a Michaelis-like complex and competitive inhibition occurs when substrate analogues are used. There is, however, still a wide gap between hydrolysis rates for the enzymes and the macrocycle. Recently, Lehn *et al.*<sup>72</sup> have reported that macrocycle **46** catalyses H/D exchange in malonate ions.

Bianchi and co-workers have investigated several polyammonium macrocycles as receptors for a variety of cations and anions in aqueous solution.<sup>73</sup>

**47****44**

Using a variety of experimental techniques receptor **47**, a branched polyazacycloalkane which contains four primary amine groups in the arms, and its interaction with anions such as ATP,  $\text{P}_2\text{O}_7^{4-}$  and the complex anions  $[\text{Co}(\text{CN})_6]^{3-}$  and  $[\text{Fe}(\text{CN})_6]^{3-}$  have been examined.<sup>74</sup> A comparison of these results with those for related macrocycle **44** revealed that stability constants were lower with branched macrocycle **47** which at neutral pH exists predominantly in its tetraprotonated form.

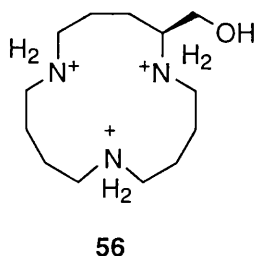
The interaction in aqueous solution of polyammonium receptor **48** with a several organic carboxylates **49-55** has been examined using a variety of experimental methods.<sup>75</sup>

**48****49****50****51****52****53****54****55**

In all cases 1:1 complex formation was observed. The overall order of the strength of interaction was found to be **51** > **53** > **52** > **49** > **50** > **54** > **55**. Selectivity was observed between the different anions, in particular guest **55** was found to interact least strongly with the host over the whole pH range under consideration. This selectivity is attributed to poorer structural matching between host and guest species since it is not pH-dependent. The protonated forms of receptor **48** appear to offer size and structural features adequate to recognise carboxyl groups centred around six-membered carbon atom ring moieties. The charge of the anion does not solely account for the interaction strengths found and structural factors appear to play a role in determining the binding, anions **49** and **50** being able to approach the receptor and implement a hydrogen bonding network more effectively than anions **54** and **55**. Of the related cyclohexane tricarboxylic acid derivatives, the all *cis* anion **53** is selectively recognised over anion **54**. Conformational analysis of these anions showed that in their tri-, di- or monoprotonated forms both **53** and **54** adopt a chair conformation with the three or two *cis*-carboxyl groups in axial disposition. In the case of the trianionic forms, however, the conformer with the three or two *cis*-carboxyl groups equatorial is found to be the most stable. When complexed with receptor **48**, it is the trianionic form of **53** which is present. Molecular modelling studies have indicated that receptor **48** acts as a flat charged surface which shows complementarity with planar guests and guest **53** is able to form a hydrogen bonding network with the host more effectively than guest **54**. For the aromatic substrates, due to their similar arrangements, charge density considerations mainly explain the order of selectivity found.

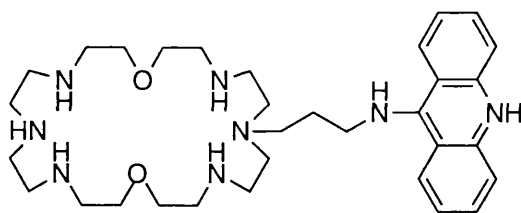
### 1.2.6 Derivatives of Polyammonium Macrocycles

Further functionalisation of polyammonium macrocycles gives rise to a wide range of structures. A simple derivative of a polyammonium macrocycle, receptor **56**, and its complexation with ATP has been described by Burrows *et al.*<sup>76</sup> The free hydroxyl group in this molecule offers the possibility of further elaboration to include additional reactive or binding functional groups. Such additional functional groups may not be involved in binding and could react as reagents or catalysts for the reactions of anionic substrates.



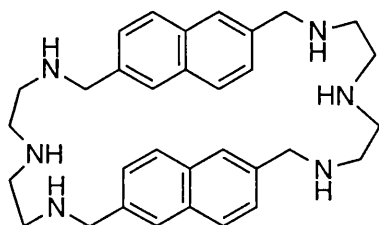
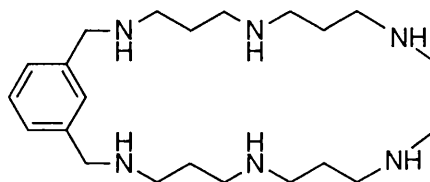


Macrocyclic polyamines, when protonated, bind strongly to nucleotides *via* electrostatic interactions between the cationic binding sites of the receptor and the negatively charged polyphosphate groups. In order to attain better recognition of nucleotides, receptor molecules need to contain other binding sites capable of interactions with the sugar moiety or nucleic base, in addition to the anion binding sites. Interactions with the nucleic base may be achieved either by stacking, or by sites capable of forming complementary hydrogen bonding patterns. The complex multifunctional anion receptor **57** has been reported by Lehn and co-workers.<sup>77</sup> This molecule contains three potential binding sites as functional subunits. Two recognition sites are present, a macrocyclic polyammonium moiety as an anion binding site and an acridine side chain for  $\pi$ -stacking interactions. A catalytic amino group is also present in the macrocycle for facilitating hydrolytic reactions.

**57**

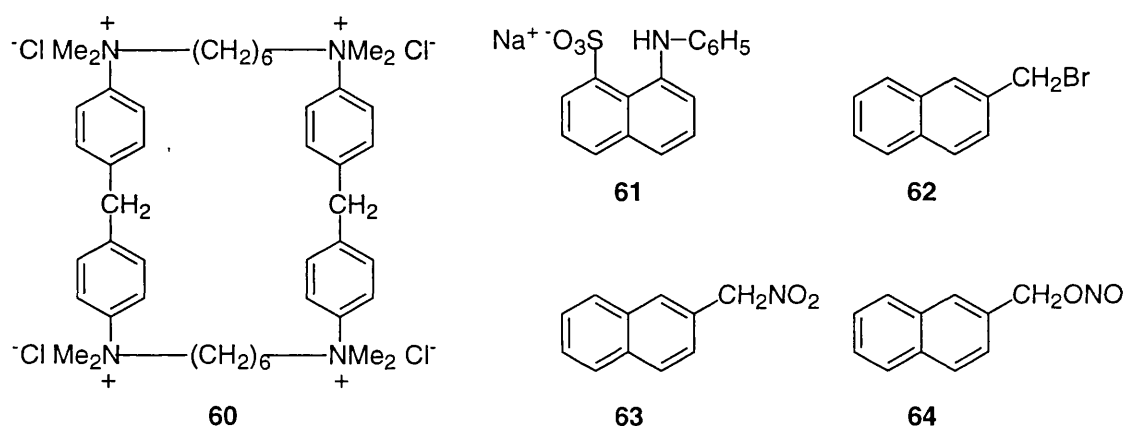
Receptor **57** shows greater selectivity between ADP and ATP than its parent macrocycle which lacks the acridine binding site. Spectroscopic methods reveal that binding of nucleotide polyphosphates occurs through simultaneous interactions between the macrocyclic polycationic moiety and the polyphosphate chain and by stacking between the acridine derivative and the nucleic base of the nucleotides. It has also been found that host **57** acts as a selective and sensitive fluorescent probe for ATP.

Receptors such as **58** and **59** have been reported which in their protonated forms complex with anionic guests through both electrostatic and  $\pi$ -stacking interactions.

**58****59**

Macrocycle **58** strongly binds planar anionic guests such as aromatic carboxylates and nucleotides.<sup>78</sup> Binding strength was found to increase with the size as well as the charge of the guest species, providing evidence that both stacking and electrostatic effects contribute to the stability of the complex. Similar effects have been observed with receptor **59**.<sup>79</sup>

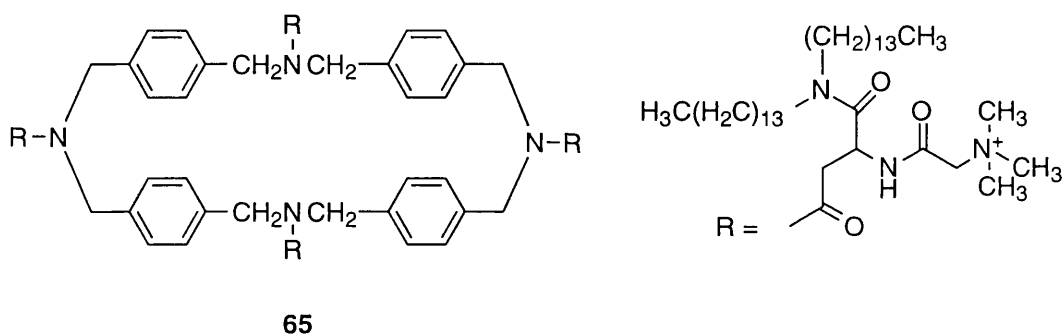
Schneider *et al.* have extensively studied the complexation behaviour of receptor **60** with anionic guests such as **61** in aqueous solution. The receptor contains four positively charged nitrogen atoms and strongly binds **61** through lipophilic and hydrophobic binding.<sup>80</sup> Neutral guests are also bound, although less strongly. Addition of salts such as sodium chloride to a mixture of host and guest decreases the strength of binding as does increasing the amount of organic solvent in the mixture.



Host **60** has been found to catalyse substrate- and product-selective reactions with ambident anions.<sup>81</sup> In the presence of **60**, the rate of reaction of 2-bromomethylnaphthalene **62** with an excess of sodium nitrite (NaNO<sub>2</sub>) is accelerated by an order of magnitude. The ratio of the two possible products is altered concomitantly, with an increase in the product bonded through nitrogen (R-NO<sub>2</sub>, **63**) over the oxygen bound product (R-ONO, **64**). Inhibition of this catalysis is observed if anion **61** is introduced into the solution since it is an effective competitor for the host cyclophane. Receptor **60** has been utilised as an analytical agent for thin layer chromatography.<sup>82</sup> Host **60** and related macrocycles have been found to stabilise DNA polymers. With RNA duplexes, however, they either stabilise the duplexes or alternatively cause base-pair opening depending on the size of the cyclophane.<sup>83</sup> Schneider and Theis<sup>84</sup> have attempted to quantify the electrostatic contributions in synthetic host-guest complexes. By comparison of the complexation free energies of host **60** with both charged and uncharged naphthalene derivatives, typical Coulomb interaction energies can be obtained. As long as electrostatic interactions dominate, a uniform value of  $5 \pm 1 \text{ kJmol}^{-1}$  per ion pair is obtained for the formation of salt bridges. A study of the equilibria in water between ion pairs with aromatic units in one or both ions yielded similar results<sup>85</sup> as did experiments with ligand-porphyrin complexes.<sup>86</sup>

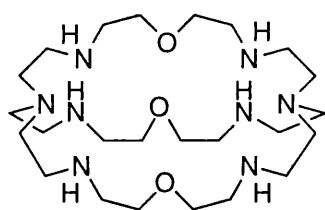
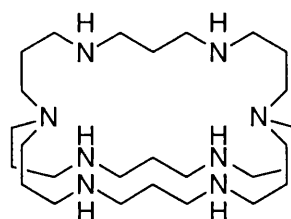
A general equation describing the contribution of hydrophobic interactions, the role of solvent and of added salts to association constants has also been put forward.<sup>87</sup>

Murakami and co-workers<sup>88</sup> have reported the synthesis and host-guest properties of a series of cyclophanes, of which receptor **65** is a representative example.



Hosts such as **65** have several interesting features which account for their complexation behaviour in aqueous solution. The molecules have deep and hydrophobic cavities which can incorporate hydrophobic guests of differing bulk through an induced-fit mechanism originating from the flexible character of the alkyl branches. In the host-guest complexation process, electrostatic and charge-transfer interactions operate in addition to the hydrophobic interactions so that the binding of guest molecules is enhanced. As long as electrostatic repulsion between guest molecules is not operative in the hydrophobic cavity, both 1:1 and 1:2 host-guest complexes can be formed. The cyclophane provides a hydrophobic cave which is highly apolar and acts to suppress the molecular motion of guests which means that such hosts may provide effective enzyme simulation models. In aqueous solution, host **65** strongly binds anionic and nonionic hydrophobic guests forming inclusion complexes with a 1:1 stoichiometry. Upon addition of a solution of the host to a solution containing the guest species, complexation immediately reached an equilibrium state. From NMR analysis the aspartate residues in the host were observed to undergo conformational changes in order to attain effective guest complexation. NMR data indicated that the guest molecule was incorporated into the three-dimensional cavity provided intramolecularly by the macrocyclic ring and the eight hydrocarbon chains.

Further derivatisation of polyammonium macrocycles can give rise to macrobicycles and macrotricycles which have a more rigorously defined three dimensional structure. Lehn has reported the synthesis and anion binding features of a series of macrobicyclic receptors exemplified by hosts **66** and **67**.

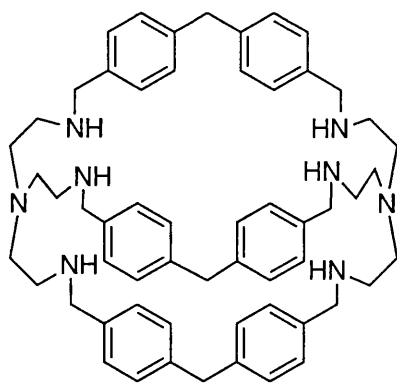
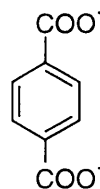
**66****67**

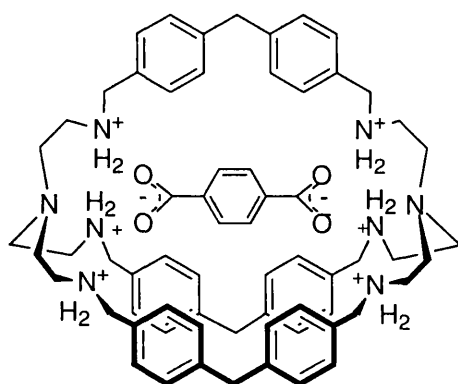
The hexaprotonated form of **66** complexes various monatomic and polyatomic anions.<sup>89,90</sup> This host has an ellipsoidal cavity and crystal structure analysis of its halide complexes reveal that the structure is distorted. The linear triatomic anion  $\text{N}_3^-$  has a shape and size complementarity to the host cavity and is bound inside by a pyramidal array of three hydrogen bonds to each terminal nitrogen. The binding constants reflect this greater efficacy for triatomic anions, being substantially higher for azide than for simple halides and other singly charged anions. Host **67** can accommodate eight protons and as a consequence stability constants are higher than those of host **66** (Table 1.2).<sup>91</sup>

	Stability Constants ( $\log K_s$ )	
	$\text{SO}_4^{2-}$	oxalate <sup>2-</sup>
<b>66</b>	4.90	4.95
<b>67</b>	7.45	6.55

**Table 1.2**

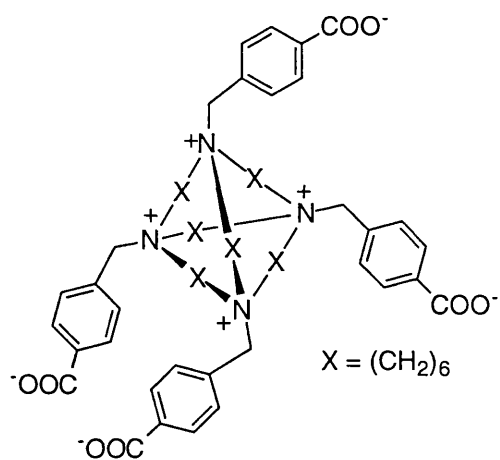
A crystal structure of related macrobicyclic **68** in its hexacationic form with the terephthalate dianion **69** shows linear recognition occurs to give supercomplex **70**.<sup>92</sup>

**68****69**

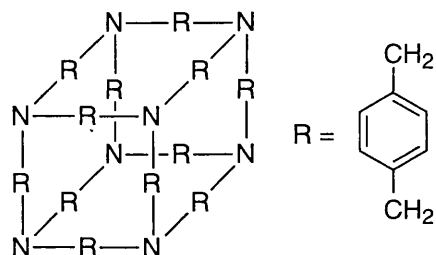


70

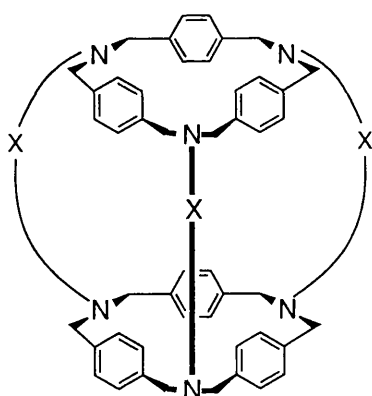
Schmidtchen and Worm<sup>93</sup> have reported the molecular recognition of halide anions in aqueous solution by the zwitterionic host molecule **71**. Iodide was found to be the most strongly bound due to its large size. A water soluble cubic macrocycle **72** has been described by Murakami *et al.*<sup>94</sup> which complexes only those guests small enough to pass through the paracyclophane ring into the inner cavity of the host. Murakami has also presented cage-type cyclophanes which have a helically twisted and cylindrical internal cavity.<sup>95</sup> Host **73** enforces guests such as **74** which can adopt one of two helical senses to assume specific chiral conformations when they are incorporated.



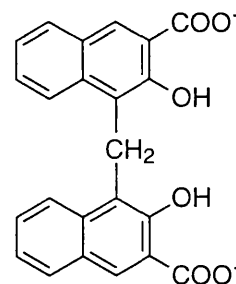
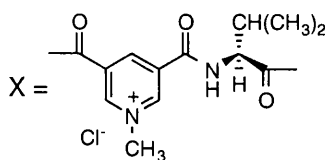
71



72



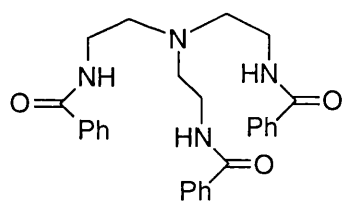
73



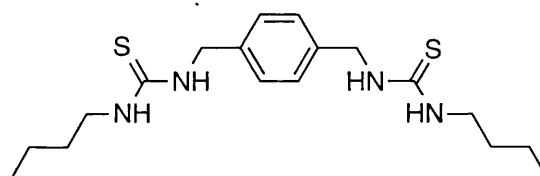
74

### 1.2.7 Non-Macrocyclic Anion Receptors

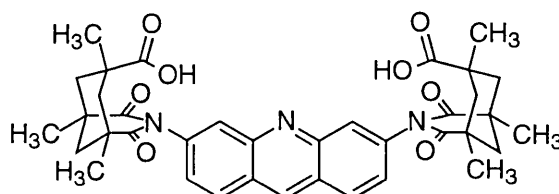
Though most anion receptors reported in the literature have been based on macrocyclic compounds, examples of non-macrocyclic anion receptors have been published. Reinhoudt *et al.*<sup>58</sup> have designed neutral ligands, such as **75**, based on diethylenetriamine and tris(aminoethyl)amine which show selective binding affinity towards anions exclusively through hydrogen-bonding. The simple molecular structure of the hosts offers the possibility of synthetic manipulation. Hamilton and co-workers<sup>96</sup> have synthesised receptor **76** which functions in highly competitive solvents such as dimethylsulfoxide through hydrogen bond donation. Rebek has reported the recognition of dicarboxylic acids by synthetic receptors such as **77**.<sup>36,97</sup> A sapphyrin dimer has been described by Sessler and co-workers which acts as an effective receptor for dicarboxylate anions.<sup>98</sup> Sapphyrins have also been employed in energy transfer systems using anion chelation.<sup>99</sup>



75



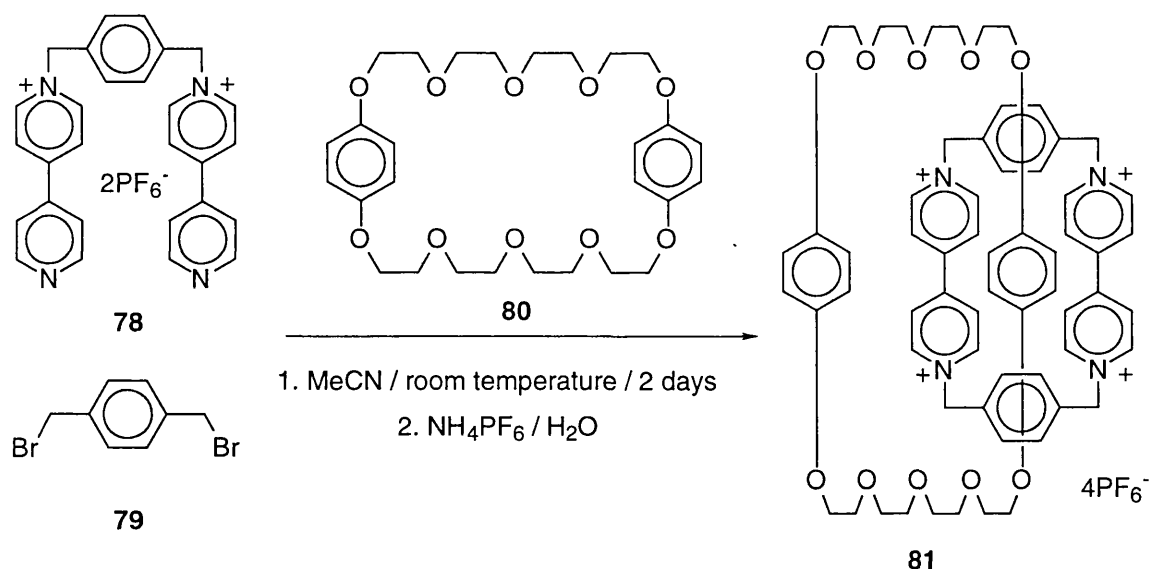
76



77

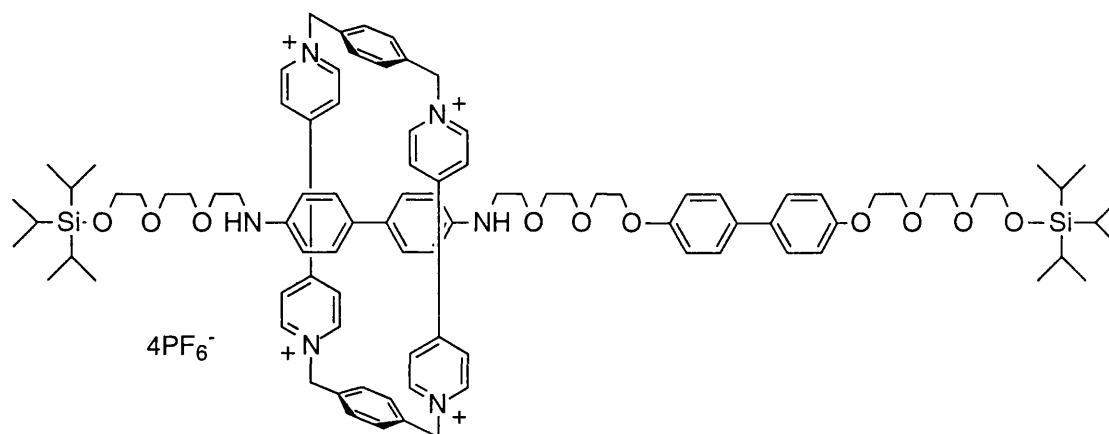
### 1.2.8 Template Synthesis

A more complex example of host-guest chemistry is illustrated by the self-assembly<sup>100</sup> of [n]catenanes and [n]rotaxanes described by Stoddart and co-workers. Electrostatic interactions play an important role in the formation of such species. The dominant noncovalent interactions involved are based on electrostatic and dispersive forces between molecular components containing  $\pi$ -electron rich and  $\pi$ -electron deficient aromatic rings. The usual host-guest relationship involves a rapid association between host and guest to form a 1:1 complex. In most cases complexation is reversible and dissociation of the complex into its molecular components occurs. If, however, the guest is trapped mechanically within or around the associated host, then dissociation is prevented and the process becomes an irreversible one. High binding constants have been observed between bisparaphenylene-34-crown-10 **80** with paraquat<sup>101</sup> and between cyclobis(paraquat-*p*-phenylene) with guests containing  $\pi$ -electron rich aromatic rings.<sup>102</sup> This suggested an efficient template-directed<sup>103</sup> self-assembly process in which **78** and **79** could be combined with **80** to give [2]catenane **81** in 70% yield.<sup>104</sup> Without the presence of polyether **80**, the macrocycle formed from **78** and **79** is only obtained in 12% yield. Two reciprocal sandwich interactions occur in the formation of [2]catenane **81**. A hydroquinone ether unit lies between two parallel bipyridinium units and a bipyridinium unit lies between two parallel hydroquinone ether units.



A variety of catenanes based on this methodology have been synthesised.<sup>105-111</sup> Expansion of the number of hydroquinone units in the macrocyclic polyether permits the self-assembly of more than one tetracationic cyclophane around the templates present in the macrocyclic polyether. Similarly, if more paraquat units are present in the cationic starting material, entrapment of more than one macrocyclic polyether may occur. Rotaxanes such as **82** have also been formed *via* similar methods to those employed in the synthesis of the catenanes.<sup>112-114</sup> Rotaxane **82**

consists of a tetracationic cyclophane threaded on a polyether chain containing biphenol and benzidine units as  $\pi$ -electron donors and terminated by stoppers in the form of tri-isopropylsilyl groups. The system forms the basis of a molecular 'switch' since the tetracationic cyclophane adopts a conformation dependent on the oxidation state of the benzidine station.<sup>113</sup>



82

### 1.3 Aim of Project

The previous sections have illustrated the importance of electrostatic interactions in supramolecular chemistry.<sup>57,115</sup> Our interest lay in using electrostatic interactions, both dispersive and attractive, to organise molecular shape and, as a consequence, molecular interactions. In many reports of molecular recognition, several different interactions have operated in parallel, for example hydrogen bonding and  $\pi$ -stacking.<sup>92</sup> Most studies have concentrated on using nonaqueous solvents. Where water has been utilised as the solvent, host molecules containing hydrophobic cavities have generally been employed. We were interested to examine electrostatic effects in aqueous solution with host molecules that did not contain significant hydrophobic regions. To examine these effects we intended to synthesise relatively simple receptors containing a number of formal positive charges through the use of quaternary ammonium centres and investigate their complexation with simple organic anions. Using these model systems, in which electrostatic interactions were the dominating force, we hoped to explore the importance of electrostatic interactions in the complexation of host and guest species employing a variety of different experimental techniques.

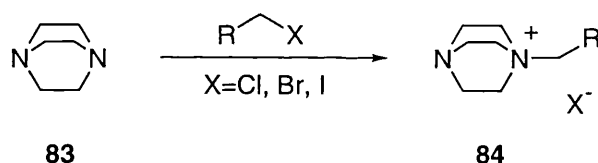


## 2 Synthesis of Polycationic Compounds

### 2.1 Introduction

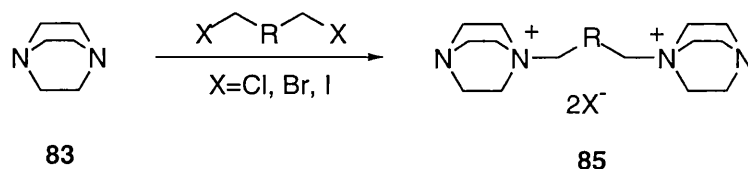
The majority of studies into molecular recognition reported have taken place in non-aqueous solution and involved structurally complex molecules, many of which have been conformationally rigid. We wished to synthesise structurally simple, conformationally flexible molecules which were water soluble, to allow us to study their behaviour in aqueous media. Such an environment might better reflect the properties of a physiological system than a non-aqueous system. We also wished to maximise the effect of electronic interaction in the molecule and allow some stability between different conformations, and thus we chose to explore the properties of symmetrically trisubstituted benzenes containing charged systems.

To introduce positive charges into our compounds we elected initially to use the commercially available base DABCO (1,4-diazabicyclo[2.2.2]octane, **83**), which has been found to react readily with alkyl halides to give compounds in which nitrogen carries a positive charge<sup>116,117</sup> (Scheme 2.1).



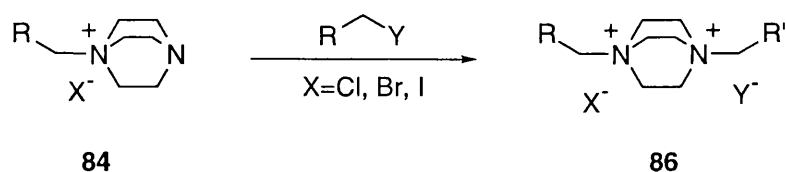
Scheme 2.1

In compounds containing more than one halide group, DABCO can react at more than one site to give multiply charged compounds<sup>118</sup> (Scheme 2.2).



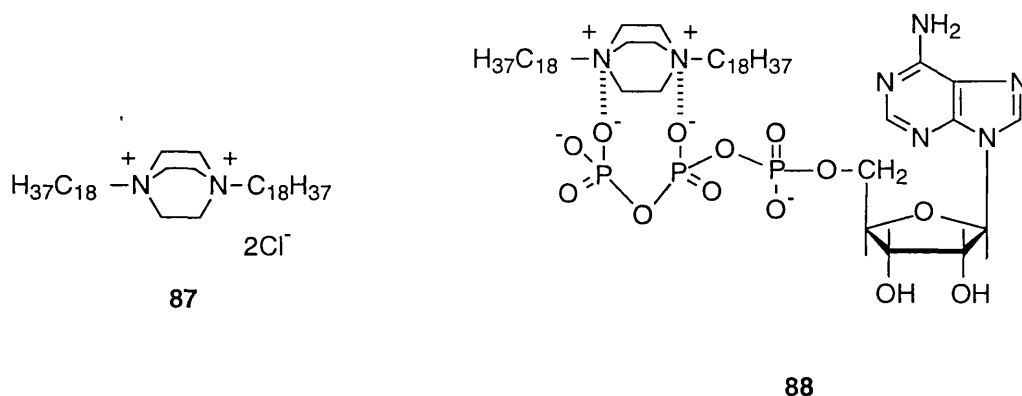
Scheme 2.2

The lone pairs of the two nitrogen atoms in DABCO have been found to behave relatively independently<sup>119</sup> (the pK<sub>a</sub> values for mono- and di-protonation being 8.8 and 3.0 respectively), meaning DABCO can react to give products in which both nitrogen atoms are positively charged (Scheme 2.3).<sup>120</sup>

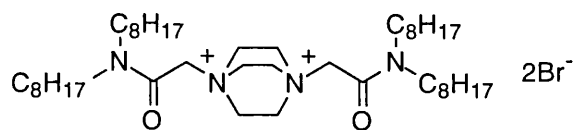


Scheme 2.3

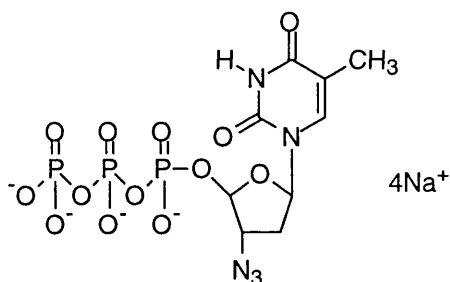
Tabushi *et al.*<sup>121-123</sup> described the use of DABCO derivatives such as **87** to selectively bind nucleoside phosphates and transport them across a liquid membrane such as chloroform. They reported remarkable selectivity toward the binding of tri- or di-anionic adenosine diphosphate compared with that of monoanionic adenosine monophosphate and attributed this selectivity to the formation of complexes such as **88**.



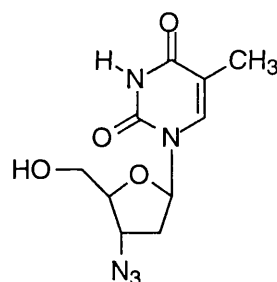
Further work by Diederich and co-workers<sup>124</sup> used DABCO derivatives as carriers for nucleotide 5'-triphosphates, as an approach to AIDS therapy. They postulated that the complexes formed between DABCO derivatives such as **89** and phosphates such as 3'-azido-2'-deoxythymidine 5'-triphosphate (AZTTP, **90**) would more easily penetrate across cell membranes than the corresponding nucleosides **91**.



89

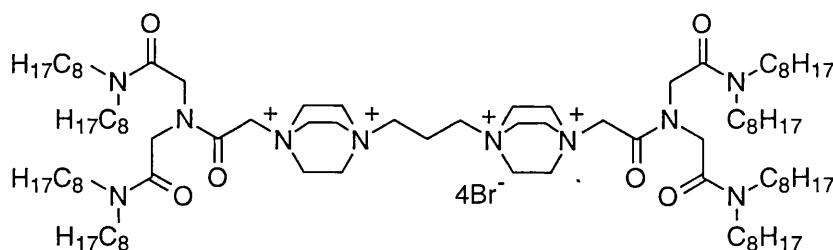


90



91

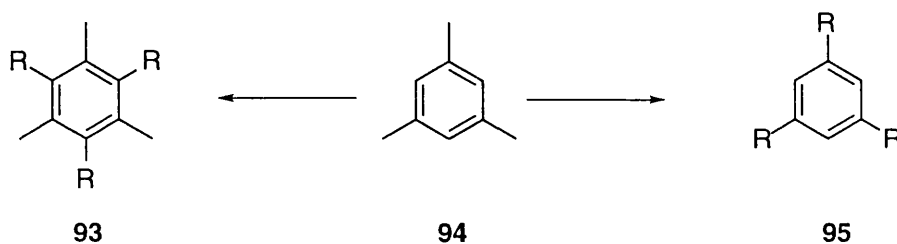
Their results showed poor nucleotide selectivity which they attributed to the fact that the complexes formed had a 2:1 stoichiometry. To improve selectivity they subsequently designed compounds such as **92** which they believed would form 1:1 complexes and act as more efficient and selective carriers.<sup>125</sup>



92

They found that the tetraquatery DABCO derivative acted as an efficient carrier of a variety of 5'-triphosphates across a dichloromethane liquid membrane, forming complexes with a 1:1 stoichiometry. However, such compounds were found not to mediate the specific transport of nucleotide 5'-triphosphates across liposomes but, above a certain concentration, acted as detergents breaking the liposomal interior.

We chose to explore compounds based on a mesitylene (1,3,5-trimethylbenzene, **94**) core, since mesitylene can be functionalised to give either tri- or hexasubstituted benzenes (Scheme 2.4).

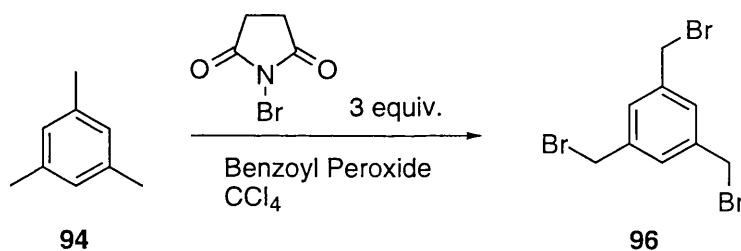


Scheme 2.4

This would allow us to directly compare compounds synthesised from the trisubstituted benzenes (**95**) with those synthesised from hexasubstituted benzenes (**93**). It was anticipated that the presence of three methyl substituents on the aromatic ring in the hexasubstituted benzenes would restrict conformational mobility relative to that in the corresponding trisubstituted compounds.

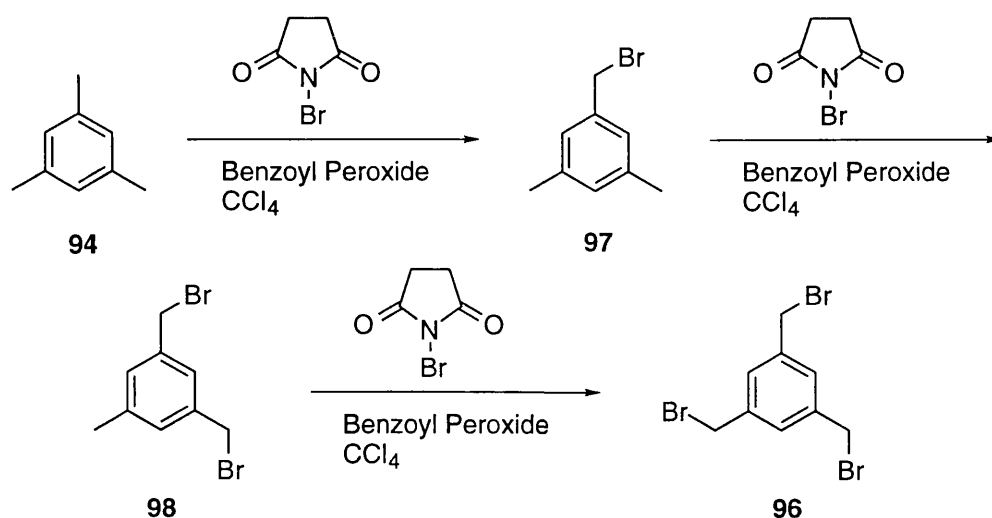
## 2.2 Routes to 1,3,5-Tris(bromomethyl)benzene

Two routes to this compound have been reported. The route reported by Vögtle *et al.*<sup>126</sup> involves the bromination of mesitylene with N-bromosuccinimide (Scheme 2.5).



Scheme 2.5

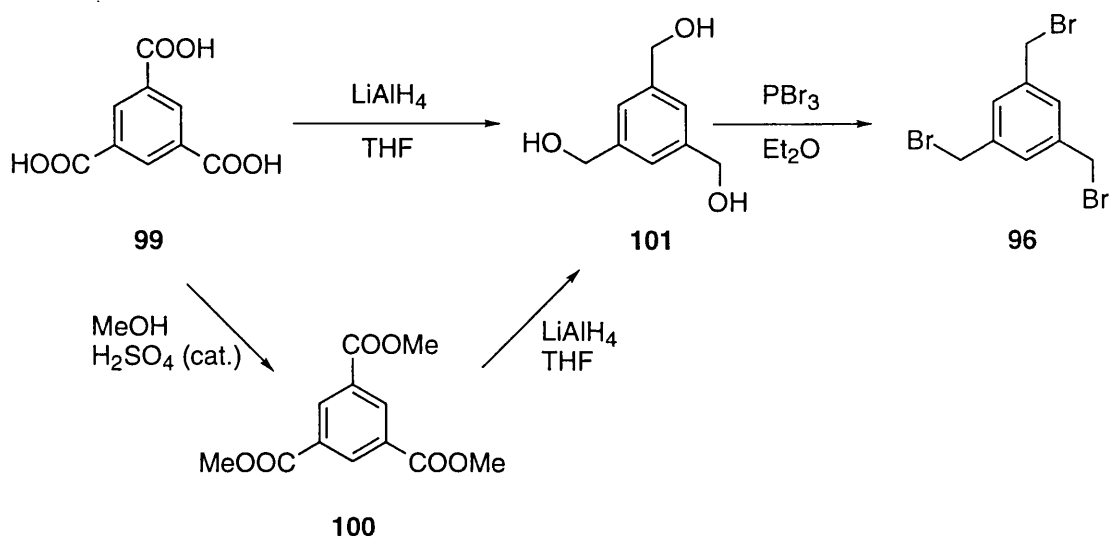
Vögtle reports an overall yield of 23% for this procedure but our attempts to carry out this reaction gave a complex mixture of products which were not easily separable, either by recrystallisation or column chromatography. For this reason we tried an alternative route in which mesitylene was sequentially brominated, with purification at each stage (Scheme 2.6).



Scheme 2.6

Our investigations into this route revealed that the first and second brominations proceed smoothly, but the third bromination leads to the formation of several products in a moderate to low yield. Presumably this reaction proceeds *via* a radical mechanism and in the reaction to give the tribromide, four methylene protons are available for abstraction versus three methyl protons. Again, these products are not easily separable, either by recrystallisation or column chromatography, and the tribromide cannot be isolated in any significant yield. For these reasons we elected not to use this route.

The alternative method reported involves a totally different strategy (Scheme 2.7) and has been reported by Cochrane *et al.*<sup>127</sup> This is a modified method based on an earlier procedure published by Hesse and Rämmish.<sup>128</sup> Here, benzene-1,3,5-tricarboxylic acid is first converted to the corresponding trimethyl ester using the method of Fuson and McKeever.<sup>129</sup> This ester is reduced with lithium aluminium hydride to the triol, which is subsequently brominated using phosphorus tribromide to give the desired tribromide **96** in an overall yield of 40%.

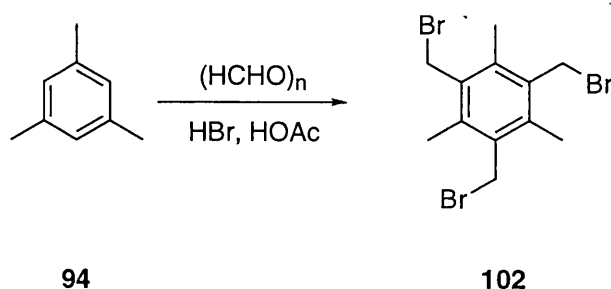


Scheme 2.7

Direct reduction of the tricarboxylic acid results in a poorer overall yield. Cochrane's original paper uses diethyl ether as the solvent for the reduction of the triester but we found improved yields were obtained with tetrahydrofuran.

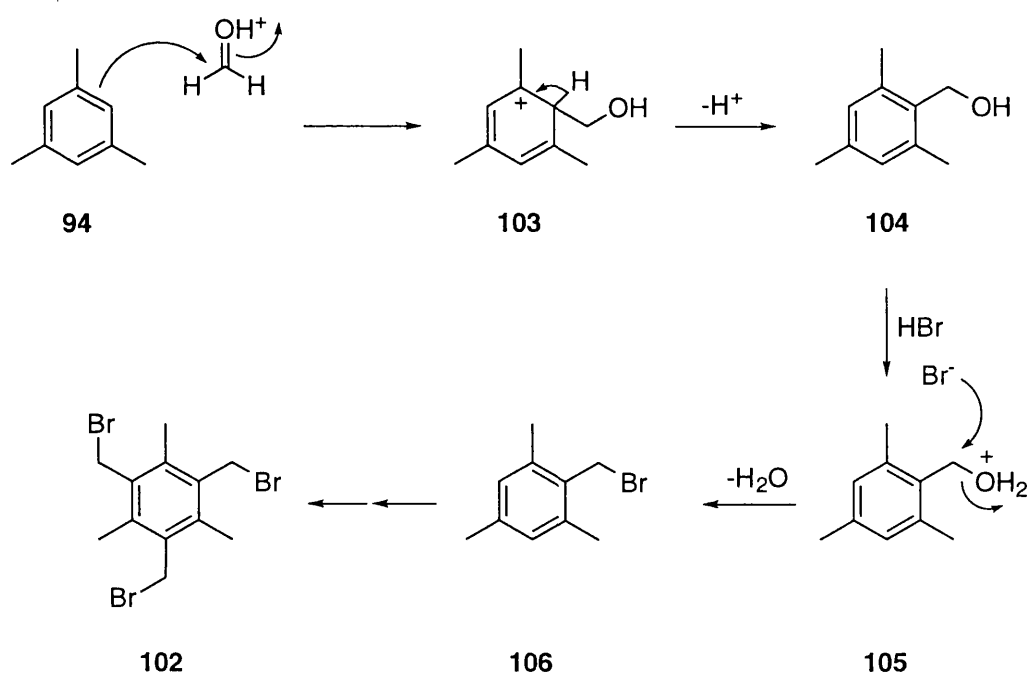
### 2.3 Synthesis of 2,4,6-Tris(bromomethyl)mesitylene

In 1993, van der Made<sup>130</sup> reported a convenient procedure for the bromomethylation of aromatic compounds in which a 30 wt % solution of HBr in acetic acid is added to a mixture of acetic acid, paraformaldehyde, and the aromatic compound. Using mesitylene as a starting material this method could be used to give 2,4,6-tris(bromomethyl)mesitylene in 86% yield (Scheme 2.8).



Scheme 2.8

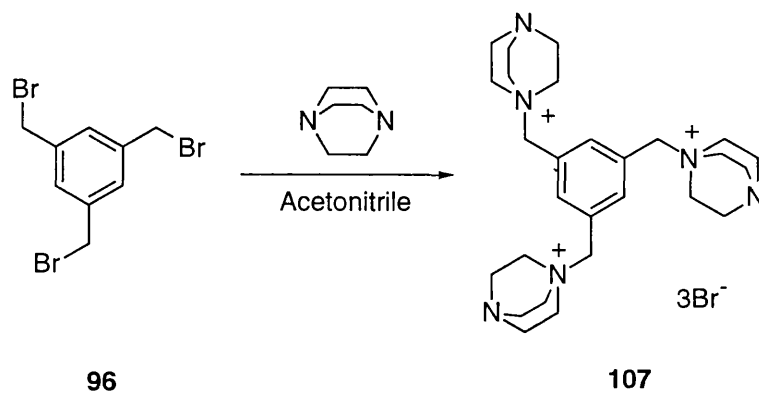
A proposed mechanism for this reaction is outlined in Scheme 2.9. The reaction proceeds *via* the electrophilic attack on mesitylene by protonated formaldehyde, followed by substitution of the hydroxyl group thus formed by bromide to give the bromomethyl-substituted compound 106. Two further substitutions occur *via* the same mechanism to give tribromide 102.



Scheme 2.9

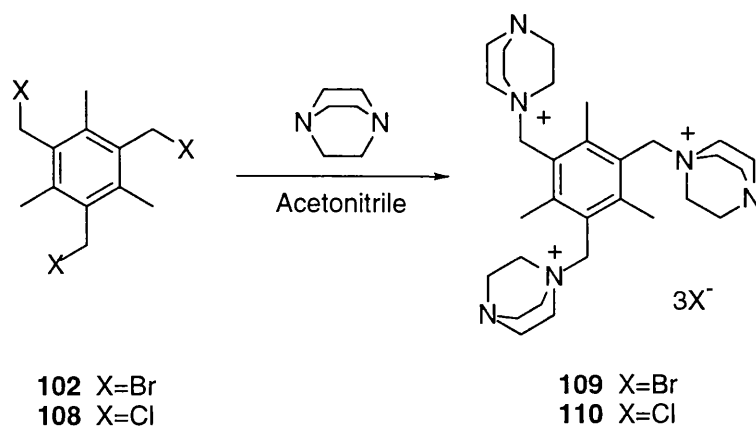
## 2.4 DABCO-based Trications

1,3,5-tris(bromomethyl)benzene **96** was stirred with DABCO in acetonitrile for 24 hours, during which time a precipitate formed. The precipitate was removed by filtration and washed with diethyl ether and acetonitrile, giving compound **107** (Scheme 2.10) in 95% yield as a white solid.



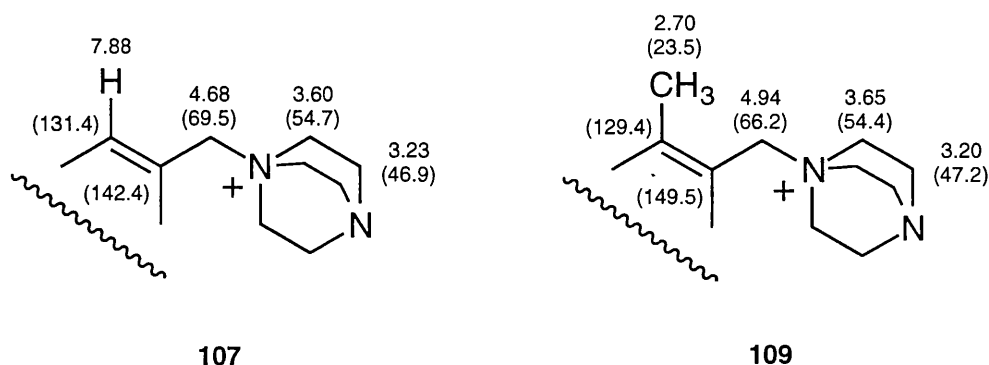
Scheme 2.10

2,4,5-Tris(chloromethyl)mesitylene (commercial sample, **108**) and 2,4,6-tris(bromomethyl)mesitylene **102** were similarly treated with DABCO to give compounds **109** and **110** (Scheme 2.11) as white solids, in 94% and 88% yields respectively.



Scheme 2.11

All of these compounds were found to be water soluble and hygroscopic. Compound **107** was particularly hygroscopic and had to be filtered under an atmosphere of dry nitrogen gas. Details of the  $^1\text{H}$  and  $^{13}\text{C}$  NMR spectra in deuterium oxide and their assignment for **107** and **109** are outlined in Figure 2.1. The methylene groups of the DABCO moieties gave rise to two triplets separated by 0.46 ppm, each integrating for 18 protons and broadened due to their proximity to the charged and uncharged nitrogen atoms. This led us to the conclusion that rotation of DABCO units was rapid on the NMR timescale, since if this were not the case we would have expected to see a more complex spectrum.

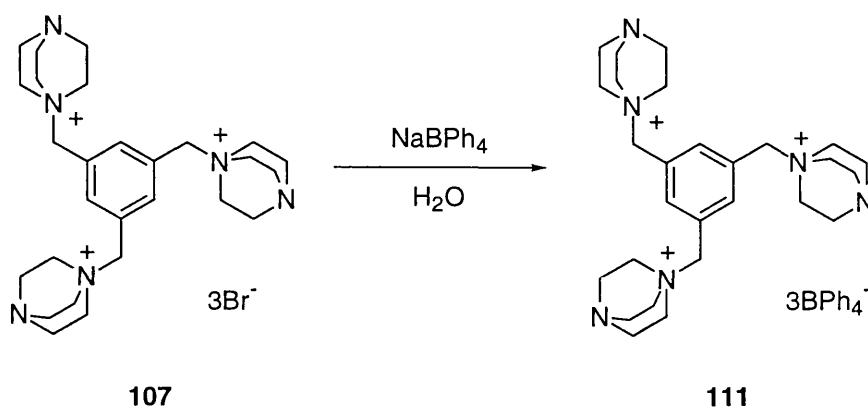
Figure 2.1 -  $^1\text{H}$  and ( $^{13}\text{C}$ ) Chemical Shifts in  $\delta$ 

The fast atom bombardment (FAB) mass spectrum of **109** showed a 1:2:1 triplet around 655, the correct isotope pattern for two bromine atoms and corresponding to the relative molecular mass minus one bromide anion ( $[\text{M}-\text{Br}]^+$ ), analogous peaks appearing in the spectra of the other tricationic compounds. Attempts were made to purify these compounds by column chromatography but proved unsuccessful as no suitable solvent system could be found. The lack of solubility in solvents other than water shown by the tricationic bromide salts precluded recrystallisation. Microanalysis of the materials revealed them to be gaining weight slowly due to



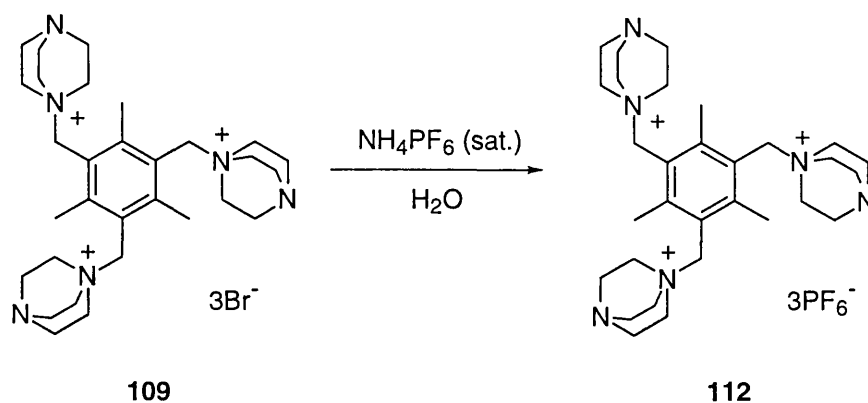
their hygroscopic nature. For these reasons an alternative counter anion was sought in order to allow an absolute measure of purity to be made.

An aqueous solution of the bromide salt **107** was converted into its tetraphenylborate salt **111** by treatment with an aqueous solution of sodium tetraphenylborate (Scheme 2.12).



Scheme 2.12

This salt was soluble in acetone and acetonitrile and insoluble in water. The  $^1\text{H}$  NMR spectrum was consistent with its structure, although it was dominated by peaks corresponding to the tetraphenylborate anion. Similar mass peaks to those observed for the halide salts appeared in the FAB spectrum. However, the dominance of the protons of the tetraphenylborate anion in the NMR spectrum led to the investigation of an alternative counter anion, hexafluorophosphate. Compound **109** in aqueous solution was converted into its hexafluorophosphate salt **112** by the addition of a saturated aqueous solution of ammonium hexafluorophosphate (Scheme 2.13).



Scheme 2.13

Compound **107** was similarly converted into its hexafluorophosphate salt **113**. The hexafluorophosphates were also soluble in acetone and acetonitrile and could be recrystallised from a mixture of acetonitrile and methanol, allowing the compounds to be completely purified and fully characterised. Recrystallisation using a mixture of acetonitrile and methanol gave colourless crystals after prolonged standing, which upon removal from the mother liquor became opaque due to the evaporation of solvent from within the crystal structure.  $^1\text{H}$  and  $^{13}\text{C}$  NMR chemical shifts in  $d_6$ -acetone for **112** and **113** are outlined in Figure 2.2. Even after prolonged drying, a significant water peak was observed in the spectra and the recrystallised materials were found to gain weight slowly during microanalysis.

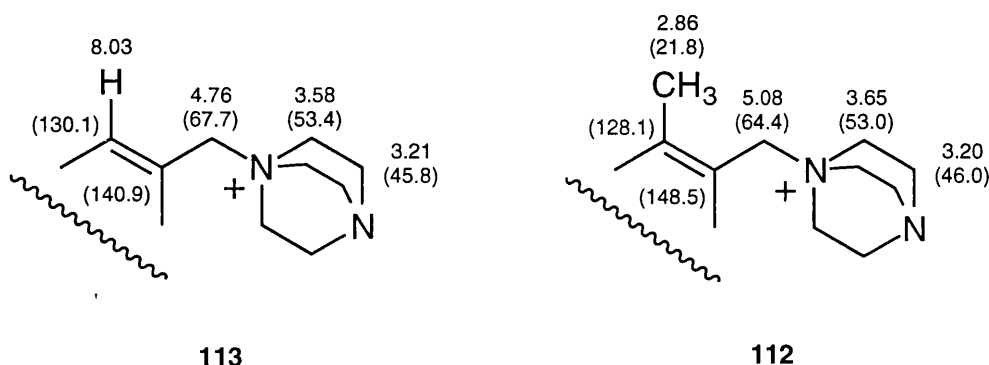


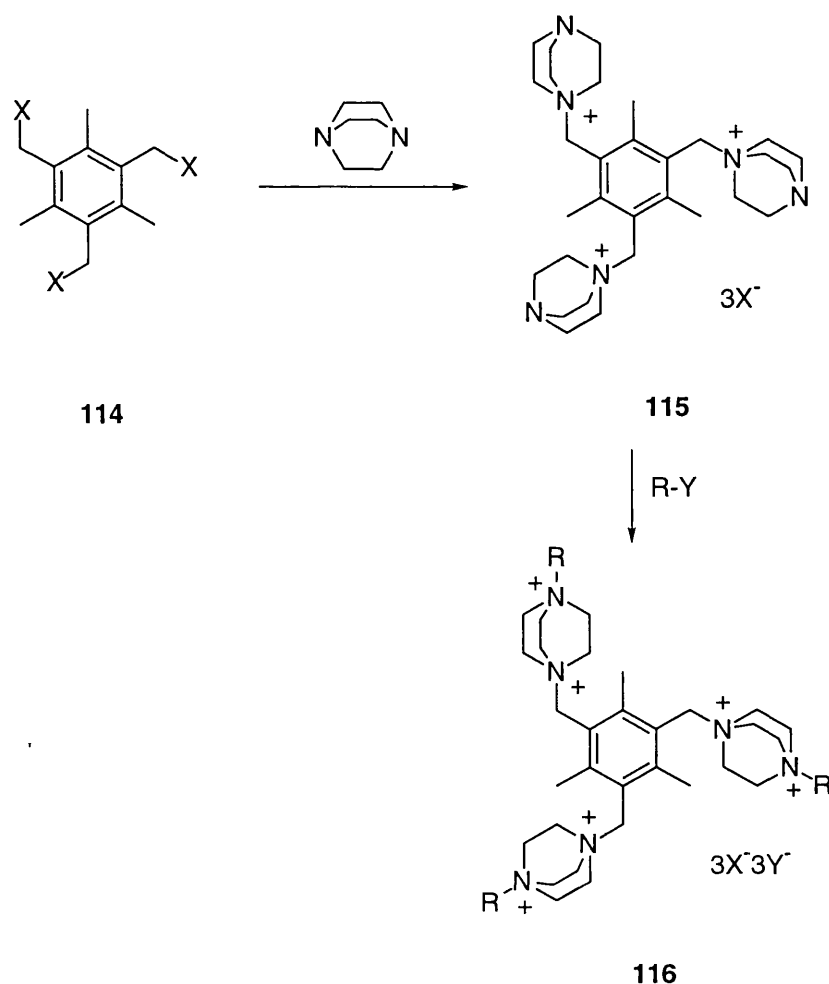
Figure 2.2 -  $^1\text{H}$  and ( $^{13}\text{C}$ ) Chemical Shifts in  $\delta$

The FAB mass spectra showed peaks corresponding to the loss of one hexafluorophosphate counter-anion. Compound **112** also showed a peak corresponding to the loss of two hexafluorophosphate anions. This peak appeared in the spectrum at 320, half the mass of the ion (640), which has two positive charges. Infra-red spectra of the materials showed characteristic peaks at *ca.* 830-840  $\text{cm}^{-1}$  corresponding to the hexafluorophosphate anion.

## 2.5 DABCO-based Hexacations

### 2.5.1 Divergent Strategy

Two possible strategies were considered in the synthesis of hexacationic compounds. The first of these, the divergent strategy, is outlined in Scheme 2.14.



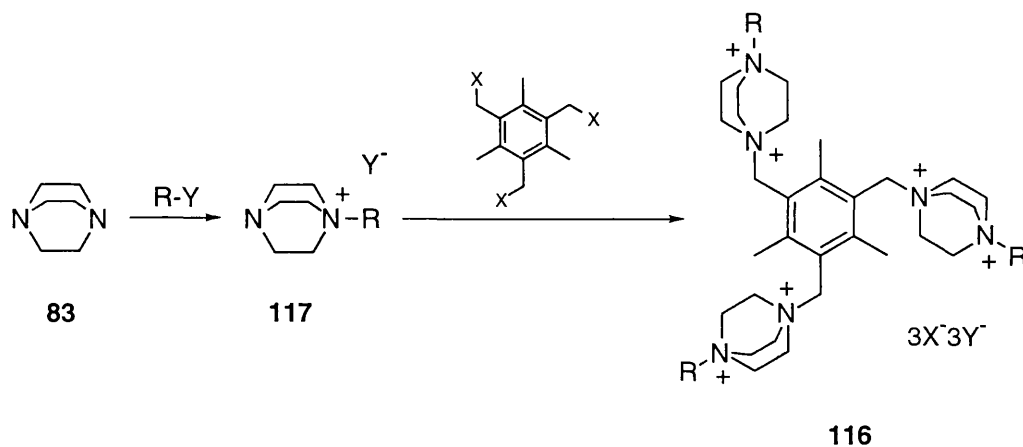
Scheme 2.14

This route suffers from several disadvantages. Incomplete reaction may occur leading to a mixture of tetra-, penta-, and hexa-cationic products, as well as any unreacted tricationic starting material, and these compounds cannot be easily separated. The halide salts are not readily soluble in organic solvents and reactions must be carried out in either water or dimethylsulfoxide, and water does not readily dissolve alkyl halides. If either the tetraphenylborate or hexafluorophosphate salts of the trication are used, any products formed will contain a mixture of counteranions which are difficult to purify and characterise.

Our attempts to alkylate the uncharged nitrogen atoms of the tricationic materials were unsuccessful, either incomplete alkylation occurring or, under more vigorous conditions, decomposition. The bromide salt **109** could be dissolved in dimethylsulfoxide but attempts to alkylate it with either bromo- or iodo-alkanes were unsuccessful. It was hoped that the hexafluorophosphate salt **112**, which is soluble in both acetone and acetonitrile, would react successfully to give hexacationic products. However, no significant reaction occurred.

### 2.5.2 Convergent Strategy

An alternative, convergent, route to hexacationic materials is outlined in Scheme 2.15.

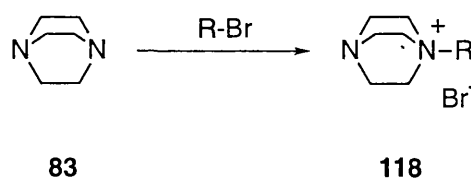


Scheme 2.15

We anticipated that this route would overcome the difficulties associated with the divergent route outlined above. In order to study this route, a series of monocation intermediates were synthesised.

### 2.5.3 Monocationic DABCO intermediates

The synthesis of monocationic DABCO derivatives has been described before<sup>120,131</sup> and the synthetic route is outlined in Scheme 2.16.



Scheme 2.16

The alkyl bromide was stirred with an excess of DABCO at room temperature to give, after workup, the monocationic derivatives as white powders in high yields (Table 2.1).

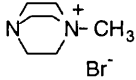
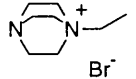
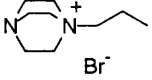
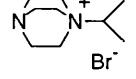
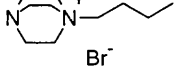
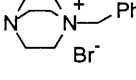
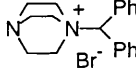
Compound	Solvent	m.p.	Yield
 <b>119</b>	Acetonitrile & Diethyl Ether	253-255 °C (dec.)	90%
 <b>120</b>	Acetonitrile	190-192 °C	83%
 <b>121</b>	Acetonitrile	144-146 °C	82%
 <b>122</b>	Acetonitrile	231-233 °C	98%
 <b>123</b>	Acetonitrile	128-130 °C	82%
 <b>124</b>	Acetonitrile	222-225 °C (dec.)	99%
 <b>125</b>	Acetonitrile	200-202 °C (dec.)	97%

Table 2.1

These compounds were generally insoluble in organic solvents, although **125** was found to be soluble in chloroform and dichloromethane. The mass spectra of the monocations showed a highest mass peak corresponding to  $[2M-Br]^+$ , as well as the expected mass peak corresponding to  $[M-Br]^+$  (**122**, Figure 2.3).

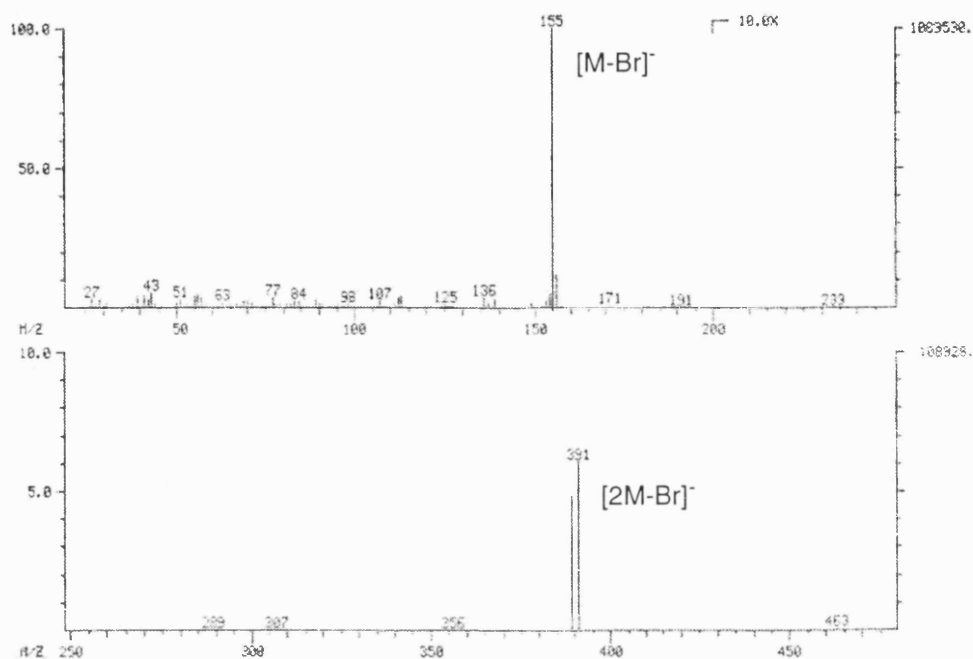


Figure 2.3

The observation of a  $[2M-Br]^+$  peak is consistent with a large amount of sample being present in the plasma matrix and the spectra being run at a relatively high pressure. The NMR spectra of the materials were consistent with their structure, with broadening of the signals due to protons adjacent to nitrogen atoms. Interestingly, fine coupling between the methyl group of **120** and the nuclear spin of the positively charged nitrogen atom was observed in the  $^1H$  NMR spectrum (Figure 2.4).

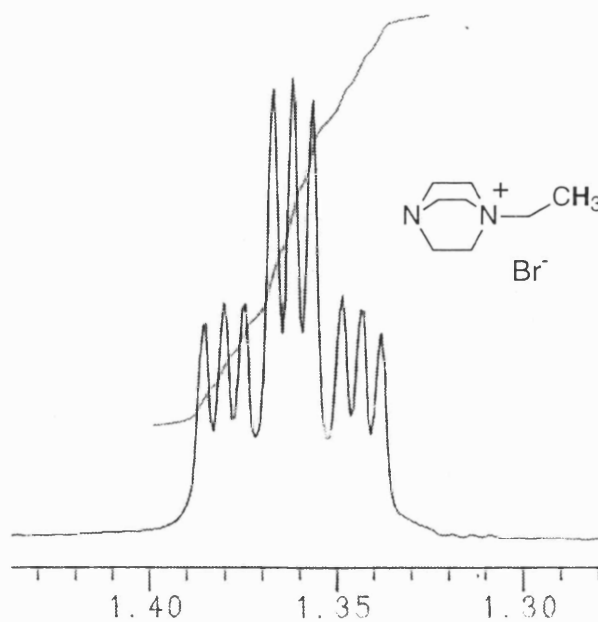
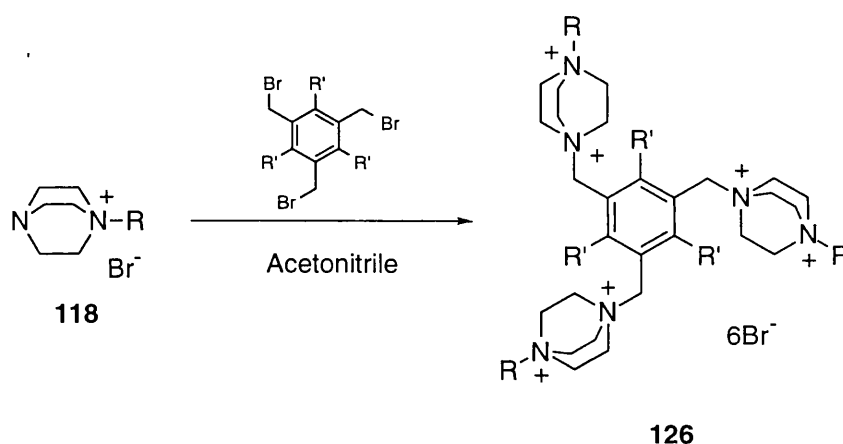


Figure 2.4

This feature was also noted in the spectrum of **122**. In the case of compound **121** the methyl group signal appears as a triplet due to coupling with the protons of the adjacent methylene group, but closer inspection reveals that each of the three lines of the triplet is further split into three signals. Each of these is of equal intensity with a coupling constant of 2.0 Hz and is due to interaction with the nitrogen nucleus, which has a nuclear spin of 1. In monocations with longer alkyl chains this splitting could no longer be resolved.

#### 2.5.4 Synthesis of DABCO-based Hexacations

A three- to four-fold excess of the monocationic intermediates discussed in the previous section, were treated with either 1,3,5-tris(bromomethyl)benzene or 2,4,6-tris(bromomethyl)mesitylene in acetonitrile to give a series of compounds containing six positive charges (**126**, Scheme 2.17) as white solids.



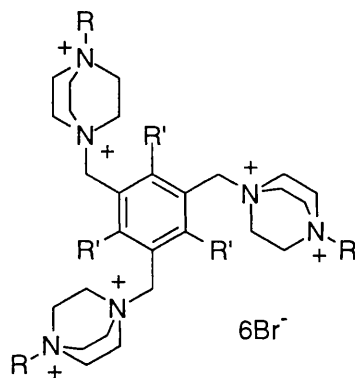
Scheme 2.17

Monitoring reactions such as these is difficult since any positively charged compounds formed tend not to move on a thin layer chromatography plate. Even the most polar solvent mixtures were found not to separate mixtures of polycations. A wide variety of solvent mixtures was tried with reverse-phase thin layer plates but no satisfactory resolution of products was observed. The colourless solution formed upon the initial combination of the reagents became opaque after stirring for 5-15 minutes, followed by gradual precipitation of the product. Reactions were generally left stirring for 24-72 hours in order to minimise the possibility of incomplete reaction occurring. The new family of compounds thus formed are illustrated in Table 2.2.

The hexacationic bromides were found to be generally soluble in water but increasing the length of the alkyl chain of the DABCO derivative led to a decrease in solubility. Indeed, the compounds obtained from the reactions of benzyl (**124**) and dibenzyl (**125**) substituted DABCO

monocations with either of the tribromide cores were insoluble in all solvents investigated precluding further characterisation.

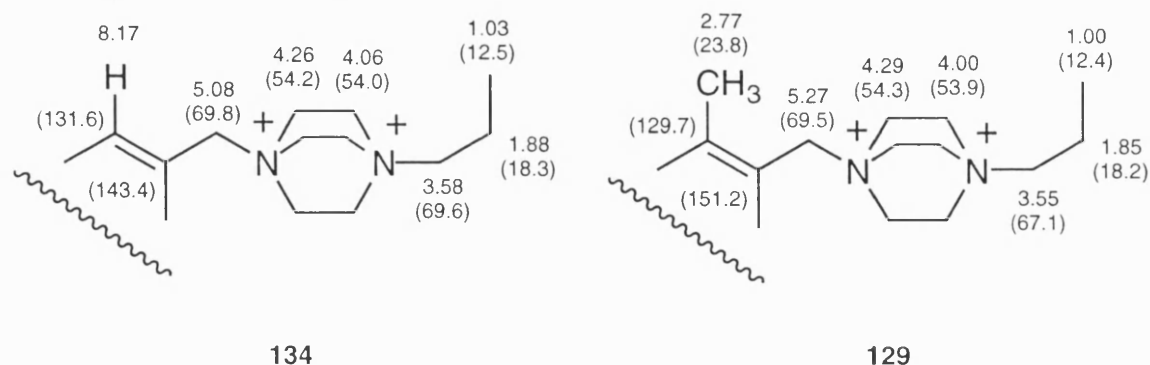
The  $^1\text{H}$  NMR and  $^{13}\text{C}$  NMR spectra of the hexacations were consistent with the structures. Two typical examples of spectra recorded in deuterium oxide and their assignments are outlined in Figure 2.5. Signals in the  $^1\text{H}$  NMR spectra corresponding to protons adjacent to the quaternised nitrogen atoms were considerably broadened, and in many cases the triplets expected for the bridging methylene groups of the DABCO moiety were observed simply as broad singlets. No evidence of conformational restriction was observed in any of the spectra, indicating rapid reorientation of the DABCO 'arms' in solution.



Compound	R'	R	Yield	m.p.
127	Me	Me	96%	234-236 °C (dec.)
128	Me	Et	95%	222-225 °C (dec.)
129	Me	1-Pr	90%	205-207 °C (dec.)
130	Me	2-Pr	81%	220-223 °C (dec.)
131	Me	1-Bu	90%	203-206 °C (dec.)
132	H	Me	81%	228-231 °C (dec.)
133	H	Et	85%	232-235 °C (dec.)
134	H	1-Pr	78%	235-238 °C (dec.)
135	H	2-Pr	78%	242-245 °C (dec.)
136	H	1-Bu	72%	243-246 °C (dec.)

Table 2.2



Figure 2.5 -  $^1\text{H}$  and ( $^{13}\text{C}$ ) Chemical Shifts in  $\delta$ 

The FAB mass spectra of the hexacationic compounds showed peaks corresponding to the molecular ion minus one bromide anion ( $[\text{M}-\text{Br}]^+$ ) with the appropriate isotope pattern (Figure 2.6, 130). Peaks also appeared corresponding to the loss of two bromide anions, but peaks corresponding to the loss of three or more bromide anions were not observed in the spectra. No significant bands were observed in the infra-red spectra of the bromide salts.

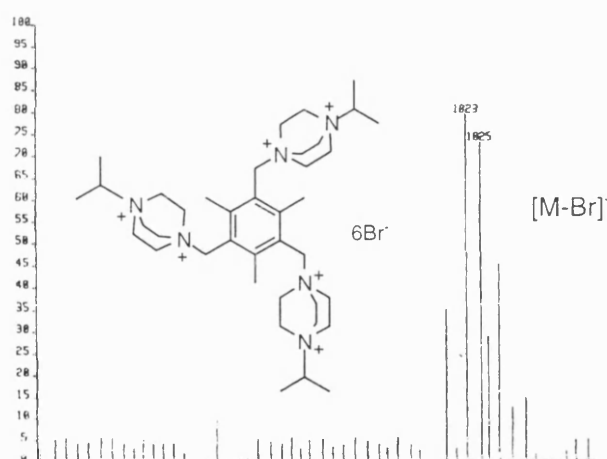
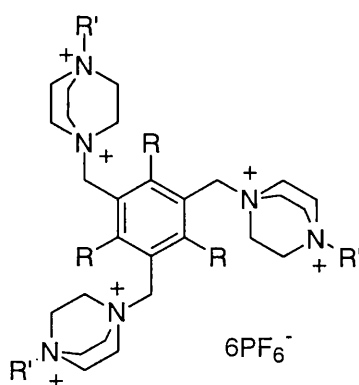


Figure 2.6

The hexacationic bromide salts were converted to their hexafluorophosphate salts by the addition of a saturated aqueous solution of ammonium hexafluorophosphate. The yields and melting points for these compounds are shown in Table 2.3.

These materials were similar in nature to the tricationic hexafluorophosphate salts discussed earlier, being soluble in acetonitrile and acetone. Recrystallisation of the materials could be achieved relatively easily in the case of the compounds based on 1,3,5-tris(bromomethyl)mesitylene. Dissolution in a small quantity of acetonitrile followed by addition of methanol and prolonged standing yielded colourless crystals which became opaque on removal

from the mother liquor. In the case of the materials based on 2,4,6-tris(bromomethyl)mesitylene, an alternative method was used whereby an aqueous solution containing an approximately twelve molar excess of ammonium hexafluorophosphate (based on hexacation) was added to an aqueous solution of the hexacation bromide salt. Prolonged standing yielded colourless crystalline materials, although again removal of the crystals from the solvent led to their becoming white and opaque. Microanalysis of the hexacations showed that they gained weight slowly, indicating they were hygroscopic. The IR spectra showed the characteristic stretch corresponding to the hexafluorophosphate anion at ca.  $840\text{ cm}^{-1}$ .  $^1\text{H}$  and  $^{13}\text{C}$  NMR spectra were consistent with the structure, but a significant water peak was observed in the proton spectra even after prolonged drying. No conformational isomerism was detected. The peaks corresponding to the bridging methylene groups of DABCO were observed, as expected to be further downfield and closer together than in the tricationic materials since both nitrogen atoms had been quaternised.



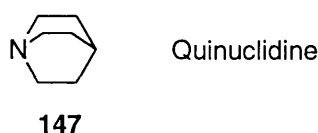
Product	R	R'	Yield	Melting Point
137	Me	Me	84%	236-239 °C (dec.)
138	Me	Et	84%	247-249 °C (dec.)
139	Me	1-Pr	77%	224-226 °C (dec.)
140	Me	2-Pr	87%	251-253 °C (dec.)
141	Me	1-Bu	81%	243-245 °C (dec.)
142	H	Me	93%	261-263 °C (dec.)
143	H	Et	90%	282-284 °C (dec.)
144	H	1-Pr	73%	261-263 °C (dec.)
145	H	2-Pr	87%	227-229 °C (dec.)
146	H	1-Bu	71%	272-274 °C (dec.)

Table 2.3

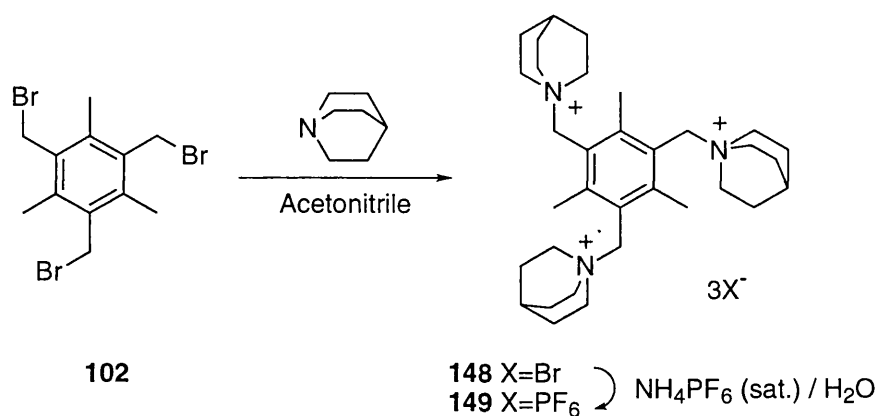
FAB mass spectroscopy revealed highest mass peaks corresponding to the loss of one counter-anion ( $[M-PF_6]^+$ ), and mass peaks corresponding to the loss of two counter-anions ( $[M-2PF_6]^+$  and  $[M-2PF_6]^{2+}$ ).

## 2.6 Other Trications

During the course of our investigations into the behaviour of the DABCO-based trications discussed previously with various organic carboxylates, we became interested in the significance of the uncharged nitrogen atoms of such species in any binding. For this reason we synthesised trications based on quinuclidine (**147**), which differs from DABCO only in that a nitrogen atom is replaced by a carbon unit.



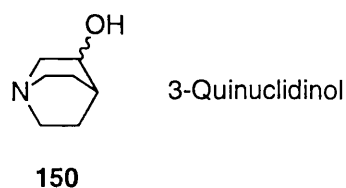
Quinuclidine was treated with 2,4,6-tris(bromomethyl)mesitylene in acetonitrile to give trication **148** as a white powder in 92% yield (Scheme 2.18). This compound showed analogous behaviour to the related compound **109** based on DABCO.



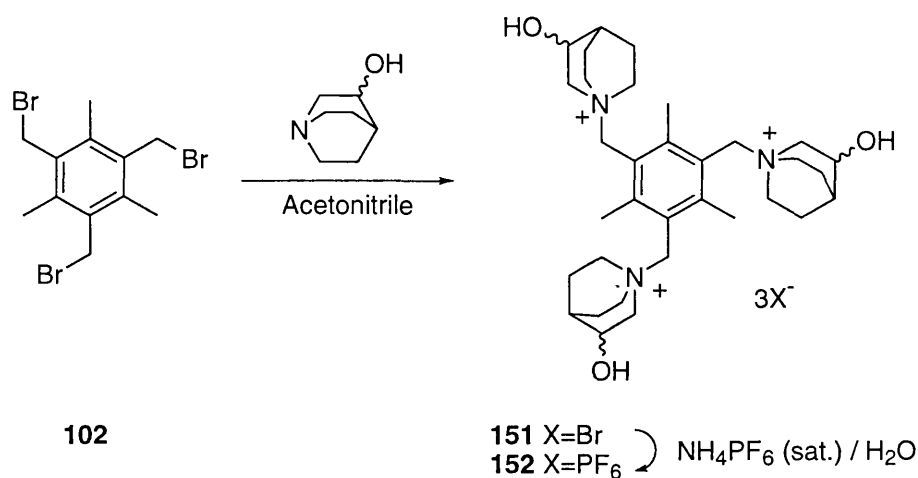
**Scheme 2.18**

The  $^1H$  NMR spectrum was more complicated than that of **109** due to the appearance of a signal corresponding to the methyne proton, and the coupling between this proton and its neighbours. The  $^{13}C$  NMR spectrum showed the anticipated seven signals and the FAB mass spectrum showed a highest mass peak corresponding to the loss of one bromide anion. Addition of a saturated aqueous solution of ammonium hexafluorophosphate to this material gave the hexafluorophosphate salt **149** which could be recrystallised from methanol and acetonitrile and fully characterised.

Further functionalisation of the DABCO-based trications discussed earlier involves the formation of hexacationic materials, as the uncharged nitrogen atoms offer the only reactive centres. We became interested in using 3-quinuclidinol (**150**) as a route to more functionalised tricationic materials since we believed that their use might overcome some of the problems of solubility associated with the hexacations discussed earlier.



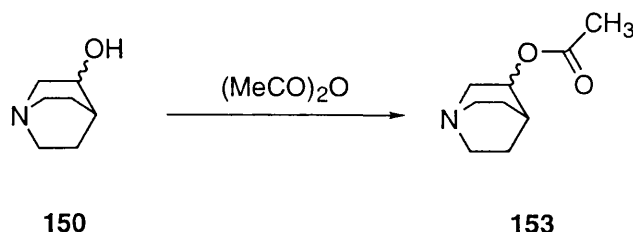
Racemic 3-quinuclidinol was treated with 2,4,6-tris(bromomethyl)mesitylene in acetonitrile to give trication **151** as a white solid in 98% yield (Scheme 2.19). As with the other tricationic materials synthesised, the product was seen precipitating out of solution during the course of the reaction. Pouring the reaction mixture into diethyl ether gave the product as a flocculent white precipitate which was removed by filtration and dried under vacuum.



**Scheme 2.19**

The <sup>1</sup>H NMR spectrum of **151** was extremely complicated since none of the protons in quinuclidinol are equivalent. Two and three bond couplings lead to complex second order splitting patterns and broad peaks. However, both the <sup>1</sup>H and <sup>13</sup>C NMR spectra were in agreement with structure as was the FAB mass spectrum. Conversion to hexafluorophosphate salt **152** was achieved using the standard method and full characterisation of the recrystallised material was possible.

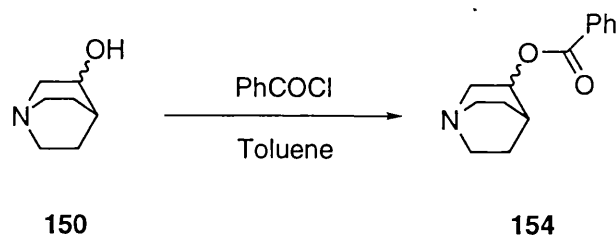
Having established its viability as a precursor to trications, we proceeded to functionalise 3-quinuclidinol *via* esterification. Using the method of Langlois,<sup>132</sup> condensation of 3-quinuclidinol and acetic anhydride under reflux gave, after work-up, 3-acetoxyquinuclidine **153** as a colourless mobile oil in 73% yield (Scheme 2.20).



Scheme 2.20

In Langlois' original paper a large quantity (ca. 30 g) of 3-quinuclidinol was used as starting material but its expense made it impracticable for us to repeat the reaction on the same scale. The literature method utilises distillation as the final stage in the work up but given the small quantities we were dealing with an alternative method was sought. We opted to purify the final product using a microdistillation apparatus under vacuum, since Kugelrohr distillation proved unsatisfactory due to inadequate separation and poor recovery.

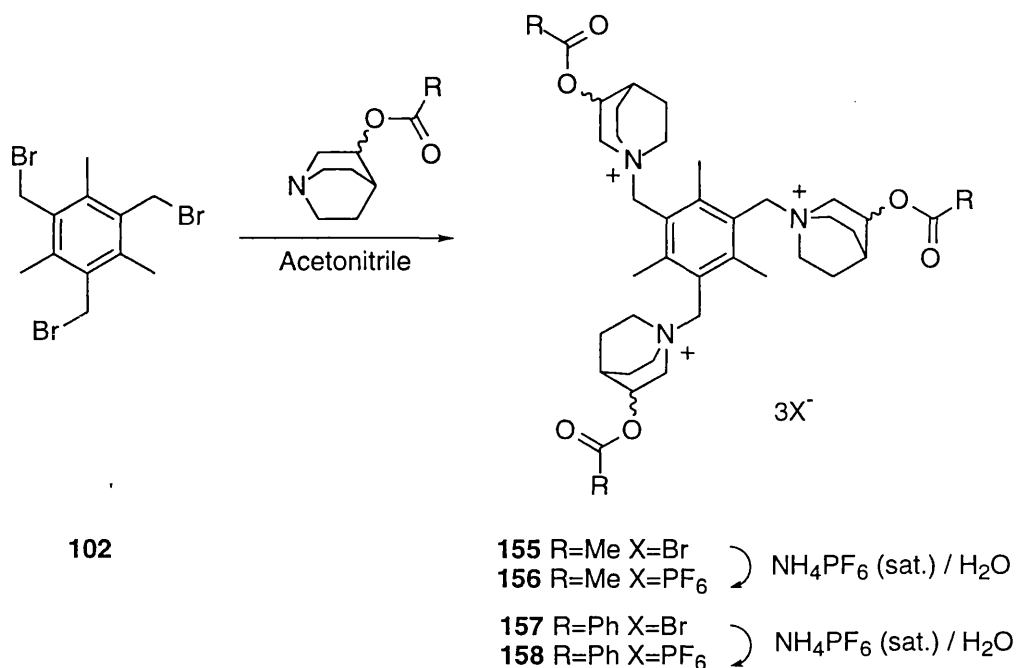
Following the procedure of Rubtsov,<sup>133</sup> 3-quinuclidinol was converted into 3-benzoyloxyquinuclidine **154** by condensation with benzoyl chloride in refluxing toluene (Scheme 2.21). Work-up gave the product as a colourless oil in 35% yield.



Scheme 2.21

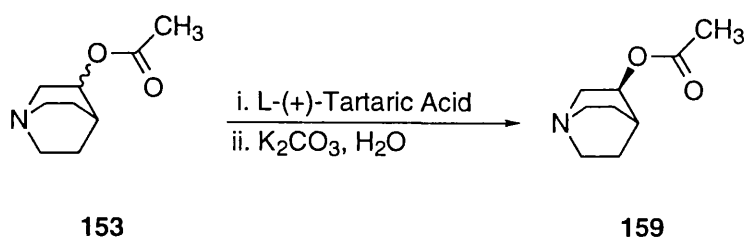
The reaction of 3-acetoxyquinuclidine and 2,4,6-tris(bromomethyl)mesitylene in acetonitrile gave trication **155** as its bromide salt in 61% yield, and subsequent ion-exchange gave the hexafluorophosphate salt **156** as a white solid in 70% yield. 3-Benzoyloxyquinuclidine reacted analogously to give trication **157** as its bromide salt in 91% yield. This material was only soluble in boiling water and was not analysed further. Conversion to the hexafluorophosphate salt **158** proceeded in 72% yield by addition of a saturated solution of ammonium hexafluorophosphate to

a solution of **157** in boiling water (Scheme 2.22). The  $^1\text{H}$  NMR spectra of these materials, like those of the 3-quinuclidinol derivatives, were complex but consistent with their structure, as were their FAB mass spectra. Recrystallisation of the hexafluorophosphate salts from acetonitrile and methanol produced materials which gave satisfactory microanalyses.



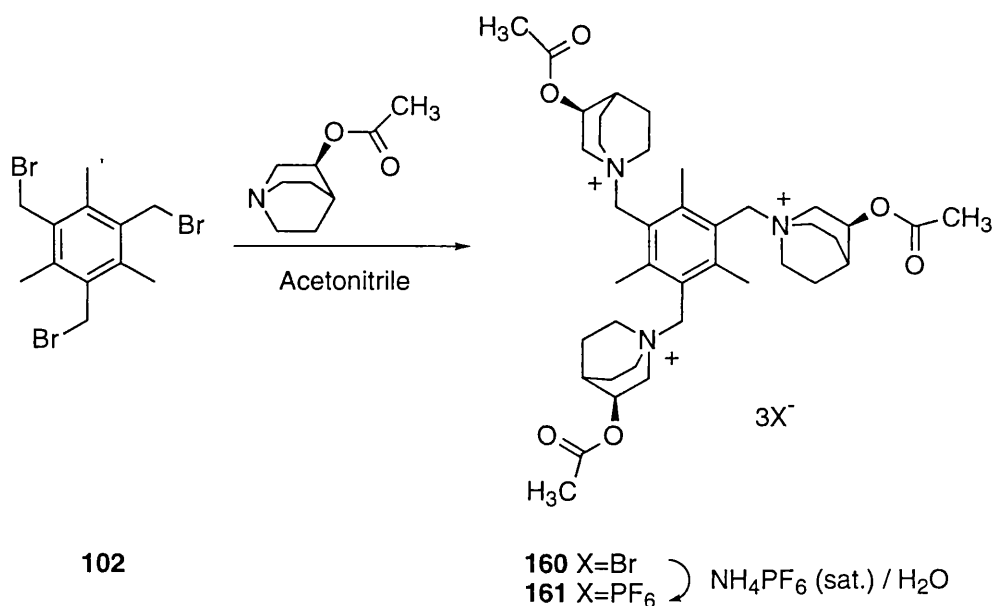
Scheme 2.22

The use of 3-quinuclidinol not only offered a route to more functionalised trications, it also offered the possibility of producing optically active material by the resolution of its derivatives. Kaiser<sup>134</sup> reported a method of resolving racemic 3-acetoxyquinuclidine into its (R)- and (S)- isomers by optical resolution using salts of tartaric acid (Scheme 2.23). Standing a 1:1 mixture of 3-acetoxyquinuclidine and L-(+)-tartaric acid in an 80% ethanol solution for several days led to the precipitation of a white solid. This solid was recrystallised from an ethanol-water mixture (4:1) to give white needles of the resolved (+)-hydrogen tartrate salt of 3-acetoxyquinuclidine. Our material had slightly higher optical rotation ( $[\alpha]_{\text{D}}^{25} = +5.3^\circ$  ( $c = 2.2$ , H<sub>2</sub>O)) than that reported in the literature ( $[\alpha]_{\text{D}}^{25} = +3.6^\circ$  ( $c = 2.2$ , H<sub>2</sub>O)).<sup>132</sup> The free base **159** was liberated using potassium carbonate. In this case our optical rotation ( $[\alpha]_{\text{D}}^{25} = +21.4^\circ$  ( $c = 2.2$ , EtOH)) was lower than that reported in the literature ( $[\alpha]_{\text{D}}^{25} = +28.5^\circ$  ( $c = 2.2$ , EtOH)).<sup>132</sup>



Scheme 2.23

Reaction of (R)-(+)-3-acetoxyquinuclidine with 2,4,6-tris(bromomethyl)mesitylene yielded **160** as a white solid in 97% yield and conversion to the hexafluorophosphate salt gave **161** in 58% yield (Scheme 2.24).



Scheme 2.24

The optical rotation of compound **160** was measured and found to be significant ( $[\alpha]_{\text{D}}^{25} = -14.7^\circ$  ( $c = 1.0$ ,  $\text{H}_2\text{O}$ )), indicating that we had made an enantiomeric trication. The NMR spectra of the compounds were identical to their racemic counterparts, as were the FAB mass spectra.

## 2.7 Conclusion

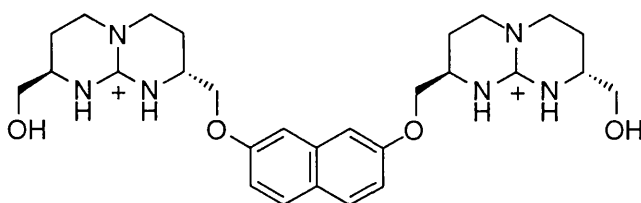
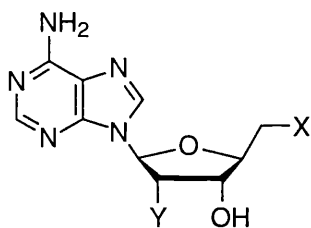
It can be seen that the use of DABCO, quinuclidine, and quinuclidinol and its derivatives offer a facile route to the synthesis of polycationic materials with a variety of functionality. As their bromide salts these materials tend to be insoluble in organic solvents but their hexafluorophosphate salts were readily soluble in acetone and acetonitrile, allowing them to be purified and fully characterised. The solubility of the bromide salts in water facilitated our studies into their host-guest properties.





selectivity of complexation, the strongest complexes being formed between species of highest charge density. A comparison between guanidinium and ammonium groups as positively charged binding sites shows that in all cases where direct matching is possible, the complexes of ammonium bearing ligands are about an order of magnitude more stable than those of the corresponding guanidinium ligands, reflecting the greater localisation of the charge in the ammonium group. The anion binding selectivities of the ligands rest on electrostatic interactions, a more highly charged anion being selectively complexed by a given ligand.

Schmidtchen and co-workers found that the foldable dicationic guanidinium host **166** bound biologically relevant phosphates in aqueous solution, with large association constants.<sup>137</sup> The host featured two chiral bicyclic guanidinium units connected to a planar and rigid naphthalene spacer and was expected to adopt a variety of extended conformations due to the electrostatic repulsion of the positive charges. Using <sup>1</sup>H NMR titration experiments association constants between **166** and phosphates **167-169** were determined, along with an association constant between the host species and inorganic phosphate (Table 3.2). All of the complexes fitted a 1:1 stoichiometry model.

**166**

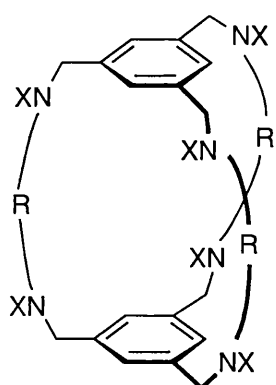
	X	Y
<b>167</b>	OH	-OPO <sub>3</sub> <sup>2-</sup>
<b>168</b>	-OPO <sub>3</sub> <sup>2-</sup>	H
<b>169</b>	-OPO <sub>3</sub> <sup>2-</sup>	OH

Association Constants of <b>166</b> and Phosphates		
Guest	Solvent	$K_a / \text{M}^{-1}$
$\text{HPO}_4^{2-}$	$\text{CD}_3\text{OD}$	18300
2'-AMP $^{2-}$ ( <b>167</b> )	$\text{CD}_3\text{OD}$	18200
2'-AMP $^{2-}$ ( <b>167</b> )	$d_6$ -DMSO	5250
2'-dAMP $^{2-}$ ( <b>168</b> )	$\text{CD}_3\text{OD}$	29200
5'-AMP $^{2-}$ ( <b>169</b> )	$\text{CD}_3\text{OD}$	3800

Table 3.2

Interestingly, inorganic phosphate was found to be bound more substantially than phosphate esters of the same charge. The organic moieties had been expected to assist in binding by hydrogen or hydrophobic bonding but they appeared instead to break up the favourable noncovalent bonding established between inorganic phosphate and the host species. The dominance of electrostatic binding interactions was illustrated by the much lower association constant obtained between **166** and **167** in  $d_6$ -DMSO compared to that found in deuterated methanol.

Heyer and Lehn<sup>138</sup> reported strong binding of anionic substrates by triply bridged cyclophane type macrocyclic polyamines, such as **170** and **171**, in their hexaprotonated forms. Using NMR titration experiments and pH-metric studies, association constants in the range  $300\text{--}10000 \text{ M}^{-1}$  were determined for the receptors with monovalent ions such as chloride and nitrate. With more highly charged anions such as sulfate and oxalate association constants up to  $3 \times 10^6 \text{ M}^{-1}$  were obtained.



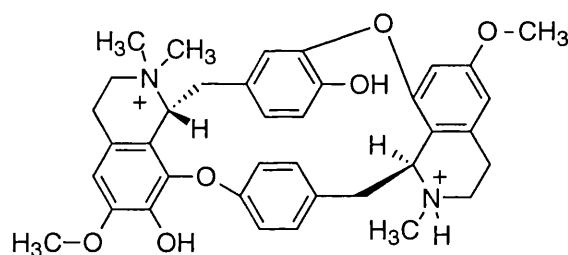
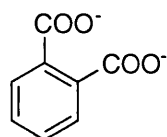
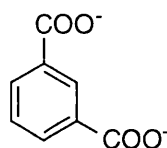
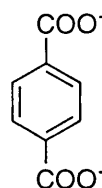
**170**  $X = \text{H}$   $R = -(\text{CH}_2)_3-$

**171**  $X = \text{H}$   $R = -\text{CH}_2\text{CH}_2\text{OCH}_2\text{CH}_2-$

Complexes formed between cyclophane macrocycles and guest anions may be of two types - those in which the anions lie outside the internal cavity of the macrocycle, and inclusive

complexes in which the guest anion lies inside the cavity. The complexation of **170** with nitrate exhibits both types of behaviour. In the solid state, crystal structure determination revealed no nitrate anion was contained in the cavity, but in solution NMR data shows a very clear 1:1 stoichiometry, supporting evidence of one nitrate anion occupying the cavity. It would appear that in the solid state the protonated amine groups adopt an 'outside' orientation in order to support a network of hydrogen bonding of the outside anions. Polyamines such as these, however, exist in the appropriate hexaprotonated form over only a small pH range, limiting their applications.

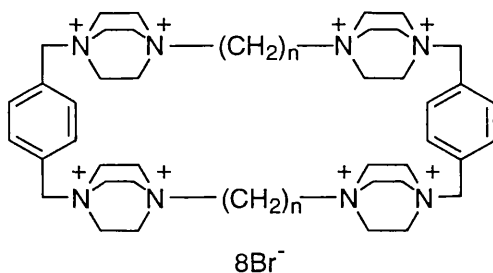
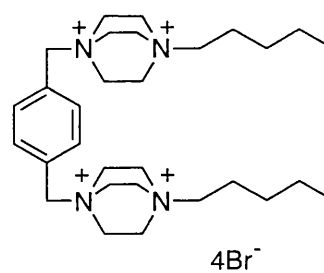
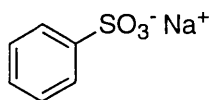
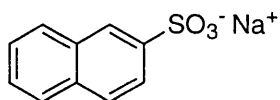
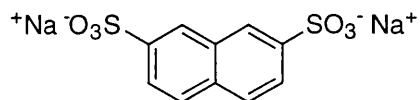
The naturally occurring alkaloid *d*-tubocurarine **172**, has found applications in medicine as a muscle relaxant due to its ability to block the acetylcholine receptor.<sup>139</sup> The macrocyclic nature of this alkaloid has no apparent relation to its biological function but its structure bears a resemblance to other polyammonium macrocycles investigated as potential host species. Alcántar *et al.*<sup>140</sup> have investigated the binding of organic anions to this macrocycle in its dicationic form using fluorometry and conductometry. In the related series of benzenedicarboxylate anions **69**, **173** and **174**, the *para*-substituted anion was found to be the most strongly bound (Table 3.3) showing the importance of the complementarity between positive charges of *d*-tubocurarine and the negative charges of the guest.

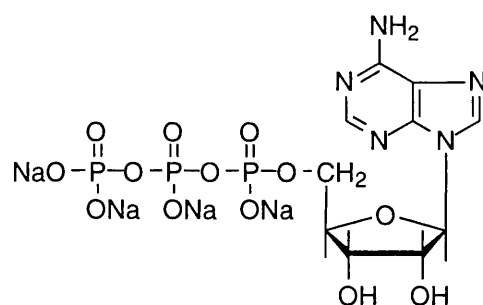
**172****173****174****69**

Complexation of <b>172</b> with	$K_a / \text{M}^{-1}$
<b>173</b>	$59 \pm 6$
<b>174</b>	$200 \pm 30$
<b>69</b>	$780 \pm 80$

Table 3.3

Menger *et al.*<sup>141</sup> report the synthesis of octacationic cyclophanes **175-177** based on DABCO, and the acyclic tetracation **178**. NMR and X-ray data revealed that the cyclophanes adsorb anions, including ATP, in aqueous media but did not bind neutral aromatic guests such as benzene and catechol. The stoichiometry of the complexes was found experimentally to be 1:1 and a summary of the association constant determinations in deuterium oxide is outlined in Table 3.4.

**175**  $n = 3$ **176**  $n = 5$ **177**  $n = 7$ **178****179****180****181**



182

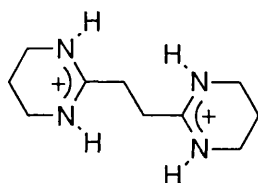
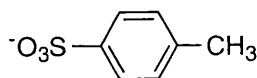
Host	Guest	$K_a / \text{M}^{-1}$
175	179	61
175	180	447
175	181	3390
175	182	13300
176	182	15900
177	182	12100
178	182	22200

Table 3.4

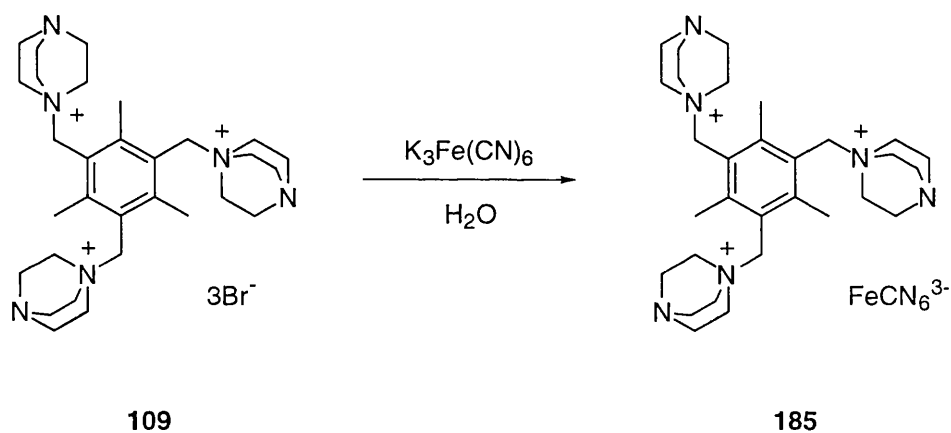
Cavity size was found not to be important in the binding of ATP to the host species and it is interesting to note that the binding of acyclic host molecule **178** to ATP was stronger than that determined from experiments with the cyclophane-type molecules. The results suggest that it is possible ATP does not enter the cavity formed by the macrocyclic compounds and that association is more of an anion exchange with the bromide counter-ions. Indeed an X-ray structure of **175** and **181** revealed that the guest molecules lay outside the cavity, reflecting the results of Lehn discussed previously.

### 3.2 Selective Crystallisation

A simple example of molecular recognition is illustrated by selective crystallisation. Brand et al.<sup>142</sup> reported the recognition of arene sulfonate **184** by bis-cyclic amidinium dication **183** in the solid state. Crystal structure analysis showed that host **183** bound two tosylate anions in a centrosymmetric fashion.

**183****184**

Both size and charge complementarity are important factors in the process of crystallisation. In the course of our investigations into our polycationic materials we found that when a solution of **109** in water was treated with an equimolar solution of potassium ferricyanide, on standing yellow-orange crystals precipitated. The crystals showed a band at  $2110\text{ cm}^{-1}$  in the IR spectrum, indicative of the presence of ferricyanide ion. An X-ray structural analysis of the crystals at 140 K showed that they were of **185** (Scheme 3.1). The crystal structure had to be carried out at low temperature since at room temperature the crystals were only weakly diffracting and a full data set could not be collected.

**Scheme 3.1**

A schematic representation of the results of the crystal structure analysis is illustrated in Figure 3.1. The ORTEP diagram is shown in Figure 3.3 (hydrogen atoms omitted for clarity), which clearly shows the interaction of the trication in its all-*cis* conformation with the ferricyanide trianion. The crystal structure analysis also revealed that each asymmetric unit had eight water molecules associated with it, whose positions are included in the ball and stick representation shown in Figure 3.2. It is probable that these water molecules are involved in some form of hydrogen bonding network. Close analysis of the bond angles in the structure show that the ferricyanide ion does not have the regular octahedral structure anticipated. The two cyanide groups perpendicular to the plane of the benzene ring are unaffected whilst two of the remaining cyanide groups bend away from the trication, and the other two bend towards it. The reason for this is not clear, since it may be either a steric or electronic effect.

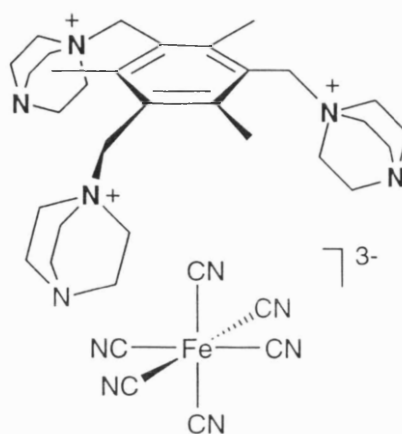


Figure 3.1

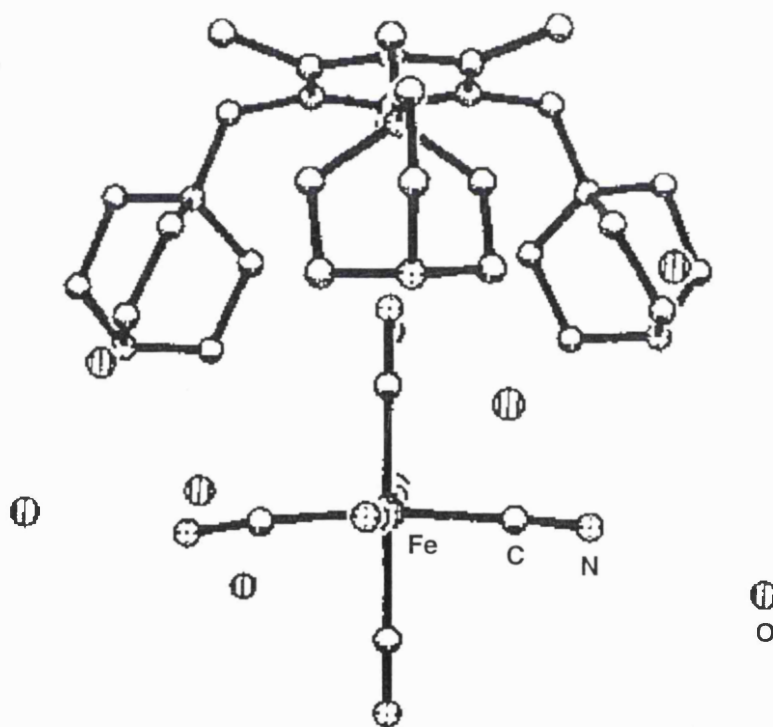


Figure 3.2

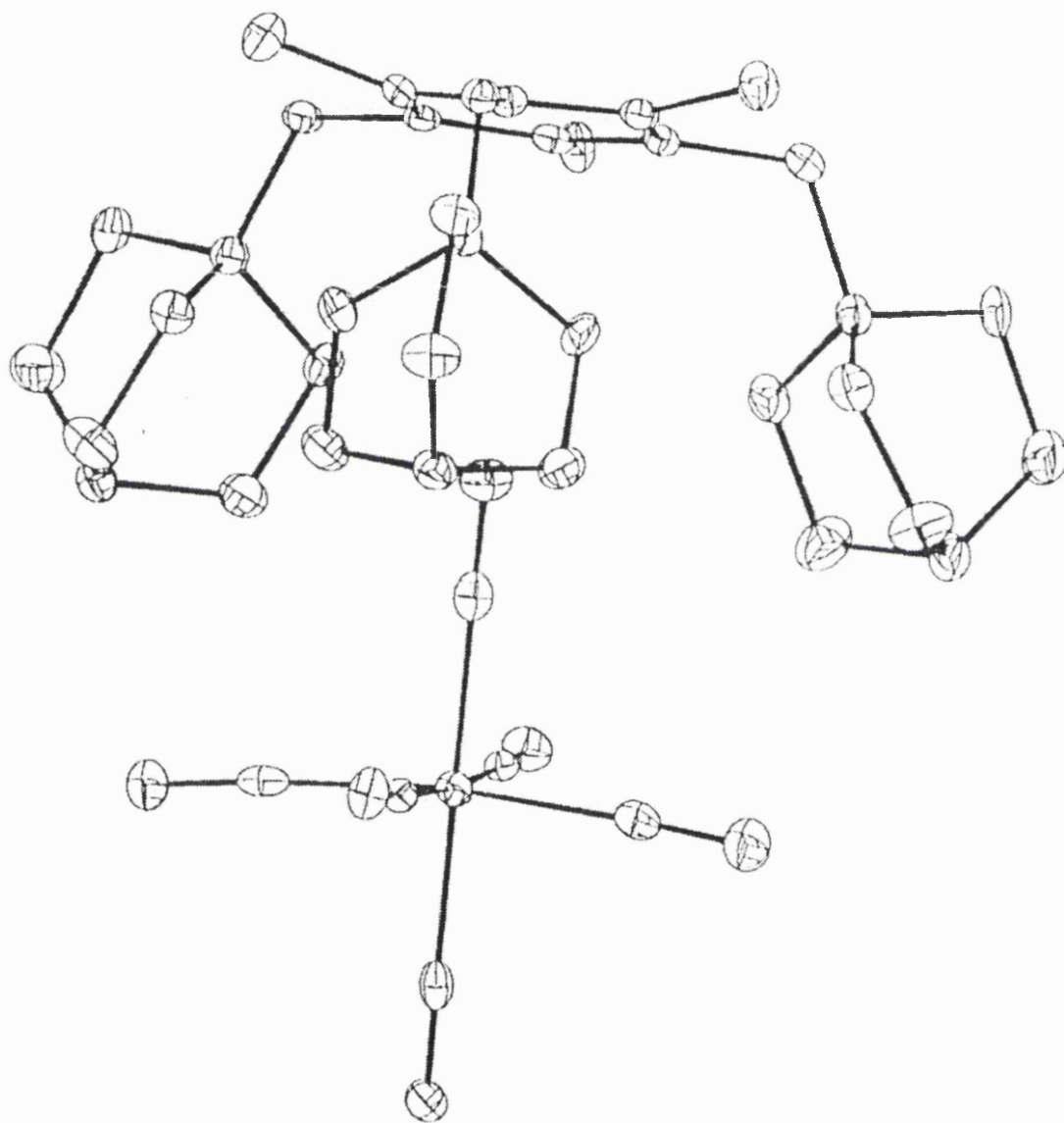
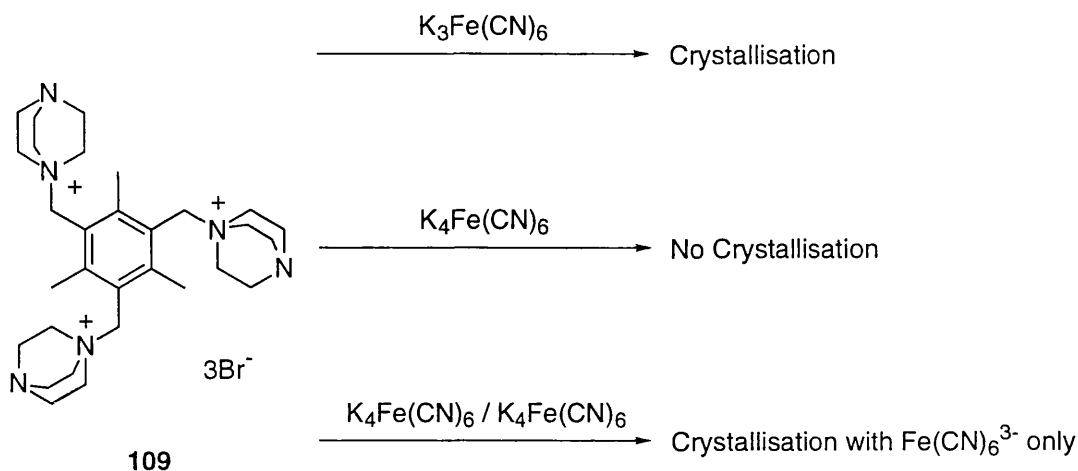


Figure 3.3

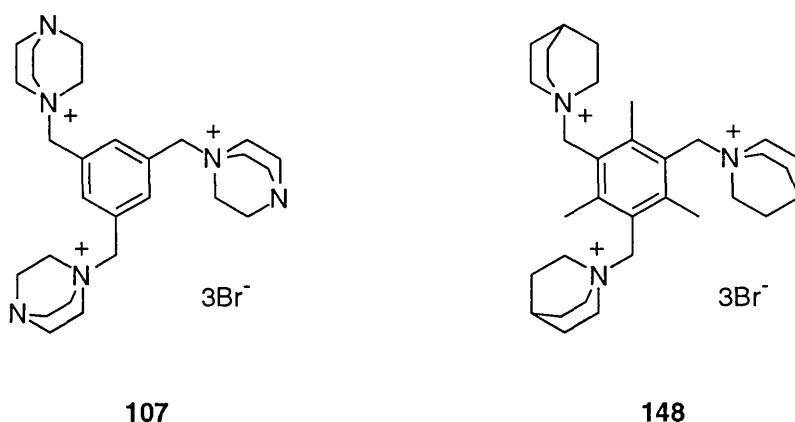


Addition of a solution of **109** to ferrocyanide gave no crystalline precipitate even after prolonged standing, while addition of **109** to a solution containing a mixture of ferri- and ferrocyanide gave crystals of the ferricyanide complex only, as shown by the IR spectrum (Scheme 3.2).



**Scheme 3.2**

The corresponding trication **107**, in which the three aromatic methyl groups are replaced by hydrogen, gave no precipitate with either ferri- or ferrocyanide even after prolonged standing, indicating the importance of the methyl substituents in prolonging the lifetime of the all-*cis* conformation of **109** in the complex, thus allowing a substantial concentration of the complex and the occurrence of nucleation. The quinuclidine analogue of **109**, trication **148**, also gave crystals when treated with ferricyanide but not ferrocyanide. In this case, however, no crystals suitable for X-ray crystallographic analysis were obtained.



### 3.2.1 Solid State $^{13}\text{C}$ NMR Spectroscopy

The ferricyanide complex **185** was found to be insoluble in all solvents, which meant we could not investigate it *via* solution NMR. Instead we utilised solid state NMR which provided some

surprising results. The solid state  $^{13}\text{C}$  NMR spectrum of the ferricyanide complex **185** recorded using magic-angle spinning and cross-polarisation, showed well resolved peaks at similar chemical shifts to the solution NMR spectrum of the corresponding trication where ferricyanide is replaced by hexafluorophosphate. This was surprising since the presence of paramagnetic iron normally precludes resolution of such spectra and the observation of well resolved spectra indicates that interaction between the paramagnetic iron atom and the organic trication is small. The most likely reason for this is that the paramagnetic coupling is reduced by rapid reorientation of the DABCO groups within the crystals at room temperature. This theory is supported by two observations. Firstly, peaks from the DABCO environments are still observed in the solid state  $^{13}\text{C}$  NMR spectrum even after a 40  $\mu\text{s}$  period of interrupted  $^1\text{H}$  decoupling and, secondly, the linewidth ( $\Delta\nu_{1/2}$ ) of the peak observed in the solid state  $^1\text{H}$  NMR spectrum is only 350 Hz (recorded using a magic-angle spinning speed of 4.5 kHz).

### 3.3 Nuclear Magnetic Resonance Techniques

There has recently been an increase in the number of groups that use NMR data for the evaluation of host-guest phenomena. The evaluation of association constants through the use of NMR data was reported 40 years ago by Huggins *et al.*<sup>143</sup> and methods for using NMR data to determine association constants have been reviewed by Connors.<sup>144</sup> In general, NMR methods have an advantage over UV and fluorescence methods because NMR is not subject to misinterpretation caused by minor impurities and NMR data can also reveal more detailed structural information than UV-VIS data. Wilcox<sup>145</sup> has reported on the errors that may arise when using NMR data. He notes that there are two sources of systematic error that are often encountered in host-guest studies based on NMR data. The first of these is the danger of carrying out titrations at concentrations inappropriate to the equilibria being measured. Second, there is the possibility of confusing acid-base chemistry with binding phenomena.

#### 3.3.1 Theory of NMR Titration

The analysis of the binding between our polycations and organic anions is based upon a simple binding equilibrium model. Considering the polycationic portion to be a host (H) to the organic anion guest (G), the two species are assumed to be in equilibrium with the complex (C).



The goal of the evaluation process is to determine the concentration equilibrium constant (association constant,  $K_a$ ) for this process. In order to simplify the analysis the question of the activity coefficients of the solutes is ignored.

$$K_a = \frac{[\text{C}]}{[\text{H}][\text{G}]} \quad (2)$$

or

$$K_d = \frac{[H][G]}{[C]} = \frac{1}{K_a} \quad (3)$$

The analysis that follows is based upon observations of changes in chemical shift in the guest species, although an analogous analysis could be made for the host species. In the cases we investigated, the rates of complex formation and breakdown were rapid. The observed chemical shift ( $\delta_{obs}$ ) of a selected proton in the guest species is therefore a weighted average of the chemical shift of the proton in two possible environments - the chemical shifts in the unbound guest environment ( $\delta_g$ ) and the chemical shift in the bound guest environment ( $\delta_c$ ). If the initial guest concentration is defined to be  $[G]_0$ , then Equation 4 applies.

$$\delta_{obs} = \frac{[G]_0 - [C]}{[G]_0} \cdot \delta_g + \frac{[C]}{[G]_0} \cdot \delta_c \quad (4)$$

Rearranging Equation 4 and defining  $\Delta\delta$  to be the difference in chemical shift for the two environments ( $\Delta\delta = \delta_c - \delta_g$ ) leads to Equation 5.

$$\delta_{obs} = \delta_g + \frac{[C]}{[G]_0} \cdot \Delta\delta \quad (5)$$

The observed chemical shift is determined by the extent of complexation. The concentration of the complex may be calculated exactly (Equation 6) provided that  $[G]_0$ ,  $[H]_0$  (the initial host concentration), and  $K_d$  (the dissociation constant for the equilibrium presented in Equation 1 and described by Equation 3) are known.

$$[C] = \frac{1}{2} \left[ K_d + [H]_0 + [G]_0 - \sqrt{(K_d + [H]_0 + [G]_0)^2 - 4[H]_0[G]_0} \right] \quad (6)$$

Combining Equations 5 and 6 gives an exact expression for the observed chemical shift as a function of  $[G]_0$ ,  $[H]_0$ ,  $K_d$ ,  $\Delta\delta$ , and  $\delta_g$ .

$$\delta_{obs} = \delta_g + \frac{\Delta\delta}{2[G]_0} \left[ K_d + [H]_0 + [G]_0 - \sqrt{(K_d + [H]_0 + [G]_0)^2 - 4[H]_0[G]_0} \right] \quad (7)$$

Or, in terms of  $[G]_0$ ,  $[H]_0$ ,  $K_a$ ,  $\Delta\delta$ , and  $\delta_g$ .

$$\delta_{obs} = \delta_g + \frac{\Delta\delta}{2[G]_0} \left[ \frac{1}{K_a} + [H]_0 + [G]_0 - \sqrt{\left( \frac{1}{K_a} + [H]_0 + [G]_0 \right)^2 - 4[H]_0[G]_0} \right] \quad (8)$$

Equation 8 describes the complexation-induced shift (CIS) of an NMR signal. The variation of  $\delta_{\text{obs}}$  with the changing ratio of guest:host ( $[G]_0/[H]_0$ ) forms the basis of NMR titration for the determination of association constants. Wilcox<sup>145</sup> points out that Equation 8 actually defines a three dimensional surface. In a titration experiment a series of measurements is obtained, each measurement being defined by three quantities  $[G]_0$ ,  $[H]_0$ , and  $\delta_{\text{obs}}$ . In our experiments  $[G]_0$  was held constant, whilst  $[H]_0$  was varied. The character of the titration curve obtained is determined solely by the relative values of  $[G]_0$ ,  $[H]_0$ , and  $K_a$ . There are several ways to use titration data to obtain an association constant. Methods have been presented by Creswell and Allred<sup>146</sup>, and Schneider *et al.*<sup>87</sup> We preferred to use the method described by Macomber.<sup>147</sup> Equation 8 requires that both  $\delta_g$  and  $\delta_c$  are known. Although the former is easily determined by direct measurement in the absence of host, the latter cannot usually be determined directly in a fast exchange system since, unless the value of  $K_a$  is large, the observed chemical shift,  $\delta_{\text{obs}}$ , may not approach the chemical shift corresponding to the complex,  $\delta_c$ , at any readily attainable ratio of  $[H]_0$  to  $[G]_0$ . Thus we are left with one equation with two unknown parameters,  $\delta_c$  and  $K_a$ . However, using non-linear curve-fitting it is possible to iteratively determine the values of  $K_a$  and  $\delta_c$  that best simulate an experimental set of  $\delta_{\text{obs}}$  versus  $[H]_0$ . A short FORTRAN program for doing this is given in Appendix 1. The program takes experimental values of  $[G]_0$ ,  $[H]_0$ , and  $\delta_{\text{obs}}$ , along with  $\delta_h$  and an initial estimate of the value of  $K_a$ . Using these data the program iteratively calculates values of  $\delta_c$  and  $K_a$  until the theoretical values of  $\delta_{\text{obs}}$  agree with those found experimentally to within 1%. It is interesting to note that any association constants determined are actually independent of the magnitude of  $\Delta\delta$ .

### 3.3.2 Method of Continuous Variations

As well as being interested in the strength of any binding between our polycations and simple guest molecules we were also interested in the nature of the binding and thus the stoichiometry of any complex formed. To determine stoichiometry we used the so-called method of continuous variations, or Job's method.<sup>148,149</sup> For the study of a simple equilibrium defined by Equation 9, a series of solutions is prepared in which the total host plus guest molar concentration,  $[H]_0 + [G]_0$ , is kept constant whilst the ratio of  $[H]_0/[G]_0$  varies.



$$x = \frac{[G]_0}{[H]_0 + [G]_0} \quad (10)$$

$$x = \frac{m}{n+m} = \frac{1}{1 + \frac{n}{m}} \quad (11)$$

It can be shown that the concentration of the complex has a maximum for an H-to-G molar ratio equal to  $n/m$ . Thus a plot of  $[C]$ , or of any property that is a linear function of  $[C]$ , against  $x$  (Equation 10) yields a curve having a maximum at a value of  $x$  defined by Equation 11, and zero values at  $x = 0$  and  $x = 1$ .

Job's method suffers from several limitations, which have been eloquently reviewed by Gil and Oliveira.<sup>149</sup> The existence of other equilibria concurrent with Equation 9 can affect the determination of  $n/m$ . However, if the concentration of other concurrent complexes is small this proves not to affect the value of  $n/m$  determined. Species other than H, G and C may be involved in the equilibrium and this may affect the value determined. The individual values of  $n$  and  $m$  are not determined and only their ratio is obtained, so this method cannot distinguish between a 1:1 and a 2:2 complex and so on. However, we expected complex formation would be from a 1:1 ratio of host and guest and thus did not anticipate any complications. The concentration of complex is given by Equation 12 and uses the value of  $\delta_c$  calculated from the association constant determination described above.

$$[C] = [G]_0 \left( \frac{\delta_{\text{obs}} - \delta_g}{\delta_c - \delta_g} \right) \quad (12)$$

Thus a plot of  $[C]$  versus  $x$  showing a maximum at a value of  $x=0.5$  indicates the formation of a 1:1 complex.

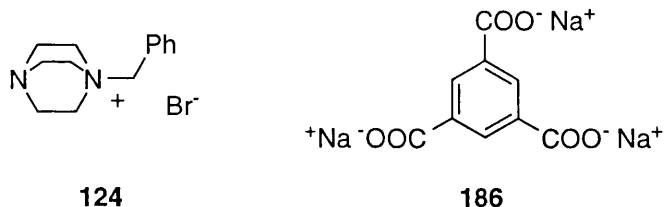
### 3.4 Binding Studies

#### 3.4.1 NMR Titration of Tricationic Compounds

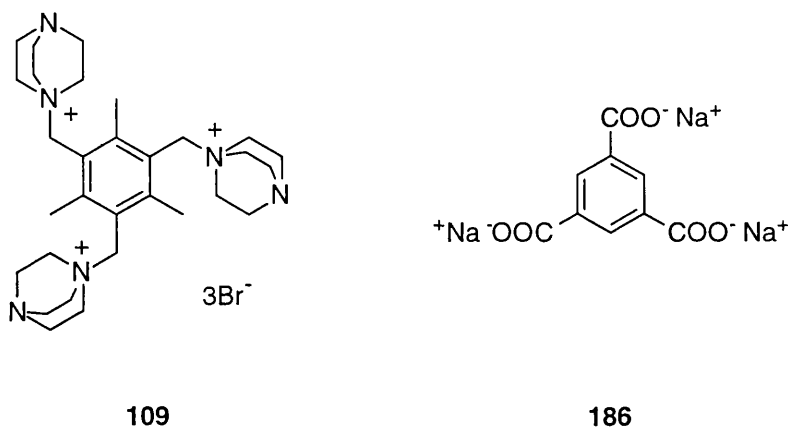
We believed that our tricationic compounds should show some selective binding affinity towards complementary trianions. Since our bromide salts were soluble in water we chose deuterium oxide as the medium in which to carry out experiments. Thus our initial experiment was the titration in deuterium oxide of host trication **109** with trisodium benzene-1,3,5-tricarboxylate **186** as guest. A standardised solution containing an approximately 5:1 mixture of host and guest was prepared, along with a standardised solution containing guest only at the same concentration. Aliquots were combined to give a constant volume of solution. The concentration of guest remained constant throughout the experiment, whilst the ratio of host:guest was varied stepwise from 5:1 to zero, the latter providing the initial position of the anion signal.  $^1\text{H}$  NMR spectra at 7 relative concentrations were recorded.

The plot of chemical shift and chemical shift difference versus the ratio of trication:trianion are shown in Figures 3.4 and 3.5 respectively. Since the association constant determination is independent of the direction of the change in chemical shift, Figure 3.5 shows the magnitude of  $\Delta\delta_{\text{obs}}$  only. An upfield shift was observed in the protons of the tricarboxylate. In a control

experiment, no significant movement was observed when monocation **124** was titrated with trication **186**.



We believe that complexation occurs *via* a face-to-face orientation of the two species, illustrated in Figure 3.6, and the upfield shifts indicate that they do not approach each other closely, as this would lead to a downfield shift being observed. Figure 3.6 shows the three DABCO substituents all lying on one side of the plane of the benzene ring. Simple molecular mechanics calculations had showed us that there was only a small energy difference between the conformer illustrated and that in which two of the DABCO substituents lie on one side of the plane of the benzene ring, with the third on the other. The NMR spectra did not show any conformational isomerism so it is not clear what the exact conformational structure of the trication is in solution but the results of the X-ray structure analysis discussed earlier showed that in complexation with the ferricyanide trianion all three DABCO groups lay on one side of the plane of the benzene ring. Iterative curve-fitting procedures discussed previously gave a value for the association constant of  $K_a = 75 \text{ M}^{-1}$ . Error bars are shown in the Figures, although these have simply been estimated to be  $\pm 0.02 \text{ ppm}$ . A number of errors can arise during the preparation and combination of the solutions, as well as errors in the recorded value of chemical shift. This makes a full error analysis difficult to apply. The chemical shift of the complex was calculated to be 7.67 ppm making the value of  $\Delta\delta$  equal to 0.73.



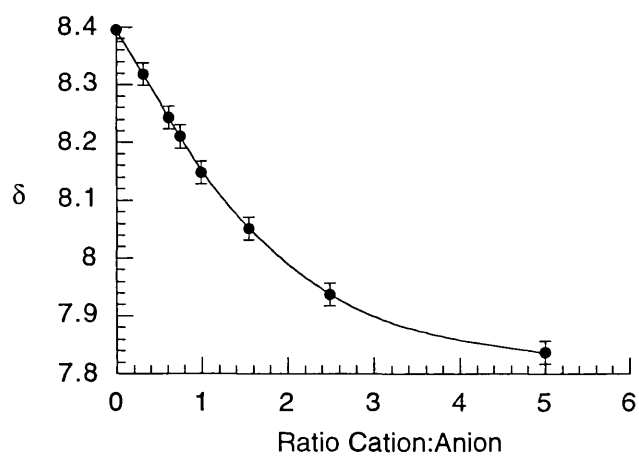


Figure 3.4

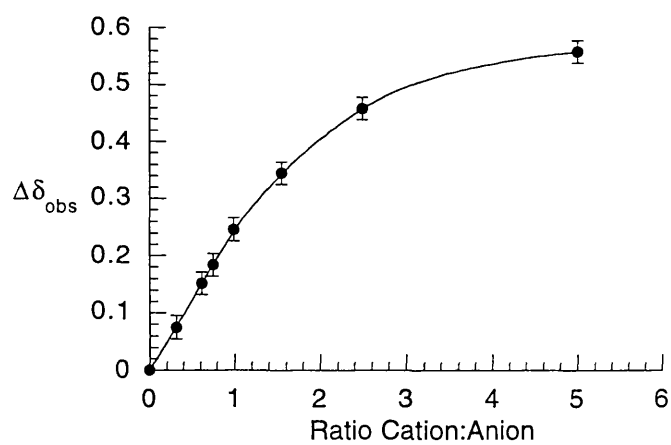


Figure 3.5

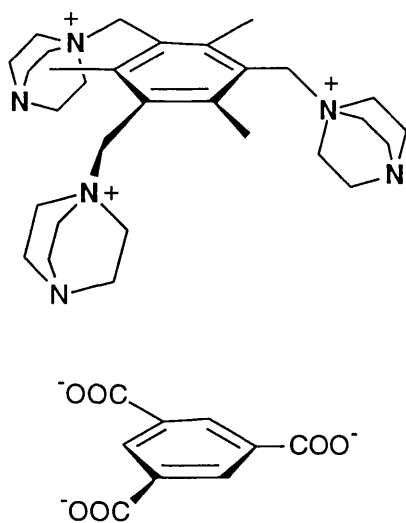


Figure 3.6

Weber<sup>150</sup> has discussed a general guideline in choosing the conditions for titration. The important parameter to consider in choosing the conditions for a titration is the ratio  $p$  defined by Equation 13.

$$p = \frac{\text{concentration of complex}}{\text{maximum concentration of complex}} \quad (13)$$

This parameter, defined by Weber as the “probability of binding”, is equal to the concentration of the complex divided by the initial concentration of the minor component. During a titration the definition of  $p$  therefore changes at the point where the initial concentration of host is equal to the initial concentration of guest (Equations 14 and 15).

$$p = \frac{[C]}{[G]_0}; \quad \text{when } [H]_0 \geq [G]_0 \quad (14)$$

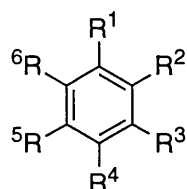
$$p = \frac{[C]}{[H]_0}; \quad \text{when } [H]_0 < [G]_0 \quad (15)$$

The important criterion that defines those data that contain the most information is that  $p$  should be between the values of 0.2 and 0.8.

$$\text{best data: } 0.2 \leq p \leq 0.8 \quad (16)$$

All data used in the determination of association constants based on the change in chemical shift of the anion were found to lie within this range.

In order to gain an insight into the selectivity of our tricationic compound towards anions of different charges, further titrations were carried out with a series of benzene carboxylates **187** - **189**. The carboxylates were chosen as guests since their <sup>1</sup>H NMR spectra are relatively simple and do not overlap with the signals in the spectra of the host molecules.



**187**  $R^1 = \text{CO}_2\text{Na}$ ;  $R^{2-6} = \text{H}$

**188**  $R^{1,3} = \text{CO}_2\text{Na}$ ;  $R^{2,4,5,6} = \text{H}$

**189**  $R^{1,2,4,5} = \text{CO}_2\text{Na}$ ;  $R^{3,6} = \text{H}$



The results of the NMR titrations carried out with these carboxylates and trication **109** are shown in Figure 3.7, which also includes the results for carboxylate **186** for comparison. The direction of the change in chemical shift was upfield in all cases. The results of the association constant determinations are shown in Table 3.5.

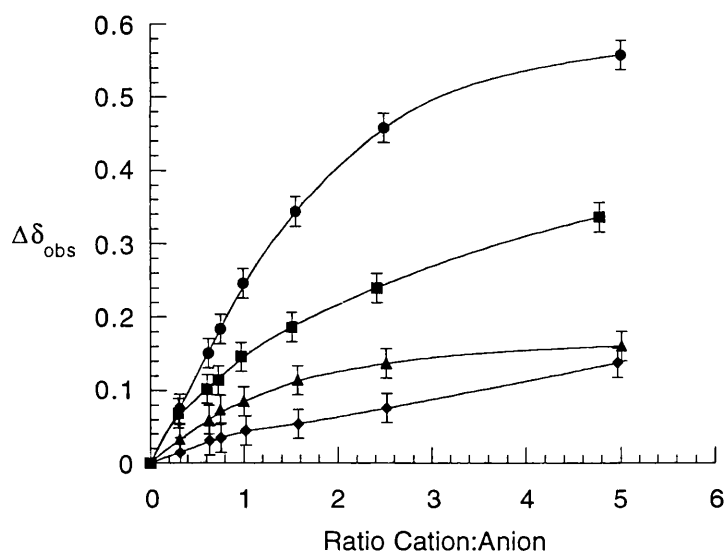


Figure 3.7

—●— 109 vs 186; —■— 109 vs 188; —▲— 109 vs 189; —◆— 109 vs 187

Cation	Anion	$K_a / \text{M}^{-1}$
109	187	16
109	188	67
109	186	75
109	189	170

Table 3.5

The results showed that as we had hoped, trication **109** bound a trianion more strongly than either a di- or monoanionic species. We were, however, surprised to note that the strongest binding was found between the trication and tetracarboxylate **189**. Figure 3.7 reveals that the magnitude of the change in chemical shift observed in the tricarboxylate is much larger than that observed in the tetracarboxylate, yet the association constant determinations show that it is the tetracarboxylate which is more strongly bound. This is due to the fact that the critical factor in the determination of association constants from NMR titration is the shape of the curve that is obtained. Figures 3.8 shows the titration curves obtained from these two experiments in terms of

the percentage of complex present based on the calculated value of the chemical shift of the complex formed in each case i.e.  $(\delta_{\text{obs}}/\Delta\delta)$ .

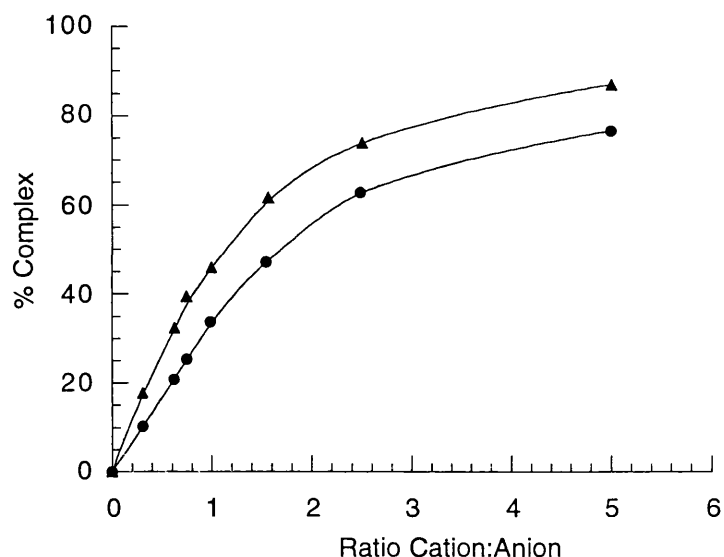


**Figure 3.8**

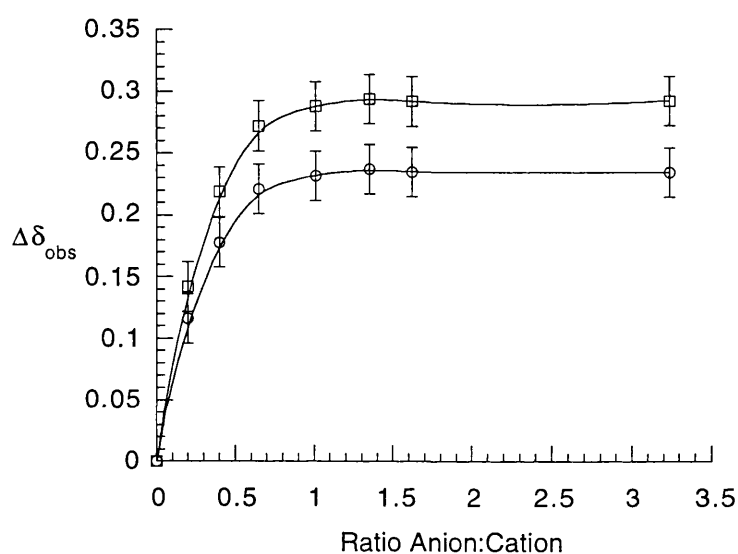
—●— 109 vs 186; —▲— 109 vs 189

Figure 3.8 shows that based on the results of the association constant determination, at a given ratio of cation:anion the proportion of complex present is larger in the case of the tetracarboxylate than the tricarboxylate. The use of the technique of NMR titration to determine association constants suffers from the fact that it tells us nothing of the nature of the complex formed in terms of the proximity of the two species to each other. It may be that the larger shift observed in the tricarboxylate is due to a closer approach of the trication than in the case of the tetracarboxylate. Table 3.6 summarises the results of the titrations in terms of the chemical shift of the free anion ( $\delta_g$ ), the anion in a 1:1 mixture of cation and anion ( $\delta_{1:1}$ ), the calculated value of the chemical shift of the complex ( $\delta_c$ ), and the difference in chemical shift between the complex and the free carboxylate ( $\Delta\delta$ ).

Cation	Anion	$\delta_g$	$\delta_{1:1}$	$\delta_c$	$\Delta\delta$
109	187	7.658	7.613	7.438	0.220
109	188	7.946	7.800	7.496	0.450
109	186	8.395	8.148	7.666	0.729
109	189	7.518	7.433	7.333	0.185

**Table 3.6**

These results led us to consider whether the technique was giving reliable results and to examine further the NMR titrations we had already performed by looking at changes in the chemical shift in the trication. Since the cation and anion were in equilibrium with the complex we anticipated that looking at the cationic portion would give the same results as looking at the anionic portion as such an equilibrium should be independent of which species is being monitored. What we found, however, was that very different results were obtained. Two different signals in the NMR corresponding to the cation were monitored - benzylic and methyl. Both showed upfield shifts and Figure 3.9 illustrates the change in chemical shift of the benzyl and methyl groups of trication **109** with tricarboxylate **186**.



**Figure 3.9**

—○— Methyl Groups; —□— Benzyl Groups

These results seem to suggest that the trication is binding the trianion far more strongly than those based on the anion shift had indicated. The change in shift of the cation protons is virtually over by the time a 1:1 equivalence is reached whilst in the anion the effect continues to much higher host:guest ratios. Indeed it was not possible to calculate an association constant from the cation shift data as they lie outside those predicted for a case of infinite binding in a 1:1 complex (Figure 3.10).

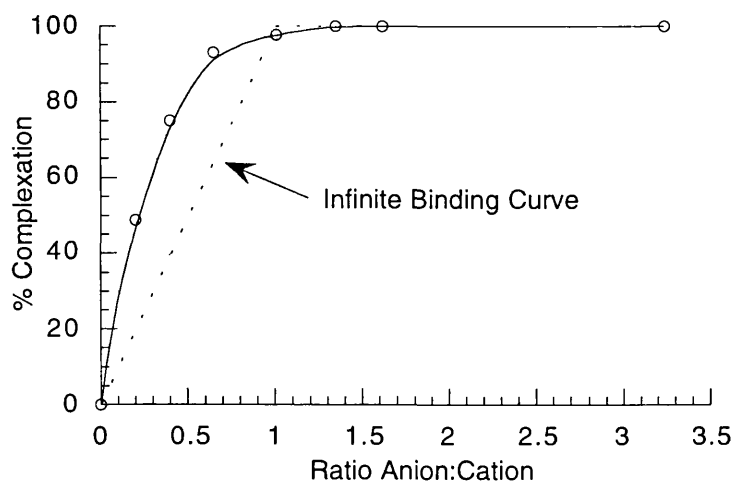


Figure 3.10

—○— 109 (Methyl Groups) vs 186

In order to show that the difference in chemical shift changes between cation and anion was not an artefact of the order of addition, an experiment was conducted where the role of host and guest was reversed. The same results were obtained under these conditions. The magnitude of the change in chemical shift is also markedly less in the trication than in the trianion. The reason for these differences in behaviour between protons in the host and guest species is unclear, though it may be due to the protons in the trication being less sensitive to the effects of complexation than those of the anion.

Similar effects were noticed in the titrations of trication **109** with the other carboxylate guests and these results are summarised in Figures 3.11 and 3.12 which show the change in chemical shift of the methyl and benzyl groups of the trication respectively. In all cases the direction of the change in chemical shift was upfield. The changes in chemical shift of the cation methyl and benzyl groups, as a function of the ratio of anion:cation, differ only in their magnitude, the shape of the curve being the same in both cases. As seen in the measurement of shifts in the carboxylate anions, the titration between the trication and trianion gives rise to the largest change in chemical shift, followed by the dianion, whilst the monoanion and tetraanion show similar, small changes in chemical shift.

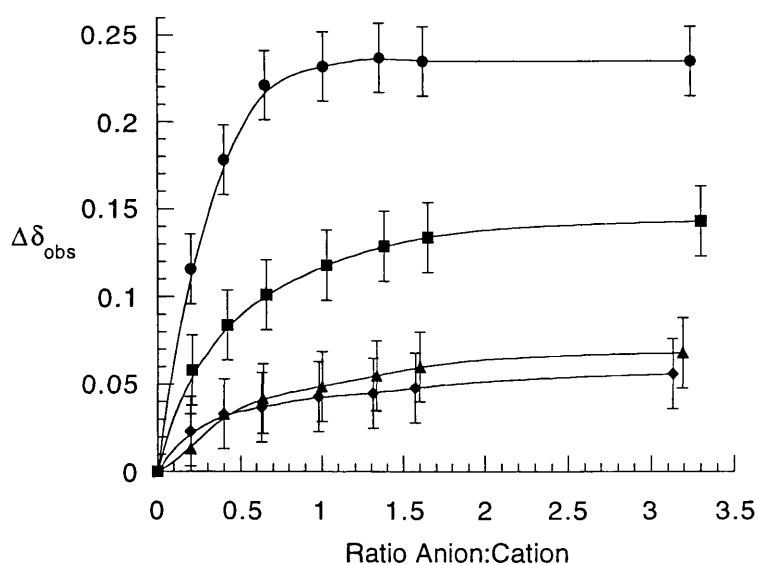


Figure 3.11 - Methyl Groups

—●— 109 vs 186; —■— 109 vs 188; —▲— 109 vs 189; —◆— 109 vs 187

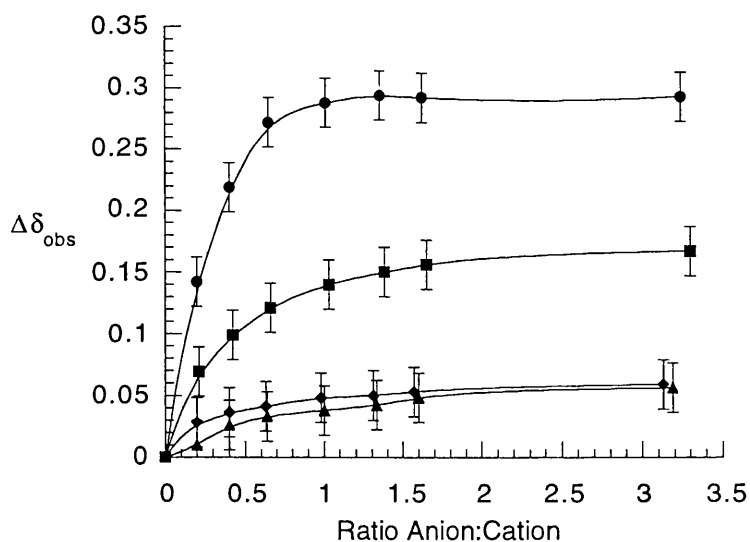


Figure 3.12 - Benzyl Groups

—●— 109 vs 186; —■— 109 vs 188; —▲— 109 vs 189; —◆— 109 vs 187

Plotting the percentage complexation in this case gives different results from those seen based on measurement of changes in chemical shift in the guest anion. Figure 3.13 shows that measurements based on the host cation indicate that the trianion is the most strongly bound guest, with the dianion the next most strongly bound and the tetraanion bound most weakly.

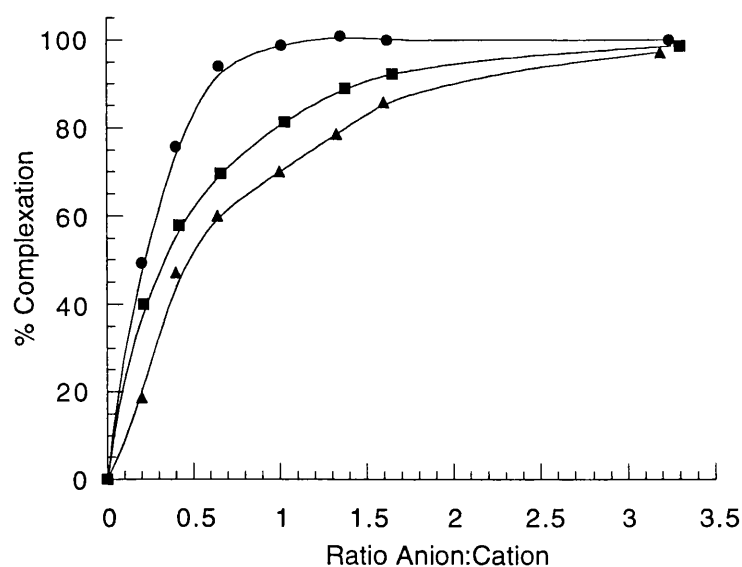
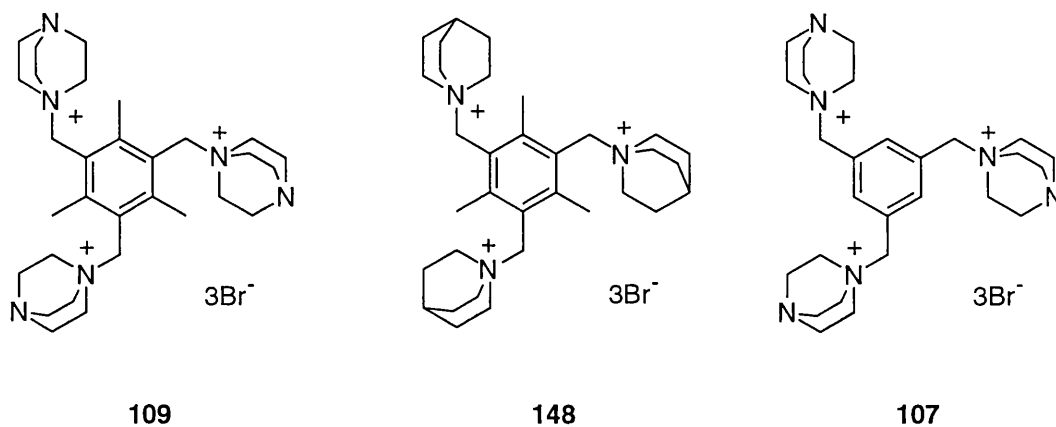


Figure 3.13

—●— 109 vs 186; —■— 109 vs 188; —▲— 109 vs 189

In order to ascertain whether the uncharged nitrogen atoms in trication **109** had any importance, a titration was also carried out between the quinuclidine-based trication **148** and tricarboxylate **186**. The importance of the methyl groups in determining the conformational ability of the trication was also assessed by carrying out titrations with trication **107** in which the methyl groups were not present. The results of these titrations are shown in Figure 3.14, whilst the association constants determined are summarised in Table 3.7.



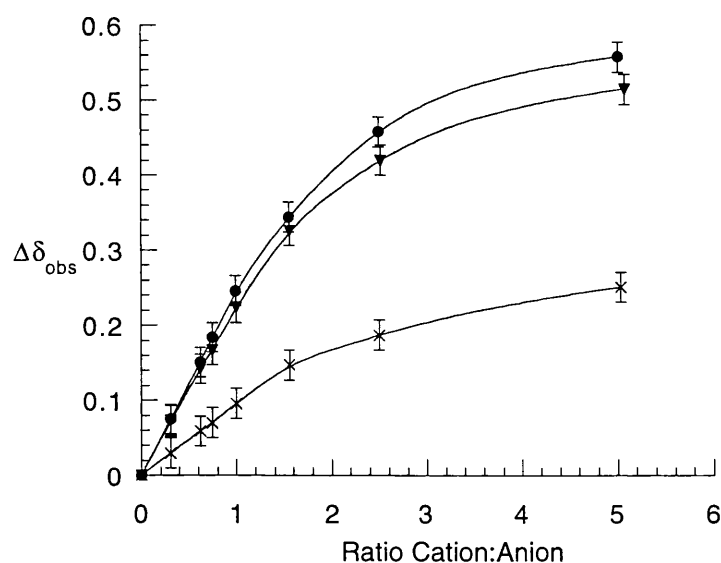


Figure 3.14

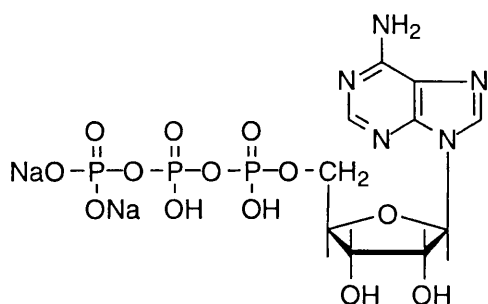
—●— 109 vs 186; —×— 107 vs 186; —▼— 148 vs 186

Cation	Anion	$\delta_g$	$\delta_{1:1}$	$\delta_c$	$\Delta\delta$	$K_a / M^{-1}$
<b>109</b>	<b>186</b>	8.395	8.148	7.666	0.729	75
<b>148</b>	<b>186</b>	8.406	8.177	7.739	0.656	78
<b>107</b>	<b>186</b>	8.399	8.303	8.020	0.379	42

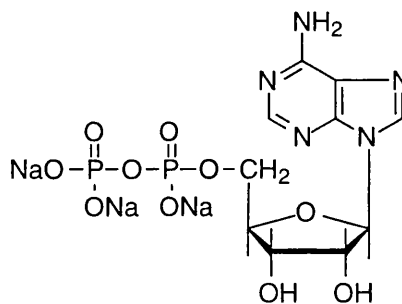
Table 3.7

The absence of the uncharged nitrogen atoms in trication **148** appears to make little difference to the strength of complexation, although the magnitude of the change in chemical shift is reduced a little. Clearly, however, the absence of the methyl substituents in trication **107** leads to more conformational mobility. This manifests itself in the reduced change in chemical shift and in the reduced strength of association which is approximately half that of the corresponding methyl-substituted trication.

Our interest in these simple systems extended into any potential biological applications for our cationic materials, since as their bromide salts they were water soluble. This led us to investigate whether trication **109** could discriminate between the biologically important anions of adenosine 5'-triphosphate (ATP) and adenosine 5'-diphosphate (ADP). For this reason titrations were carried out between trication **109** and these two anions in their di- and trianionic forms respectively (**190** and **191**). The chemical shifts of the anomeric protons in the anions were monitored. In both cases upfield shifts were observed. The association constants determined and a summary of the other data are given in Table 3.8.



190



191

Cation	Anion	$\delta_g$	$\delta_{1:1}$	$\delta_c$	$\Delta\delta$	$K_a / M^{-1}$
<b>109</b>	ADP ( <b>191</b> )	6.165	6.093	5.877	0.216	42
<b>109</b>	ATP ( <b>190</b> )	6.146	6.083	5.877	0.206	43

Table 3.8

The data show that trication **109** was unable to distinguish between the two anions, and only very weak binding was observed.

### 3.4.2 Job Plots - Trications

Separate experiments were conducted in order to determine the stoichiometry of the binding between the host and guest species in which the total concentration of ions was constant with different ratios of host and guest. In the cases of trication **109** with dicarboxylate **188** and tetracarboxylate **189**, symmetric curves were obtained with maxima at equivalent concentrations of the two components (Figure 3.15).

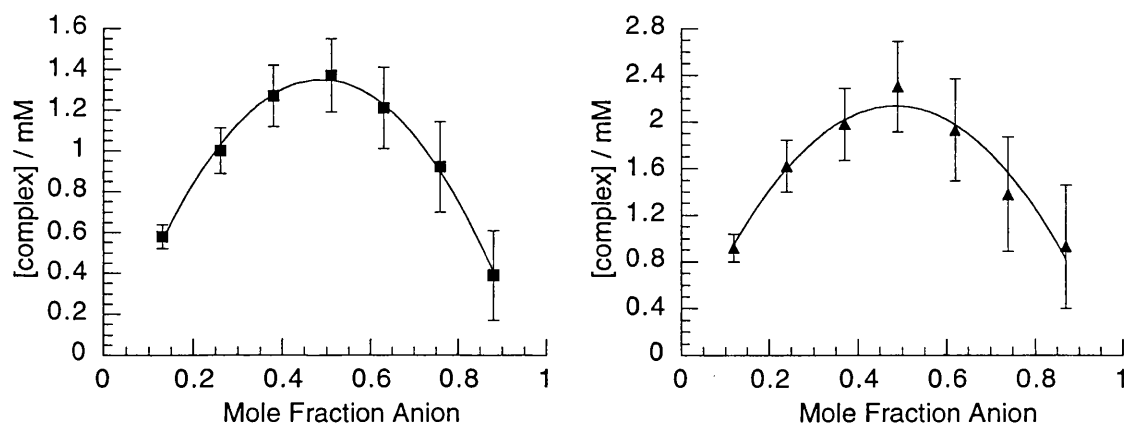


Figure 3.15

—■— 109 vs 188; —▲— 109 vs 189



The error bars in Job Plots increase in size with increasing mole fraction of anion. Recalling Equation 12 shows that the concentration of the complex is calculated from the difference between the observed chemical shift and that of the free guest. Thus, the smaller the difference between these two figures, the larger the error. It is also worthwhile to note that the value of the chemical shift of the complex calculated in the determination of the association constant affects only the scale of the y-axis in the Job Plots and thus its absolute value is unimportant in ascertaining the stoichiometry of the complex. The Job Plot of trication **109** and sodium benzoate **187** resulted in very small shifts, though analysis of these showed a stoichiometry deviating from 1:1. The magnitude of the shifts, however, meant that these results could not be treated as reliable.

Since trication **109** and tricarboxylate **186** have charge complementarity we anticipated that the formation of a 1:1 complex would be observed. This was not, however, what we found. Figure 3.16 shows that the curve passes through a maximum at a mole fraction of anion of approximately 0.4 indicating a host:guest stoichiometry of 3:2. The same stoichiometry was observed when DABCO-based trication **109** was replaced with the corresponding quinuclidine-based trication **148** (Figure 3.17). Possible explanations for this phenomenon lie in the fact that we may be simultaneously observing more than one equilibrium. Any plot will not distinguish between such equilibria and an averaged curve will be seen. It would appear that the case which we presumed would be the most simple is actually a more complex set of equilibria.

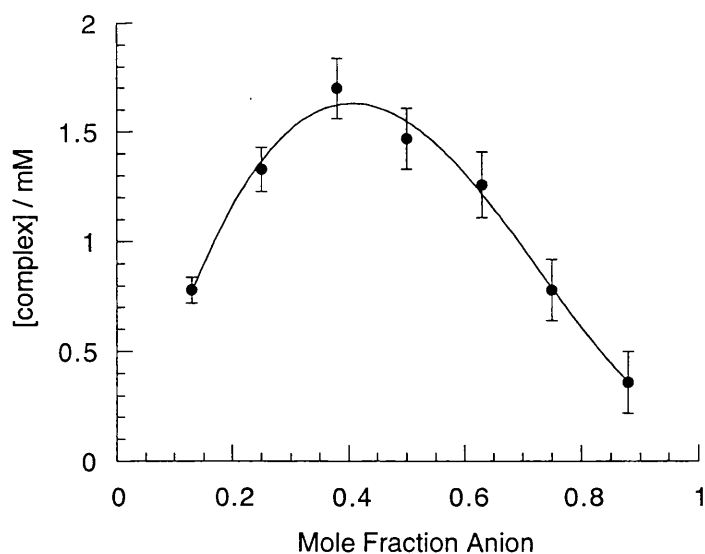
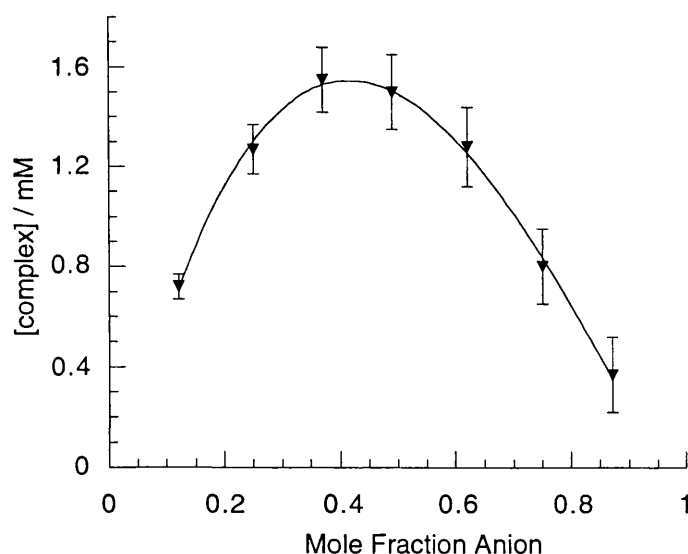


Figure 3.16

—●— 109 vs 186

**Figure 3.17****—▼— 148 vs 186**

Job Plots based on the changes in chemical shift of the cationic species showed no difference in shape from those based on the anion shifts, though obviously the calculated concentration of complex was much larger due to the difference in the results of the NMR titrations.

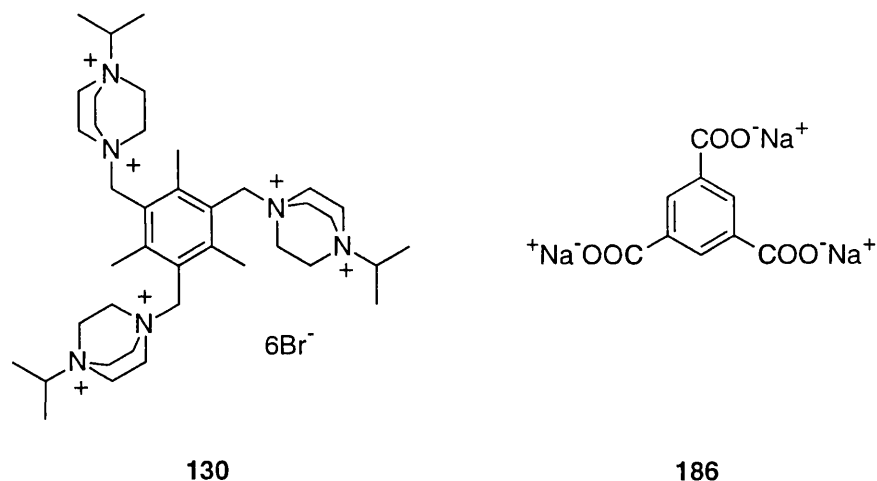
### 3.4.3 NMR Titration of Hexacationic Compounds

The strength of binding between the tricationic compounds and simple organic carboxylates was only weak to moderate. Given that the DABCO-based hexacations we had synthesised contained twice the number of positive charges as the tricationic materials, we were interested to discover whether this resulted in enhanced binding to simple guest species, and what, if any, was the effect of the further substitution of DABCO in the hexacations.

The same protocol as that discussed for the tricationic materials was used in the NMR titration of the hexacationic compounds, although lower concentrations were employed in some of the experiments to reduce the mass of compound to be dissolved. Changes in the chemical shift of the protons in the anion were monitored, along with those of the methyl and benzyl groups in the hexacations. The non-linear curve fitting methods used were as for previous titrations.

Trisodium-1,3,5-benzenetricarboxylate was chosen as the standard guest for use in the titration of the hexacations since it had given rise to the largest shifts in the titrations with the tricationic species. Despite the results of the association constants determinations, we believed this meant that it was the most strongly bound, or at least that the cation and anion showed the most close approach with one other.

To see whether any binding was observed between our trianion and the hexacationic materials, a titration was carried out between hexacation **130** and tricarboxylate **186** in deuterium oxide.



As had been observed with the trications, an upfield change in chemical shift was observed in the trianion, with concomitant changes in the chemical shifts of the methyl and benzyl groups of the hexacation. A plot of the change in chemical shift of the trianion is shown in Figure 3.18. The curve differs from that observed with the cation in that the line appears to be reaching a maximum more quickly and this was confirmed in the determination of the association constant resulted in a value of  $5360 \text{ M}^{-1}$ , a seventy-fold increase on the binding of the trianion with the corresponding trication.

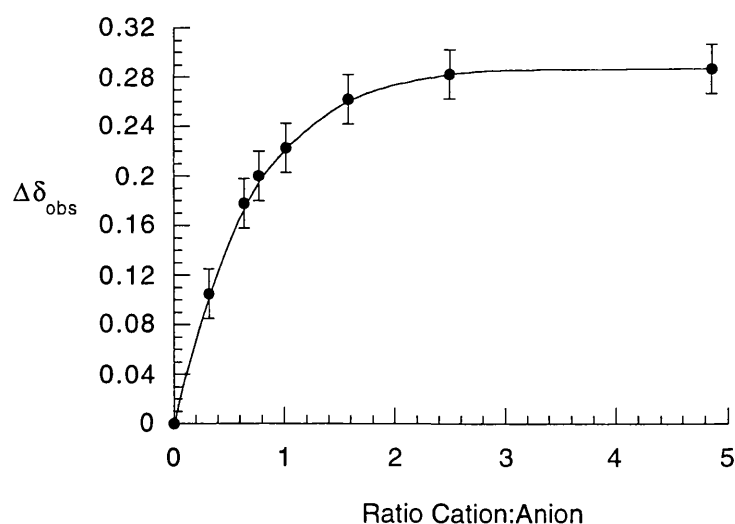


**Figure 3.18**

—●— **130 vs 186**

Unlike titrations involving the tricationic compounds, the upfield changes in chemical shift in the cation were more closely related to those seen in the anion. Figure 3.19 illustrates the change in chemical shift of the methyl group of hexacation **130** during its titration with tricarboxylate **186**. Not only are the shapes of the curves similar, but the magnitude of the change in chemical shift is also of the same order.

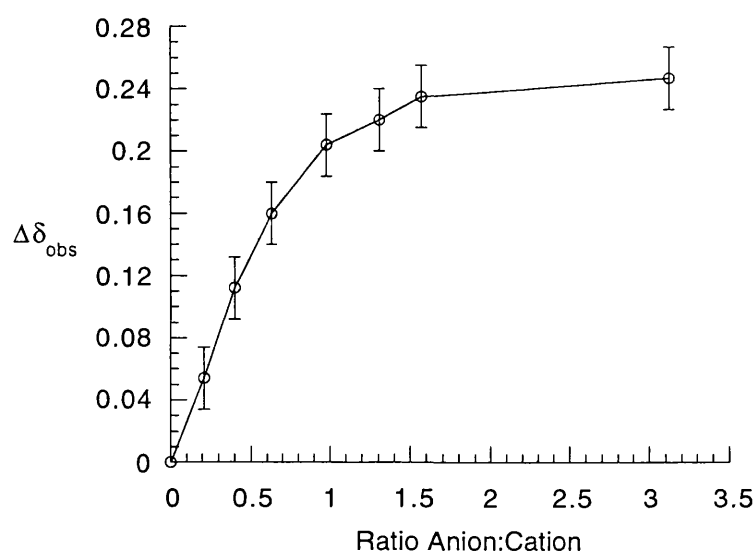


**Figure 3.19**

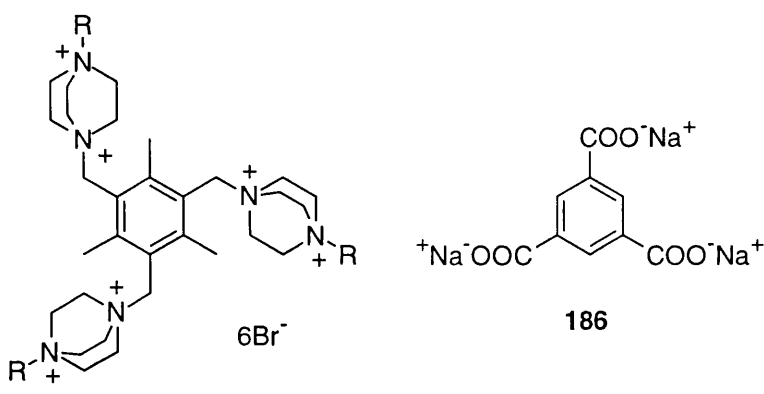
—○— **130 vs 186**

Using the hexacation methyl group shift data, an association constant of  $18140 \text{ M}^{-1}$  was determined. A similar result was obtained using the data from the chemical shifts of the hexacation benzyl group data (Table 3.9). Although these association constants were larger by threefold than that determined from the anion shift, they illustrated that the correlation between cation and anion shifts was greater than in the titrations of the tricationic compounds discussed previously.

NMR Titration of <b>130</b> and <b>186</b>			
Signal	$\Delta\delta_{1:1}$	$\Delta\delta$	$K_a / \text{M}^{-1}$
Trianion	0.223	0.290	5360
Hexacation Benzyl	0.252	0.305	17140
Hexacation Methyl	0.204	0.245	18140

**Table 3.9**

NMR titrations were carried out between the other hexacationic materials that we had synthesised and trianion **186**. The results of these titrations are summarised in Table 3.10.

					
R	Compound	Signal	$\Delta\delta_{1:1}$	$\Delta\delta_{\max}$	$K_a / \text{M}^{-1}$
Me	<b>127</b>	Trianion	0.209	0.24	ND
		Hexacation Benzyl	0.246	0.309	ND
		Hexacation Methyl	0.188	0.247	ND
Et	<b>128</b>	Trianion	0.253	0.407	815
		Hexacation Benzyl	0.261	0.311	38260
		Hexacation Methyl	0.213	0.269	6660
1-Pr	<b>129</b>	Trianion	0.238	0.311	4070
		Hexacation Benzyl	0.234	0.308	3530
		Hexacation Methyl	0.188	0.243	3920
2-Pr	<b>130</b>	Trianion	0.223	0.290	5360
		Hexacation Benzyl	0.252	0.305	17140
		Hexacation Methyl	0.204	0.245	18140
1-Bu	<b>131</b>	Trianion	0.215	0.290	2820
		Hexacation Benzyl	0.237	0.292	11220
		Hexacation Methyl	0.187	0.229	8360

ND indicates that the program used in the determination of  $K_a$  produced no result

**Table 3.10**

A full error analysis for the values of the association constants is difficult to apply but percentage errors are expected to be larger for the smaller association constant values and decrease as the size of the association constant increases.

The magnitude of the change in chemical shift of the tricarboxylate anion varied between titrations, the largest overall shift (0.407 ppm) occurring during titration with ethyl substituted hexacation **128**. The changes in chemical shift of the methyl (0.23-0.27 ppm) and benzyl (0.29-0.31 ppm) groups of the hexacations, however, were all of approximately the same magnitude.

The most consistent results are obtained for 1-propyl substituted hexacation **129**, which gives association constants of the same order for all three signals monitored. The behaviour of the chemical shift of the anion in the titration of methyl substituted hexacation **127** and tricarboxylate **186** was unusual and the plot of the NMR titration is shown in Figure 3.20, which shows that after rising to a maximum value, the magnitude of the change in chemical shift decreases with an increasing ratio of cation:anion.

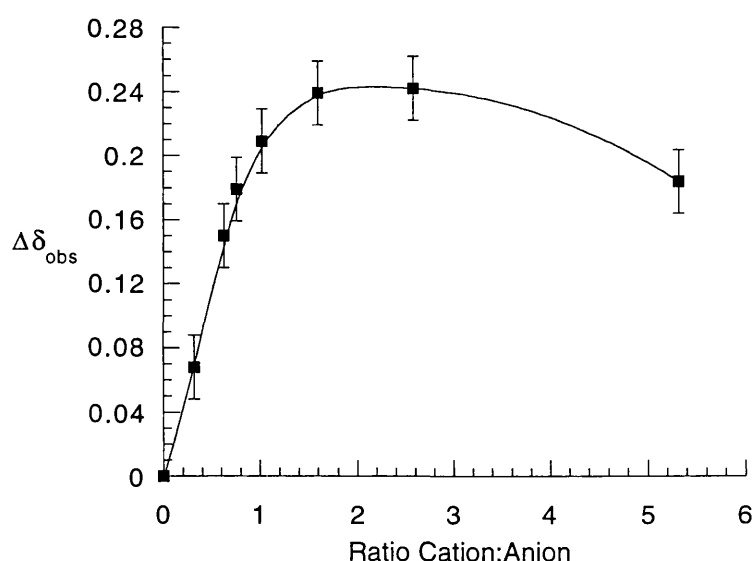
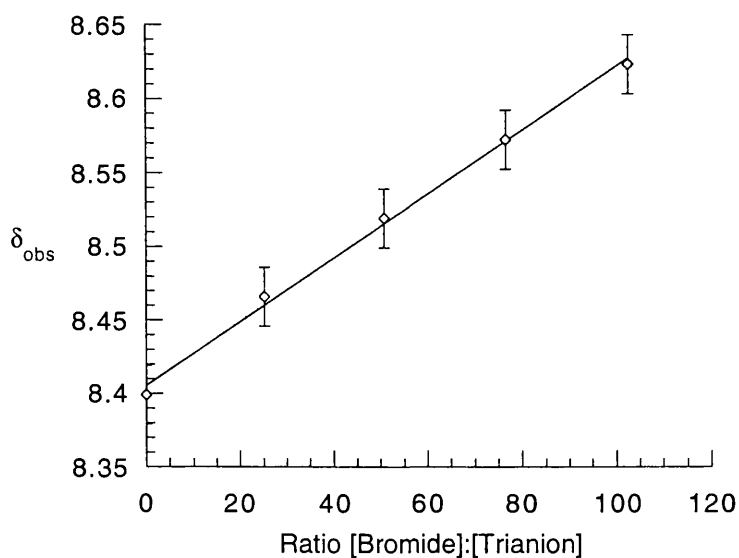


Figure 3.20

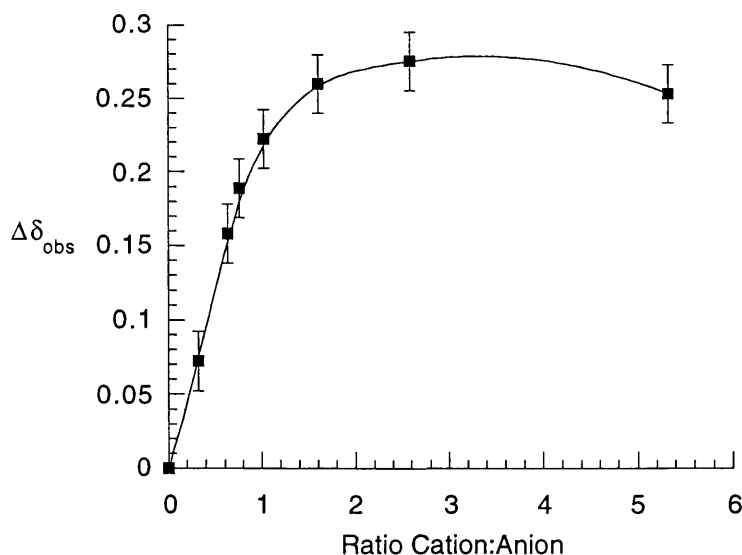
—■— 127 vs 186

We were interested to try and discover the cause of this effect and hypothesised that it may be due to the presence of an excess of bromide ions. For each hexacation in solution there are six bromide anions present also. To investigate whether this excess of bromide ions had any effect on the chemical shift of the tricarboxylate we performed an experiment in which the chemical shift of a solution of tricarboxylate **186** in deuterium oxide was monitored in varying concentrations of sodium bromide. The results of this experiment are outlined in Figure 3.21 which shows that as the concentration of sodium bromide, and thus the concentration of bromide anions, increases, the chemical shift of the trianion moves downfield.

**Figure 3.21**

—◇— 186 vs NaBr

Using these results, corrected shifts were calculated for the trianion in the titration of **127** and **186**, these results being shown in Figure 3.22. This shows that although the decline in the magnitude of  $\Delta\delta_{\text{obs}}$  is still present, it has been somewhat reduced. Even using these data, however, an association constant could not be determined.

**Figure 3.22**

—■— 127 vs 186

No clear pattern emerges in relation to the length of the alkyl chain substitution, whichever of the chemical shifts is being used in the determination of the association constants (Figure 3.23).

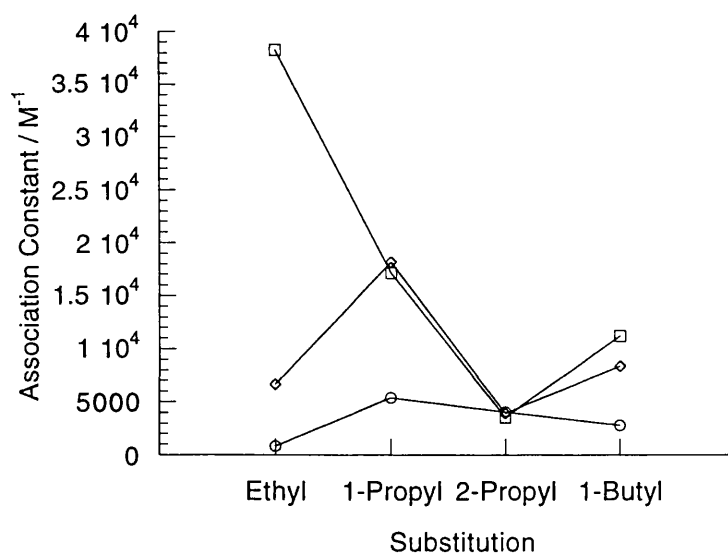
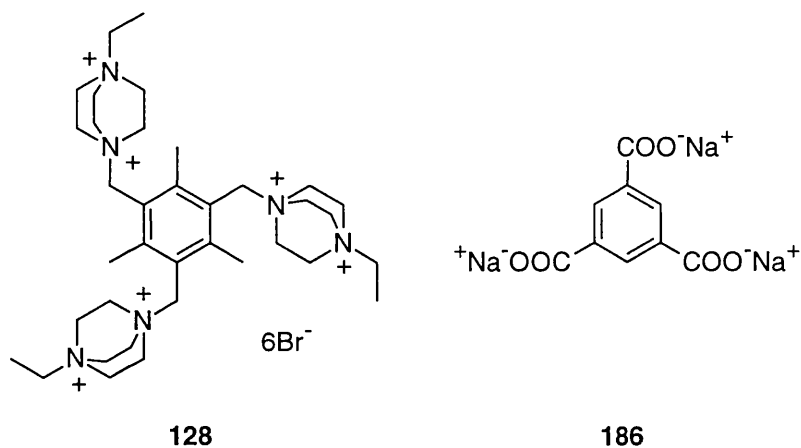


**Figure 3.23**

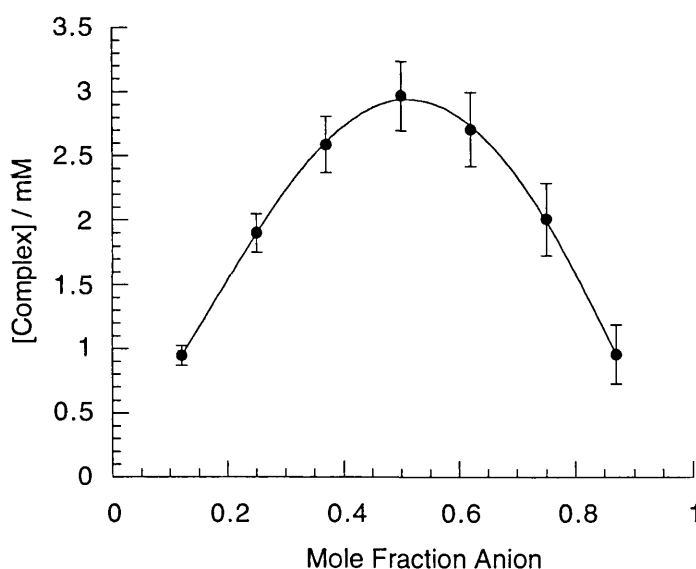
—○— Anion; —□— Cation Benzyl; —◇— Cation Methyl

### 3.4.4 Job Plots - Hexacations

As with the investigation into the tricationic materials, separate experiments were carried out in order to determine the stoichiometry of the complexes formed between the hexacations and the trianion. In all cases the curves showed a maximum at a mole fraction of guest of 0.5, corresponding to a 1:1 stoichiometry. If charge balancing was an important requirement a host:guest stoichiometry of 1:2 might have been expected, but this was not observed. As an example, the Job plot for ethyl-substituted hexacation **128** and tricarboxylate **186** is shown in Figure 3.24.





**Figure 3.24**

—●— 128 vs 186

Similarly shaped curves were obtained based on measurements of changes in chemical shift in the hexacation.

### 3.5 Microcalorimetry

The discrepancies in the  $^1\text{H}$  NMR chemical shift parameters for the combinations of cations and anions and the consequent uncertainty over the association constants led us to investigate an alternative method.

#### 3.5.1 Introduction

Calorimeters are instruments used for the direct measurement of heat quantities, heat production rates and heat capacities. Such information can be used to probe the extent of a reaction and thus in the determination of an association constant for a given process. A calorimeter is a thermodynamic instrument but can also be employed as an analytical tool, for example as a 'process monitor'. Though traditionally used in biological work, Wadsö<sup>151</sup> has reviewed the scope of microcalorimetry in the field of macrocyclic chemistry and points out three important areas for calorimetric experiments: (i) investigations of the thermodynamic properties of host-guest complex formation; (ii) thermodynamic characterisation of macrocyclic compounds with respect to their intermolecular interactions in the condensed state and in solutions; (iii) characterisation of the effect of interactions between living cellular systems and macrocyclic compounds and complexes. Our interest lay in the first of these three uses. Most of the reports into the investigation of macrocyclic compounds have been on cyclodextrins,<sup>152-156</sup> whilst few experiments have been reported on crown ethers,<sup>157,158</sup> cryptands,<sup>158</sup> and calixarenes,<sup>159</sup> but the total number of experiments reported in the literature remains small. In experiments where the

heat evolved is small, and the temperature remains effectively constant, a sensitive calorimeter is used, often referred to as an isothermal calorimeter. Experiments carried out with such an instrument are generically termed Isothermal Titration Calorimetry (ITC) experiments.

A schematic diagram of a standard ITC instrument is shown in Figure 3.25. In an ITC experiment the enthalpy of binding is measured from a small reaction cell. There are two such cells, one of which is a thermal reference and is typically filled with water and the other is filled with one of the interacting species under study, which are kept at a constant reaction temperature by heating (the 'ambient' temperature is maintained at temperatures below that of the reaction by an external waterbath). Aliquots of the other interacting species are injected into the 'sample' cell and depending on the endo- or exothermic nature of the reaction the amount of heat applied to the sample cell will be increased or decreased respectively to maintain thermal parity. It is this change in heat requirement that is measured.

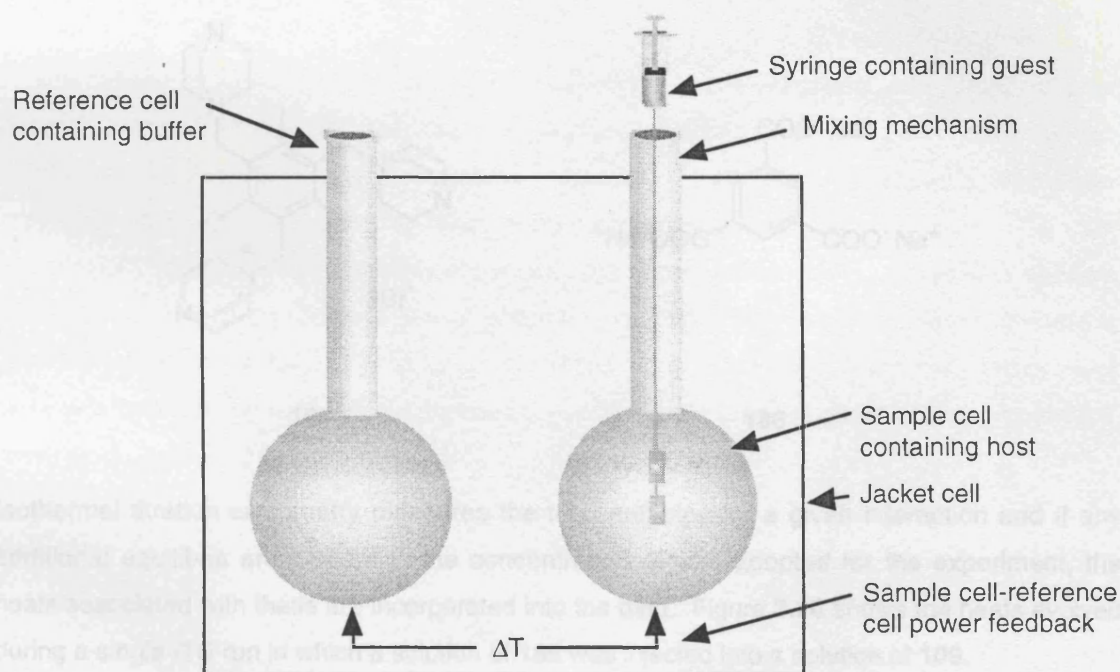


**Figure 3.25 - Schematic Diagram of a Commercially Available ITC Instrument**

The concentrations of the reactants chosen are such that any binding sites will be gradually saturated throughout an experiment and the last few injections should effectively represent the heat of dilution of the reactant in the syringe into the solvent employed, which is also separately determined in a control experiment. The heat of each injection minus its respective heat of dilution is calculated and plotted against the molar ratio of reactants. For a simple 1:1 binding event the resultant curve is sigmoidal, the profile being determined by the binding constant. The curve is fitted to a simple algorithm which allows for the determination of the binding constant,  $K_B$ ,

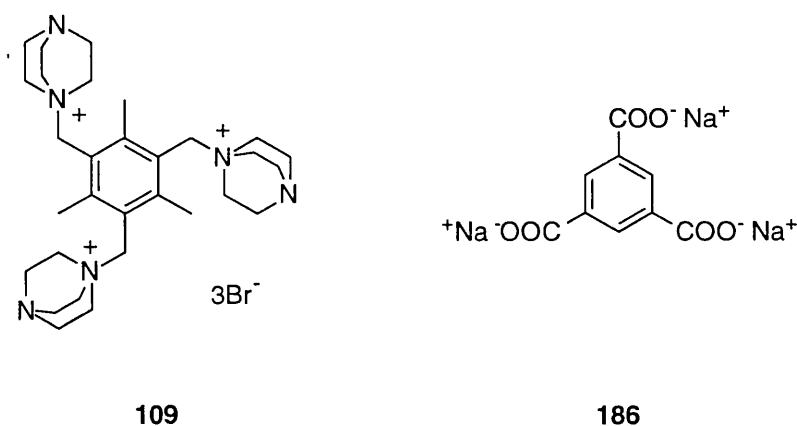
and the enthalpy,  $\Delta H$ . From this a full thermodynamic characterisation can be obtained using Equation 17:<sup>160,161</sup>

$$-RT\ln K_B = \Delta H - T\Delta S = \Delta G \quad (17)$$

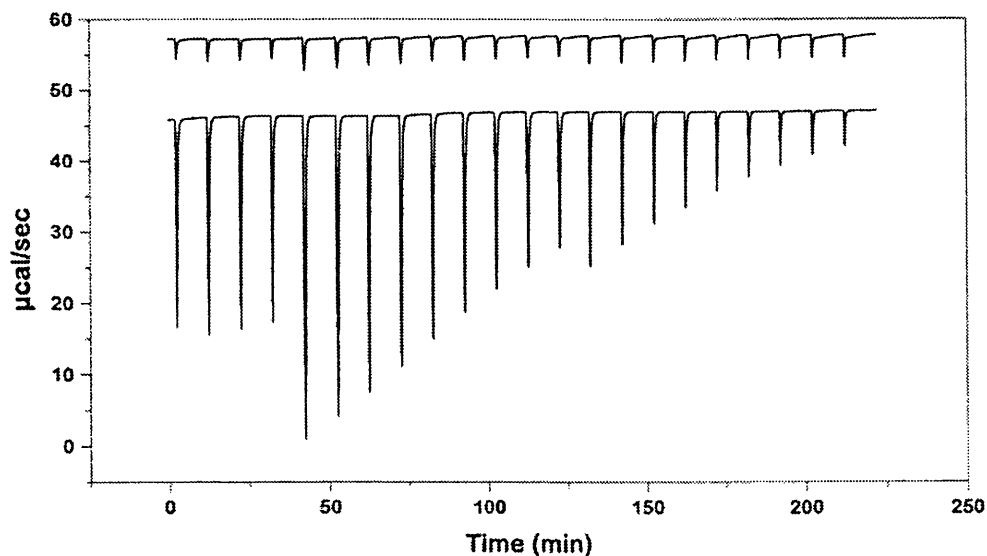
Where  $R$  is the gas constant,  $T$  is the absolute temperature,  $\Delta S$  is the entropy change and  $\Delta G$  is the free energy change for the interaction.

### 3.5.2 Calorimetric Analysis of Polycationic Materials

We chose initially to investigate the interaction between trication **109** and trianion **186** since of all the interactions studied this would appear to have the best stereo- and electronic complementarity and thus was anticipated to give rise to a large association constant, despite the results obtained from NMR methods.



Isothermal titration calorimetry measures the total enthalpy for a given interaction and if any additional equilibria are present in the concentration regime adopted for the experiment, the heats associated with these are incorporated into the data. Figure 3.26 shows the heats evolved during a single ITC run in which a solution of **186** was injected into a solution of **109**.

**Figure 3.26**

In many cases it is possible to deconvolute the heat effects of several events. The titration curves obtained (Figure 3.27) showed that the trication:trianion interaction did not occur with a simple 1:1 stoichiometry, as had also been noted from NMR experiments. It appears that larger complexes are more stable, possibly resulting from interaction of the monomeric units. The data for titrations performed under a variety of conditions is shown in Table 3.11. There also appears to be a small effect of the concentration of cation on the titration curve which could result from the anion induced oligomerisation of the cation in the cell. This is not unexpected since solvation of the largely hydrophobic interacting molecules is due to the presence of charge which on complex formation is unable to interact with solvent.

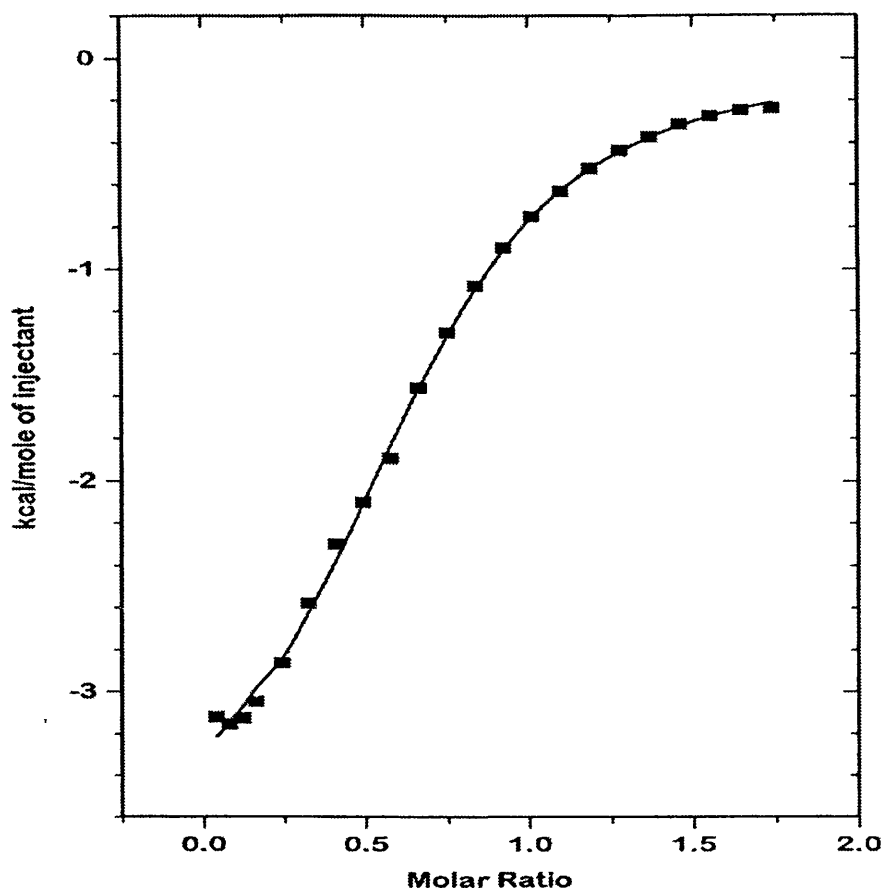


Figure 3.27

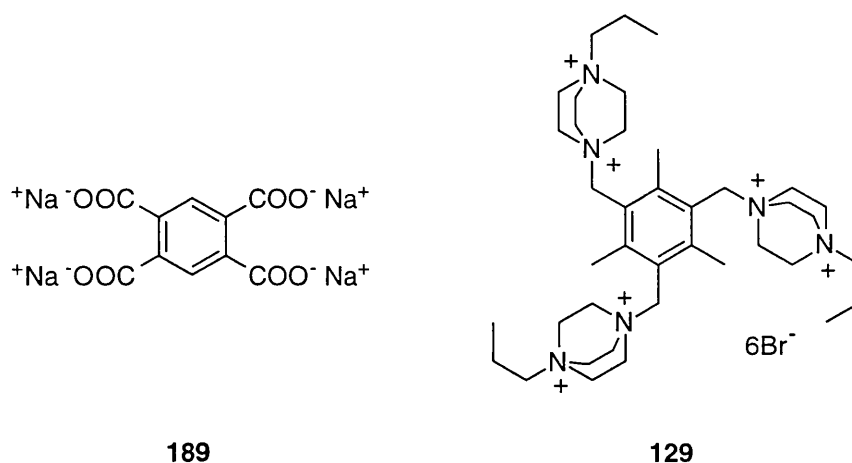
[Anion] in syringe mM	[Cation] in cell mM	Stoichiometry N	$K_B$ $M^{-1}$	$\Delta H$ $kJ\ mol^{-1}$
30	3.0	0.526	1070	-17.70
40	4.5	0.621	1720	-16.72
40	6.0	0.619	990	-21.21
56	9.6	0.619	585	-25.82
56	9.6	0.597	496	-26.03

Table 3.11

The stoichiometry,  $N$ , of this reaction was determined as 0.596 with a large standard deviation. The binding constant  $K_B$  was found to be  $972\ M^{-1}$ , again with a large standard deviation, and the mean enthalpy of reaction,  $\Delta H$ , was  $-21.5 \pm 3.9\ kJ\ mol^{-1}$ . Although the errors in these determinations are high, this is to be expected for a system of this type in which the interaction is weak and in which other processes are occurring. From Equation 17, a mean value for  $\Delta G$  of  $-16.8 \pm 1.1\ kJ\ mol^{-1}$  was derived.

That most of the binding of the two ions is enthalpic is not surprising if we assume that all of the binding is electrostatic in origin, a not unreasonable assumption given the nature of the reacting species and their mode of interaction. If it is assumed that the binding affinity for each bridge is the same, which presumes a 1:1 complex despite the complexity of the process, a value for  $\Delta H/n$  ( $n=3$ ), the enthalpy of binding of a salt bridge, of  $-7.2 \text{ kJ mol}^{-1}$  is obtained. This is very similar to the value of  $\Delta G/n$  determined by Schneider *et al.*,<sup>84</sup> from  $^1\text{H}$  NMR titration studies, who suggested a value of  $-5 \pm 1 \text{ kJ mol}^{-1}$ . In the present case the addition of the entropy term gives a value of  $\Delta G/n$  of  $-5.6 \text{ kJ mol}^{-1}$ .

Isothermal titration calorimetry experiments were also carried out using trication **109** and tetraanion **189**. In this case the interaction was too weak for an accurate determination of the thermodynamic parameters to be made using ITC. Unlike the interaction between **109** and **186**, this process is endothermic and any interaction must be entropy driven. This result illustrates the problem with the  $^1\text{H}$  NMR method for these systems - although the chemical shift change in the complexation of **109** with **189** was much smaller than that between **109** and **186**, because the latter took longer to reach its maximum value a greater association constant was determined for the trication/tetraanion combination.



Since our  $^1\text{H}$  NMR experiments with hexacation **129** and trianion **186** had shown the most closely correlated association constants in terms of which spectral signal was used in the determination, ITC experiments were carried out on this system. The additional charged groups present on the hexacation compared to the trication add to the complexity of the titration and the titration curve appears to incorporate an additional interaction (Figure 3.28). This is attributed to the trianion induced association of the hexacation giving rise to higher order complexes. As the trianion is added to the calorimetric cell containing the hexacations, the huge excess of positively charged host molecules could result in structures involving a network of molecules in which the

guest trianion binds a number of hexacationic molecules. As further anions are added these networks dissociate to give rise to smaller intermolecular complexes. The titration curves are too complex for reliable fitting and hence no thermodynamic data is reported.

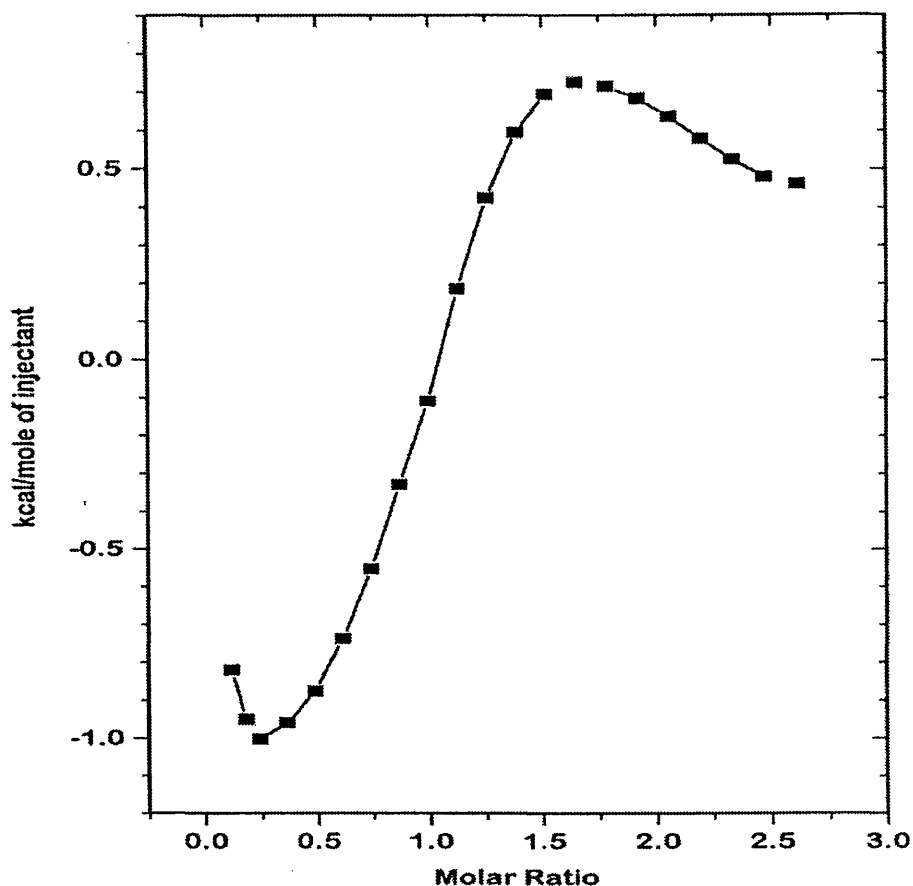


Figure 3.28

Further ITC experiments were carried out between hexacation **129** and tetraanion **189**, a summary of the results being given in Table 3.12. The reaction was endothermic, indicating that the binding was again entropic in character. The stoichiometry of the reaction suggests that the model is more complex than that taken to derive these results, but there does seem to be a significant difference in the nature of the trication/trianion interaction compared with those of the other systems investigated by isothermal calorimetry. The large increase in entropy in this system may derive from the release of complexed water molecules to the bulk environment.

Summary of ITC of <b>129</b> and <b>189</b>	
$K_B / M^{-1}$	1170
N	1.63
$\Delta H / kJ mol^{-1}$	$+11.7 \pm 2.8$
$\Delta G / kJ mol^{-1}$	$-17.4 \pm 0.9$

Table 3.12

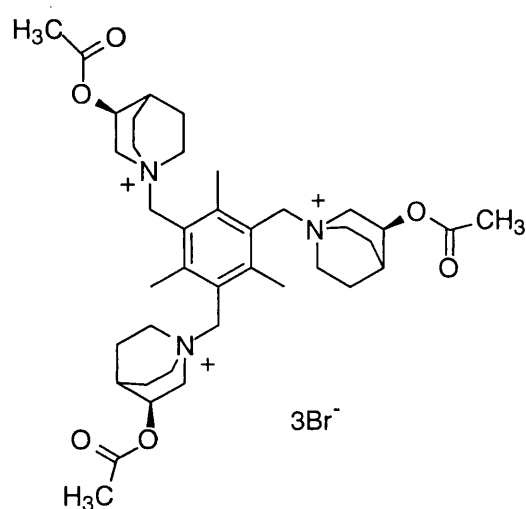
### 3.5.3 Comparison of Results from $^1H$ NMR Titrations and ITC

$^1H$  NMR titration showed that the two systems with the assumed best-fit with regard to charge equivalence, that is DABCO-based trication **109** and trianion **186**, and quinuclidine-based trication **148** and trianion **186**, showed much the largest change in chemical shift of the anion protons ( $\Delta\delta \sim 0.5$ ). When the values of  $K_a$  were determined from the data, however, they were found to be smaller than those obtained for other systems. This reflects the slower attainment of maximum  $\Delta\delta$  for these combinations compared to other systems. Since ITC shows that the combination of DABCO-based trication **109** and trianion **186** is enthalpically driven and the most tightly bound we may here be observing combinations in which, after the initial binding, further arrangement of the two ligands together with the solvent and other counter-ions occurs to give a tighter ion-pair,<sup>162,163</sup> so that the chemical shift does not reflect the actual chemical shift of the initially formed ion-pair. Such complications do, of course, tend to invalidate the original assumptions by which  $K_a$  was determined from the  $^1H$  chemical shift changes.

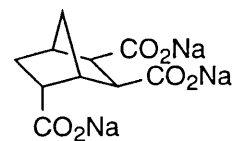
## 3.6 Future Perspectives

The use of isothermal titration calorimetry in the field of host-guest chemistry is relatively new and continued work using this technique is anticipated. Our successful synthesis of chiral trication **160** has provided the opportunity for new avenues of research and the development of materials with novel host-guest properties. In particular, these compounds may be able to discriminate between chiral anions such as **192** and **193**. This area is currently under investigation by co-workers.





160



192



193

### 3.7 Conclusion

The comparatively simple polycations synthesised during the course of the project exhibit a number of interesting features and pose a number of questions regarding the interactions of ions in aqueous solution. Restricting the conformational mobility of the polycation clearly changes its behaviour and allows it to interact at all cationic centres at the same time with a complementary polyanion. This is most strikingly seen in the precipitation of ferricyanide salts of the hexasubstituted trications derived from either DABCO or quinuclidine, which does not occur with the corresponding trisubstituted benzene analogues. Charge matching is probably the dominant factor in the interactions of these polycations, although the shape of the polyanion component is also of importance. We had hoped that these systems would be of sufficient simplicity that a value for a salt-bridge between a cationic and anionic charge would could have been measured or estimated with some accuracy. As the results from isothermal titration calorimetry show, however, the interaction between the designated ions, the spectator counterions and the water molecules in these systems is already complex. It would appear that, when the concentration of polycation is high compared to the polyanion, networks are formed in which the polyanion species is shared by more than one polycation. Increasing the concentration of the polyanion leads to regrouping of these species and eventually, in favourable cases, to the formation of a system in which there approximates a one-to-one correspondence between the polycation and polyanion. As these changes occur it seems likely that water molecules are displaced from solvation sites in the charged species to the bulk water. The spectator ions are themselves not indifferent, as we have shown by measuring the effects of salt concentration on the  $^1\text{H}$  NMR chemical shifts. Our results also pose problems for the use of  $^1\text{H}$  NMR titrations in determining binding constants, at least in aqueous solution. Because the determination of the binding constant depends on the shape of the binding curve and not on the change in chemical shift, those systems which appear to dock together with the displacement of water molecules and spectator ions take time to attain the

maximum chemical shift and show "weak" binding from analysis of the titration curves. When the complete process is explored by ITC then these systems have much greater enthalpies of binding and higher binding constants.

---

## 4 Experimental

### 4.1 Synthesis

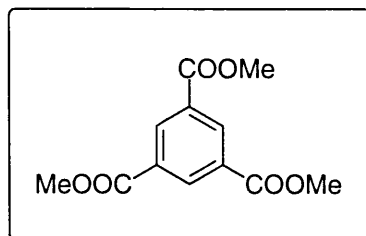
Unless otherwise stated, IR spectra were recorded on a Perkin-Elmer 1605 FT-IR spectrophotometer. Melting points were determined on a Reichert melting point apparatus and are uncorrected. Optical rotations were measured on an Optical Activity Ltd Polaar 2000 automatic polarimeter. Mass spectra were recorded on either a VG micromass 305 electron impact (EI) or VG-ZAB SE fast atom bombardment (FAB) mass spectrometer with Finnigan Incos II data system at University College London. In some cases overloaded spectra were recorded in order to see the parent-ion, and in this case neither the relative intensities nor a base peak are recorded. For hexabromide salts a complex splitting pattern is observed in the parent-ion and in such cases only the most intense peak in the group is noted.  $^1\text{H}$  and  $^{13}\text{C}$  NMR spectra were recorded at 400 MHz and 100 MHz respectively on a Varian VXR-400 instrument, with residual protic solvent as the internal standard, except where  $\text{D}_2\text{O}$  was used as the solvent. In the latter case the spectrometer was referenced to 3-(trimethylsilyl)propionic-2,2,3,3- $d_4$  acid, sodium salt, before insertion of the sample to be examined. Spectra were recorded in the solvent specified, with chemical shifts expressed in parts per million ( $\delta$ ) relative to the internal standard, and coupling constants  $J$  measured in Hertz (Hz). Microanalyses were carried out by the microanalytical section of the Chemistry Department, University College London.

Chemical reagents were purchased from Aldrich Chemical Co., Lancaster Synthesis, ACROS and BDH. Diethyl ether and tetrahydrofuran (sodium and benzophenone) were distilled under an atmosphere of nitrogen immediately prior to use. All other solvents and reagents were used as received unless otherwise stated.

Analytical thin layer chromatography (tlc) was performed on pre-coated aluminium backed plates (Merck Kieselgel 60  $\text{F}_{254}$ ) and visualised using ultraviolet light (254 nm), iodine or potassium permanganate [add 62.5 g of  $\text{Na}_2\text{CO}_3$  in water (1.25 L) to 12.5 g of  $\text{KMnO}_4$  in water (1.25 L)] as appropriate.

## 4.2 Starting Materials

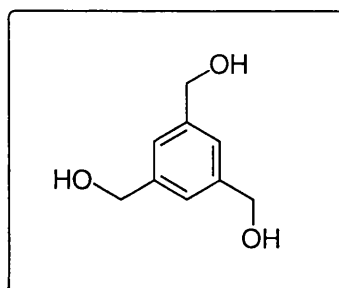
### 4.2.1 Trimethyl benzene-1,3,5-tricarboxylate 100



1,3,5-Benzene tricarboxylic acid (2.02 g, 9.61 mmol) was dissolved in methanol (55 mL). Concentrated sulfuric acid (3 mL) was added and the mixture was heated to reflux for 4 h. As the solution cooled a precipitate was formed. This precipitate was removed by filtration and the filtrate extracted with ether (3x50 mL). The combined organic extracts were washed with sodium hydrogen carbonate (1 M, 3x30 mL) and water (1x30 mL). The ethereal solution was dried over magnesium sulfate and the solvent removed under reduced pressure to yield a white solid. This solid and the initial precipitate were combined and the material recrystallised from methanol to yield the triester as white plates (2.08 g, 7.17 mmol, 86%).

Mp	143-145 °C, lit. <sup>129</sup> 144-145 °C
<sup>1</sup> H NMR (CDCl <sub>3</sub> )	3.95 (s, 9H, CH <sub>3</sub> ), 8.82 (s, 3H, ArH)
<sup>13</sup> C NMR (CDCl <sub>3</sub> )	52.6, 131.1, 134.5, 165.4
IR (KBr disc, cm <sup>-1</sup> )	1729 (s), 1452 (m), 1432 (m), 1342 (m), 1247 (s), 1000 (m), 740 (m)
MS (EI) (m/z %)	252 (62.5) (M <sup>+</sup> ), 221 (100)
C <sub>12</sub> H <sub>12</sub> O <sub>6</sub>	calc. C 57.14 H 4.80
(252.22)	found 57.10 4.64

### 4.2.2 1,3,5-Trishydroxymethylbenzene 101

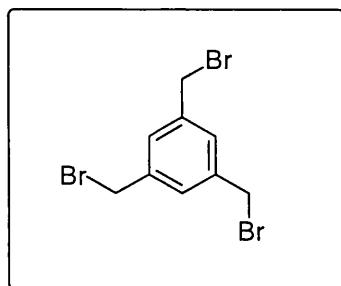


Trimethyl benzene-1,3,5-tricarboxylate (4.94 g, 19.6 mmol) dissolved in THF (100 mL) was added dropwise over 90 min to a suspension of lithium aluminium hydride (2.10 g, 55.3 mmol) in THF

(100 mL) at room temperature, under nitrogen, to give a yellow coloured suspension. The mixture was heated to reflux for 6 h after which it was stirred overnight at room temperature. The reaction mixture was then quenched with 10% w/v sodium hydroxide (5 mL) and stirred for 2 h. The resultant aluminium oxides were then removed by filtration and the filtrate dried over magnesium sulfate. Evaporation of the solvent, followed by recrystallisation of the residue from hot ethyl acetate yielded the product as white needles (1.56 g, 9.3 mmol, 47%).

Mp	77-78 °C, lit. <sup>127</sup> 77-78 °C.			
<sup>1</sup> H NMR (D <sub>2</sub> O)	4.67 (s, 6H, CH <sub>2</sub> ) 7.33 (s, 3H, ArH)			
<sup>13</sup> C NMR (D <sub>2</sub> O)	66.5, 128.5, 143.8			
IR (KBr disc, cm <sup>-1</sup> )	3297 (br s), 3190 (br s), 1610 (w), 1445 (m), 1361 (m)			
MS (EI) (m/z %)	168 (35.1) (M <sup>+</sup> ), 150 (9.0), 79 (100)			
C <sub>9</sub> H <sub>12</sub> O <sub>3</sub>	calc.	C 64.27	H 7.19	O 28.54
(168.19)	found	64.17	7.26	28.57

#### 4.2.3 1,3,5-Tris(bromomethyl)benzene 96



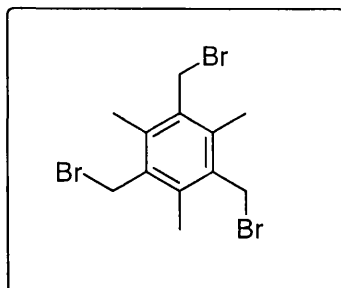
A solution of phosphorus tribromide (2.0 mL, 20.69 mmol) in dry ether (60 mL) was slowly added to a suspension of 1,3,5-tris(hydroxymethyl)benzene (1.48 g, 8.80 mmol) in dry ether (100 mL), at 0 °C. The reaction mixture was stirred for 2 h at 0 °C, then for a further 2 h at room temperature. Water (100 mL) was added and two layers formed. The organic layer was separated, washed with water (3x25 mL) and dried over magnesium sulfate. Removal of the solvent under reduced pressure afforded the tribromide as a white solid (2.66 g, 7.45 mmol, 85%).

Mp	93-94 °C, lit. <sup>127</sup> 93-95 °C.			
<sup>1</sup> H NMR (CDCl <sub>3</sub> )	4.44 (s, 6H, CH <sub>2</sub> ), 7.33 (s, 3H, ArH)			
<sup>13</sup> C NMR (CDCl <sub>3</sub> )	32.2, 129.5, 139.0			
IR (KBr disc, cm <sup>-1</sup> )	1213 (s), 894 (w), 704 (m), 582 (s)			
MS (EI) (m/z %)	360 (0.1), 358 (1.6), 356 (1.7), 354 (0.2) (M <sup>+</sup> ), 277 (100)			

---

$C_9H_9Br_3$	calc.	C 30.29	H 2.54
(356.88)	found	30.73	2.44

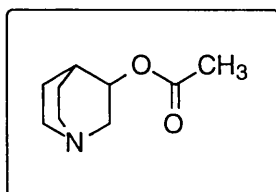
#### 4.2.4 2,4,6-Tris(bromomethyl)mesitylene 102



A solution of hydrogen bromide in acetic acid (45% w/v, 17.5 mL) was added rapidly to a mixture of mesitylene (3.02 g, 25.1 mmol), paraformaldehyde (2.51 g, 83.6 mmol) and glacial acetic acid (25 mL). The mixture was stirred for 20 h at 95 °C and then poured into water (100 mL). A precipitate formed which was removed by filtration on a glass frit and dried under vacuum. Recrystallisation from chloroform/light petroleum yielded the product as white needles (8.62 g, 21.6 mmol, 86%).

Mp	184-186 °C, lit. <sup>130</sup> 186 °C.
$^1H$ NMR ( $CDCl_3$ )	2.45 (s, 9H, $ArCH_3$ ), 4.56 (s, 6H, $CH_2$ )
$^{13}C$ NMR ( $CDCl_3$ )	15.4, 29.9, 133.2, 137.9
IR (KBr disc, $cm^{-1}$ )	1560 (w), 1444 (w), 1379 (w), 1206 (s), 1196 (s), 786 (m), 572 (m), 468 (m)
MS (EI) (m/z %)	400 (1.2), 398 (2.1) ( $M^+$ ), 319 (46.2), 159 (100)
$C_{12}H_{15}Br_3$	calc. C 36.13 H 3.79
(398.96)	found 36.28 3.56

#### 4.2.5 3-Acetoxyquinuclidine 153



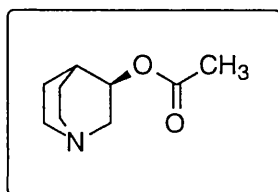
Racemic 3-quinuclidinol (1.01 g, 7.94 mmol) and acetic anhydride (30 mL) were heated to reflux for 5 h. The solution was concentrated under reduced pressure, neutralised with saturated sodium hydrogen carbonate solution (30 mL) and extracted with chloroform (3x80 mL). The

---

combined organic extracts were dried over magnesium sulfate and evaporated. The residue was distilled (~40 °C, 0.1 mmHg) using a microdistillation apparatus with a dowel rod inserted in the distillation flask to prevent bumping, providing a colourless oil (0.98 g, 5.79 mmol, 73%).

$^1\text{H}$ NMR ( $\text{CDCl}_3$ )	1.35-1.39 (m, 1H, CH), 1.50-1.56 (m, 1H, CH), 1.62-1.69 (m, 1H, CH), 1.78-1.84 (m, 1H, CH), 1.95-2.00 (m, 1H, CH), 2.02 (s, 3H, $\text{CH}_3$ ), 2.63-2.88 (m, 6H, $\text{N}(\text{CH}_2)_3$ ), 3.17-3.23 (m, 1H, $\text{NCH}_2\text{CH}_2\text{CH}$ ), 4.74-4.78 (m, 1H, $\text{HCOAc}$ )
$^{13}\text{C}$ NMR ( $\text{CDCl}_3$ )	19.4, 21.1, 24.4, 25.0, 46.3, 47.2, 55.3, 71.2, 170.7
IR (neat film, $\text{cm}^{-1}$ )	2944 (s), 2871 (m), 1733 (s), 1656 (w), 1450 (w), 1369 (m), 1318 (w), 1246 (s), 1029 (m), 784 (w)
MS (FAB) ( $m/z$ %)	170 (100) ( $\text{MH}^+$ )

#### 4.2.6 (R)-(+)-3-Acetoxyquinuclidine 159



L-(+)-tartaric acid (0.51 g, 3.40 mmol) was dissolved in 80% ethanol (10 mL) and racemic 3-acetoxyquinuclidine (0.58 g, 3.40 mmol) was added. The solution was left for 72 h at room temperature. A white solid precipitated and was removed by filtration. The solid was recrystallised in 80% ethanol affording white needles of resolved (R)-(+)-3-Acetoxyquinuclidine tartrate (0.35 g, 1.10 mmol, 65%).

Mp	93-95 °C, lit. <sup>132</sup> 94-95 °C
$[\alpha]^{25}_{\text{D}}$	+5.3 ° ( $c = 2.2$ , $\text{H}_2\text{O}$ ) (lit. <sup>132</sup> +3.6 ° ( $c = 2.2$ , $\text{H}_2\text{O}$ ))

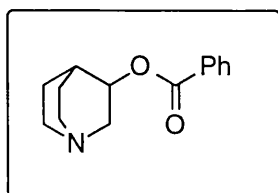
The resolved tartrate was dissolved in water and the solution made alkaline with potassium carbonate. The ester was extracted with chloroform (3x50 mL). The extracts were dried over magnesium sulfate, filtered and concentrated to provide a colourless oil.

$[\alpha]^{25}_{\text{D}}$	+21.4 ° ( $c = 2.2$ , $\text{H}_2\text{O}$ ) (lit. <sup>132</sup> +28.5 ° ( $c = 2.2$ , $\text{EtOH}$ ))
$^1\text{H}$ NMR ( $\text{CDCl}_3$ )	1.35-1.39 (m, 1H, CH), 1.50-1.56 (m, 1H, CH), 1.62-1.69 (m, 1H, CH), 1.78-1.84 (m, 1H, CH), 1.95-2.00 (m, 1H, CH), 2.02 (s, 3H, $\text{CH}_3$ ), 2.63-2.88 (m, 6H, $\text{N}(\text{CH}_2)_3$ ), 3.17-3.23 (m, 1H, $\text{NCH}_2\text{CH}_2\text{CH}$ ), 4.74-4.78 (m, 1H, $\text{HCOAc}$ )

---

$^{13}\text{C}$ NMR ( $\text{CDCl}_3$ )	19.4, 21.1, 24.4, 25.0, 46.3, 47.2, 55.3, 71.2, 170.7
IR (neat film, $\text{cm}^{-1}$ )	2944 (s), 2871 (m), 1733 (s), 1656 (w), 1450 (w), 1369 (m), 1318 (w), 1246 (s), 1029 (m), 784 (w)
MS (FAB) ( $m/z$ %)	170 (100) ( $\text{MH}^+$ )

#### 4.2.7 3-Benzoyloxyquinuclidine 154



Racemic 3-quinuclidinol (0.41 g, 3.22 mmol) and benzoyl chloride (1.50 mL, 12.9 mmol) were heated to reflux overnight in toluene (35 mL). The mixture was extracted with 10% sulfuric acid (30 mL). The acid layer was extracted with diethyl ether (3x60 mL). The sulfuric acid solution was treated with a saturated sodium carbonate solution until all no more gas was evolved and then treated with diethyl ether (3x60 mL). The ether extract was dried over magnesium sulfate and the solvent evaporated yielding a colourless oil (0.26 g, 1.12 mmol, 35%).

$^1\text{H}$ NMR ( $\text{CDCl}_3$ )	1.41-1.49 (m, 1H, CH), 1.58-1.65 (m, 1H, CH), 1.68-1.75 (m, 1H, CH), 1.92-2.00 (m, 1H, CH), 2.12-2.14 (m, 1H, CH), 2.74-3.00 (m, 6H, $\text{N}(\text{CH}_2)_3$ ), 3.30-3.36 (m, 1H, $\text{NCH}_2\text{CH}_2\text{CH}$ ), 5.00-5.04 (m, 1H, $\text{HCOCOPh}$ ), 7.43 (t, $^3J_{\text{H-H}} = 7.6$ Hz, 2H, $\text{H}_3$ ), 7.55 (t, $^3J_{\text{H-H}} = 7.4$ Hz, 1H, $\text{H}_4$ ), 8.03 (d, $^3J_{\text{H-H}} = 7.1$ Hz, 2H, $\text{H}_2$ )
$^{13}\text{C}$ NMR ( $\text{CDCl}_3$ )	19.8, 24.6, 25.4, 46.6, 47.5, 55.7, 71.9, 128.4, 129.6, 130.5, 133.0, 166.3
IR (neat film, $\text{cm}^{-1}$ )	2943 (s), 2870 (w), 1714 (s), 1601 (w), 1451 (w), 1316 (m), 1275 (s), 1113 (m), 1064 (m), 1021 (m), 714 (m)
MS (FAB) ( $m/z$ %)	232 (100) ( $\text{MH}^+$ )

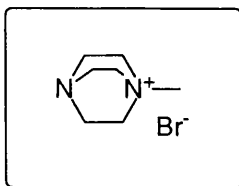
### 4.3 Monocations

#### 4.3.1 General Procedure

The bromoalkane was added via a syringe to a solution of DABCO in acetonitrile over a period of 15 min. The resultant mixture was stirred for either 4-6 h or overnight, after which time the solution was poured into diethyl ether (400-700 mL) and stirred for 1 h. A precipitate formed which was removed by filtration and dried *in vacuo*.



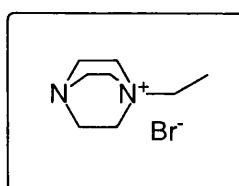
## 4.3.2 N-Methyl-DABCO Bromide 119



To a solution of DABCO (2.50 g, 22.3 mmol) in acetonitrile (40 mL) was added bromomethane in diethyl ether (2.0 M solution, 6.0 mL, 12 mmol). The mixture was stirred for 4 h after which time it was poured into diethyl ether (400 mL) and stirred for 30 min. The precipitate formed was removed by filtration and dried *in vacuo* giving the product as a white hygroscopic powder (2.23 g, 10.8 mmol, 90%).

Mp	253-255 °C (dec.)
$^1\text{H}$ NMR ( $\text{D}_2\text{O}$ )	3.09 (s, 3H, $\text{CH}_3$ ), 3.23 (t, 6H, $^3J_{\text{H-H}} = 7.4$ Hz, $\text{N-CH}_2$ ), 3.43 (t, 6H, $^3J_{\text{H-H}} = 7.6$ Hz, $\text{N}^+\text{-CH}_2$ )
$^{13}\text{C}$ NMR ( $\text{D}_2\text{O}$ )	46.8, 54.2, 56.6
IR (KBr disc, $\text{cm}^{-1}$ )	1636 (br w), 1469 (m), 1354 (w), 1326 (w), 1119 (m), 1056 (m), 993 (w), 917 (w), 842 (m), 794 (m)
FAB-MS ( $m/z$ %)	335 (7.9), 333 (8.1) ( $[\text{2M-Br}]^+$ ), 127 (100) ( $[\text{M-Br}]^+$ )

## 4.3.3 N-Ethyl-DABCO Bromide 120



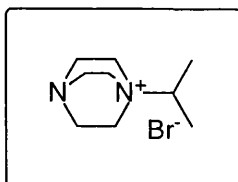
DABCO (2.78 g, 24.8 mmol) and 1-bromoethane (1.00 mL, 13.4 mmol) in acetonitrile (40 mL) were treated as described in the general procedure to give the product as a white hygroscopic powder (2.47 g, 11.2 mmol, 83%).

Mp	190-192 °C
$^1\text{H}$ NMR ( $\text{D}_2\text{O}$ )	1.38 (t, 3H, $^3J_{\text{H-H}} = 7.1$ Hz, $\text{CH}_3$ ), 3.25 (br, 6H, $\text{N-CH}_2$ ), 3.41 (m, 8H, $\text{N}^+\text{-CH}_2\text{CH}_2\text{-N}$ & $\text{CH}_3\text{CH}_2\text{-N}^+$ )
$^{13}\text{C}$ NMR ( $\text{D}_2\text{O}$ )	9.8, 47.0, 54.3, 62.8

---

IR (KBr disc, $\text{cm}^{-1}$ )	1654 (br w), 1464 (m), 1412 (w), 1324 (w), 1095 (m), 1058 (m), 999 (w), 846 (w), 799 (w)
FAB-MS ( $m/z$ %)	363 (7.5), 361 (7.7) ( $[2\text{M}-\text{Br}]^+$ ), 141 (100) ( $[\text{M}-\text{Br}]^+$ )

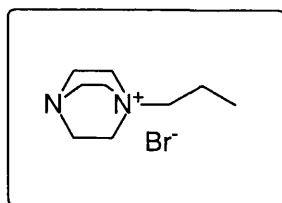
#### 4.3.4 N-2-Propyl DABCO Bromide 122



DABCO (5.05 g, 45.0 mmol) and 2-bromopropane (2.50 mL, 26.6 mmol) in acetonitrile (100 mL) were treated as described in the general procedure to give the product as a white hygroscopic powder (6.13 g, 26.0 mmol, 98%).

Mp	231-233 °C, lit. <sup>120</sup> 228 °C.
$^1\text{H}$ NMR ( $\text{D}_2\text{O}$ )	1.38 (d, 6H, $^3J_{\text{H-H}} = 6.7$ Hz, $(\text{CH}_3)_2$ ), 3.19 (t, 6H, $^3J_{\text{H-H}} = 7.3$ Hz, $\text{CH}_2\text{-N}$ ), 3.40 (t, 6H, $^3J_{\text{H-H}} = 7.3$ Hz, $\text{CH}_2\text{-N}^+$ ), 3.57 (heptet, 1H, $^3J_{\text{H-H}} = 6.6$ Hz, $\text{CH}(\text{CH}_3)_2$ )
$^{13}\text{C}$ NMR ( $\text{D}_2\text{O}$ )	18.2, 47.1, 51.9, 69.2
IR (KBr disc, $\text{cm}^{-1}$ )	1634 (br w), 1463 (w), 1394 (w), 1322 (w), 1122 (m), 1059 (m), 846 (m)
FAB-MS ( $m/z$ %)	391 (6.1), 389 (4.8) ( $[2\text{M}-\text{Br}]^+$ ), 155 (100) ( $[\text{M}-\text{Br}]^+$ )

#### 4.3.5 N-1-Propyl-DABCO Bromide 121



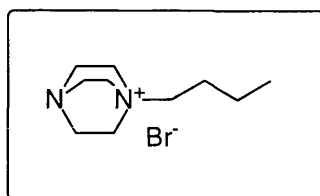
DABCO (2.48 g, 22.1 mmol) and 1-bromopropane (1.00 mL, 11.3 mmol) in acetonitrile (30 mL) were treated as described in the general procedure to give the product as a white hygroscopic powder (2.18 g, 9.3 mmol, 82%).

Mp	144-146 °C
----	------------

---

$^1\text{H}$ NMR ( $\text{D}_2\text{O}$ )	0.98 (t, 3H, $^3J_{\text{H-H}} = 7.3$ Hz, $\text{CH}_2\text{CH}_3$ ), 1.79 (sextet, 2H, $^3J_{\text{H-H}} = 8.2$ Hz, $\text{CH}_2\text{CH}_3$ ), 3.21 (m, 8H, $\text{N-CH}_2\text{CH}_2\text{-N}^+$ & $\text{CH}_3\text{CH}_2\text{CH}_2$ ) 3.41 (br t, 6H, $\text{N-CH}_2\text{CH}_2\text{-N}^+$ )
$^{13}\text{C}$ NMR ( $\text{D}_2\text{O}$ )	12.8, 17.8, 47.0, 54.9, 68.8
IR (KBr disc, $\text{cm}^{-1}$ )	2970 (m), 1654 (br w), 1467 (m), 1381 (w), 1098 (m), 1058 (m), 999 (w), 845 (w), 796 (w)
FAB-MS ( $m/z$ %)	390 (14.3), 388 (14.0) ( $[\text{2M-Br}]^+$ ), 155 (100) ( $[\text{M-Br}]^+$ )

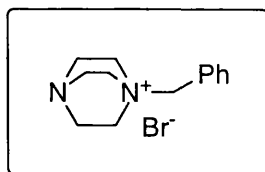
#### 4.3.6 N-1-Butyl-DABCO Bromide 123



DABCO (2.61 g, 23.3 mmol) and 1-bromobutane (1.00 mL, 9.2 mmol) in acetonitrile (100 mL) were treated as described in the general procedure to give the product as a white hygroscopic powder (1.88 g, 7.5 mmol, 82%).

Mp	128-130 °C
$^1\text{H}$ NMR ( $\text{D}_2\text{O}$ )	0.96 (t, 3H, $^3J_{\text{H-H}} = 7.4$ Hz, $\text{CH}_3$ ), 1.39 (m, 2H, $\text{CH}_2\text{CH}_3$ ), 1.75 (m, 2H, $\text{CH}_2\text{CH}_2\text{CH}_3$ ), 3.21 (t, 6H, $^3J_{\text{H-H}} = 6.5$ Hz, $\text{N-CH}_2\text{CH}_2\text{-N}^+$ ), 3.27 (t, 2H, $^3J_{\text{H-H}} = 8.1$ Hz, $\text{N}^+\text{-CH}_2\text{-nPr}$ ), 3.42 (t, 6H, $^3J_{\text{H-H}} = 6.9$ Hz, $\text{N-CH}_2\text{CH}_2\text{-N}^+$ )
$^{13}\text{C}$ NMR ( $\text{D}_2\text{O}$ )	15.6, 22.0, 26.0, 47.0, 54.9, 67.3
IR (KBr disc, $\text{cm}^{-1}$ )	1650 (br w), 1463 (m), 1098 (m), 1058 (m), 845 (w), 796 (w)
FAB-MS ( $m/z$ %)	418 (2.4), 416 (2.4) ( $[\text{2M-Br}]^+$ ), 169 (100) ( $[\text{M-Br}]^+$ )

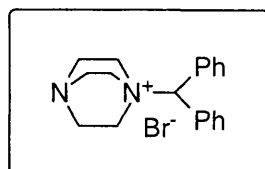
## 4.3.7 N-Benzyl-DABCO Bromide 124



DABCO (0.44 g, 3.92 mmol) and benzyl bromide (0.21 mL, 1.77 mmol) in acetonitrile (50 mL) were treated as described in the general procedure to give the product as a white hygroscopic powder (0.52 g, 1.84 mmol, 99%).

Mp	222-225 °C (dec.), lit. <sup>131</sup> 230 °C (dec.)
<sup>1</sup> H NMR (D <sub>2</sub> O)	3.18 (t, 6H, <sup>3</sup> J <sub>H-H</sub> = 7.4 Hz, N-CH <sub>2</sub> CH <sub>2</sub> -N <sup>+</sup> ), 3.47 (t, 6H, <sup>3</sup> J <sub>H-H</sub> = 7.4 Hz, N-CH <sub>2</sub> CH <sub>2</sub> -N <sup>+</sup> ), 4.81 (s, 2H, ArCH <sub>2</sub> ), 7.57 (m, 5H, ArH)
<sup>13</sup> C NMR (D <sub>2</sub> O)	47.1, 54.8, 71.1, 128.8, 132.1, 133.6, 135.9
IR (KBr disc, cm <sup>-1</sup> )	2960 (s), 2888 (m), 1576 (w br), 1454 (m), 1314 (s), 1216 (m), 1077 (m), 1058 (s), 1004 (m), 899 (w), 842 (m), 798 (m), 764 (s), 702 (s)
FAB-MS (m/z %)	487 (2.3), 485 (2.1) ([2M-Br] <sup>+</sup> ), 203 (100) ([M-Br] <sup>+</sup> )

## 4.3.8 N-Dibenzyl-DABCO Bromide 125



DABCO (0.74 g, 6.60 mmol) and bromodiphenylmethane (0.58 g, 2.35 mmol) in acetonitrile (45 mL) were treated as described in the general procedure to give the product as a white hygroscopic powder (0.82 g, 2.28 mmol, 97%).

Mp	200-202 °C (dec.)
<sup>1</sup> H NMR (CDCl <sub>3</sub> )	3.13 (t, 6H, <sup>3</sup> J <sub>H-H</sub> = 7.4 Hz, N-CH <sub>2</sub> CH <sub>2</sub> -N <sup>+</sup> ), 3.78 (t, 6H, <sup>3</sup> J <sub>H-H</sub> = 7.4 Hz, N-CH <sub>2</sub> CH <sub>2</sub> -N <sup>+</sup> ), 7.00 (s, 1H, Ar <sub>2</sub> CH), 7.40 (m, 6H, <b>H</b> <sub>3</sub> & <b>H</b> <sub>4</sub> ), 7.98 (d, 4H, <sup>3</sup> J <sub>H-H</sub> = 8.2 Hz, <b>H</b> <sub>2</sub> )
<sup>13</sup> C NMR (CDCl <sub>3</sub> )	45.6, 50.7, 79.8, 129.6, 130.2, 131.6, 131.9
IR (KBr disc, cm <sup>-1</sup> )	3059 (w), 2953 (w), 1499 (w), 1456 (m), 1342 (w), 1178 (w), 1059 (m), 995 (w), 871 (w), 813 (w), 759 (m), 712 (m)

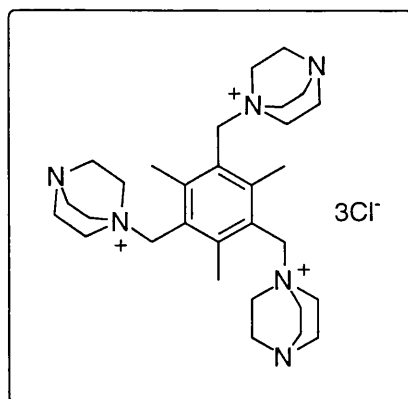
FAB-MS (m/z %)	639 (5.8), 637 (5.5) ([2M-Br] <sup>+</sup> ), 279 (99.8) ([M-Br] <sup>+</sup> ), 167 (100)
----------------	-----------------------------------------------------------------------------------------------

## 4.4 Trications

### 4.4.1 General Procedure

A mixture of the aromatic trihalide and amine was stirred in acetonitrile at room temperature for 24-36 h during which time precipitation occurred. The flask contents were poured into diethyl ether (400-700 mL) and stirred for 1 h. The precipitate was removed by filtration, washed with diethyl ether (3x50 mL) and acetonitrile (3x15 mL), then dried *in vacuo*. The hexafluorophosphate salt was obtained by dissolving the halide product in water (*ca.* 5% w/v) and then adding a saturated aqueous solution of ammonium hexafluorophosphate until no further precipitation occurred. The precipitate was collected by filtration, dissolved in acetone and dried over potassium carbonate. Evaporation of the solvent, followed by recrystallisation of the residue from a mixture of acetonitrile and methanol yielded the hexafluorophosphate salt.

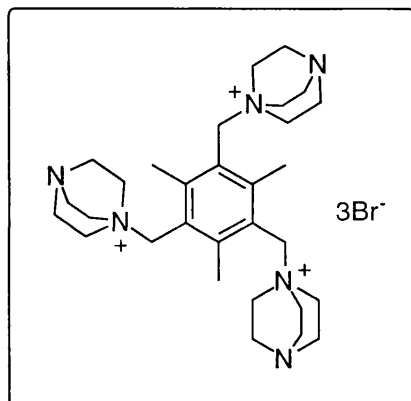
### 4.4.2 2,4,6-Tris(DABCO-N-methyl)mesitylene Trichloride 110



2,4,6-Tris(chloromethyl)mesitylene (0.30 g, 1.35 mmol) and DABCO (3.00 g, 26.8 mmol) were treated in acetonitrile (100 mL) as described in the general procedure to give the product as a hygroscopic white powder (0.71 g, 1.18 mmol, 94%).

Mp	252-255 °C (dec.)
<sup>1</sup> H NMR (D <sub>2</sub> O)	2.67 (s, 9H, ArCH <sub>3</sub> ), 3.20 (br, 18H, N-CH <sub>2</sub> ), 3.64 (br, 18H, N <sup>+</sup> -CH <sub>2</sub> CH <sub>2</sub> -N), 4.92 (s, 6H, ArCH <sub>2</sub> )
<sup>13</sup> C NMR (D <sub>2</sub> O)	23.8, 47.4, 54.6, 66.5, 129.6, 149.7
IR (KBr disc, cm <sup>-1</sup> )	2962 (w), 1630 (br w), 1465 (w), 1366 (m), 1191 (w), 1059 (m), 991 (w), 890 (w), 858 (m), 798 (w)
FAB-MS (m/z %)	567 (0.9), 566 (0.2), 565 (2.2) ([M-Cl] <sup>+</sup> ), 113 (100)

## 4.4.3 2,4,6-Tris(DABCO-N-methyl)mesitylene Tribromide 109



A solution of 2,4,6-tris(bromomethyl)mesitylene (1.98 g, 4.96 mmol) and DABCO (5.85 g, 52.2 mmol) in acetonitrile (150 mL) were treated as outlined in the general procedure to yield the product as a hygroscopic white powder (3.22 g, 4.4 mmol, 88%).

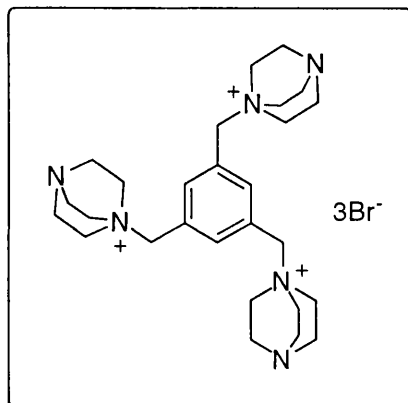
Mp	227-229 °C (dec.)
$^1\text{H}$ NMR ( $\text{D}_2\text{O}$ )	2.70 (s, 9H, $\text{ArCH}_3$ ), 3.22 (br t, 18H, N- $\text{CH}_2$ ), 3.68 (br t, 18H, N- $\text{CH}_2\text{CH}_2\text{-N}^+$ ), 4.94 (s, 6H, $\text{ArCH}_2$ )
$^{13}\text{C}$ NMR ( $\text{D}_2\text{O}$ )	23.5, 47.2, 54.4, 66.2, 129.4, 149.5
IR (KBr disc, $\text{cm}^{-1}$ )	2962 (m), 2883 (w), 1631 (br w), 1466 (m), 1366 (m), 1194 (w), 1059 (s), 992 (m), 887 (w), 855 (m), 802 (m)
FAB-MS ( $m/z$ %)	657 (7.5), 655 (13.9), 653(7.0) ( $[\text{M-Br}]^+$ ), 137 (100)

## 4.4.4 2,4,6-Tris(DABCO-N-methyl)mesitylene Tri(hexafluorophosphate) 112

Compound **109** (0.22 g, 0.30 mmol) was converted to its hexafluorophosphate salt as outlined in the general procedure to yield colourless plates, which upon removal from the mother liquor and drying *in vacuo* gave a white solid (0.21 g, 0.23 mmol, 75%).

Mp	234-236 °C (dec.)
$^1\text{H}$ NMR ( $d_6$ -acetone)	2.86 (s, 9H, $\text{ArCH}_3$ ), 3.20 (br t, 18H, N- $\text{CH}_2$ ), 3.65 (br t, 18H, N- $\text{CH}_2\text{CH}_2\text{-N}^+$ ), 5.08 (s, 6H, $\text{ArCH}_2$ )
$^{13}\text{C}$ NMR ( $d_6$ -acetone)	21.8, 46.0, 53.0, 64.4, 128.1, 148.5
IR (KBr disc, $\text{cm}^{-1}$ )	1634 (br w), 1468 (w), 1368 (w), 1064 (w), 838 (br s)
FAB-MS ( $m/z$ %)	785 (34.0) ( $[\text{M-PF}_6]^+$ ), 320 (8.6) ( $[\text{M-2PF}_6]^{2+}$ ), 192 (100)
$\text{C}_{30}\text{H}_{51}\text{N}_6\text{F}_{18}\text{P}_3 \cdot 3\text{H}_2\text{O}$	calc. C 36.57 H 5.83 N 8.53
(984.72)	found 36.59 5.68 8.44

#### 4.4.5 1,3,5-Tris(DABCO-N-methyl)benzene Tribromide 107



To a solution of DABCO (1.04 g, 9.27 mmol) in acetonitrile (30 mL) was added dropwise a solution of 1,3,5-tris(bromomethyl)benzene (0.19 g, 0.53 mmol) in acetonitrile (35 mL). The solution was stirred for 48 h, during which time a precipitate formed. The contents of the flask were poured into ether (350 mL) and stirred for 10 min. The precipitate was filtered off under nitrogen and dried *in vacuo* giving the product as a white hygroscopic solid (0.35 g, 0.50 mmol, 95%).

Mp	255-258 °C (dec.)
$^1\text{H}$ NMR ( $\text{D}_2\text{O}$ )	3.23 (t, 18H, $^3J_{\text{H-H}} = 7.1$ Hz, N-CH <sub>2</sub> ), 3.60 (t, 18H, $^3J_{\text{H-H}} = 7.1$ Hz, N-CH <sub>2</sub> CH <sub>2</sub> -N <sup>+</sup> ), 4.68 (s, 6H, ArCH <sub>2</sub> ), 7.88 (s, 3H, ArH)
$^{13}\text{C}$ NMR ( $\text{D}_2\text{O}$ )	46.9, 54.7, 69.5, 131.4, 142.4
IR (KBr disc, $\text{cm}^{-1}$ )	1634 (br w), 1463 (m), 1372 (m), 1080 (m), 1058 (s), 896 (w), 849 (m), 798 (w)
FAB-MS ( $m/z$ %)	615 (34.6), 613 (67.6), 611 (37.2) ([M-Br] <sup>+</sup> ), 112 (100)

#### 4.4.6 1,3,5-Tris(DABCO-N-methyl)benzene Trihexafluorophosphate 113

Compound **107** (0.20 g, 0.29 mmol) was converted to its hexafluorophosphate salt as outlined in the general procedure to yield colourless plates, which upon removal from the mother liquor and drying *in vacuo* gave a white solid (0.16g, 0.18 mmol, 62%).

Mp	221-223 °C
$^1\text{H}$ NMR ( $d_6$ -acetone)	3.21 (t, 18H, $^3J_{\text{H-H}} = 7.3$ Hz, N-CH <sub>2</sub> ), 3.58 (t, 18H, $^3J_{\text{H-H}} = 7.4$ Hz, N-CH <sub>2</sub> CH <sub>2</sub> -N <sup>+</sup> ), 4.76 (s, 6H, ArCH <sub>2</sub> ), 8.03 (s, 3H, ArH)
$^{13}\text{C}$ NMR ( $d_6$ -acetone)	45.8, 53.4, 67.7, 130.1, 140.9
IR (KBr disc, $\text{cm}^{-1}$ )	1629 (br w), 1466 (w), 1374 (w), 1083 (w), 1059 (m), 992 (w), 835 (br s), 557 (s)

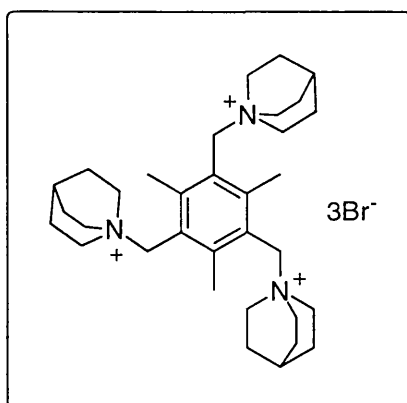
FAB-MS (m/z %)	743 (100) ([M-PF <sub>6</sub> ] <sup>+</sup> )
C <sub>27</sub> H <sub>45</sub> N <sub>6</sub> F <sub>18</sub> P <sub>3</sub>	calc. C 36.50 H 5.10 N 9.46
(888.59)	found 37.23 5.34 9.71

#### 4.4.7 1,3,5-Tris(DABCO-N-methyl)benzene Tri(tetraphenylborate) 111

Compound **107** was dissolved in water (25 mL) and to the solution was added tetraphenylboron sodium (0.20 g, 0.58 mmol) in water (25 mL). A hydrophobic precipitate formed which was filtered off and dried *in vacuo*. After dissolution of the material in acetonitrile followed by filtration and removal of the solvent under reduced pressure, the product was isolated as an off-white solid (0.67 g, 0.47 mmol, 89%).

Mp	143-146 °C (dec.)
<sup>1</sup> H NMR (d <sub>6</sub> -DMSO)	3.03 (t, 18H, <sup>3</sup> J <sub>H-H</sub> = 7.1 Hz, N-CH <sub>2</sub> ), 3.26 (t, 18H, <sup>3</sup> J <sub>H-H</sub> = 7.1 Hz, N-CH <sub>2</sub> CH <sub>2</sub> N <sup>+</sup> ), 4.55 (s, 6H, ArCH <sub>2</sub> ), 6.78 (t, 12H, <sup>3</sup> J <sub>H-H</sub> = 7.2 Hz, <b>H</b> <sub>4</sub> [BPh <sub>4</sub> ]), 6.91 (t, 24H, <sup>3</sup> J <sub>H-H</sub> = 7.4 Hz, <b>H</b> <sub>2</sub> [BPh <sub>4</sub> ]), 7.16 (br m, 24H, <b>H</b> <sub>3</sub> [BPh <sub>4</sub> ]), 7.68 (s, 3H, ArH)
<sup>13</sup> C NMR (d <sub>6</sub> -DMSO)	44.7, 51.7, 65.5, 121.5, 125.3, 128.6, 135.5, 139.4, 163.3
IR (KBr disc, cm <sup>-1</sup> )	3054 (m), 1578 (w), 1478 (m), 1426 (m), 1364 (w), 1056 (m), 839 (w), 736 (s), 707 (s), 612 (m)
FAB-MS (m/z %)	1092 (5.0) ([M-BPh <sub>4</sub> ] <sup>+</sup> ), 112 (100)

#### 4.4.8 2,4,6-Tris(Quinuclidine-N-methyl)mesitylene Tribromide 148



A solution of 2,4,6-tris(bromomethyl)mesitylene (0.45 g, 1.13 mmol) and quinuclidine (0.46 g, 4.14 mmol) in acetonitrile (40 mL) were treated as outlined in the general procedure to yield the product as a hygroscopic white powder (0.76 g, 1.03 mmol, 92%).

Mp	267-270 °C (dec.)
----	-------------------



---

$^1\text{H}$ NMR ( $\text{D}_2\text{O}$ )	2.01 (br, 18H, $\text{CH}_2\text{CH}_2\text{-N}^+$ ), 2.18 (m, 3H, $\text{CH}(\text{CH}_2)_3$ ), 2.66 (s, 9H, $\text{ArCH}_3$ ), 3.66 (br, 18H, $\text{CH}_2\text{CH}_2\text{-N}^+$ ), 4.77 (s, 6H, $\text{ArCH}_2$ )
$^{13}\text{C}$ NMR ( $\text{D}_2\text{O}$ )	21.3, 23.5, 26.4, 57.2, 65.8, 129.9, 149.0
IR (KBr disc, $\text{cm}^{-1}$ )	2957 (s), 1653 (br w), 1458 (m), 1380 (w), 1068 (m), 992 (m), 937 (w), 886 (w), 846 (m)
FAB-MS ( $m/z$ %)	654 (11.5), 652 (22.1), 650 (10.5) ( $[\text{M-Br}]^+$ ), 541.1 (28.8), 112.1 (100)

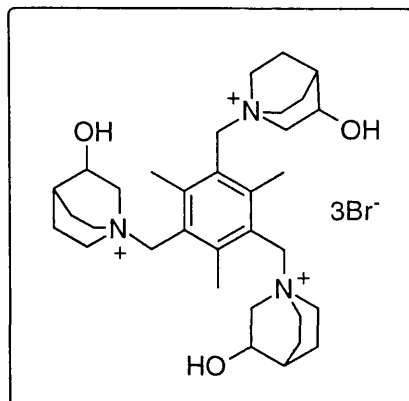
#### 4.4.9 2,4,6-Tris(Quinuclidine-N-methyl)mesitylene Tri(hexafluorophosphate) 149

Compound **148** (0.30 g, 0.41 mmol) was converted to its hexafluorophosphate salt as outlined in the general procedure to yield colourless plates, which upon removal from the mother liquor and drying *in vacuo* gave a white solid (0.30 g, 0.32 mmol, 79%).

Mp	290-292 °C (dec.)
$^1\text{H}$ NMR ( $d_6$ -acetone)	2.04 (m, 18H, $\text{CH}_2\text{CH}_2\text{-N}^+$ ), 2.13 (m, 3H, $\text{CH}(\text{CH}_2)_3$ ), 2.82 (s, 9H, $\text{ArCH}_3$ ), 3.75 (t, $^3J_{\text{H-H}} = 7.9$ Hz, 18H, $\text{CH}_2\text{CH}_2\text{-N}^+$ ), 4.96 (s, 6H, $\text{ArCH}_2$ )
$^{13}\text{C}$ NMR ( $d_6$ -acetone)	19.4, 21.3, 24.2, 55.1, 63.7, 128.0, 147.6
IR (KBr disc, $\text{cm}^{-1}$ )	2979 (w), 2894 (w), 1628 (br w), 1470 (m), 1375 (w), 1327 (w), 1067 (w), 835 (br s), 558 (s)
FAB-MS ( $m/z$ %)	782 (37.0) ( $[\text{M-PF}_6]^+$ ), 319 (24.5) ( $[\text{M-2PF}_6]^{2+}$ ), 137 (100)
$\text{C}_{33}\text{H}_{54}\text{N}_3\text{F}_{18}\text{P}_3$	calc. C 42.73 H 5.87 N 4.53
(927.70)	found 42.48 5.85 4.73

---

#### 4.4.10 2,4,6-Tris(3-Quinuclidinol-N-methyl)mesitylene Tribromide 151



A solution of 2,4,6-tris(bromomethyl)mesitylene (0.28 g, 0.70 mmol) and racemic 3-quinuclidinol (0.31 g, 2.44 mmol) in acetonitrile (30 mL) were treated as outlined in the general procedure to yield the product as a hygroscopic white powder (0.54 g, 0.69 mmol, 98%).

Mp	258-261 °C (dec.)
$^1\text{H}$ NMR ( $\text{D}_2\text{O}$ )	1.93 (br m, 3H, CH), 2.01-2.09 (br m, 3H, CH), 2.22-2.27 (br m, 6H, $\text{CH}_2$ ), 2.59-2.61 (br m, 3H, CH), 2.67 (s, 9H, $\text{ArCH}_3$ ), 3.20-3.65 (br m, 18H, $\text{N}(\text{CH}_2)_3$ ), 3.98-4.01 (br m, 3H, $\text{N}^+-\text{CH}_2\text{CH}_2\text{CH}$ ), 4.33 (br, 3H, $\text{CHOH}$ ), 4.85 (s, 6H, $\text{ArCH}_2$ )
$^{13}\text{C}$ NMR ( $\text{D}_2\text{O}$ )	20.3, 23.6, 23.8, 28.2, 55.3, 57.8, 65.5, 65.8, 67.1, 129.8, 149.3
IR (KBr disc, $\text{cm}^{-1}$ )	2969 (m), 1636 (br w), 1492 (w), 1456 (m), 1413 (w), 1374 (w), 1119 (m), 1094 (m), 1047 (m), 886 (m), 839 (w), 803 (w)
FAB-MS ( $m/z$ %)	702 (1.7), 700 (3.4), 698 (1.7) ( $[\text{M}-\text{Br}]^+$ ) 575 (1.3), 573 (2.4), 571 (1.3) ( $[\text{M}-\text{C}_7\text{H}_{13}\text{NO}-\text{Br}]^+$ ) 154 (100)

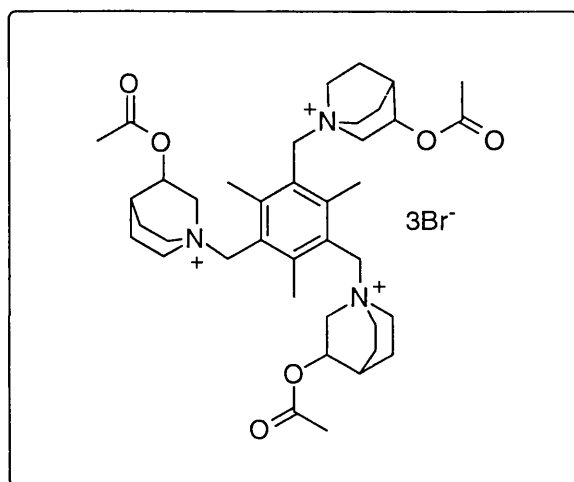
#### 4.4.11 2,4,6-Tris(3-Quinuclidinol-N-methyl)mesitylene Tri(hexafluorophosphate) 152

Compound **151** (0.30 g, 0.41 mmol) was converted to its hexafluorophosphate salt as outlined in the general procedure to yield colourless plates, which upon removal from the mother liquor and drying *in vacuo* gave a white solid (0.30 g, 0.32 mmol, 79%).

Mp	252-255 °C (dec.)
$^1\text{H}$ NMR ( $d_6$ -acetone)	1.90-1.95 (br m, 3H, CH), 2.00-2.08 (m, 3H, CH), 2.16 (br, 3H, CH), 2.31-2.35 (br m, 3H, CH), 2.84 (s, 9H, $\text{ArCH}_3$ ), 2.90-2.95 (br, 3H, $\text{N}^+-\text{CH}_2$ ), 3.48-3.75 (br m, 12H, $\text{N}^+(\text{CH}_2)_2$ ), 3.79-3.83 (br

	m, 3H, N <sup>+</sup> -CH <sub>2</sub> CHOH), 3.95-3.98 (br, 3H, N <sup>+</sup> -CH <sub>2</sub> CH <sub>2</sub> CH), 4.29 (br, 3H, CHOH), 5.03 (s, 6H, ArCH <sub>2</sub> )
<sup>13</sup> C NMR (d <sub>6</sub> -acetone)	18.5, 21.8, 27.1, 29.5, 53.1, 56.3, 64.0, 64.9, 65.1, 128.4, 148.2
IR (KBr disc, cm <sup>-1</sup> )	2972 (w), 1637 (br w), 1466 (w), 1412 (w), 1375 (w), 1121 (w), 1092 (w), 1052 (w), 1914 (w), 837 (br s), 558 (s)
FAB-MS (m/z %)	830 (100) ([M-PF <sub>6</sub> ] <sup>+</sup> )
C <sub>33</sub> H <sub>54</sub> N <sub>3</sub> O <sub>3</sub> F <sub>18</sub> P <sub>3</sub> ·2H <sub>2</sub> O	calc. C 39.18 H 5.78 N 4.15
(1011.72)	found 39.41 5.64 4.27

#### 4.4.12 2,4,6-Tris(3-Acetoxyquinuclidine-N-methyl)mesitylene Tribromide 155



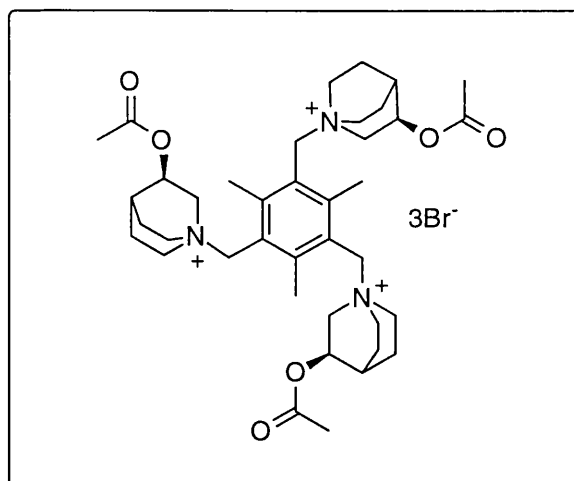
A solution of 2,4,6-tris(bromomethyl)mesitylene (0.18 g, 0.45 mmol) and racemic 3-acetoxyquinuclidine (0.26 g, 1.54 mmol) in acetonitrile (25 mL) were treated as outlined in the general procedure to yield the product as a hygroscopic white powder (0.25 g, 0.28 mmol, 61%).

Mp	223-225 °C (dec.)
<sup>1</sup> H NMR (D <sub>2</sub> O)	2.01-2.16 (br, 6H, CH <sub>2</sub> ), 2.18 (s, 9H, COCH <sub>3</sub> ), 2.34-2.44 (br, 6H, CH <sub>2</sub> ), 2.63 (s, 9H, ArCH <sub>3</sub> ), 3.63-3.75 (br m, 18H, N <sup>+</sup> -(CH <sub>2</sub> ) <sub>3</sub> ), 4.16-4.19 (br m, 3H, N <sup>+</sup> -CH <sub>2</sub> CH <sub>2</sub> CH), 4.83 (s, 6H, ArCH <sub>2</sub> ), 5.02-5.06 (br m, 3H, HCOCOCH <sub>3</sub> )
<sup>13</sup> C NMR (D <sub>2</sub> O)	21.0, 23.4, 23.8, 23.9, 26.2, 55.8, 58.3, 62.5, 65.9, 71.3, 129.9, 149.6, 176.5
IR (KBr disc, cm <sup>-1</sup> )	2962 (m), 1723 (s), 1637 (br w), 1460 (w), 1372 (m), 1247 (s), 1117 (w), 1093 (w), 1048 (m), 924 (w), 883 (w), 841 (w)
FAB-MS (m/z)	828, 826, 824 ([M-Br] <sup>+</sup> )

**4.4.13 2,4,6-Tris(3-Quinuclidinol-N-methyl)mesitylene****Tri(hexafluorophosphate) 156**

Compound **155** (0.20 g, 0.22 mmol) was converted to its hexafluorophosphate salt as outlined in the general procedure to yield colourless plates, which upon removal from the mother liquor and drying *in vacuo* gave a white solid (0.17 g, 0.15 mmol, 70%).

Mp	193-195 °C (dec.)
$^1\text{H}$ NMR ( $d_6$ -acetone)	2.02-2.14 (m, 6H, $\text{CH}_2$ ), 2.07 (s, 9H, $\text{COCH}_3$ ), 2.11-2.38 (br m, 6H, $\text{CH}_2$ ), 2.78 (s, 9H, $\text{ArCH}_3$ ), 3.62-3.89 (br m, 18H, $\text{N}^+(\text{CH}_2)_3$ ), 4.15-4.19 (br m, 3H, $\text{N}^+-\text{CH}_2\text{CH}_2\text{CH}$ ), 5.02 (s, 6H, $\text{ArCH}_2$ ), 5.02-5.08 (obsc. m, 3H, $\text{HCOCOCH}_3$ )
$^{13}\text{C}$ NMR ( $d_6$ -acetone)	19.0, 20.7, 21.7, 21.9, 24.5, 53.6, 55.7, 62.2, 64.0, 68.6, 128.3, 148.4, 171.2
IR (KBr disc, $\text{cm}^{-1}$ )	2975 (w), 1741 (m), 1466 (w), 1420 (w), 1374 (m), 1248 (m), 1048 (w), 841 (br s), 558 (s)
FAB-MS ( $m/z$ %)	957 (100) ( $[\text{M}-\text{PF}_6]^+$ ) 406 (18.2) ( $[\text{M}-2\text{PF}_6]^{2+}$ )
$\text{C}_{39}\text{H}_{60}\text{N}_3\text{O}_6\text{F}_{18}\text{P}_3 \cdot \text{H}_2\text{O}$ (1119.84)	calc. C 41.83 H 5.58 N 3.75 found 41.86 5.59 3.56

**4.4.14 2,4,6-Tris((R)-(+)-3-Acetoxyquinuclidine-N-methyl)mesitylene****Tribromide 160**

A solution of 2,4,6-tris(bromomethyl)mesitylene (0.10 g, 0.25 mmol) and (R)-(+)-3-acetoxyquinuclidine (0.16 g, 0.95 mmol) in acetonitrile (15 mL) were treated as outlined in the general procedure to yield the product as a hygroscopic white powder (0.22 g, 0.24 mmol, 97%).

---

Mp	249-252 °C (dec.)
$[\alpha]^{25}_D$	-14.7 ° (c = 1.0, H <sub>2</sub> O)
<sup>1</sup> H NMR (D <sub>2</sub> O)	2.04-2.17 (br, 6H, CH <sub>2</sub> ), 2.17 (s, 9H, COCH <sub>3</sub> ), 2.33-2.43 (br, 6H, CH <sub>2</sub> ), 2.62 (s, 9H, ArCH <sub>3</sub> ), 3.63-3.75 (br m, 18H, N <sup>+</sup> -(CH <sub>2</sub> ) <sub>3</sub> ), 4.16-4.18 (br m, 3H, N <sup>+</sup> -CH <sub>2</sub> CH <sub>2</sub> CH), 4.82 (s, 6H, ArCH <sub>2</sub> ), 5.02 (br m, 3H, HCOCOCH <sub>3</sub> )
<sup>13</sup> C NMR (D <sub>2</sub> O)	20.8, 23.1, 23.5, 23.6, 25.9, 55.4, 58.1, 62.3, 65.7, 71.1, 129.7, 149.3, 176.3
IR (KBr disc, cm <sup>-1</sup> )	2965 (m), 1724 (s), 1637 (br w), 1459 (w), 1372 (m), 1247 (s), 1047 (m), 1026 (m), 883 (w)
FAB-MS (m/z %)	828 (<1), 826 (2.3), 824 (<1) ([M-Br] <sup>+</sup> ) 659 (9.7), 657 (19.0), 655 (9.7) ([M-Br-C <sub>9</sub> H <sub>15</sub> NO <sub>2</sub> ] <sup>+</sup> ) 170 (100)

#### 4.4.15 2,4,6-Tris((R)-(+)-3-Acetoxyquinuclidine-N-methyl)mesitylene

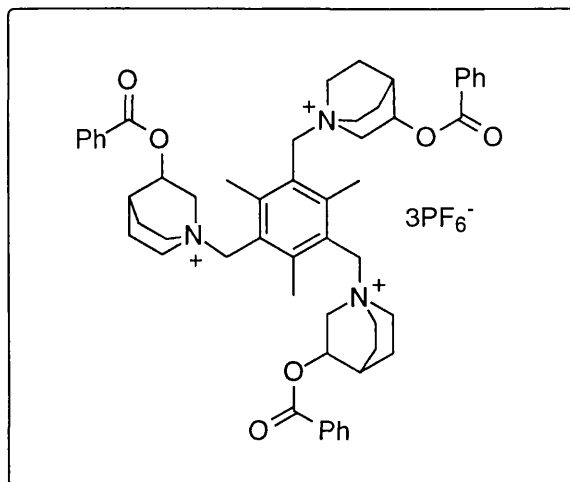
##### Tri(hexafluorophosphate) 161

Compound **160** (0.10 g, 0.11 mmol) was converted to its hexafluorophosphate salt as outlined in the general procedure to yield colourless plates, which upon removal from the mother liquor and drying *in vacuo* gave a white solid (0.07 g, 0.06 mmol, 58%).

Mp	198-200 °C
<sup>1</sup> H NMR (d <sub>6</sub> -acetone)	1.98-2.16 (obsc. m, 6H, CH <sub>2</sub> ), 2.07 (s, 9H, COCH <sub>3</sub> ), 2.10-2.38 (br m, 6H, CH <sub>2</sub> ), 2.80 (s, 9H, ArCH <sub>3</sub> ), 3.63-3.89 (br m, 18H, N <sup>+</sup> (CH <sub>2</sub> ) <sub>3</sub> ), 4.17-4.21 (br m, 3H, N <sup>+</sup> -CH <sub>2</sub> CH <sub>2</sub> CH), 5.03 (s, 6H, ArCH <sub>2</sub> ), 5.03-5.06 (obsc. m, 3H, HCOCOCH <sub>3</sub> )
IR (KBr disc, cm <sup>-1</sup> )	2977 (w), 1743 (m), 1367 (br w), 1467 (w), 1416 (w), 1374 (m), 1243 (m), 1048 (w), 838 (br s), 558 (s)
FAB-MS (m/z %)	957 (100) ([M-PF <sub>6</sub> ] <sup>+</sup> ) 406 (30.2) ([M-2PF <sub>6</sub> ] <sup>2+</sup> )

---

**4.4.16 2,4,6-Tris(3-Benzoyloxyquinuclidine-N-methyl)mesitylene  
Tri(hexafluorophosphate) 158**



A solution of 2,4,6-tris(bromomethyl)mesitylene (0.12 g, 0.30 mmol) and racemic 3-benzoyloxyquinuclidine (0.24 g, 1.04 mmol) in acetonitrile (30 mL) was stirred at room temperature for 48 h during which time precipitation occurred. The flask contents were poured into diethyl ether (300 mL) and stirred for 1 h. The precipitate was removed by filtration, washed with diethyl ether (3x50 mL) and acetonitrile (3x15 mL), then dried *in vacuo* giving the tribromide salt as a white solid (0.30 g, 0.27 mmol, 91%).

Mp	247-250 °C (dec.)
IR (KBr disc, cm <sup>-1</sup> )	2964 (m), 1716 (s), 1600 (m), 1491 (w), 1451 (m), 1275 (s), 1178 (w), 1111 (s), 1026 (m), 990 (m), 885 (m), 842 (w), 800 (w) 716 (s)
FAB-MS (m/z)	1014, 1012, 1010 ([M-Br] <sup>+</sup> )

The solid was dissolved in boiling water (15 mL) and a saturated solution of ammonium hexafluorophosphate (4 mL) added. A white solid formed on cooling which was collected by filtration. Recrystallisation of the residue from a mixture of acetonitrile and propan-2-ol yielded the hexafluorophosphate salt as white hemispheres (0.28g, 0.22 mmol, 72%).

Mp	278-282 °C (dec.)
<sup>1</sup> H NMR (d <sub>6</sub> -acetone)	2.20-2.26 (br m, 9H, CH <sub>2</sub> ), 2.85 (s, 9H, ArCH <sub>3</sub> ), 3.50-3.92 (br m, 12H, (N <sup>+</sup> -(CH <sub>2</sub> ) <sub>2</sub> )), 4.11-4.14 (br m, 6H, (N <sup>+</sup> -CH <sub>2</sub> )), 4.28-4.31 (br m, 3H, N <sup>+</sup> -CH <sub>2</sub> CH <sub>2</sub> CH), 5.10 (s, ArCH <sub>2</sub> ), 5.36-5.43 (br m, 3H, HCOCOPh), 7.52 (m, 6H, H <sub>3</sub> ), 7.68 (m, 3H, H <sub>4</sub> ), 8.07 (m, 6H, H <sub>2</sub> )

---

$^{13}\text{C}$ NMR ( $d_6$ -acetone)	19.3, 21.7, 21.9, 24.6, 53.2, 56.3, 62.1, 64.0, 69.3, 128.2, 128.4, 129.5, 130.5, 134.4, 148.6, 166.4
IR (KBr disc, $\text{cm}^{-1}$ )	2971 (w), 1714 (s), 1601 (w), 1453 (w), 1318 (w), 1274 (s), 1112 (m), 1072 (w), 1026 (w), 840 (br s), 716 (m), 558 (s)
FAB-MS ( $m/z$ %)	1143 (100) ( $[\text{M-PF}_6]^+$ )
$\text{C}_{54}\text{H}_{66}\text{N}_3\text{O}_6\text{F}_{18}\text{P}_3$	calc. C 50.36 H 5.16 N 3.26
(1288.04)	found 50.01 5.04 3.10

---

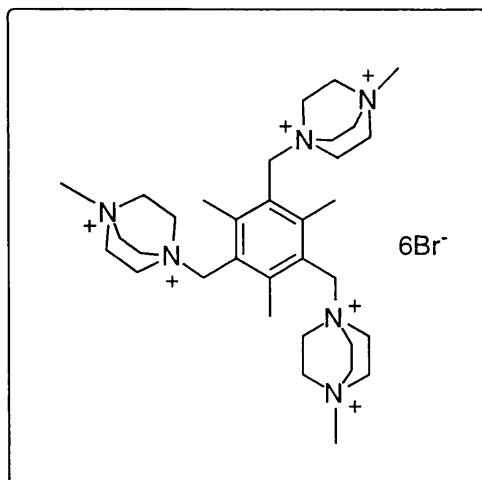
## 4.5 Hexacations

### 4.5.1 General Procedure

A mixture of the aromatic trihalide and amine were stirred in acetonitrile at room temperature for 24–72 h during which time precipitation of a white solid occurred. This precipitate was removed by filtration, washed with acetonitrile (3x20 mL), and then dried *in vacuo*. The hexafluorophosphate salt was obtained by dissolving the halide product in water (*ca.* 5% w/v), followed by addition of a saturated aqueous solution of ammonium hexafluorophosphate until no further precipitation occurred. This precipitate was removed by filtration, dissolved in acetone and dried over potassium carbonate. Evaporation of the solvent, followed by recrystallisation of the residue from a mixture of acetonitrile and methanol yielded the hexafluorophosphate salt. Samples for microanalysis were prepared by dissolving the halide product in water (*ca.* 5% w/v), followed by addition of a 12 molar excess of ammonium hexafluorophosphate in water (*ca.* 5% w/v). On standing, precipitation occurred. The precipitate was removed by filtration, washed with water, and dried *in vacuo* yielding the hexafluorophosphate salt.

---

#### 4.5.2 2,4,6-Tris(N'-methyl-DABCO-N-methyl)mesitylene hexabromide 127



2,4,6-Tris(bromomethyl)mesitylene (0.20 g, 0.50 mmol) and **119** (0.52 g, 2.51 mmol) in acetonitrile (40 mL) were treated as described in the general procedure to yield the product as a white powder (0.49 g, 0.48 mmol, 96%).

Mp	234-236 °C (dec.)
$^1\text{H}$ NMR ( $\text{D}_2\text{O}$ )	2.78 (s, 9H, $\text{ArCH}_3$ ), 3.41 (s, 9H, $\text{CH}_3\text{-N}^+$ ), 4.06 (t, 18H, $^3J_{\text{H-H}} = 7.0$ Hz, $\text{CH}_3\text{-N}^+\text{-CH}_2$ ), 4.31 (t, 18H, $^3J_{\text{H-H}} = 7.2$ Hz, $\text{ArCH}_2\text{-N}^+\text{-CH}_2$ ), 5.27 (s, 6H, $\text{ArCH}_2$ )
$^{13}\text{C}$ NMR ( $\text{D}_2\text{O}$ )	23.8, 53.9, 55.4, 56.4, 67.2, 129.7, 151.3
IR (KBr disc, $\text{cm}^{-1}$ )	3000 (s), 1636 (br w), 1475 (m), 1377 (m), 1123 (s), 1060 (m), 951 (w), 856 (s)
FAB-MS ( $m/z$ )	939 ( $[\text{M-Br}]^+$ ), 860 ( $[\text{M-2Br}]^+$ ), 460

#### 4.5.3 2,4,6-Tris(N'-methyl-DABCO-N-methyl)mesitylene hexa(hexafluorophosphate) 137

Compound **127** (0.25 g, 0.25 mmol) was converted to its hexafluorophosphate salt as outlined in the general procedure to yield, after drying *in vacuo*, the product as a white solid (0.29 g, 0.21 mmol, 84%).

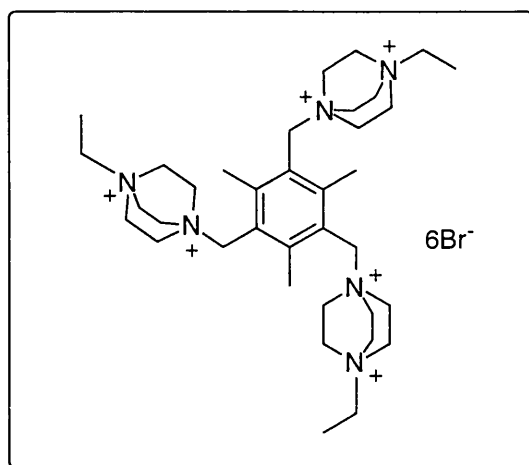
Mp	236-239 °C (dec.)
$^1\text{H}$ NMR ( $d_6$ -acetone)	2.98 (s, 9H, $\text{ArCH}_3$ ), 3.68 (s, 9H, $\text{CH}_3\text{-N}^+$ ), 4.19 (t, 18H, $^3J_{\text{H-H}} = 7.0$ Hz, $\text{CH}_3\text{-N}^+\text{-CH}_2$ ), 4.41 (t, 18H, $^3J_{\text{H-H}} = 7.0$ Hz, $\text{ArCH}_2\text{-N}^+\text{-CH}_2$ ), 5.59 (s, 6H, $\text{ArCH}_2$ )
$^{13}\text{C}$ NMR ( $d_6$ -acetone)	21.2, 51.8, 53.3, 54.1, 65.1, 127.6, 150.2



---

IR (KBr disc, $\text{cm}^{-1}$ )	3056 (w), 1637 (br w), 1478 (m), 1124 (w), 1060 (w), 834 (br s), 559 (s)
FAB-MS ( $m/z$ )	1265 ( $[\text{M-PF}_6]^+$ ), 1120 ( $[\text{M-2PF}_6]^+$ ), 460

#### 4.5.4 2,4,6-Tris(N'-ethyl-DABCO-N-methyl)mesitylene hexabromide 128



2,4,6-Tris(bromomethyl)mesitylene (0.34 g, 0.85 mmol) and **120** (0.73 g, 3.30 mmol) in acetonitrile (45 mL) were treated as described in the general procedure to yield the product as a white powder (0.86 g, 0.81 mmol, 95%).

Mp	222-225 °C (dec.)
$^1\text{H}$ NMR ( $\text{D}_2\text{O}$ )	1.46 (t, 9H, $^3J_{\text{H-H}} = 7.3$ Hz, $\text{CH}_3\text{CH}_2\text{-N}^+$ ), 2.80 (s, 9H, $\text{ArCH}_3$ ), 3.71 (q, 6H, $^3J_{\text{H-H}} = 7.3$ Hz, $\text{CH}_3\text{CH}_2\text{-N}^+$ ), 4.00 (t, 18H, $^3J_{\text{H-H}} = 7.1$ Hz, $\text{CH}_3\text{CH}_2\text{-N}^+\text{-CH}_2$ ), 4.32 (t, 18H, $^3J_{\text{H-H}} = 7.1$ Hz, $\text{ArCH}_2\text{-N}^+\text{-CH}_2$ ), 5.29 (s, 6H, $\text{ArCH}_2$ )
$^{13}\text{C}$ NMR ( $\text{D}_2\text{O}$ )	9.8, 23.6, 53.6, 53.7, 63.9, 67.0, 129.5, 151.0
IR (KBr disc, $\text{cm}^{-1}$ )	3003 (s), 1630 (br w), 1459 (m), 1417 (m), 1101 (s), 1061 (m), 929 (w), 856 (s), 813 (w)
FAB-MS ( $m/z$ )	983 ( $[\text{M-Br}]^+$ ), 901 ( $[\text{M-2Br}]^+$ ), 459

#### 4.5.5 2,4,6-Tris(N'-ethyl-DABCO-N-methyl)mesitylene hexa(hexafluorophosphate) 138

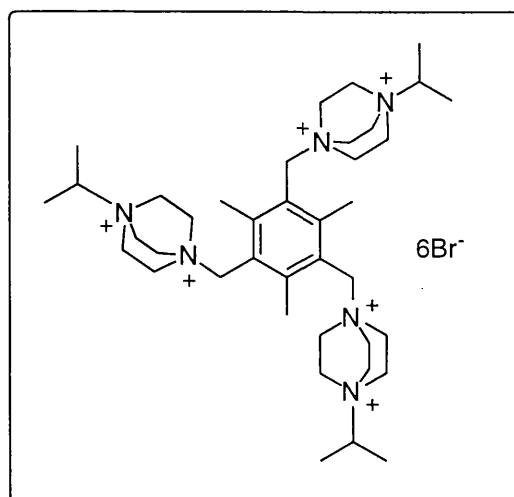
Compound **128** (0.30 g, 0.28 mmol) was converted to its hexafluorophosphate salt as outlined in the general procedure to yield, after drying *in vacuo*, the product as a white solid (0.34 g, 0.23 mmol, 84%).

Mp	247-249 °C (dec.)
----	-------------------

---

$^1\text{H}$ NMR ( $d_6$ -acetone)	1.45 (t, 9H, $^3J_{\text{H-H}} = 7.2$ Hz, $\text{CH}_3\text{CH}_2\text{-N}^+$ ), 2.95 (s, 9H, $\text{ArCH}_3$ ), 3.94 (q, 6H, $^3J_{\text{H-H}} = 7.3$ Hz, $\text{CH}_3\text{CH}_2\text{-N}^+$ ), 4.11 (t, 18H, $^3J_{\text{H-H}} = 7.2$ Hz, $\text{CH}_3\text{CH}_2\text{-N}^+\text{-CH}_2$ ), 4.38 (t, 18H, $^3J_{\text{H-H}} = 7.0$ Hz, $\text{ArCH}_2\text{-N}^+\text{-CH}_2$ ), 5.59 (s, 6H, $\text{ArCH}_2$ )
$^{13}\text{C}$ NMR ( $d_6$ -acetone)	7.9, 21.5, 51.6, 52.1, 61.9, 65.1, 128.0, 150.2
IR (KBr disc, $\text{cm}^{-1}$ )	1635 (br w), 1478 (w), 1420 (w), 1113 (w), 834 (br s), 559 (s)
FAB-MS ( $m/z$ %)	1307 (1.3) ( $[\text{M-PF}_6]^+$ ), 581 (0.8) ( $[\text{M-2PF}_6]^{2+}$ ), 141 (100)
$\text{C}_{36}\text{H}_{66}\text{N}_6\text{F}_6\text{P}_6$	calc. C 29.76 H 4.58 N 5.78
(1452.74)	found 29.10 4.60 5.39

#### 4.5.6 2,4,6-Tris( $\text{N}'$ -2-propyl-DABCO- $\text{N}$ -methyl)mesitylene hexabromide 130



2,4,6-Tris(bromomethyl)mesitylene (0.08 g, 0.20 mmol) and **122** (0.17 g, 0.72 mmol) in acetonitrile (25 mL) were treated as described in the general procedure to yield the product as a white powder (0.18 g, 0.16 mmol, 81%).

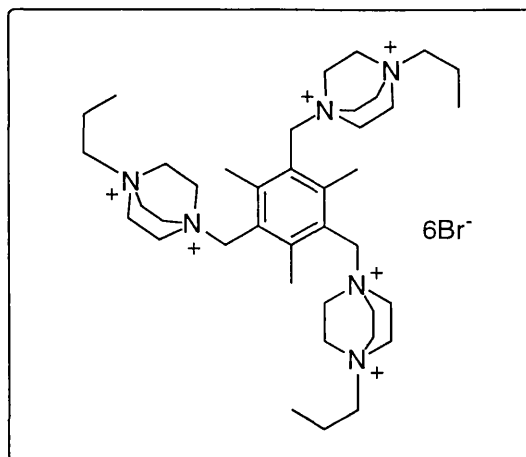
Mp	220-223 °C (dec.)
$^1\text{H}$ NMR ( $\text{D}_2\text{O}$ )	1.48 (d, 18H, $^3J_{\text{H-H}} = 6.5$ Hz, $\text{CH}(\text{CH}_3)_2$ ), 2.78 (s, 9H, $\text{ArCH}_3$ ), 3.96 (br t, 18H, $(\text{CH}_3)_2\text{CH-N}^+\text{-CH}_2$ ), 4.18 (br, 3H, $\text{CH}(\text{CH}_3)_2$ ), 4.28 (br t, 18H, $\text{ArCH}_2\text{-N}^+\text{-CH}_2$ ), 5.28 (s, 6H, $\text{ArCH}_2$ )
$^{13}\text{C}$ NMR ( $\text{D}_2\text{O}$ )	18.3, 23.8, 51.5, 53.8, 66.9, 71.4, 129.8, 151.1
IR (KBr disc, $\text{cm}^{-1}$ )	3010 (s), 1635 (br m), 1475 (m), 1414 (m), 1173 (w), 1120 (s), 1078 (m), 886 (w), 863 (m), 840 (m), 800 (w)
FAB-MS ( $m/z$ %)	1023 (2.7) ( $[\text{M-Br}]^+$ ), 473 (2.5) ( $[\text{M-2Br}]^{2+}$ ), 155 (100)

#### 4.5.7 2,4,6-Tris(N'-2-propyl-DABCO-N-methyl)mesitylene hexa(hexafluorophosphate) 140

Compound **130** (0.22 g, 0.20 mmol) was converted to its hexafluorophosphate salt as outlined in the general procedure to yield, after drying *in vacuo*, the product as a white solid (0.26 g, 0.17 mmol, 87%).

Mp	251-253 °C (dec.)		
$^1\text{H}$ NMR ( $d_6$ -acetone)	1.52 (d, 18H, $^3J_{\text{H-H}} = 5.7$ Hz, $\text{CH}(\text{CH}_3)_2$ ), 2.95 (s, 9H, $\text{ArCH}_3$ ), 4.10 (br, 18H, $(\text{CH}_3)_2\text{CH-N}^+-\text{CH}_2$ ), 4.21 (br, 3H, $\text{CH}(\text{CH}_3)_2$ ), 4.36 (br, 18H, $\text{ArCH}_2-\text{N}^+-\text{CH}_2$ ), 5.60 (s, 6H, $\text{ArCH}_2$ )		
$^{13}\text{C}$ NMR ( $d_6$ -acetone)	15.7, 21.1, 49.4, 51.6, 64.3, 68.6, 128.0, 149.1		
IR (KBr disc, $\text{cm}^{-1}$ )	3066 (w), 1636 (br w), 1482 (w), 1420 (m), 1402 (m), 1174 (w), 1121 (m), 1073 (w), 832 (br s), 741 (m), 557 (s)		
FAB-MS (m/z)	1349 ( $[\text{M-PF}_6]^+$ ), 1204 ( $[\text{M-2PF}_6]^+$ ), 602 ( $[\text{M-2PF}_6]^{2+}$ )		
$\text{C}_{39}\text{H}_{72}\text{N}_6\text{F}_6\text{P}_6\cdot\text{H}_2\text{O}$	calc.	C 30.96	H 4.93
(1512.83)	found	30.81	4.76
			N 5.56
			5.57

#### 4.5.8 2,4,6-Tris(N'-1-propyl-DABCO-N-methyl)mesitylene hexabromide 129



2,4,6-Tris(bromomethyl)mesitylene (0.20 g, 0.50 mmol) and **121** (0.84 g, 3.63 mmol) in acetonitrile (45 mL) were treated as described in the general procedure to yield the product as a white powder (0.51 g, 0.46 mmol, 90%).

Mp	205-207 °C (dec.)		
$^1\text{H}$ NMR ( $\text{D}_2\text{O}$ )	1.00 (t, 9H, $^3J_{\text{H-H}} = 7.2$ Hz, $\text{CH}_2\text{CH}_2\text{CH}_3$ ), 1.85 (m, 6H, $\text{CH}_2\text{CH}_2\text{CH}_3$ ), 2.77 (s, 9H, $\text{ArCH}_3$ ), 3.55 (m, 6H, $\text{CH}_2\text{CH}_2\text{CH}_3$ ), 4.00 (br t, 18H, $\text{CH}_3\text{CH}_2\text{CH}_2-\text{N}^+-\text{CH}_2$ ), 4.29 (br t, 18H, $\text{ArCH}_2-\text{N}^+-\text{CH}_2$ ), 5.27 (s, 6H, $\text{ArCH}_2$ )		

---

$^{13}\text{C}$ NMR ( $\text{D}_2\text{O}$ )	12.4, 18.2, 23.8, 53.9, 54.3, 67.1, 69.5, 129.7, 151.2
IR (KBr disc, $\text{cm}^{-1}$ )	2974 (s), 1636 (br w), 1457 (m), 1420 (w), 1388 (w), 1103 (m), 1061 (w), 852 (m)
FAB-MS ( $m/z$ )	1023 ( $[\text{M}-\text{Br}]^+$ ), 944 ( $[\text{M}-2\text{Br}]^+$ ), 473 ( $[\text{M}-2\text{Br}]^{2+}$ )

#### 4.5.9 2,4,6-Tris(*N*'-1-propyl-DABCO-*N*-methyl)mesitylene

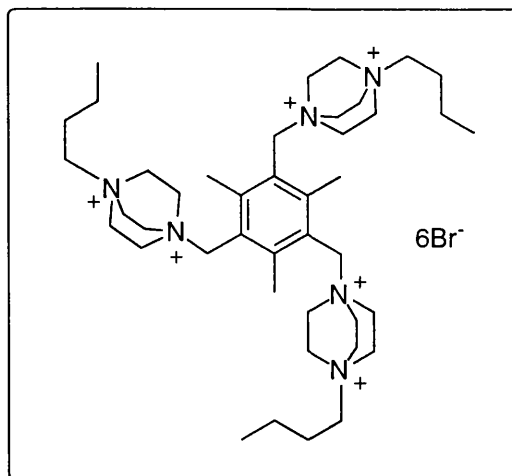
##### hexa(hexafluorophosphate 140

Compound **130** (0.45 g, 0.41 mmol) was converted to its hexafluorophosphate salt as outlined in the general procedure to yield, after drying *in vacuo*, the product as a white solid (0.47 g, 0.31 mmol, 77%).

Mp	224-226 °C (dec.)
$^1\text{H}$ NMR ( $d_6$ -acetone)	1.02 (t, 9H, $^3J_{\text{H-H}} = 7.3$ Hz, $\text{CH}_2\text{CH}_2\text{CH}_3$ ), 1.86 (m, 6H, $\text{CH}_2\text{CH}_2\text{CH}_3$ ), 2.95 (s, 9H, $\text{ArCH}_3$ ), 3.80 (br, 6H, $\text{CH}_2\text{CH}_2\text{CH}_3$ ), 4.12 (br t, 18H, $\text{CH}_3\text{CH}_2\text{CH}_2\text{-N}^+\text{-CH}_2$ ), 4.40 (br t, 18H, $\text{ArCH}_2\text{-N}^+\text{-CH}_2$ ), 5.58 (s, 6H, $\text{ArCH}_2$ )
$^{13}\text{C}$ NMR ( $d_6$ -acetone)	10.4, 11.3, 21.5, 52.1, 52.3, 65.1, 67.2, 128.1, 150.8
IR (KBr disc, $\text{cm}^{-1}$ )	2982 (w), 1637 (br w), 1475 (w), 1421 (w), 1104 (m), 833 (br s), 741 (m), 559 (s)
FAB-MS ( $m/z$ )	1349 ( $[\text{M}-\text{PF}_6]^+$ ), 1203 ( $[\text{M}-2\text{PF}_6]^+$ ), 602 ( $[\text{M}-2\text{PF}_6]^{2+}$ )
$\text{C}_{39}\text{H}_{72}\text{N}_6\text{F}_6\text{P}_6$	calc. C 31.34 H 4.85 N 5.62
(1494.82)	found 30.81 4.86 5.54

---

#### 4.5.10 2,4,6-Tris(N'-1-butyl-DABCO-N-methyl)mesitylene hexabromide 131



2,4,6-Tris(bromomethyl)mesitylene (0.20 g, 0.50 mmol) and **123** (0.93 g, 3.73 mmol) in acetonitrile (45 mL) were treated as described in the general procedure to yield the product as a white powder (0.52 g, 0.45 mmol, 90%).

Mp	203-206 °C (dec.)
$^1\text{H}$ NMR ( $\text{D}_2\text{O}$ )	0.98 (t, 9H, $^3\text{J}_{\text{H-H}} = 7.3$ Hz, $\text{CH}_2\text{CH}_3$ ), 1.42 (m, 6H, $\text{CH}_2\text{CH}_3$ ), 1.82 (m, 6H, $\text{CH}_2\text{CH}_2\text{CH}_3$ ), 2.78 (s, 9H, $\text{ArCH}_3$ ), 3.60 (m, 6H, $\text{CH}_2\text{CH}_2\text{CH}_2\text{CH}_3$ ), 4.00 (t, 18H, $^3\text{J}_{\text{H-H}} = 6.6$ Hz, $\text{ArCH}_2\text{-N}^+\text{-CH}_2\text{CH}_2$ ), 4.30 (t, 18H, $^3\text{J}_{\text{H-H}} = 6.6$ Hz, $\text{ArCH}_2\text{-N}^+\text{-CH}_2\text{CH}_2$ ), 5.27 (s, 6H, $\text{ArCH}_2$ )
$^{13}\text{C}$ NMR ( $\text{D}_2\text{O}$ )	15.3, 21.5, 23.5, 26.0, 53.6, 54.0, 66.8, 67.9, 129.4, 150.9
IR (KBr disc, $\text{cm}^{-1}$ )	2965 (s), 1633 (br m), 1465 (m), 1418 (w), 1388 (m), 1103 (m), 1059 (m), 856 (s)
FAB-MS ( $m/z$ )	1067 ( $[\text{M-Br}]^+$ ), 986 ( $[\text{M-2Br}]^+$ )

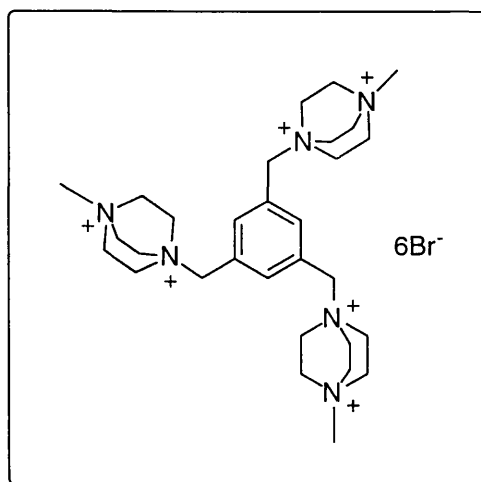
#### 4.5.11 2,4,6-Tris(N'-1-butyl-DABCO-N-methyl)mesitylene hexa(hexafluorophosphate) 141

Compound **131** (0.37 g, 0.32 mmol) was converted to its hexafluorophosphate salt as outlined in the general procedure to yield, after drying *in vacuo*, the product as a white solid (0.40 g, 0.26 mmol, 81%).

Mp	243-245 °C (dec.)
$^1\text{H}$ NMR ( $d_6$ -acetone)	0.96 (t, 9H, $^3\text{J}_{\text{H-H}} = 7.3$ Hz, $\text{CH}_2\text{CH}_3$ ), 1.44 (m, 6H, $\text{CH}_2\text{CH}_3$ ), 1.82 (m, 6H, $\text{CH}_2\text{CH}_2\text{CH}_3$ ), 2.94 (s, 9H, $\text{ArCH}_3$ ), 3.85 (br m, 6H,

	$\text{CH}_2\text{CH}_2\text{CH}_2\text{CH}_3$ ), 4.12 (br t, 18H, $\text{ArCH}_2\text{-N}^+\text{-CH}_2\text{CH}_2$ ), 4.43 (br t, 18H, $\text{ArCH}_2\text{-N}^+\text{-CH}_2\text{CH}_2$ ), 5.60 (s, 6H, $\text{ArCH}_2$ )
$^{13}\text{C}$ NMR ( $d_6$ -acetone)	14.4, 15.9, 20.8, 21.8, 52.1, 52.2, 65.1, 65.8, 128.0, 150.3
IR (KBr disc, $\text{cm}^{-1}$ )	2971 (w), 1636 (br w), 1473 (m), 1420 (w), 1390 (w), 1104 (m), 1062 (w), 832 (br s), 740 (w), 559 (s)
FAB-MS ( $m/z$ %)	1391 (2.2) ( $[\text{M-PF}_6]^+$ ), 623 (1.6) ( $[\text{M-2PF}_6]^{2+}$ ), 169 (100)
$\text{C}_{42}\text{H}_{78}\text{N}_6\text{F}_6\text{P}_3$	calc. C 32.82 H 5.12 N 5.47
(1536.90)	found 32.41 5.23 5.24

#### 4.5.12 1,3,5-Tris(N'-methyl-DABCO-N-methyl)benzene hexabromide 132



1,3,5-Tris(bromomethyl)benzene (0.18 g, 0.50 mmol) and **119** (0.38 g, 1.83 mmol) in acetonitrile (30 mL) were treated as described in the general procedure to yield the product as a white powder (0.40 g, 0.41 mmol, 81%).

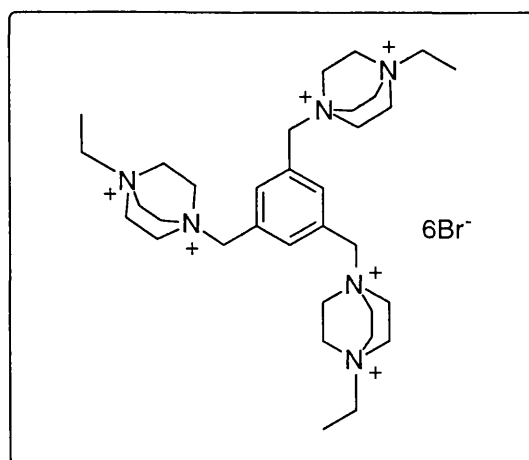
Mp	228-231 °C (dec.)
$^1\text{H}$ NMR ( $\text{D}_2\text{O}$ )	3.44 (s, 9H, $\text{CH}_3\text{-N}^+$ ), 4.11 (t, $^3J_{\text{H-H}} = 6.9$ Hz, 18H, $\text{CH}_3\text{-N}^+\text{-CH}_2$ ), 4.28 (t, $^3J_{\text{H-H}} = 6.8$ Hz, 18H, $\text{ArCH}_2\text{-N}^+\text{-CH}_2$ ), 5.08 (s, 6H, $\text{ArCH}_2$ ), 8.16 (s, 3H, $\text{ArH}$ )
$^{13}\text{C}$ NMR ( $\text{D}_2\text{O}$ )	53.7, 55.3, 56.1, 69.7, 131.3, 143.2
IR (KBr disc, $\text{cm}^{-1}$ )	3009 (s), 1636 (br w), 1471 (m), 1420 (w), 1382 (m), 1127 (m), 1059 (m), 853 (s), 744 (w)
FAB-MS ( $m/z$ )	899 ( $[\text{M-Br}]^+$ ), 693

#### 4.5.13 1,3,5-Tris(N'-methyl-DABCO-N-methyl)benzene hexa(hexafluorophosphate) 142

Compound **132** (0.34 g, 0.35 mmol) was converted to its hexafluorophosphate salt as outlined in the general procedure to yield, after drying *in vacuo*, the product as a white solid (0.44 g, 0.32 mmol, 93%).

Mp	261-263 °C		
<sup>1</sup> H NMR ( <i>d</i> <sub>6</sub> -acetone)	3.65 (s, 9H, CH <sub>3</sub> -N <sup>+</sup> ), 4.29 (m, 36H, CH <sub>3</sub> -N <sup>+</sup> -CH <sub>2</sub> & ArCH <sub>2</sub> -N <sup>+</sup> -CH <sub>2</sub> ), 5.21 (s, 6H, ArCH <sub>2</sub> ), 8.20 (s, 3H, ArH)		
<sup>13</sup> C NMR ( <i>d</i> <sub>6</sub> -acetone)	52.2, 53.6, 54.3, 67.9, 129.8, 141.5		
IR (KBr disc, cm <sup>-1</sup> )	1629 (br w), 1478 (w), 1388 (w), 1128 (w), 831 (br s), 741 (w), 558 (s)		
FAB-MS (m/z)	1223 ([M-PF <sub>6</sub> ] <sup>+</sup> ), 1077 ([M-2PF <sub>6</sub> ] <sup>+</sup> ), 539 ([M-2PF <sub>6</sub> ] <sup>2+</sup> )		
C <sub>30</sub> H <sub>54</sub> N <sub>6</sub> F <sub>36</sub> P <sub>6</sub>	calc.	C 26.33	H 3.98
(1368.57)	found	26.17	4.04
			N 6.14
			6.06

#### 4.5.14 1,3,5-Tris(N'-ethyl-DABCO-N-methyl)benzene hexabromide 133



1,3,5-Tris(bromomethyl)benzene (0.19 g, 0.53 mmol) and **120** (0.51 g, 2.31 mmol) in acetonitrile (35 mL) were treated as described in the general procedure to yield the product as a white powder (0.46 g, 0.45 mmol, 85%).

Mp	232-235 °C (dec.)		
<sup>1</sup> H NMR (D <sub>2</sub> O)	1.46 (t, 9H, <sup>3</sup> J <sub>H-H</sub> = 6.2 Hz, CH <sub>2</sub> CH <sub>3</sub> ), 3.71 (br q, 6H, <sup>3</sup> J <sub>H-H</sub> = 7.1 Hz, CH <sub>2</sub> CH <sub>3</sub> ), 4.04 (br, 18H, ArCH <sub>2</sub> -N <sup>+</sup> -CH <sub>2</sub> CH <sub>2</sub> ), 4.26 (br, 18H, ArCH <sub>2</sub> -N <sup>+</sup> -CH <sub>2</sub> CH <sub>2</sub> ), 5.08 (s, 6H, ArCH <sub>2</sub> ), 8.17 (s, 3H, ArH)		
<sup>13</sup> C NMR (D <sub>2</sub> O)	9.9, 53.5, 53.8, 64.0, 69.6, 131.4, 143.2		

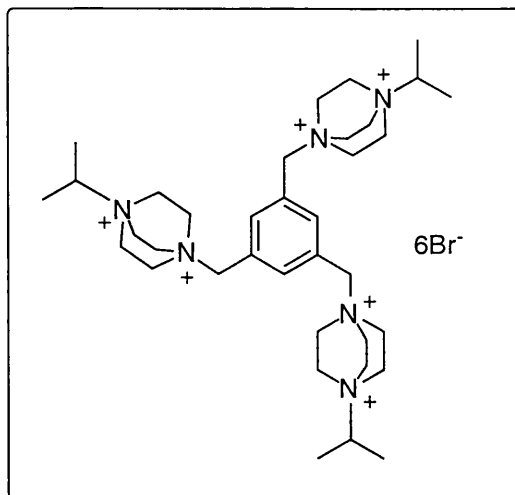
IR (KBr disc, $\text{cm}^{-1}$ )	3000 (s), 1627 (br m), 1459 (m), 1419 (m), 1183 (w), 1110 (s), 1062 (m), 921 (w), 854 (s), 746 (w)
FAB-MS ( $m/z$ )	939 ( $[\text{M}-\text{Br}]^+$ ), 859 ( $[\text{M}-2\text{Br}]^+$ ), 363

#### 4.5.15 1,3,5-Tris(N'-ethyl-DABCO-N-methyl)benzene hexa(hexafluorophosphate) 143

Compound **133** (0.29 g, 0.28 mmol) was converted to its hexafluorophosphate salt as outlined in the general procedure to yield, after drying *in vacuo*, the product as a white solid (0.36 g, 0.26 mmol, 90%).

Mp	282-284 °C
$^1\text{H}$ NMR ( $d_6$ -acetone)	1.47 (t, 9H, $^3J_{\text{H-H}} = 7.2$ Hz, $\text{CH}_2\text{CH}_3$ ), 3.89 (q, 6H, $^3J_{\text{H-H}} = 7.3$ Hz, $\text{CH}_2\text{CH}_3$ ), 4.16 (br t, 18H, $\text{ArCH}_2\text{-N}^+\text{-CH}_2\text{CH}_2$ ), 4.28 (br t, 18H, $\text{ArCH}_2\text{-N}^+\text{-CH}_2\text{CH}_2$ ), 5.22 (s, 6H, $\text{ArCH}_2$ ), 8.26 (s, 3H, $\text{ArH}$ )
$^{13}\text{C}$ NMR ( $d_6$ -acetone)	7.9, 51.5, 52.1, 62.0, 67.7, 129.8, 141.4
IR (KBr disc, $\text{cm}^{-1}$ )	3056 (m), 1636 (br w), 1484 (m), 1420 (w), 1395 (w), 1115 (m), 1066 (w), 836 (br s), 740 (m), 558 (s)
FAB-MS ( $m/z$ )	1265 ( $[\text{M}-\text{PF}_6]^+$ ), 1120 ( $[\text{M}-2\text{PF}_6]^+$ ), 560 ( $[\text{M}-2\text{PF}_6]^{2+}$ ), 459
$\text{C}_{33}\text{H}_{60}\text{N}_6\text{F}_{36}\text{P}_6$	calc. C 28.10 H 4.29 N 5.96
(1410.65)	found 28.10 4.30 5.73

#### 4.5.16 1,3,5-Tris(N'-2-propyl-DABCO-N-methyl)benzene hexabromide 135



1,3,5-Tris(bromomethyl)benzene (0.19 g, 0.53 mmol) and **122** (0.60 g, 2.55 mmol) in acetonitrile (35 mL) were treated as described in the general procedure to yield the product as a white powder (0.44 g, 0.41 mmol, 78%).



---

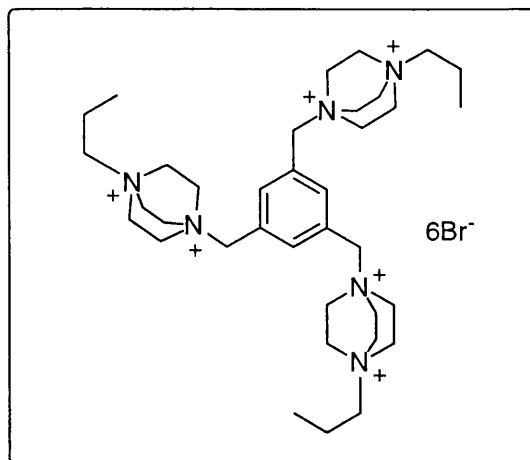
Mp	242-245 °C (dec.)
$^1\text{H}$ NMR ( $\text{D}_2\text{O}$ )	1.49 (d, 18H, $^3J_{\text{H-H}} = 5.8$ Hz, $\text{CH}(\text{CH}_3)_2$ ), 4.00 (br, 18H, $\text{ArCH}_2\text{-N}^+\text{-CH}_2\text{CH}_2$ ), 4.22 (br, 21H, $\text{ArCH}_2\text{-N}^+\text{-CH}_2\text{CH}_2$ & $\text{CH}(\text{CH}_3)_2$ ), 5.05 (s, 6H, $\text{ArCH}_2$ ), 8.15 (s, 3H, $\text{ArH}$ )
$^{13}\text{C}$ NMR ( $\text{D}_2\text{O}$ )	18.0, 51.1, 53.8, 69.3, 71.3, 131.4, 143.0
IR (KBr disc, $\text{cm}^{-1}$ )	3007 (s), 1636 (br w), 1474 (s), 1414 (m), 1398 (m), 1172 (w), 1120 (m), 1086 (w), 1062 (w), 887 (w), 857 (m), 839 (s), 746 (w)
FAB-MS (m/z)	983 ( $[\text{M-Br}]^+$ ), 901 ( $[\text{M-2Br}]^+$ ), 452 ( $[\text{M-2Br}]^{2+}$ )

**4.5.17 1,3,5-Tris(N'-2-propyl-DABCO-N-methyl)benzene  
hexa(hexafluorophosphate) 145**

Compound **135** (0.31 g, 0.29 mmol) was converted to its hexafluorophosphate salt as outlined in the general procedure to yield, after drying *in vacuo*, the product as a white solid (0.37 g, 0.26 mmol, 87%).

Mp	227-229 °C			
$^1\text{H}$ NMR ( $d_6$ -acetone)	1.55 (d, 18H, $^3J_{\text{H-H}} = 6.4$ Hz, $\text{CH}(\text{CH}_3)_2$ ), 4.17 (br, 18H, $\text{ArCH}_2\text{-N}^+\text{-CH}_2\text{CH}_2$ ), 4.25 (br, 21H, $\text{ArCH}_2\text{-N}^+\text{-CH}_2\text{CH}_2$ & $\text{CH}(\text{CH}_3)_2$ ), 5.22 (s, 6H, $\text{ArCH}_2$ ), 8.29 (s, 3H, $\text{ArH}$ )			
$^{13}\text{C}$ NMR ( $d_6$ -acetone)	15.5, 48.8, 51.7, 66.9, 68.9, 129.4, 140.8			
IR (KBr disc, $\text{cm}^{-1}$ )	3007 (w), 1636 (br w), 1481 (m), 1418 (m), 1173 (w), 1120 (m), 1088 (w), 832 (br s), 741 (w), 558 (s)			
FAB-MS (m/z)	1307 ( $[\text{M-PF}_6]^+$ ), 1162 ( $[\text{M-2PF}_6]^+$ ), 581 ( $[\text{M-2PF}_6]^{2+}$ )			
$\text{C}_{36}\text{H}_{66}\text{N}_6\text{F}_{36}\text{P}_6$	calc.	C 29.76	H 4.58	N 5.78
(1452.73)	found	29.80	4.64	5.96

#### 4.5.18 1,3,5-Tris(N'-1-propyl-DABCO-N-methyl)benzene hexabromide 134



1,3,5-Tris(bromomethyl)benzene (0.17 g, 0.48 mmol) and **121** (0.44 g, 1.87 mmol) in acetonitrile (30 mL) were treated as described in the general procedure to yield the product as a white powder (0.33 g, 0.31 mmol, 78%).

Mp	235-238 °C (dec.)
$^1\text{H}$ NMR ( $\text{D}_2\text{O}$ )	1.03 (t, 9H, $^3J_{\text{H-H}} = 7.1$ Hz, $\text{CH}_2\text{CH}_2\text{CH}_3$ ), 1.88 (br, 6H, $\text{CH}_2\text{CH}_2\text{CH}_3$ ) 3.58 (br t, 6H, $^3J_{\text{H-H}} = 8.1$ Hz, $\text{CH}_2\text{CH}_2\text{CH}_3$ ), 4.06 (br, 18H, $\text{ArCH}_2\text{-N}^+\text{-CH}_2\text{CH}_2$ ), 4.26 (br, 18H, $\text{ArCH}_2\text{-N}^+\text{-CH}_2\text{CH}_2$ ), 5.08 (s, 6H, $\text{ArCH}_2$ ), 8.17 (s, 3H, $\text{ArH}$ )
$^{13}\text{C}$ NMR ( $\text{D}_2\text{O}$ )	12.5, 18.3, 54.0, 54.2, 69.6, 69.8, 131.6, 143.4
IR (KBr disc, $\text{cm}^{-1}$ )	3011 (s), 1624 (br m), 1465 (m), 1419 (w), 1389 (m), 1183 (w), 1109 (s), 1062 (m), 915 (w), 854 (s), 748 (w)
FAB-MS ( $m/z$ )	983 ( $[\text{M-Br}]^+$ ), 902 ( $[\text{M-2Br}]^+$ )

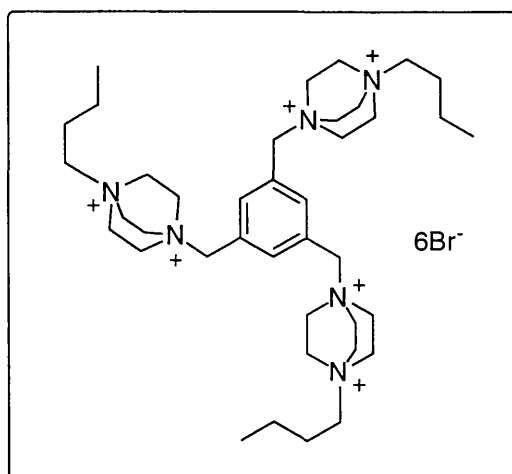
#### 4.5.19 1,3,5-Tris(N'-1-propyl-DABCO-N-methyl)benzene hexa(hexafluorophosphate) 144

Compound **134** (0.11 g, 0.10 mmol) was converted to its hexafluorophosphate salt as outlined in the general procedure to yield, after drying *in vacuo*, the product as a white solid (0.11 g, 0.08 mmol, 73%).

Mp	261-263 °C
$^1\text{H}$ NMR ( $d_6$ -acetone)	0.99 (t, 9H, $^3J_{\text{H-H}} = 7.3$ Hz, $\text{CH}_2\text{CH}_2\text{CH}_3$ ), 1.91 (m, 6H, $\text{CH}_2\text{CH}_2\text{CH}_3$ ), 3.75 (m, 6H, $\text{CH}_2\text{CH}_2\text{CH}_3$ ), 4.18 (br, 18H, $\text{ArCH}_2\text{-N}^+\text{-CH}_2\text{CH}_2$ ), 4.28 (br, 18H, $\text{ArCH}_2\text{-N}^+\text{-CH}_2\text{CH}_2$ ), 5.20 (s, 6H, $\text{ArCH}_2$ ), 8.24 (s, 3H, $\text{ArH}$ )
$^{13}\text{C}$ NMR ( $d_6$ -acetone)	10.4, 16.2, 52.1, 52.2, 67.3, 67.7, 129.8, 141.4

IR (KBr disc, $\text{cm}^{-1}$ )	3056 (w), 1636 (br w), 1475 (w), 1397 (w), 1108 (w), 834 (br s), 740 (w), 558 (s)
FAB-MS (m/z %)	1307 (42.9) ( $[\text{M}-\text{PF}_6]^+$ ), 581 (12.2) ( $[\text{M}-2\text{PF}_6]^{2+}$ ), 155 (100)
$\text{C}_{36}\text{H}_{66}\text{N}_6\text{F}_{36}\text{P}_6$ (1452.73)	calc. C 29.76 H 4.58 N 5.78 found 29.67 4.57 5.85

#### 4.5.20 1,3,5-Tris(N'-1-butyl-DABCO-N-methyl)benzene hexabromide 136



1,3,5-Tris(bromomethyl)benzene (0.17 g, 0.48 mmol) and **123** (0.43 g, 1.73 mmol) in acetonitrile (30 mL) were treated as described in the general procedure to yield the product as a white powder (0.38 g, 0.34 mmol, 72%).

Mp	243-246 °C (dec.)
$^1\text{H}$ NMR ( $\text{D}_2\text{O}$ )	0.96 (t, 9H, $^3\text{J}_{\text{H-H}} = 7.3$ Hz, $\text{CH}_2\text{CH}_3$ ), 1.41 (q, 6H, $^3\text{J}_{\text{H-H}} = 7.2$ Hz, $\text{CH}_2\text{CH}_3$ ), 1.81 (br, 6H, $\text{CH}_2\text{CH}_2\text{CH}_3$ ), 3.60 (m, 6H, $\text{CH}_2\text{CH}_2\text{CH}_2\text{CH}_3$ ), 4.03 (br, 18H, $\text{ArCH}_2\text{-N}^+\text{-CH}_2\text{CH}_2$ ), 4.23 (br, 18H, $\text{ArCH}_2\text{-N}^+\text{-CH}_2\text{CH}_2$ ), 5.04 (s, 6H, $\text{ArCH}_2$ ), 8.13 (s, 3H, $\text{ArH}$ )
$^{13}\text{C}$ NMR ( $\text{D}_2\text{O}$ )	15.3, 21.5, 26.1, 53.8, 53.9, 68.0, 69.6, 131.4, 143.1
IR (KBr disc, $\text{cm}^{-1}$ )	2964 (s), 1634 (br m), 1464 (s), 1391 (m), 1108 (s), 1061 (w), 854 (s)
FAB-MS (m/z)	1023 (1.4) ( $[\text{M}-\text{Br}]^+$ ), 169 (100)

#### 4.5.21 1,3,5-Tris(N'-1-butyl-DABCO-N-methyl)benzene hexa(hexafluorophosphate) 146

Compound **136** (0.23 g, 0.21 mmol) was converted to its hexafluorophosphate salt as outlined in the general procedure to yield, after drying *in vacuo*, the product as a white solid (0.22 g, 0.15 mmol, 71%).

---

Mp	272-274 °C (dec.)
$^1\text{H}$ NMR ( $d_6$ -acetone)	0.94 (t, 9H, $^3J_{\text{H-H}} = 7.3$ Hz, $\text{CH}_2\text{CH}_3$ ), 1.42 (m, 6H, $\text{CH}_2\text{CH}_3$ ), 1.88 (m, 6H, $\text{CH}_2\text{CH}_2\text{CH}_3$ ), 3.83 (m, 6H, $\text{CH}_2\text{CH}_2\text{CH}_2\text{CH}_3$ ), 4.23 (br, 18H, $\text{ArCH}_2\text{-N}^+\text{-CH}_2\text{CH}_2$ ), 4.28 (br, 18H, $\text{ArCH}_2\text{-N}^+\text{-CH}_2\text{CH}_2$ ), 5.21 (s, 6H, $\text{ArCH}_2$ ), 8.23 (s, 3H, $\text{ArH}$ )
$^{13}\text{C}$ NMR ( $d_6$ -acetone)	13.3, 19.5, 24.1, 51.7, 51.9, 65.6, 67.4, 129.5, 141.1
IR (KBr disc, $\text{cm}^{-1}$ )	2972 (w), 1635 (br w), 1474 (w), 1396 (w), 1108 (w), 833 (br s), 741 (w), 558 (s)
FAB-MS (m/z %)	1349 ( $[\text{M-PF}_6]^+$ ), 601 ( $[\text{M-2PF}_6]^{2+}$ ), 169.1 (100)
$\text{C}_{39}\text{H}_{72}\text{N}_6\text{F}_{36}\text{P}_6$	calc. C 31.34 H 4.85 N 5.62
(1494.81)	found 30.74 5.18 5.28

---

## 4.6 NMR Titrations and Job Plots

This section consists of a series of tables summarising the results of investigations into the behaviour of some of the polycations synthesised with a variety of organic anions using nuclear magnetic resonance spectroscopy. Throughout this section the letter **C** refers to the polycationic component whilst the letter **A** refers to the anion. **AC** refers to the complex formed between the two species. Carboxylate salts were prepared from their corresponding acids by reaction with a stoichiometric quantity of sodium hydroxide in water, followed by precipitation from water and acetone, except for sodium benzoate, adenosine 5'-diphosphate, trisodium salt (ADP) and adenosine 5'-triphosphate, disodium salt (ATP) where commercial samples were used. All reagents were dried under vacuum overnight before use. Where ADP or ATP was the anion, the chemical shift of the anomeric proton was observed. For anions where more than one aryl signal was observed, a weighted average chemical shift ( $\delta_{\text{ave}}$ ) is quoted:

e.g.



### 4.6.1 General Protocol - NMR Titrations

Standardised solutions of (i) a mixture of polycation and polyanion and (ii) polyanion were prepared in D<sub>2</sub>O and aliquots combined to give a constant volume of solution. The polycation was initially considered to be the host and the ratio of host:guest was varied stepwise from 5:1 to zero, the latter providing the initial position of the anion signals, and <sup>1</sup>H NMR spectra were taken at 7 relative concentrations. Spectra were recorded at 400 MHz on a Varian VXR-400 instrument. The spectrometer was referenced to 3-(trimethylsilyl)propionic-2,2,3,3-*d*<sub>4</sub> acid, sodium salt, before and after each titration. The changes in the <sup>1</sup>H NMR spectral chemical shifts of the anion protons in association with the polycation were recorded. In most cases, the chemical shifts of the benzylic and methyl groups in the polycation for each sample were also recorded along with a reference sample of polycation. Where more than one titration was performed, the results shown are the average over all experiments. Plots of chemical shift difference against the ratio of host-guest concentrations were fitted by iterative curve-fitting procedures, using data within the values 0.2 and 0.8 of the parameter *p* of Weber<sup>145</sup>, and association constants were derived from these curves.

### 4.6.2 General Protocol - Job Plots

Standardised solutions of polycation and anion were prepared in D<sub>2</sub>O and aliquots combined to give a constant volume of solution such that the total concentration of host and guest remained constant. <sup>1</sup>H NMR spectra were taken at 7 relative proportions. Spectra were recorded at 400

---

MHz on a Varian VXR-400 instrument. The spectrometer was referenced to 3-(trimethylsilyl)propionic-2,2,3,3- $d_4$  acid, sodium salt, before and after each run. The changes in the  $^1\text{H}$  NMR spectral chemical shifts of the anion protons in association with the polycation were recorded. In most cases, the chemical shifts of the benzylic and methyl groups in the polycation for each sample were also recorded along with a reference sample of polycation. In cases where more than one run was performed, the results shown are the average over all experiments. From observations of protons in the anion, the concentration of the complex was estimated as follows:

$$[\text{AC}] = [\text{A}]_{\text{tot}}(\delta_{\text{obs}} - \delta_{\text{A}})/(\delta_{\text{AC}} - \delta_{\text{A}})$$

where:  $[\text{A}]_{\text{tot}}$  = the total concentration of A in solution

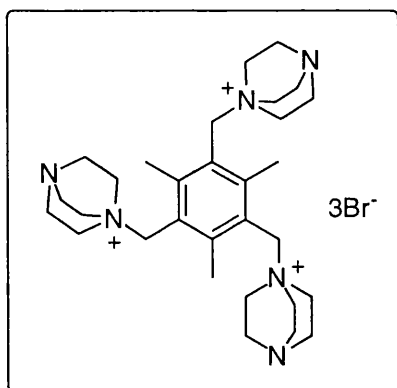
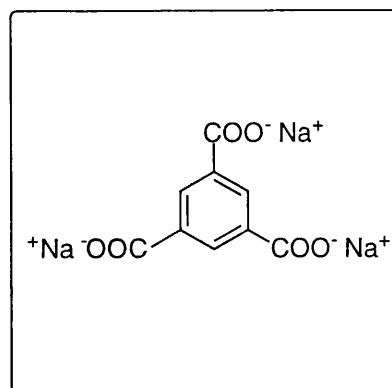
$\delta_{\text{obs}}$  = observed chemical shift

$\delta_{\text{A}}$  = chemical shift of the observed protons in A

$\delta_{\text{AC}}$  = chemical shift of the observed protons of A in the complex  
(estimated on the basis of NMR titration data).

Corresponding methods were used to determine the concentration of complex from measurements of the chemical shifts in the polycations.

#### 4.6.3 NMR Titration of 2,4,6-Tris(DABCO-N-methyl)mesitylene Tribromide 109 and Trisodium Benzene-1,3,5-tricarboxylate 186

**C****A**

	Solution X			Solution Y	
	C / mg	A / mg	D <sub>2</sub> O / mL	A / mg	D <sub>2</sub> O / mL
Run 1	183.4	13.6	5.00	13.6	5.00
Run 2	183.1	13.8	5.00	14.0	5.00
Run 3	183.1	13.8	5.00	14.2	5.00
Run 4	184.2	13.9	5.00	13.7	5.00

#### Anion Shift (Average of 4 Runs)

X / mL	Y / mL	[C] / mM	[A] / mM	[C]/[A]	$\delta$	$\Delta\delta$
0.00	0.80	0.00	10.05	0.00	8.395	0.000
0.05	0.75	3.12	10.05	0.31	8.319	0.075
0.10	0.70	6.24	10.04	0.62	8.243	0.151
0.12	0.68	7.48	10.04	0.75	8.210	0.184
0.16	0.64	9.98	10.04	0.99	8.148	0.246
0.25	0.55	15.59	10.03	1.55	8.051	0.344
0.40	0.40	24.94	10.01	2.49	7.937	0.458
0.80	0.00	49.88	9.98	5.00	7.837	0.558

## Cation Methyl Shift (Average of 4 Runs)

X / mL	Y / mL	[C] / mM	[A] / mM	[A]/[C]	$\delta$	$\Delta\delta$
Cation Reference		10.00	0.00	0.00	2.687	0.000
0.80	0.00	49.82	9.95	0.20	2.572	0.116
0.40	0.40	24.91	10.02	0.40	2.509	0.178
0.25	0.55	15.57	10.05	0.65	2.466	0.221
0.16	0.64	9.96	10.06	1.01	2.455	0.232
0.12	0.68	7.47	10.07	1.35	2.450	0.237
0.10	0.70	6.23	10.07	1.62	2.453	0.235
0.05	0.75	3.11	10.08	3.24	2.452	0.235

## Cation Benzyl Shift (Average of 4 Runs)

X / mL	Y / mL	[C] / mM	[A] / mM	[A]/[C]	$\delta$	$\Delta\delta$
Cation Reference		10.00	0.00	0.00	4.930	0.000
0.80	0.00	49.82	9.95	0.20	4.788	0.142
0.40	0.40	24.91	10.02	0.40	4.711	0.219
0.25	0.55	15.57	10.05	0.65	4.658	0.272
0.16	0.64	9.96	10.06	1.01	4.643	0.288
0.12	0.68	7.47	10.07	1.35	4.636	0.294
0.10	0.70	6.23	10.07	1.62	4.639	0.292
0.05	0.75	3.11	10.08	3.24	4.638	0.293

## 4.6.4 Job Plot of 2,4,6-Tris(DABCO-N-methyl)mesitylene Tribromide 109 and Trisodium Benzene-1,3,5-tricarboxylate 186

	Solution X		Solution Y	
	C / mg	D <sub>2</sub> O / mL	A / mg	D <sub>2</sub> O / mL
Run 1	37.2	5.00	14.1	5.00
Run 2	74.4	10.00	14.0	5.00
Run 3	37.3	5.00	27.8	10.00



## Anion Shift (Average of 3 Runs)

X / mL	Y / mL	[C] / mM	[A] / mM	$\frac{[A]}{[A]+[C]}$	$\delta$	$\Delta\delta$	[AC] / mM	Error / mM
0.00	0.80	0.00	10.10	1.00	8.395	0.000	0.00	
0.10	0.70	1.30	8.90	0.88	8.365	0.030	0.36	0.14
0.20	0.60	2.50	7.60	0.75	8.320	0.075	0.78	0.14
0.30	0.50	3.80	6.30	0.63	8.249	0.145	1.26	0.15
0.40	0.40	5.10	5.10	0.50	8.183	0.212	1.47	0.14
0.50	0.30	6.30	3.80	0.38	8.074	0.320	1.70	0.14
0.60	0.20	7.60	2.50	0.25	8.013	0.382	1.33	0.10
0.70	0.10	8.90	1.30	0.13	7.944	0.451	0.78	0.06

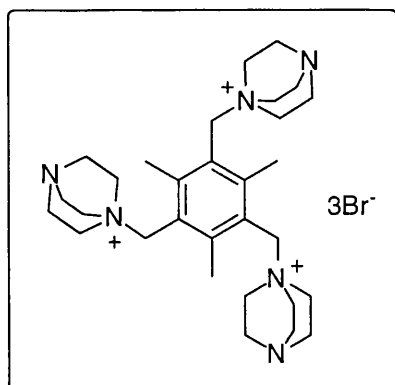
## Cation Methyl Shift (Average of 3 Runs)

X / mL	Y / mL	[C] / mM	[A] / mM	$\frac{[C]}{[A]+[C]}$	$\delta$	$\Delta\delta$	[AC] / mM	Error / mM
0.80	0.00	10.12	0.00	1.00	2.687	0.000	0.00	
0.70	0.10	8.86	1.27	0.87	2.618	0.069	2.48	0.48
0.60	0.20	7.59	2.54	0.75	2.545	0.142	4.37	0.53
0.50	0.30	6.33	3.80	0.62	2.502	0.185	4.75	0.49
0.40	0.40	5.06	5.07	0.50	2.468	0.219	4.48	0.43
0.30	0.50	3.80	6.34	0.37	2.457	0.230	3.53	0.33
0.20	0.60	2.53	7.61	0.25	2.458	0.230	2.35	0.22
0.10	0.70	1.27	8.87	0.12	2.458	0.230	1.18	0.11

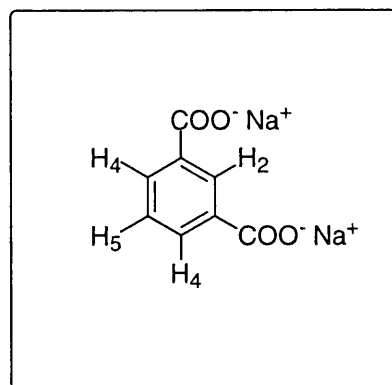
## Cation Benzyl Shift (Average of 3 Runs)

X / mL	Y / mL	[C] / mM	[A] / mM	$\frac{[C]}{[A]+[C]}$	$\delta$	$\Delta\delta$	[AC] / mM	Error / mM
0.80	0.00	10.12	0.00	1.00	4.930	0.000	0.00	
0.70	0.10	8.86	1.27	0.87	4.850	0.080	2.30	0.40
0.60	0.20	7.59	2.54	0.75	4.756	0.174	4.26	0.46
0.50	0.30	6.33	3.80	0.62	4.703	0.227	4.64	0.44
0.40	0.40	5.06	5.07	0.50	4.660	0.270	4.41	0.38
0.30	0.50	3.80	6.34	0.37	4.645	0.285	3.49	0.30
0.20	0.60	2.53	7.61	0.25	4.644	0.286	2.34	0.20
0.10	0.70	1.27	8.87	0.12	4.646	0.284	1.16	0.10

#### 4.6.5 NMR Titration of 2,4,6-Tris(DABCO-N-methyl)mesitylene Tribromide 109 and Disodium Benzene-1,3-dicarboxylate 188



C



A

	Solution X			Solution Y	
	C / mg	A / mg	D <sub>2</sub> O / mL	A / mg	D <sub>2</sub> O / mL
Run 1	187.5	10.7	5.00	10.9	5.00
Run 2	184.7	11.3	5.00	11.4	5.00
Run 3	184.7	11.3	5.00	10.5	5.00

#### Anion Shift (Average of 3 Runs)

X / mL	Y / mL	[C] / mM	[A] / mM	[C]/[A]	$\delta_2$	$\delta_4$	$\delta_5$	$\delta_{ave}$	$\Delta\delta_{ave}$
0.00	0.80	0.00	10.41	0.00	8.286	8.085	7.526	7.946	0.000
0.05	0.75	3.15	10.42	0.30	8.199	7.923	7.464	7.877	0.069
0.10	0.70	6.31	10.43	0.61	8.156	7.894	7.433	7.844	0.102
0.12	0.68	7.57	10.43	0.73	8.146	7.880	7.424	7.833	0.114
0.16	0.64	10.10	10.44	0.97	8.102	7.852	7.395	7.800	0.146
0.25	0.55	15.77	10.46	1.51	8.053	7.814	7.359	7.760	0.187
0.40	0.40	25.24	10.49	2.41	7.985	7.765	7.312	7.706	0.240
0.80	0.00	50.48	10.57	4.78	7.842	7.680	7.236	7.610	0.337

## Cation Methyl Shift (Average of 3 Runs)

X / mL	Y / mL	[C] / mM	[A] / mM	[A]/[C]	$\delta$	$\Delta\delta$
Cation Reference		10.00	0.00	0.00	2.687	0.000
0.80	0.00	50.48	10.57	0.21	2.629	0.058
0.40	0.40	25.24	10.49	0.42	2.604	0.084
0.25	0.55	15.77	10.46	0.66	2.587	0.101
0.16	0.64	10.10	10.44	1.03	2.569	0.118
0.12	0.68	7.57	10.43	1.38	2.558	0.129
0.10	0.70	6.31	10.43	1.65	2.554	0.134
0.05	0.75	3.15	10.42	3.30	2.544	0.143

## Cation Benzyl Shift (Average of 3 Runs)

X / mL	Y / mL	[C] / mM	[A] / mM	[A]/[C]	$\delta$	$\Delta\delta$
Cation Reference		10.00	0.00	0.00	4.930	0.000
0.80	0.00	50.48	10.57	0.21	4.861	0.069
0.40	0.40	25.24	10.49	0.42	4.831	0.099
0.25	0.55	15.77	10.46	0.66	4.809	0.121
0.16	0.64	10.10	10.44	1.03	4.790	0.140
0.12	0.68	7.57	10.43	1.38	4.780	0.150
0.10	0.70	6.31	10.43	1.65	4.775	0.156
0.05	0.75	3.15	10.42	3.30	4.763	0.167

## 4.6.6 Job Plot of 2,4,6-Tris(DABCO-N-methyl)mesitylene Tribromide 109 and Disodium Benzene-1,3-dicarboxylate 188

	Solution X		Solution Y	
	C / mg	D <sub>2</sub> O / mL	A / mg	D <sub>2</sub> O / mL
Run 1	73.6	10.00	11.1	5.00
Run 2	36.7	5.00	10.2	5.00
Run 3	37.0	5.00	11.2	5.00

## Anion Shift (Average of 3 Runs)

X / mL	Y / mL	[C] / mM	[A] / mM	$\frac{[A]}{[A]+[C]}$	$\delta_2$	$\delta_4$	$\delta_5$	$\delta_{ave}$	$\Delta\delta_{ave}$	[AC] / mM	Error / mM
0.00	0.80	0.00	10.31	1.00	8.288	7.986	7.527	7.947	0.000	0.00	
0.10	0.70	1.25	9.02	0.88	8.259	7.968	7.515	7.927	0.020	0.39	0.22
0.20	0.60	2.50	7.73	0.76	8.217	7.938	7.480	7.893	0.054	0.92	0.22
0.30	0.50	3.76	6.45	0.63	8.178	7.909	7.453	7.862	0.085	1.21	0.20
0.40	0.40	5.01	5.16	0.51	8.134	7.877	7.419	7.827	0.120	1.37	0.18
0.50	0.30	6.26	3.87	0.38	8.098	7.850	7.395	7.798	0.148	1.27	0.15
0.60	0.20	7.51	2.58	0.26	8.062	7.827	7.369	7.771	0.176	1.00	0.11
0.70	0.10	8.76	1.29	0.13	8.025	7.801	7.346	7.743	0.204	0.58	0.06

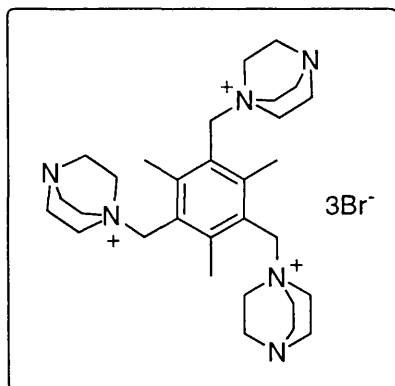
## Cation Methyl Shift (Average of 3 Runs)

X / mL	Y / mL	[C] / mM	[A] / mM	$\frac{[C]}{[A]+[C]}$	$\delta$	$\Delta\delta$	[AC] / mM	Error / mM
0.80	0.00	10.02	0.00	1.00	2.687	0.000	0.00	
0.70	0.10	8.76	1.29	0.87	2.651	0.036	2.07	0.68
0.60	0.20	7.51	2.58	0.74	2.631	0.056	2.77	0.63
0.50	0.30	6.26	3.87	0.62	2.611	0.076	3.12	0.57
0.40	0.40	5.01	5.16	0.49	2.587	0.100	3.29	0.49
0.30	0.50	3.76	6.45	0.37	2.565	0.122	3.02	0.40
0.20	0.60	2.50	7.73	0.24	2.550	0.138	2.26	0.28
0.10	0.70	1.25	9.02	0.12	2.538	0.149	1.22	0.14

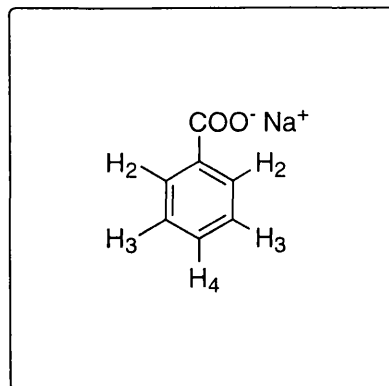
## Cation Benzyl Shift (Average of 3 Runs)

X / mL	Y / mL	[C] / mM	[A] / mM	$\frac{[C]}{[A]+[C]}$	$\delta$	$\Delta\delta$	[AC] / mM	Error / mM
0.80	0.00	10.02	0.00	1.00	4.930	0.000	0.00	
0.70	0.10	8.76	1.29	0.87	4.894	0.036	1.77	0.57
0.60	0.20	7.51	2.58	0.74	4.869	0.061	2.55	0.54
0.50	0.30	6.26	3.87	0.62	4.841	0.090	3.11	0.50
0.40	0.40	5.01	5.16	0.49	4.822	0.108	3.01	0.43
0.30	0.50	3.76	6.45	0.37	4.790	0.141	2.93	0.36
0.20	0.60	2.50	7.73	0.24	4.778	0.152	2.12	0.24
0.10	0.70	1.25	9.02	0.12	4.782	0.149	1.03	0.12

#### 4.6.7 NMR Titration of 2,4,6-Tris(DABCO-N-methyl)mesitylene Tribromide 109 and Sodium Benzoate 187



C



A

	Solution X			Solution Y	
	C / mg	A / mg	D <sub>2</sub> O / mL	A / mg	D <sub>2</sub> O / mL
Run 1	183.2	6.9	5.00	6.9	5.00
Run 2	183.2	6.9	5.00	14.2	10.00
Run 3	184.4	7.9	5.00	14.2	10.00

#### Anion Shift (Average of 3 Runs)

X / mL	Y / mL	[C] / mM	[A] / mM	[C]/[A]	$\delta_2$	$\delta_3$	$\delta_4$	$\delta_{ave}$	$\Delta\delta_{ave}$
0.00	0.80	0.00	9.76	0.00	7.878	7.487	7.667	7.658	0.000
0.05	0.75	3.12	9.78	0.32	7.859	7.475	7.549	7.643	0.015
0.10	0.70	6.24	9.80	0.64	7.841	7.460	7.536	7.628	0.031
0.12	0.68	7.49	9.80	0.76	7.838	7.454	7.533	7.623	0.035
0.16	0.64	9.99	9.82	1.02	7.826	7.444	7.526	7.613	0.045
0.25	0.55	15.60	9.85	1.58	7.814	7.437	7.518	7.604	0.054
0.40	0.40	24.96	9.90	2.52	7.789	7.417	7.499	7.582	0.076
0.80	0.00	49.93	10.04	4.97	7.717	7.358	7.450	7.520	0.138

## Cation Methyl Shift (Average of 3 Runs)

X / mL	Y / mL	[C] / mM	[A] / mM	[A]/[C]	$\delta$	$\Delta\delta$
Cation Reference		10.00	0.00	0.00	2.687	0.000
0.80	0.00	49.93	10.04	0.20	2.664	0.023
0.40	0.40	24.96	9.90	0.40	2.655	0.033
0.25	0.55	15.60	9.85	0.63	2.650	0.037
0.16	0.64	9.99	9.82	0.98	2.644	0.043
0.12	0.68	7.49	9.80	1.31	2.643	0.045
0.10	0.70	6.24	9.80	1.57	2.639	0.048
0.05	0.75	3.12	9.78	3.13	2.632	0.056

## Cation Benzyl Shift (Average of 3 Runs)

X / mL	Y / mL	[C] / mM	[A] / mM	[A]/[C]	$\delta$	$\Delta\delta$
Cation Reference		10.00	0.00	0.00	4.930	0.000
0.80	0.00	49.93	10.04	0.20	4.903	0.028
0.40	0.40	24.96	9.90	0.40	4.894	0.036
0.25	0.55	15.60	9.85	0.63	4.889	0.041
0.16	0.64	9.99	9.82	0.98	4.882	0.048
0.12	0.68	7.49	9.80	1.31	4.880	0.050
0.10	0.70	6.24	9.80	1.57	4.877	0.053
0.05	0.75	3.12	9.78	3.13	4.872	0.059

## 4.6.8 Job Plot of 2,4,6-Tris(DABCO-N-methyl)mesitylene Tribromide 109 and Sodium Benzoate 187

	Solution X		Solution Y	
	C / mg	D <sub>2</sub> O / mL	A / mg	D <sub>2</sub> O / mL
Run 1	75.2	10.00	7.7	5.00

## Anion Shift (1 Run)

X / mL	Y / mL	[C] / mM	[A] / mM	$\frac{[A]}{[A]+[C]}$	$\delta_2$	$\delta_3$	$\delta_4$	$\delta_{ave}$	$\Delta\delta_{ave}$	[AC] / mM	Error / mM
0.00	0.80	0.00	10.69	1.00	7.870	7.478	7.552	7.650	0.000	0.00	
0.10	0.70	1.28	9.35	0.88	7.869	7.476	7.555	7.649	0.001	0.03	0.44
0.20	0.60	2.56	8.01	0.76	7.858	7.482	7.546	7.645	0.004	0.17	0.39
0.30	0.50	3.83	6.68	0.64	7.856	7.468	7.547	7.639	0.011	0.34	0.33
0.40	0.40	5.11	5.34	0.51	7.836	7.477	7.538	7.633	0.017	0.43	0.27
0.50	0.30	6.39	4.01	0.39	7.836	7.456	7.534	7.624	0.026	0.49	0.21
0.60	0.20	7.67	2.67	0.26	7.823	7.442	7.521	7.610	0.040	0.50	0.15
0.70	0.10	8.95	1.34	0.13	7.813	7.434	7.515	7.602	0.048	0.30	0.08

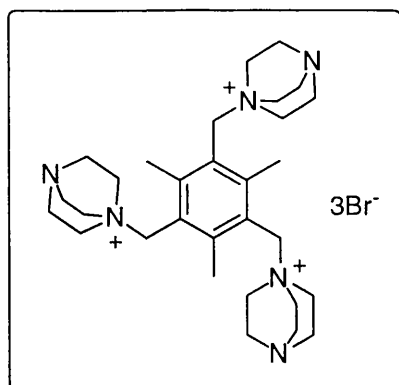
## Cation Methyl Shift (1 Run)

X / mL	Y / mL	[C] / mM	[A] / mM	$\frac{[C]}{[A]+[C]}$	$\delta$	$\Delta\delta$	[AC] / mM	Error / mM
0.80	0.00	10.22	0.00	1.00	2.687	0.000	0.00	
0.70	0.10	8.95	1.34	0.87	2.661	0.026	4.20	1.80
0.60	0.20	7.67	2.67	0.74	2.654	0.033	4.55	1.59
0.50	0.30	6.39	4.01	0.61	2.654	0.033	3.79	1.32
0.40	0.40	5.11	5.34	0.49	2.654	0.033	3.01	1.06
0.30	0.50	3.83	6.68	0.36	2.647	0.041	2.76	0.82
0.20	0.60	2.56	8.01	0.24	2.643	0.044	2.00	0.55
0.10	0.70	1.28	9.35	0.12	2.631	0.056	1.27	0.29

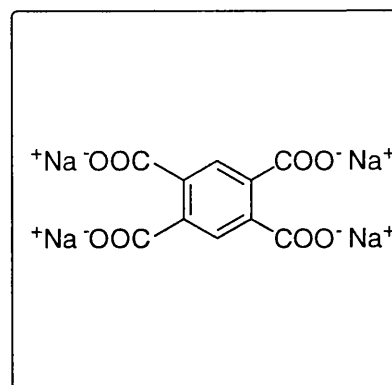
## Cation Benzyl Shift (1 Run)

X / mL	Y / mL	[C] / mM	[A] / mM	$\frac{[C]}{[A]+[C]}$	$\delta$	$\Delta\delta$	[AC] / mM	Error / mM
0.80	0.00	10.22	0.00	1.00	4.930	0.000	0.00	
0.70	0.10	8.95	1.34	0.87	4.906	0.024	3.55	1.64
0.60	0.20	7.67	2.67	0.74	4.900	0.031	3.85	1.45
0.50	0.30	6.39	4.01	0.61	4.898	0.032	3.39	1.21
0.40	0.40	5.11	5.34	0.49	4.890	0.040	3.33	1.00
0.30	0.50	3.83	6.68	0.36	4.884	0.047	2.93	0.77
0.20	0.60	2.56	8.01	0.24	4.872	0.058	2.43	0.54
0.10	0.70	1.28	9.35	0.12	4.869	0.061	1.27	0.27

#### 4.6.9 NMR Titration of 2,4,6-Tris(DABCO-N-methyl)mesitylene Tribromide 109 and Tetrasodium Benzene-1,2,4,5-tetracarboxylate 189



C



A

	Solution X			Solution Y	
	C / mg	A / mg	D <sub>2</sub> O / mL	A / mg	D <sub>2</sub> O / mL
Run 1	184.4	17.1	5.00	16.9	5.00
Run 2	184.4	17.1	5.00	34.2	10.00
Run 3	184.1	17.1	5.00	17.3	5.00

#### Anion Shift (Average of 3 Runs)

X / mL	Y / mL	[C] / mM	[A] / mM	[C]/[A]	$\delta$	$\Delta\delta$
0.00	0.80	0.00	10.00	0.00	7.518	0.000
0.05	0.75	3.13	10.00	0.31	7.485	0.033
0.10	0.70	6.26	10.00	0.63	7.459	0.060
0.12	0.68	7.52	10.00	0.75	7.445	0.073
0.16	0.64	10.02	10.00	1.00	7.433	0.085
0.25	0.55	15.66	10.00	1.57	7.404	0.114
0.40	0.40	25.06	10.00	2.51	7.381	0.137
0.80	0.00	50.12	10.00	5.01	7.357	0.161



## Cation Methyl Shift (Average of 3 Runs)

X / mL	Y / mL	[C] / mM	[A] / mM	[A]/[C]	$\delta$	$\Delta\delta$
Cation Reference		10.00	0.00	0.00	2.687	0.000
0.80	0.00	50.12	10.00	0.20	2.674	0.013
0.40	0.40	25.06	10.00	0.40	2.654	0.033
0.25	0.55	15.66	10.00	0.64	2.645	0.042
0.16	0.64	10.02	10.00	1.00	2.638	0.049
0.12	0.68	7.52	10.00	1.33	2.632	0.055
0.10	0.70	6.26	10.00	1.60	2.627	0.060
0.05	0.75	3.13	10.00	3.19	2.620	0.068

## Cation Benzyl Shift (Average of 3 Runs)

X / mL	Y / mL	[C] / mM	[A] / mM	[A]/[C]	$\delta$	$\Delta\delta$
Cation Reference		10.00	0.00	0.00	4.930	0.000
0.80	0.00	50.12	10.00	0.20	4.920	0.010
0.40	0.40	25.06	10.00	0.40	4.904	0.026
0.25	0.55	15.66	10.00	0.64	4.898	0.033
0.16	0.64	10.02	10.00	1.00	4.893	0.038
0.12	0.68	7.52	10.00	1.33	4.888	0.042
0.10	0.70	6.26	10.00	1.60	4.882	0.048
0.05	0.75	3.13	10.00	3.19	4.875	0.056

## 4.6.10 Job Plot of 2,4,6-Tris(DABCO-N-methyl)mesitylene Tribromide 109 and Tetrasodium Benzene-1,2,4,5-tetracarboxylate 189

	Solution X		Solution Y	
	C / mg	D <sub>2</sub> O / mL	A / mg	D <sub>2</sub> O / mL
Run 1	75.2	10.00	16.8	5.00

## Anion Shift (1 Run)

X / mL	Y / mL	[C] / mM	[A] / mM	$\frac{[A]}{[A]+[C]}$	$\delta$	$\Delta\delta$	[AC] / mM	Error / mM
0.00	0.80	0.00	9.82	1.00	7.510	0.000	0.00	
0.10	0.70	1.28	8.59	0.87	7.491	0.019	0.93	0.53
0.20	0.60	2.56	7.37	0.74	7.477	0.033	1.38	0.49
0.30	0.50	3.83	6.14	0.62	7.454	0.055	1.93	0.44
0.40	0.40	5.11	4.91	0.49	7.427	0.083	2.30	0.39
0.50	0.30	6.39	3.68	0.37	7.415	0.095	1.98	0.31
0.60	0.20	7.67	2.46	0.24	7.393	0.117	1.62	0.22
0.70	0.10	8.95	1.23	0.12	7.377	0.133	0.92	0.12

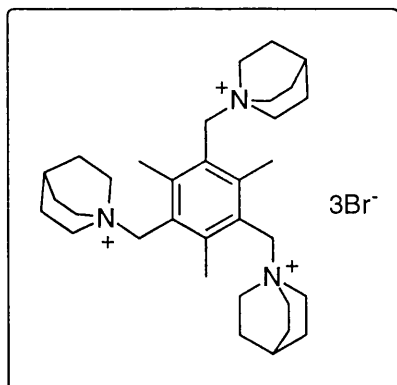
## Cation Methyl Shift (1 Run)

X / mL	Y / mL	[C] / mM	[A] / mM	$\frac{[C]}{[A]+[C]}$	$\delta$	$\Delta\delta$	[AC] / mM	Error / mM
0.80	0.00	10.22	0.00	1.00	2.687	0.000	0.00	
0.70	0.10	8.95	1.23	0.88	2.657	0.030	1.43	0.55
0.60	0.20	7.67	2.46	0.76	2.651	0.036	1.48	0.48
0.50	0.30	6.39	3.68	0.63	2.643	0.044	1.50	0.42
0.40	0.40	5.11	4.91	0.51	2.624	0.063	1.73	0.36
0.30	0.50	3.83	6.14	0.38	2.621	0.067	1.36	0.27
0.20	0.60	2.56	7.37	0.26	2.612	0.075	1.03	0.19
0.10	0.70	1.28	8.59	0.13	2.599	0.088	0.60	0.10

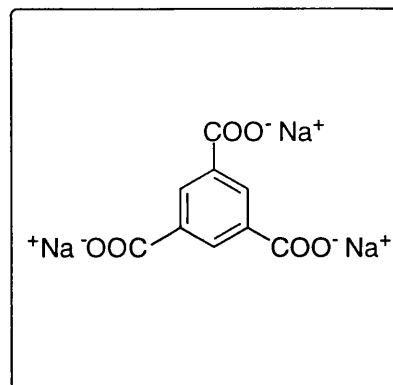
## Cation Benzyl Shift (1 Run)

X / mL	Y / mL	[C] / mM	[A] / mM	$\frac{[C]}{[A]+[C]}$	$\delta$	$\Delta\delta$	[AC] / mM	Error / mM
0.80	0.00	10.22	0.00	1.00	4.930	0.000	0.00	
0.70	0.10	8.95	1.23	0.88	4.906	0.024	1.66	0.77
0.60	0.20	7.67	2.46	0.76	4.902	0.029	1.68	0.67
0.50	0.30	6.39	3.68	0.63	4.897	0.033	1.63	0.57
0.40	0.40	5.11	4.91	0.51	4.882	0.048	1.90	0.49
0.30	0.50	3.83	6.14	0.38	4.879	0.051	1.50	0.37
0.20	0.60	2.56	7.37	0.26	4.863	0.067	1.32	0.26
0.10	0.70	1.28	8.59	0.13	4.839	0.092	0.90	0.14

#### 4.6.11 NMR Titration of 2,4,6-Tris(Quinuclidine-N-methyl)mesitylene Tribromide 148 and Trisodium Benzene-1,3,5-tricarboxylate 186



C



A

	Solution X			Solution Y	
	C / mg	A / mg	D <sub>2</sub> O / mL	A / mg	D <sub>2</sub> O / mL
Run 1	366.0	27.2	10.00	13.9	5.00
Run 2	366.0	27.2	10.00	14.2	5.00
Run 3	366.0	27.2	10.00	13.5	5.00

#### Anion Shift (Average of 3 Runs)

X / mL	Y / mL	[C] / mM	[A] / mM	[C]/[A]	$\delta$	$\Delta\delta$
0.00	0.80	0.00	10.07	0.00	8.402	0.000
0.05	0.75	3.12	10.06	0.31	8.329	0.073
0.10	0.70	6.25	10.04	0.62	8.260	0.142
0.12	0.68	7.49	10.04	0.75	8.235	0.167
0.16	0.64	9.99	10.03	1.00	8.178	0.224
0.25	0.55	15.61	10.00	1.56	8.076	0.326
0.40	0.40	24.98	9.96	2.51	7.981	0.420
0.80	0.00	49.96	9.85	5.07	7.887	0.515

## Cation Methyl Shift (Average of 3 Runs)

X / mL	Y / mL	[C] / mM	[A] / mM	[A]/[C]	$\delta$	$\Delta\delta$
Cation Reference		10.00	0.00	0.00	2.649	0.000
0.80	0.00	49.96	9.85	0.20	2.550	0.099
0.40	0.40	24.98	9.95	0.40	2.486	0.163
0.25	0.55	15.61	9.98	0.64	2.455	0.194
0.16	0.64	9.99	10.01	1.00	2.435	0.214
0.12	0.68	7.49	10.02	1.34	2.433	0.216
0.10	0.70	6.25	10.02	1.60	2.427	0.222
0.05	0.75	3.12	10.03	3.21	2.425	0.224

## Cation Benzyl Shift (Average of 3 Runs)

X / mL	Y / mL	[C] / mM	[A] / mM	[A]/[C]	$\delta$	$\Delta\delta$
Cation Reference		10.00	0.00	0.00	4.759	0.000
0.80	0.00	49.96	9.85	0.20	4.638	0.121
0.40	0.40	24.98	9.95	0.40	4.561	0.198
0.25	0.55	15.61	9.98	0.64	4.523	0.236
0.16	0.64	9.99	10.01	1.00	4.499	0.260
0.12	0.68	7.49	10.02	1.34	4.497	0.261
0.10	0.70	6.25	10.02	1.60	4.492	0.267
0.05	0.75	3.12	10.03	3.21	4.491	0.267

## 4.6.12 Job Plot of 2,4,6-Tris(Quinuclidine-N-methyl)mesitylene Tribromide 148 and Trisodium Benzene-1,3,5-tricarboxylate 186

	Solution X		Solution Y	
	C / mg	D <sub>2</sub> O / mL	A / mg	D <sub>2</sub> O / mL
Run 1	74.3	10.00	27.3	10.00
Run 2	74.3	10.00	27.3	10.00
Run 3	74.3	10.00	13.7	5.00

## Anion Shift (Average of 3 Runs)

X / mL	Y / mL	[C] / mM	[A] / mM	$\frac{[A]}{[A]+[C]}$	$\delta$	$\Delta\delta$	[AC] / mM	Error / mM
0.00	0.80	0.00	9.90	1.00	8.397	0.000	0.00	
0.10	0.70	1.27	8.66	0.87	8.369	0.028	0.37	0.15
0.20	0.60	2.54	7.42	0.75	8.327	0.071	0.80	0.15
0.30	0.50	3.80	6.19	0.62	8.261	0.136	1.28	0.16
0.40	0.40	5.07	4.95	0.49	8.197	0.200	1.50	0.15
0.50	0.30	6.34	3.71	0.37	8.123	0.274	1.55	0.13
0.60	0.20	7.61	2.47	0.25	8.059	0.338	1.27	0.10
0.70	0.10	8.88	1.24	0.12	8.015	0.383	0.72	0.05

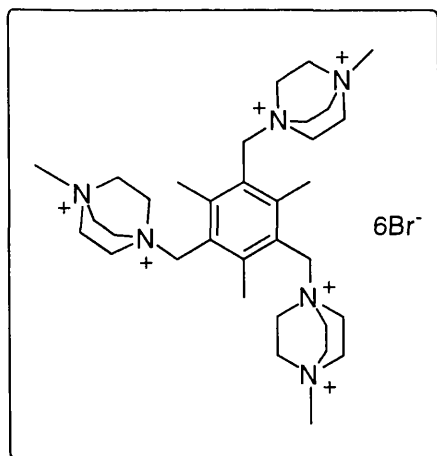
## Cation Methyl Shift (Average of 3 Runs)

X / mL	Y / mL	[C] / mM	[A] / mM	$\frac{[C]}{[A]+[C]}$	$\delta$	$\Delta\delta$	[AC] / mM	Error / mM
0.80	0.00	10.14	0.00	1.00	2.649	0.000	0.00	
0.70	0.10	8.88	1.24	0.88	2.579	0.070	2.73	0.52
0.60	0.20	7.61	2.47	0.75	2.526	0.123	4.09	0.54
0.50	0.30	6.34	3.71	0.63	2.480	0.169	4.69	0.51
0.40	0.40	5.07	4.95	0.51	2.442	0.207	4.58	0.45
0.30	0.50	3.80	6.19	0.38	2.432	0.217	3.60	0.35
0.20	0.60	2.54	7.42	0.25	2.428	0.221	2.45	0.23
0.10	0.70	1.27	8.66	0.13	2.426	0.223	1.24	0.12

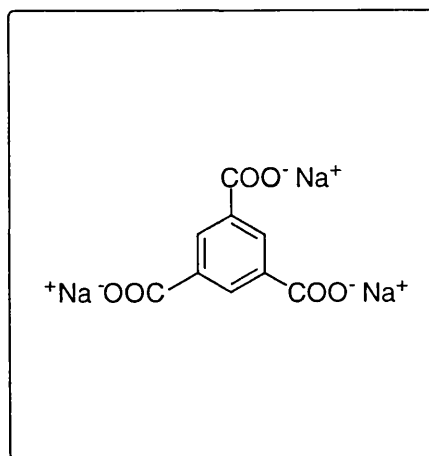
## Cation Benzyl Shift (Average of 3 Runs)

X / mL	Y / mL	[C] / mM	[A] / mM	$\frac{[C]}{[A]+[C]}$	$\delta$	$\Delta\delta$	[AC] / mM	Error / mM
0.80	0.00	10.14	0.00	1.00	4.759	0.000	0.00	
0.70	0.10	8.88	1.24	0.88	4.680	0.078	2.58	0.46
0.60	0.20	7.61	2.47	0.75	4.615	0.143	4.06	0.49
0.50	0.30	6.34	3.71	0.63	4.559	0.199	4.71	0.47
0.40	0.40	5.07	4.95	0.51	4.513	0.245	4.63	0.42
0.30	0.50	3.80	6.19	0.38	4.501	0.258	3.65	0.32
0.20	0.60	2.54	7.42	0.25	4.497	0.262	2.47	0.22
0.10	0.70	1.27	8.66	0.13	4.500	0.259	1.22	0.11

#### 4.6.13 NMR Titration of 2,4,6-Tris(N'-Methyl-DABCO-N-methyl)mesitylene Hexabromide 127 and Trisodium Benzene-1,3,5-tricarboxylate 186



C



A

	Solution X			Solution Y	
	C / mg	A / mg	D <sub>2</sub> O / mL	A / mg	D <sub>2</sub> O / mL
Run 1	257.4	13.1	5.00	27.7	10.00
Run 2	257.4	13.1	5.00	27.7	10.00
Run 3	126.1	6.4	5.00	6.8	5.00

#### Anion Shift (Average of 3 Runs)

X / mL	Y / mL	[C] / mM	[A] / mM	[C]/[A]	$\delta$	$\Delta\delta$
0.00	0.80	0.00	8.33	0.00	8.395	0.000
0.05	0.75	2.62	8.30	0.32	8.327	0.068
0.10	0.70	5.23	8.27	0.63	8.245	0.150
0.12	0.68	6.28	8.26	0.76	8.216	0.179
0.16	0.64	8.38	8.24	1.02	8.185	0.209
0.25	0.55	13.09	8.19	1.60	8.155	0.239
0.40	0.40	20.94	8.10	2.58	8.153	0.242
0.80	0.00	41.88	7.87	5.32	8.211	0.184

## Cation Methyl Shift (Average of 3 Runs)

X / mL	Y / mL	[C] / mM	[A] / mM	[A]/[C]	$\delta$	$\Delta\delta$
Cation Reference		10.00	0.00	0.00	2.754	0.000
0.80	0.00	41.88	7.87	0.19	2.738	0.016
0.40	0.40	20.94	8.10	0.39	2.670	0.084
0.25	0.55	13.09	8.19	0.63	2.608	0.146
0.16	0.64	8.38	8.24	0.98	2.566	0.188
0.12	0.68	6.28	8.26	1.32	2.546	0.207
0.10	0.70	5.23	8.27	1.58	2.529	0.225
0.05	0.75	2.62	8.30	3.17	2.514	0.240

## Cation Benzyl Shift (Average of 3 Runs)

X / mL	Y / mL	[C] / mM	[A] / mM	[A]/[C]	$\delta$	$\Delta\delta$
Cation Reference		10.00	0.00	0.00	5.265	0.000
0.80	0.00	41.88	7.87	0.19	5.217	0.048
0.40	0.40	20.94	8.10	0.39	5.139	0.126
0.25	0.55	13.09	8.19	0.63	5.068	0.197
0.16	0.64	8.38	8.24	0.98	5.019	0.246
0.12	0.68	6.28	8.26	1.32	4.996	0.269
0.10	0.70	5.23	8.27	1.58	4.977	0.288
0.05	0.75	2.62	8.30	3.17	4.961	0.304

4.6.14 Job Plot of 2,4,6-Tris(N'-Methyl-DABCO-N-methyl)mesitylene Hexabromide 127 and Trisodium Benzene-1,3,5-tricarboxylate 186

	Solution X		Solution Y	
	C / mg	D <sub>2</sub> O / mL	A / mg	D <sub>2</sub> O / mL
Run 1	36.1	5.00	9.4	5.00
Run 2	50.6	5.00	13.6	5.00
Run 3	50.3	5.00	13.4	5.00

**Anion Shift (Average of 3 Runs)**

X / mL	Y / mL	[C] / mM	[A] / mM	$\frac{[A]}{[A]+[C]}$	$\delta$	$\Delta\delta$	[AC] / mM	Error / mM
0.00	0.80	0.00	8.79	1.00	8.394	0.000	0.00	
0.10	0.70	1.12	7.69	0.87	8.358	0.036	0.99	0.32
0.20	0.60	2.24	6.59	0.75	8.298	0.097	2.19	0.34
0.30	0.50	3.36	5.49	0.62	8.238	0.157	2.93	0.33
0.40	0.40	4.48	4.39	0.49	8.189	0.205	3.07	0.30
0.50	0.30	5.59	3.30	0.37	8.170	0.224	2.86	0.27
0.60	0.20	6.71	2.20	0.25	8.210	0.184	1.40	0.15
0.70	0.10	7.83	1.10	0.12	8.304	0.091	0.38	0.06

**Cation Methyl Shift (Average of 3 Runs)**

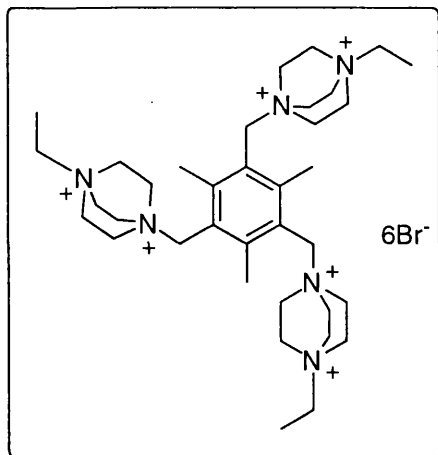
X / mL	Y / mL	[C] / mM	[A] / mM	$\frac{[C]}{[A]+[C]}$	$\delta$	$\Delta\delta$	[AC] / mM	Error / mM
0.80	0.00	8.95	0.00	1.00	2.754	0.000	0.00	
0.70	0.10	7.83	1.10	0.88	2.729	0.025	0.77	0.35
0.60	0.20	6.71	2.20	0.75	2.688	0.066	1.75	0.35
0.50	0.30	5.59	3.30	0.63	2.616	0.138	3.07	0.38
0.40	0.40	4.48	4.39	0.51	2.567	0.187	3.29	0.34
0.30	0.50	3.36	5.49	0.38	2.531	0.223	2.94	0.28
0.20	0.60	2.24	6.59	0.25	2.512	0.242	2.13	0.19
0.10	0.70	1.12	7.69	0.13	2.507	0.247	1.09	0.10

**Cation Benzyl Shift (Average of 3 Runs)**

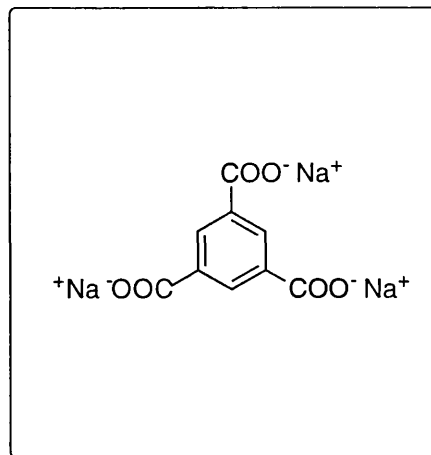
X / mL	Y / mL	[C] / mM	[A] / mM	$\frac{[C]}{[A]+[C]}$	$\delta$	$\Delta\delta$	[AC] / mM	Error / mM
0.80	0.00	8.95	0.00	1.00	5.262	0.000	0.00	
0.70	0.10	7.83	1.10	0.88	5.226	0.036	0.80	0.26
0.60	0.20	6.71	2.20	0.75	5.172	0.090	1.97	0.32
0.50	0.30	5.59	3.30	0.63	5.094	0.169	2.66	0.29
0.40	0.40	4.48	4.39	0.51	5.025	0.238	2.93	0.27
0.30	0.50	3.36	5.49	0.38	4.979	0.283	2.62	0.22
0.20	0.60	2.24	6.59	0.25	4.961	0.301	2.06	0.17
0.10	0.70	1.12	7.69	0.13	4.954	0.308	0.95	0.08



#### 4.6.15 NMR Titration of 2,4,6-Tris(N'-ethyl-N-methyl)mesitylene Hexabromide 128 and Trisodium Benzene-1,3,5-tricarboxylate 186



C



A

	Solution X			Solution Y	
	C / mg	A / mg	D <sub>2</sub> O / mL	A / mg	D <sub>2</sub> O / mL
Run 1	132.0	6.6	5.00	14.6	10.00
Run 2	132.0	6.6	5.00	14.6	10.00
Run 3	132.0	6.6	5.00	6.3	5.00

#### Anion Shift (Average of 3 Runs)

X / mL	Y / mL	[C] / mM	[A] / mM	[C]/[A]	$\delta$	$\Delta\delta$
0.00	0.80	0.00	5.05	0.00	8.393	0.000
0.05	0.75	1.55	5.03	0.31	8.292	0.101
0.10	0.70	3.11	5.01	0.62	8.198	0.195
0.12	0.68	3.73	5.01	0.74	8.186	0.207
0.16	0.64	4.97	4.99	1.00	8.141	0.253
0.25	0.55	7.77	4.96	1.56	8.095	0.298
0.40	0.40	12.42	4.91	2.53	8.058	0.335
0.80	0.00	24.85	4.78	5.20	8.009	0.384

## Cation Methyl Shift (Average of 3 Runs)

X / mL	Y / mL	[C] / mM	[A] / mM	[A]/[C]	$\delta$	$\Delta\delta$
Cation Reference		10.00	0.00	0.00	2.783	0.000
0.80	0.00	24.85	4.78	0.19	2.719	0.064
0.40	0.40	12.42	4.91	0.40	2.656	0.126
0.25	0.55	7.77	4.96	0.64	2.616	0.166
0.16	0.64	4.97	4.99	1.00	2.570	0.213
0.12	0.68	3.73	5.01	1.34	2.549	0.233
0.10	0.70	3.11	5.01	1.61	2.539	0.244
0.05	0.75	1.55	5.03	3.24	2.527	0.256

## Cation Benzyl Shift (Average of 3 Runs)

X / mL	Y / mL	[C] / mM	[A] / mM	[A]/[C]	$\delta$	$\Delta\delta$
Cation Reference		10.00	0.00	0.00	5.279	0.000
0.80	0.00	24.85	4.78	0.19	5.193	0.086
0.40	0.40	12.42	5.03	0.41	5.116	0.163
0.25	0.55	7.77	5.13	0.66	5.074	0.205
0.16	0.64	4.97	5.19	1.04	5.018	0.261
0.12	0.68	3.73	5.21	1.40	4.993	0.286
0.10	0.70	3.11	5.22	1.68	4.983	0.297
0.05	0.75	1.55	5.26	3.38	4.969	0.310

## 4.6.16 Job Plot of 2,4,6-Tris(N'-ethyl-N-methyl)mesitylene Hexabromide 128 and Trisodium Benzene-1,3,5-tricarboxylate 186

	Solution X		Solution Y	
	C / mg	D <sub>2</sub> O / mL	A / mg	D <sub>2</sub> O / mL
Run 1	105.4	10.00	27.1	10.00
Run 2	105.4	10.00	27.1	10.00
Run 3	105.4	10.00	27.1	10.00

## Anion Shift (Average of 3 Runs)

X / mL	Y / mL	[C] / mM	[A] / mM	$\frac{[A]}{[A]+[C]}$	$\delta$	$\Delta\delta$	[AC] / mM	Error / mM
0.00	0.80	0.00	9.82	1.00	8.395	0.000	0.00	
0.10	0.70	1.24	8.59	0.87	8.342	0.052	0.96	0.23
0.20	0.60	2.48	7.36	0.75	8.283	0.112	2.01	0.28
0.30	0.50	3.72	6.13	0.62	8.214	0.181	2.71	0.29
0.40	0.40	4.96	4.91	0.50	8.147	0.247	2.97	0.27
0.50	0.30	6.20	3.68	0.37	8.104	0.291	2.59	0.22
0.60	0.20	7.44	2.45	0.25	8.079	0.316	1.90	0.15
0.70	0.10	8.68	1.23	0.12	8.080	0.315	0.95	0.08

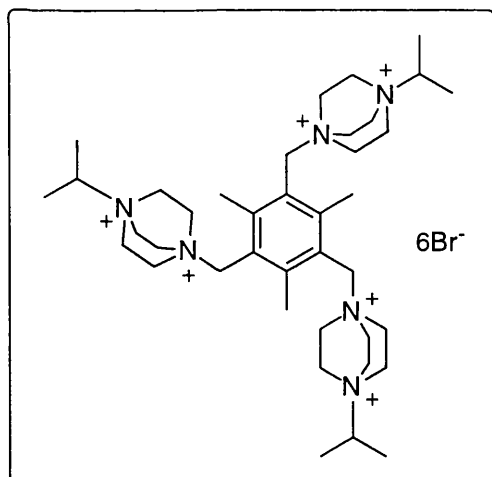
## Cation Methyl Shift (Average of 3 Runs)

X / mL	Y / mL	[C] / mM	[A] / mM	$\frac{[C]}{[A]+[C]}$	$\delta$	$\Delta\delta$	[AC] / mM	Error / mM
0.80	0.00	9.92	0.00	1.00	2.779	0.000	0.00	
0.70	0.10	8.68	1.23	0.88	2.721	0.058	1.90	0.42
0.60	0.20	7.44	2.45	0.75	2.651	0.128	3.58	0.46
0.50	0.30	6.20	3.68	0.63	2.621	0.159	3.71	0.42
0.40	0.40	4.96	4.91	0.50	2.569	0.210	3.93	0.38
0.30	0.50	3.72	6.13	0.38	2.531	0.248	3.48	0.31
0.20	0.60	2.48	7.36	0.25	2.521	0.258	2.41	0.21
0.10	0.70	1.24	8.59	0.13	2.519	0.261	1.22	0.11

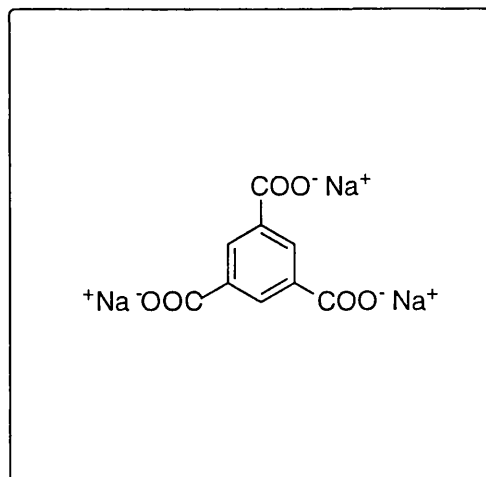
## Cation Benzyl Shift (Average of 3 Runs)

X / mL	Y / mL	[C] / mM	[A] / mM	$\frac{[C]}{[A]+[C]}$	$\delta$	$\Delta\delta$	[AC] / mM	Error / mM
0.80	0.00	10.47	0.00	1.00	5.272	0.000	0.00	
0.70	0.10	9.16	1.24	0.88	5.210	0.062	1.86	0.39
0.60	0.20	7.85	2.48	0.76	5.125	0.147	3.38	0.40
0.50	0.30	6.54	3.73	0.64	5.085	0.187	4.04	0.42
0.40	0.40	5.23	4.97	0.51	5.022	0.250	4.31	0.39
0.30	0.50	3.93	6.21	0.39	4.977	0.295	3.82	0.32
0.20	0.60	2.62	7.45	0.26	4.965	0.307	2.74	0.23
0.10	0.70	1.31	8.69	0.13	4.961	0.310	1.31	0.11

#### 4.6.17 NMR Titration of 2,4,6-Tris(N'-2-propyl-DABCO-N-methyl)mesitylene Hexabromide 130 and Trisodium Benzene-1,3,5-tricarboxylate 186



C



A

	Solution X			Solution Y	
	C / mg	A / mg	D <sub>2</sub> O / mL	A / mg	D <sub>2</sub> O / mL
Run 1	138.0	7.1	5.00	13.5	10.00
Run 2	138.0	7.1	5.00	13.5	10.00
Run 3	138.0	7.1	5.00	6.6	5.00

#### Anion Shift (Average of 3 Runs)

X / mL	Y / mL	[C] / mM	[A] / mM	[C]/[A]	$\delta$	$\Delta\delta$
0.00	0.80	0.00	4.85	0.00	8.398	0.000
0.05	0.75	1.56	4.87	0.32	8.293	0.105
0.10	0.70	3.12	4.89	0.64	8.220	0.178
0.12	0.68	3.75	4.90	0.77	8.197	0.200
0.16	0.64	5.00	4.91	1.02	8.175	0.223
0.25	0.55	7.81	4.94	1.58	8.136	0.262
0.40	0.40	12.49	5.00	2.50	8.114	0.283
0.80	0.00	24.99	5.14	4.86	8.110	0.287

## Cation Methyl Shift (Average of 3 Runs)

X / mL	Y / mL	[C] / mM	[A] / mM	[A]/[C]	$\delta$	$\Delta\delta$
Cation Reference		10.00	0.00	0.00	2.784	0.000
0.80	0.00	24.99	5.14	0.21	2.730	0.054
0.40	0.40	12.49	5.00	0.40	2.672	0.112
0.25	0.55	7.81	4.94	0.63	2.623	0.160
0.16	0.64	5.00	4.91	0.98	2.580	0.204
0.12	0.68	3.75	4.90	1.31	2.564	0.220
0.10	0.70	3.12	4.89	1.57	2.549	0.235
0.05	0.75	1.56	4.87	3.12	2.537	0.247

## Cation Benzyl Shift (Average of 3 Runs)

X / mL	Y / mL	[C] / mM	[A] / mM	[A]/[C]	$\delta$	$\Delta\delta$
Cation Reference		10.00	0.00	0.00	5.280	0.000
0.80	0.00	24.99	5.14	0.21	5.204	0.076
0.40	0.40	12.49	5.00	0.40	5.138	0.142
0.25	0.55	7.81	4.94	0.63	5.082	0.198
0.16	0.64	5.00	4.91	0.98	5.028	0.252
0.12	0.68	3.75	4.90	1.31	5.010	0.271
0.10	0.70	3.12	4.89	1.57	4.991	0.290
0.05	0.75	1.56	4.87	3.12	4.977	0.303

4.6.18 Job Plot of 2,4,6-Tris(N'-2-propyl-DABCO-N-methyl)mesitylene Hexabromide 130 and Trisodium Benzene-1,3,5-tricarboxylate 186

	Solution X		Solution Y	
	C / mg	D <sub>2</sub> O / mL	A / mg	D <sub>2</sub> O / mL
Run 1	114.1	10.00	27.6	10.00
Run 2	114.1	10.00	27.6	10.00
Run 3	114.1	10.00	27.6	10.00

## Anion Shift (Average of 3 Runs)

X / mL	Y / mL	[C] / mM	[A] / mM	$\frac{[A]}{[A]+[C]}$	$\delta$	$\Delta\delta$	[AC] / mM	Error / mM
0.00	0.80	0.00	10.00	1.00	8.402	0.000	0.00	
0.10	0.70	1.29	8.75	0.87	8.359	0.043	1.22	0.35
0.20	0.60	2.58	7.50	0.74	8.289	0.113	2.87	0.40
0.30	0.50	3.87	6.25	0.62	8.230	0.172	3.66	0.40
0.40	0.40	5.17	5.00	0.49	8.172	0.230	3.91	0.37
0.50	0.30	6.46	3.75	0.37	8.141	0.261	3.29	0.29
0.60	0.20	7.75	2.50	0.24	8.136	0.266	2.26	0.20

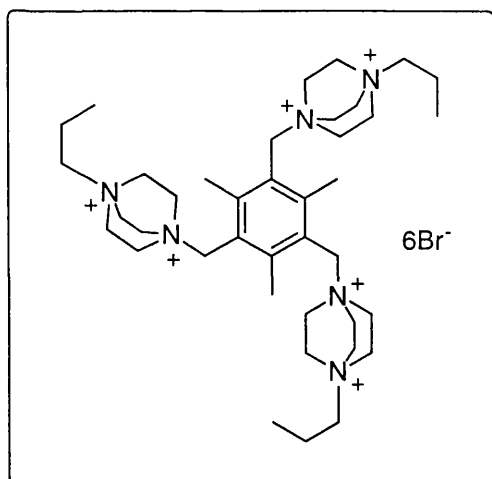
## Cation Methyl Shift (Average of 3 Runs)

X / mL	Y / mL	[C] / mM	[A] / mM	$\frac{[C]}{[A]+[C]}$	$\delta$	$\Delta\delta$	[AC] / mM	Error / mM
0.80	0.00	10.33	0.00	1.00	2.784	0.000	0.00	
0.70	0.10	9.04	1.25	0.88	2.755	0.029	1.06	0.42
0.60	0.20	7.75	2.50	0.76	2.691	0.092	2.92	0.46
0.50	0.30	6.46	3.75	0.63	2.643	0.141	3.71	0.45
0.40	0.40	5.17	5.00	0.51	2.586	0.198	4.17	0.42
0.30	0.50	3.87	6.25	0.38	2.549	0.235	3.71	0.34
0.20	0.60	2.58	7.50	0.26	2.539	0.245	2.58	0.23
0.10	0.70	1.29	8.75	0.13	2.541	0.243	1.28	0.12

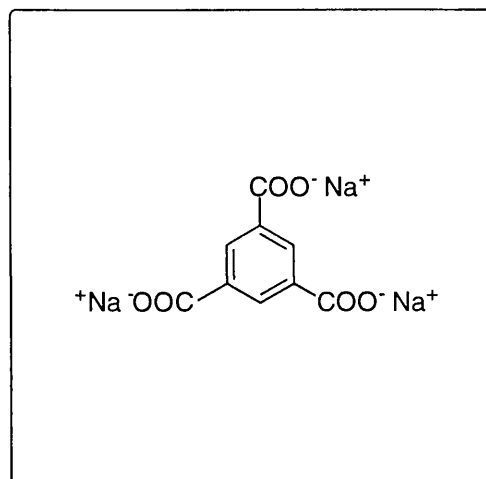
## Cation Benzyl Shift (Average of 3 Runs)

X / mL	Y / mL	[C] / mM	[A] / mM	$\frac{[C]}{[A]+[C]}$	$\delta$	$\Delta\delta$	[AC] / mM	Error / mM
0.80	0.00	10.33	0.00	1.00	5.280	0.000	0.00	
0.70	0.10	9.04	1.25	0.88	5.251	0.029	0.86	0.34
0.60	0.20	7.75	2.50	0.76	5.176	0.104	2.39	0.35
0.50	0.30	6.46	3.75	0.63	5.106	0.175	3.69	0.40
0.40	0.40	5.17	5.00	0.51	5.035	0.245	4.15	0.38
0.30	0.50	3.87	6.25	0.38	4.990	0.290	3.69	0.31
0.20	0.60	2.58	7.50	0.26	4.978	0.302	2.54	0.21
0.10	0.70	1.29	8.75	0.13	4.977	0.303	1.28	0.11

#### 4.6.19 NMR Titration of 2,4,6-Tris(N'-1-propyl-DABCO-N-methyl)mesitylene Hexabromide 129 and Trisodium Benzene-1,3,5-tricarboxylate 186



C



A

	Solution X			Solution Y	
	C / mg	A / mg	D <sub>2</sub> O / mL	A / mg	D <sub>2</sub> O / mL
Run 1	137.4	7.5	5.00	13.7	10.00
Run 2	137.4	7.5	5.00	13.7	10.00
Run 3	137.4	7.5	5.00	6.8	5.00

#### Anion Shift (Average of 3 Runs)

X / mL	Y / mL	[C] / mM	[A] / mM	[C]/[A]	$\delta$	$\Delta\delta$
0.00	0.80	0.00	4.95	0.00	8.395	0.000
0.05	0.75	1.56	4.98	0.31	8.287	0.108
0.10	0.70	3.11	5.01	0.62	8.209	0.185
0.12	0.68	3.73	5.02	0.74	8.188	0.206
0.16	0.64	4.98	5.05	0.99	8.157	0.238
0.25	0.55	7.78	5.10	1.52	8.123	0.271
0.40	0.40	12.44	5.19	2.40	8.100	0.294
0.80	0.00	24.88	5.43	4.58	8.088	0.307

**Cation Methyl Shift (Average of 3 Runs)**

X / mL	Y / mL	[C] / mM	[A] / mM	[A]/[C]	$\delta$	$\Delta\delta$
Cation Reference		10.00	0.00	0.00	2.760	0.000
0.80	0.00	24.88	5.43	0.22	2.712	0.048
0.40	0.40	12.44	5.19	0.42	2.656	0.103
0.25	0.55	7.78	5.10	0.66	2.620	0.140
0.16	0.64	4.98	5.05	1.01	2.572	0.188
0.12	0.68	3.73	5.02	1.35	2.546	0.214
0.10	0.70	3.11	5.01	1.61	2.540	0.220
0.05	0.75	1.56	4.98	3.20	2.524	0.236

**Cation Benzyl Shift (Average of 3 Runs)**

X / mL	Y / mL	[C] / mM	[A] / mM	[A]/[C]	$\delta$	$\Delta\delta$
Cation Reference		10.00	0.00	0.00	5.259	0.000
0.80	0.00	24.88	5.43	0.22	5.188	0.071
0.40	0.40	12.44	5.20	0.42	5.125	0.135
0.25	0.55	7.78	5.11	0.66	5.082	0.177
0.16	0.64	4.98	5.06	1.02	5.025	0.234
0.12	0.68	3.73	5.03	1.35	4.993	0.266
0.10	0.70	3.11	5.02	1.61	4.986	0.273
0.05	0.75	1.56	4.99	3.21	4.966	0.293

**4.6.20 Job Plot of 2,4,6-Tris(N'-1-propyl-DABCO-N-methyl)mesitylene Hexabromide 129 and Trisodium Benzene-1,3,5-tricarboxylate 186**

	Solution X		Solution Y	
	C / mg	D <sub>2</sub> O / mL	A / mg	D <sub>2</sub> O / mL
Run 1	108.1	10.00	27.4	10.00
Run 2	108.1	10.00	27.4	10.00
Run 3	108.1	10.00	27.4	10.00



## Anion Shift (Average of 3 Runs)

X / mL	Y / mL	[C] / mM	[A] / mM	$\frac{[A]}{[A]+[C]}$	$\delta$	$\Delta\delta$	[AC] / mM	Error / mM
0.00	0.80	0.00	9.92	1.00	8.392	0.000	0.00	
0.10	0.70	1.22	8.68	0.88	8.349	0.043	1.18	0.33
0.20	0.60	2.45	7.44	0.75	8.299	0.094	2.26	0.35
0.30	0.50	3.67	6.20	0.63	8.234	0.158	3.18	0.36
0.40	0.40	4.89	4.96	0.50	8.176	0.217	3.49	0.34
0.50	0.30	6.12	3.72	0.38	8.151	0.241	2.90	0.26
0.60	0.20	7.34	2.48	0.25	8.153	0.240	1.93	0.18
0.70	0.10	8.56	1.24	0.13	8.237	0.156	0.63	0.07

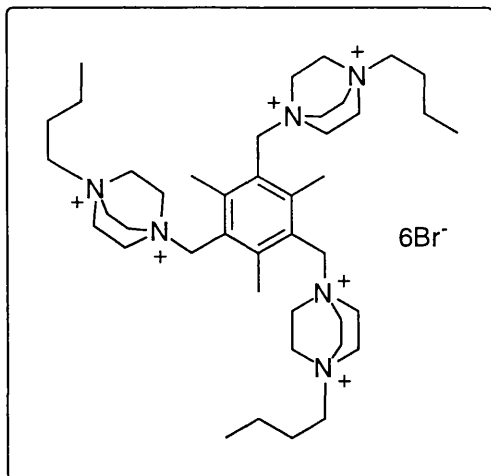
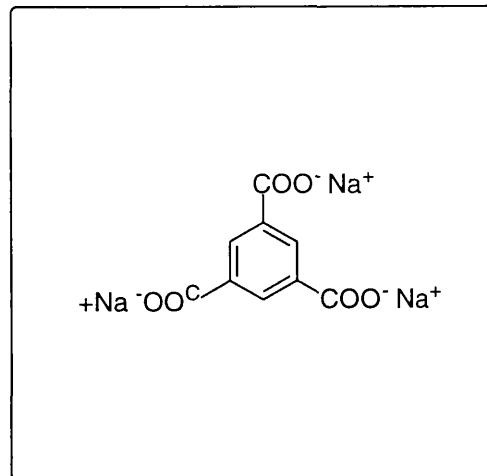
## Cation Methyl Shift (Average of 3 Runs)

X / mL	Y / mL	[C] / mM	[A] / mM	$\frac{[C]}{[A]+[C]}$	$\delta$	$\Delta\delta$	[AC] / mM	Error / mM
0.80	0.00	9.79	0.00	1.00	2.760	0.000	0.00	
0.70	0.10	8.56	1.24	0.87	2.727	0.032	1.14	0.41
0.60	0.20	7.34	2.48	0.75	2.670	0.090	2.71	0.44
0.50	0.30	6.12	3.72	0.62	2.632	0.128	3.22	0.41
0.40	0.40	4.89	4.96	0.50	2.570	0.189	3.82	0.39
0.30	0.50	3.67	6.20	0.37	2.534	0.226	3.42	0.32
0.20	0.60	2.45	7.44	0.25	2.524	0.236	2.38	0.22
0.10	0.70	1.22	8.68	0.12	2.525	0.234	1.18	0.11

## Cation Benzyl Shift (Average of 3 Runs)

X / mL	Y / mL	[C] / mM	[A] / mM	$\frac{[C]}{[A]+[C]}$	$\delta$	$\Delta\delta$	[AC] / mM	Error / mM
0.80	0.00	9.79	0.00	1.00	5.259	0.000	0.00	
0.70	0.10	8.56	1.24	0.87	5.217	0.042	1.17	0.34
0.60	0.20	7.34	2.48	0.75	5.144	0.115	2.75	0.38
0.50	0.30	6.12	3.72	0.62	5.099	0.160	3.18	0.36
0.40	0.40	4.89	4.96	0.50	5.021	0.238	3.78	0.35
0.30	0.50	3.67	6.20	0.37	4.978	0.281	3.35	0.29
0.20	0.60	2.45	7.44	0.25	4.966	0.293	2.33	0.20
0.10	0.70	1.22	8.68	0.12	4.961	0.297	1.18	0.10

**4.6.21 NMR Titration of 2,4,6-Tris(N'-1-butyl-DABCO-N-methyl)mesitylene Hexabromide 131 and Trisodium Benzene-1,3,5-tricarboxylate 186**

**C****A**

	Solution X			Solution Y	
	C / mg	A / mg	D <sub>2</sub> O / mL	A / mg	D <sub>2</sub> O / mL
Run 1	144.4	7.0	5.00	13.8	10.00
Run 2	144.4	7.0	5.00	13.8	10.00
Run 3	144.4	7.0	5.00	6.8	5.00

**Anion Shift (Average of 3 Runs)**

X / mL	Y / mL	[C] / mM	[A] / mM	[C]/[A]	$\delta$	$\Delta\delta$
0.00	0.80	0.00	4.97	0.00	8.395	0.000
0.05	0.75	1.57	4.98	0.32	8.306	0.089
0.10	0.70	3.15	4.99	0.63	8.221	0.174
0.12	0.68	3.78	4.99	0.76	8.213	0.182
0.16	0.64	5.04	4.99	1.01	8.180	0.215
0.25	0.55	7.87	5.00	1.57	8.149	0.246
0.40	0.40	12.59	5.02	2.51	8.110	0.285
0.80	0.00	25.19	5.07	4.97	8.109	0.286

## Cation Methyl Shift (Average of 3 Runs)

X / mL	Y / mL	[C] / mM	[A] / mM	[A]/[C]	$\delta$	$\Delta\delta$
Cation Reference		10.00	0.00	0.00	2.761	0.000
0.80	0.00	25.19	5.07	0.20	2.721	0.040
0.40	0.40	12.59	5.02	0.40	2.660	0.101
0.25	0.55	7.87	5.00	0.64	2.614	0.147
0.16	0.64	5.04	4.99	0.99	2.574	0.187
0.12	0.68	3.78	4.99	1.32	2.554	0.207
0.10	0.70	3.15	4.99	1.58	2.548	0.213
0.05	0.75	1.57	4.98	3.16	2.534	0.227

## Cation Benzyl Shift (Average of 3 Runs)

X / mL	Y / mL	[C] / mM	[A] / mM	[A]/[C]	$\delta$	$\Delta\delta$
Cation Reference		10.00	0.00	0.00	5.262	0.000
0.80	0.00	25.19	5.07	0.20	5.198	0.064
0.40	0.40	12.59	5.02	0.40	5.128	0.134
0.25	0.55	7.87	5.00	0.64	5.074	0.188
0.16	0.64	5.04	4.99	0.99	5.025	0.237
0.12	0.68	3.78	4.99	1.32	5.001	0.261
0.10	0.70	3.15	4.99	1.58	4.993	0.269
0.05	0.75	1.57	4.98	3.16	4.968	0.294

4.6.22 Job Plot of 2,4,6-Tris(N'-butyl-DABCO-N-methyl)mesitylene Hexabromide 131 and Trisodium Benzene-1,3,5-tricarboxylate 186

	Solution X		Solution Y	
	C / mg	D <sub>2</sub> O / mL	A / mg	D <sub>2</sub> O / mL
Run 1	116.0	10.00	28.2	10.00
Run 2	116.0	10.00	28.2	10.00
Run 3	116.0	10.00	28.2	10.00

**Anion Shift (Average of 3 Runs)**

X / mL	Y / mL	[C] / mM	[A] / mM	$\frac{[A]}{[A]+[C]}$	$\delta$	$\Delta\delta$	[AC] / mM	Error / mM
0.00	0.80	0.00	10.21	1.00	8.392	0.000	0.00	
0.10	0.70	1.26	8.94	0.88	8.352	0.040	1.23	0.37
0.20	0.60	2.53	7.66	0.75	8.305	0.088	2.34	0.38
0.30	0.50	3.79	6.38	0.63	8.257	0.136	3.01	0.37
0.40	0.40	5.06	5.11	0.50	8.190	0.202	3.60	0.36
0.50	0.30	6.32	3.83	0.38	8.164	0.229	3.05	0.29
0.60	0.20	7.59	2.55	0.25	8.180	0.213	1.89	0.18
0.70	0.10	8.85	1.28	0.13	8.298	0.094	0.42	0.07

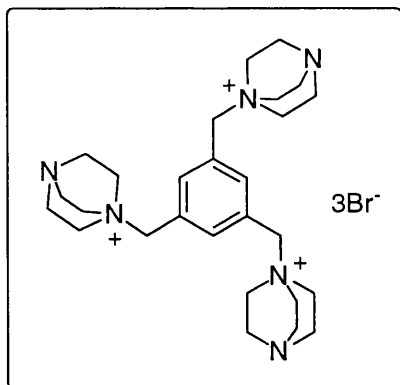
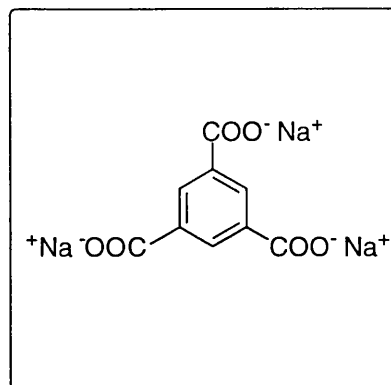
**Cation Methyl Shift (Average of 3 Runs)**

X / mL	Y / mL	[C] / mM	[A] / mM	$\frac{[C]}{[A]+[C]}$	$\delta$	$\Delta\delta$	[AC] / mM	Error / mM
0.80	0.00	10.12	0.00	1.00	2.760	0.000	0.00	
0.70	0.10	8.85	1.28	0.87	2.736	0.024	0.92	0.43
0.60	0.20	7.59	2.55	0.75	2.679	0.081	2.69	0.47
0.50	0.30	6.32	3.83	0.62	2.616	0.144	3.99	0.48
0.40	0.40	5.06	5.11	0.50	2.572	0.188	4.17	0.43
0.30	0.50	3.79	6.38	0.37	2.540	0.220	3.66	0.35
0.20	0.60	2.53	7.66	0.25	2.533	0.227	2.52	0.24
0.10	0.70	1.26	8.94	0.12	2.534	0.226	1.25	0.12

**Cation Benzyl Shift (Average of 3 Runs)**

X / mL	Y / mL	[C] / mM	[A] / mM	$\frac{[C]}{[A]+[C]}$	$\delta$	$\Delta\delta$	[AC] / mM	Error / mM
0.80	0.00	10.12	0.00	1.00	5.260	0.000	0.00	
0.70	0.10	8.85	1.28	0.87	5.227	0.032	0.99	0.36
0.60	0.20	7.59	2.55	0.75	5.158	0.102	2.67	0.40
0.50	0.30	6.32	3.83	0.62	5.080	0.180	3.93	0.41
0.40	0.40	5.06	5.11	0.50	5.016	0.244	4.26	0.39
0.30	0.50	3.79	6.38	0.37	4.983	0.277	3.62	0.31
0.20	0.60	2.53	7.66	0.25	4.973	0.286	2.50	0.21
0.10	0.70	1.26	8.94	0.12	4.971	0.288	1.26	0.11

#### 4.6.23 NMR Titration of 1,3,5-Tris(DABCO-N-methyl)mesitylene Tribromide 107 and Trisodium Benzene-1,3,5-tricarboxylate 186

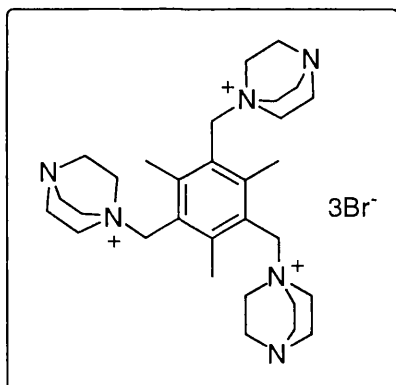
**C****A**

	Solution X			Solution Y	
	C / mg	A / mg	D <sub>2</sub> O / mL	A / mg	D <sub>2</sub> O / mL
Run 1	172.9	13.9	5.00	27.8	10.00
Run 2	173.4	13.6	5.00	14.2	5.00
Run 3	173.4	13.6	5.00	13.5	5.00

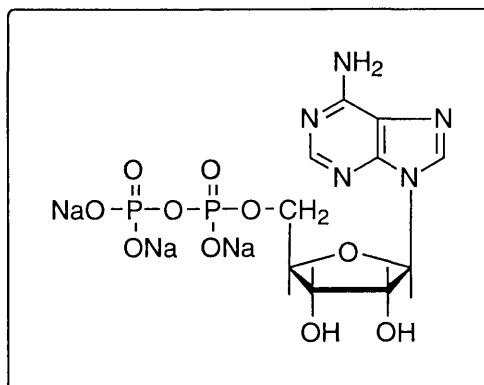
#### Anion Shift (Average of 3 Runs)

X / mL	Y / mL	[C] / mM	[A] / mM	[C]/[A]	$\delta$	$\Delta\delta$
0.00	0.80	0.00	10.04	0.00	8.399	0.000
0.05	0.75	3.12	10.04	0.31	8.369	0.030
0.10	0.70	6.25	10.03	0.62	8.340	0.059
0.12	0.68	7.49	10.03	0.75	8.329	0.070
0.16	0.64	9.99	10.02	1.00	8.303	0.096
0.25	0.55	15.61	10.01	1.56	8.252	0.147
0.40	0.40	24.98	9.98	2.50	8.212	0.187
0.80	0.00	49.97	9.92	5.03	8.148	0.251

#### 4.6.24 NMR Titration of 2,4,6-Tris(DABCO-N-methyl)mesitylene Tribromide 109 and Adenosine 5'-diphosphate, trisodium salt 190



C



A

	Solution X			Solution Y	
	C / mg	A / mg	D <sub>2</sub> O / mL	A / mg	D <sub>2</sub> O / mL
Run 1	184.3	24.2	5.00	24.5	5.00

#### Anion Shift (1 Run)

X / mL	Y / mL	[C] / mM	[A] / mM	[C]/[A]	$\delta$	$\Delta\delta$
0.00	0.80	0.00	10.06	0.00	6.165	0.000
0.05	0.75	3.13	10.05	0.31	6.145	0.020
0.10	0.70	6.26	10.04	0.62	6.118	0.047
0.12	0.68	7.52	10.04	0.75	6.108	0.057
0.16	0.64	10.02	10.03	1.00	6.093	0.072
0.25	0.55	15.66	10.02	1.56	6.066	0.099
0.40	0.40	25.06	10.00	2.51	6.032	0.133
0.80	0.00	50.12	9.93	5.04	5.979	0.186

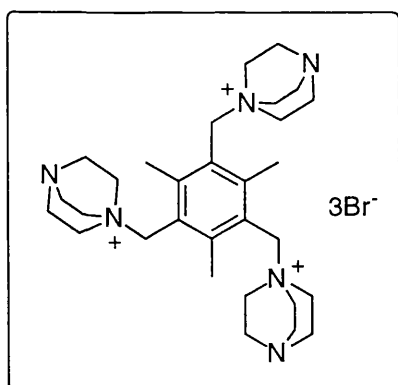
#### 4.6.25 Job Plot of 2,4,6-Tris(DABCO-N-methyl)mesitylene Tribromide 109 and Adenosine 5'-diphosphate, trisodium salt 191

	Solution X		Solution Y	
	C / mg	D <sub>2</sub> O / mL	A / mg	D <sub>2</sub> O / mL
Run 1	73.6	10.00	24.8	5.00

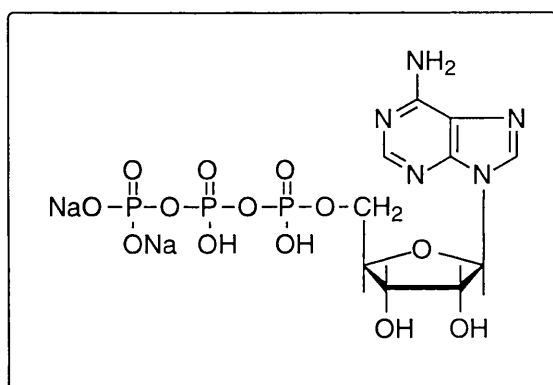
## Anion Shift (1 Run)

X / mL	Y / mL	[C] / mM	[A] / mM	$\frac{[A]}{[A]+[C]}$	$\delta$	$\Delta\delta$	[AC] / mM	Error / mM
0.00	0.80	0.00	10.18	1.00	6.173	0.000	0.00	
0.10	0.70	1.25	8.91	0.88	6.164	0.009	0.25	0.32
0.20	0.60	2.50	7.64	0.75	6.152	0.021	0.55	0.29
0.30	0.50	3.75	6.36	0.63	6.137	0.036	0.78	0.26
0.40	0.40	5.00	5.09	0.5	6.118	0.055	0.95	0.22
0.50	0.30	6.25	3.82	0.38	6.101	0.071	0.93	0.18
0.60	0.20	7.50	2.55	0.25	6.080	0.093	0.81	0.13
0.70	0.10	8.75	1.27	0.13	6.027	0.146	0.63	0.07

## 4.6.26 NMR Titration of 2,4,6-Tris(DABCO-N-methyl)mesitylene Tribromide 109 and Adenosine 5'-triphosphate, disodium salt 191



C



A

	Solution X			Solution Y	
	C / mg	A / mg	D <sub>2</sub> O / mL	A / mg	D <sub>2</sub> O / mL
Run 1	184.6	28.0	5.00	28.1	5.00

**Anion Shift (1 Run)**

X / mL	Y / mL	[C] / mM	[A] / mM	[C]/[A]	$\delta$	$\Delta\delta$
0.00	0.80	0.00	10.20	0.00	6.146	0.000
0.05	0.75	3.14	10.19	0.31	6.124	0.022
0.10	0.70	6.27	10.19	0.62	6.107	0.039
0.12	0.68	7.53	10.19	0.74	6.099	0.047
0.16	0.64	10.04	10.19	0.99	6.083	0.063
0.25	0.55	15.69	10.19	1.54	6.059	0.087
0.40	0.40	25.10	10.18	2.47	6.015	0.131
0.80	0.00	50.20	10.16	4.94	5.977	0.169

**4.7 Isothermal Titration Calorimetry**

All samples were dissolved in HPLC grade water. Calorimetric measurements were made at 20°C using an MCS ITC (MicroCal Inc., Northampton, MA, USA). The heats of dilution were determined in separate experiments by titration of the injection of the component in the syringe into water and the injection of water into the component in the calorimetric cell. The heats derived from these control experiments were subtracted from the total heats of reaction before data analysis. In the systems in which no oligomerisation of the interacting components occurs the heats of dilution are approximately constant during the course of the titration. It was thus possible to clearly identify interactions where the unbound components were associated. To assess the effects of possible protonation, experiments were performed in 5 mM MOPS at pH 7.0. No differences in data were, however, observed from those obtained in water.



---

## References

- (1) Cram, D. J.; Cram, J. M. *Science (Washington)* **1974**, *183*, 803-809.
  - (2) Perutz, M. F. *Science* **1978**, *201*, 1187-1191.
  - (3) Náray-Szabó, G.; Ferenczy, G. G. *Chem. Rev.* **1995**, *95*, 829-847.
  - (4) Moore, W. J. *Physical Chemistry*; 5th ed.; Longman: Harlow, 1972.
  - (5) Debye, P.; Hückel, E. *Phys. Z.* **1923**, *24*, 185.
  - (6) Harned, H. S.; Morrison, J. O.; Walker, F.; Donelson, J. G.; Calmon, C. J. *Am. Chem. Soc.* **1939**, *61*, 49-54.
  - (7) Bjerrum, N. Z. *Z. Physik. Chem.* **1923**, *106*, 219-242.
  - (8) Gane, R.; Ingold, C. K. *J. Chem. Soc.* **1928**, 1595-1600.
  - (9) Gane, R.; Ingold, C. K. *J. Chem. Soc.* **1928**, 2267-2272.
  - (10) Gane, R.; Ingold, C. K. *J. Chem. Soc.* **1929**, 1691-1700.
  - (11) Gane, R.; Ingold, C. K. *J. Chem. Soc.* **1931**, 2153-2169.
  - (12) Kirkwood, J. G.; Westheimer, F. H. *J. Chem. Phys.* **1938**, *6*, 506-512.
  - (13) Westheimer, F. H.; Kirkwood, J. G. *J. Chem. Phys.* **1938**, *6*, 513-517.
  - (14) Westheimer, F. H. *Tetrahedron* **1995**, *51*, 3-20.
  - (15) Barton, D. H. R.; Schmeidler, G. A. *J. Chem. Soc.* **1948**, 1197-1203.
  - (16) Rajasekaran, E.; Jayaram, B.; Honig, B. *J. Am. Chem. Soc.* **1994**, *116*, 8238-8240.
  - (17) Potter, M. J.; Gilson, M. K.; McCammon, J. A. *J. Am. Chem. Soc.* **1994**, *116*, 10298-10299.
  - (18) Baldwin, J. M. *Br. Med. Bull.* **1976**, *32*, 213-218.
  - (19) Perutz, M. F. *Br. Med. Bull.* **1976**, *32*, 195-208.
  - (20) Kilmartin, J. V. *Br. Med. Bull.* **1976**, *32*, 209-212.
  - (21) Mehler, E. L.; Eichele, G. *Biochemistry* **1984**, *23*, 3887-3891.
  - (22) Honig, B.; Nicholls, A. *Science* **1995**, *268*, 1144-1149.
  - (23) Gilson, M. K.; Honig, B. H. *Nature* **1987**, *330*, 84-86.
  - (24) Sternberg, M. J. E.; Hayes, F. R. F.; Russell, A. J.; Thomas, P. G.; Fersht, A. R. *Nature* **1987**, *330*, 86-88.
  - (25) Mehler, E. L.; Solmajer, T. *Protein Engng* **1991**, *4*, 903-910.
  - (26) Lemieux, R. U. *Acc. Chem. Res.* **1996**, *29*, 373-380.
  - (27) Tam, S.-C.; Williams, R. J. P. *J. Chem. Soc., Faraday Trans. I* **1984**, *80*, 2255-2267.
  - (28) Dietrich, B.; Fyles, D. L.; Fyles, T. M.; Lehn, J.-M. *Helv. Chim. Acta* **1979**, *62*, 2763-2787.
  - (29) Pedersen, C. J. *J. Am. Chem. Soc.* **1967**, *89*, 7017-7036.
  - (30) Pedersen, C. J. *J. Am. Chem. Soc.* **1967**, *89*, 2495-2496.
  - (31) Dietrich, B.; Lehn, J.-M.; Sauvage, J. P. *Tetrahedron Lett.* **1969**, 2889-2892.
  - (32) Dietrich, B.; Lehn, J.-M.; Sauvage, J. P. *Tetrahedron Lett.* **1969**, 2885-2888.
-

- 
- (33) Kyba, E. P.; Helgeson, R. C.; Madan, K.; Gokel, G. W.; Tarnowski, T. L.; Moore, S. S.; Cram, D. J. *J. Am. Chem. Soc.* **1977**, *99*, 2564-2571.
- (34) Cram, D. J. *Angew. Chem. Int. Ed. Engl.* **1988**, *27*, 1009-1020.
- (35) Lehn, J.-M. *Acc. Chem. Res.* **1978**, *11*, 49-57.
- (36) Rebek, J., Jr. *Angew. Chem. Int. Ed. Engl.* **1990**, *29*, 245-255.
- (37) Adrian, J. C., Jr.; Wilcox, C. S. *J. Am. Chem. Soc.* **1991**, *113*, 678-680.
- (38) Seel, C.; Vögtle, F. *Angew. Chem. Int. Ed. Engl.* **1992**, *31*, 528-549.
- (39) Hildebrand, J. H. *Proc. Natl. Acad. Sci. USA* **1979**, *76*, 194.
- (40) Diederich, F.; Dick, K. *J. Am. Chem. Soc.* **1984**, *106*, 8024-8036.
- (41) Diederich, F.; Griebel, D. *J. Am. Chem. Soc.* **1984**, *106*, 8037-8046.
- (42) Diederich, F. *Angew. Chem. Int. Ed. Engl.* **1988**, *27*, 362-386.
- (43) Smithrud, D. B.; Diederich, F. *J. Am. Chem. Soc.* **1990**, *112*, 339-343.
- (44) Carcanague, D. R.; Knobler, C. B.; Diederich, F. *J. Am. Chem. Soc.* **1992**, *114*, 1515-1517.
- (45) Chastrette, M.; Carretto, J. *Tetrahedron* **1982**, *38*, 1615-1618.
- (46) Diederich, F.; Dick, K.; Griebel, D. *J. Am. Chem. Soc.* **1986**, *108*, 2273-2286.
- (47) Whitlock, B. J.; Whitlock, H. W. *J. Am. Chem. Soc.* **1990**, *112*, 3910-3915.
- (48) Kennan, A. J.; Whitlock, H. W. *J. Am. Chem. Soc.* **1996**, *118*, 3027-3028.
- (49) Stauffer, D. A.; Dougherty, D. A. *Tetrahedron Lett.* **1988**, *29*, 6039-6042.
- (50) Shepodd, T. J.; Petti, M. A.; Dougherty, D. A. *J. Am. Chem. Soc.* **1988**, 1983-1985.
- (51) Petti, M. A.; Shepodd, T. J.; Barrans, R. E., Jr.; Dougherty, D. A. *J. Am. Chem. Soc.* **1988**, *110*, 6825-6840.
- (52) Stauffer, D. A.; Barrans, R. E., Jr.; Dougherty, D. A. *J. Org. Chem.* **1990**, *55*, 2762-2767.
- (53) Kearney, P. C.; Mizoue, L. S.; Kumpf, R. A.; Forman, J. E.; McCurdy, A.; Dougherty, D. A. *J. Am. Chem. Soc.* **1993**, *115*, 9907-9919.
- (54) Forman, J. E.; Barrans, R. E., Jr.; Dougherty, D. A. *J. Am. Chem. Soc.* **1995**, *117*, 9213-9228.
- (55) Schneider, H.-J.; Güttles, D.; Schneider, U. *J. Am. Chem. Soc.* **1988**, *110*, 6449-6454.
- (56) Dietrich, B. *Pure & Appl. Chem.* **1993**, *65*, 1457-1464.
- (57) Lehn, J.-M. *Angew. Chem. Int. Ed. Engl.* **1988**, *27*, 89-112.
- (58) Verboom, W.; Rudkevich, D. M.; Reinhoudt, D. N. *Pure & Appl. Chem.* **1994**, *66*, 679-686.
- (59) Kneeland, D. M.; Ariga, K.; Lynch, V. M.; Huang, C.-Y.; Anslyn, E. V. *J. Am. Chem. Soc.* **1993**, *115*, 10042-10055.
- (60) Albert, J. S.; Goodman, M. S.; Hamilton, A. D. *J. Am. Chem. Soc.* **1995**, *117*, 1143-1144.
- (61) Kimura, E. *Top. Curr. Chem.* **1985**, *128*, 113-141.
- (62) Cullinane, J. *J. Am. Chem. Soc.* **1982**, *104*, 3048-3053.
- (63) Gelb, R. I.; Lee, B. T.; Zompa, L. J. *J. Am. Chem. Soc.* **1985**, *107*, 909-916.
-

- 
- (64) Gelb, R. I.; Schwartz, L. M.; Zompa, L. J. *Inorg. Chem.* **1986**, *25*, 1527-1535.
- (65) Santos, M. A.; Drew, M. G. B. *J. Chem. Soc. Faraday Trans.* **1991**, *87*, 1321-1331.
- (66) Suet, E. *Tetrahedron Lett.* **1984**, *25*, 645-648.
- (67) Dietrich, B.; Hosseini, M. W.; Lehn, J. M.; Sessions, R. B. *J. Am. Chem. Soc.* **1981**, *103*, 1282-1283.
- (68) Dietrich, B.; Hosseini, M. W.; Lehn, J.-M.; Sessions, R. B. *Helv. Chim. Acta* **1983**, *66*, 1262-1278.
- (69) Kimura, E.; Kodoma, M.; Yatsunami, T. *J. Am. Chem. Soc.* **1982**, *104*, 3182-3187.
- (70) Hosseini, M. W.; Lehn, J.-M. *Helv. Chim. Acta* **1987**, *70*, 1312-1319.
- (71) Mertes, M. P.; Mertes, K. B. *Acc. Chem. Res.* **1990**, *23*, 413-418.
- (72) Fenniri, H.; Lehn, J.-M.; Marquis-Rigault, A. *Angew. Chem. Int. Ed. Engl.* **1996**, *35*, 337-339.
- (73) Bencini, A.; Bianchi, A.; Paoletti, P.; Paoli, P. *Pure & Appl. Chem.* **1993**, *65*, 381-386.
- (74) Bencini, A.; Bianchi, A.; Burguete, M. I.; Domenech, A.; Garcia-España, E.; Luis, S. V.; Niño, M. A.; Ramírez, J. A. *J. Chem. Soc. Perkin Trans. 2* **1991**, 1445-1451.
- (75) Bencini, A.; Bianchi, A.; Burguete, M. I.; Dapporto, P.; Doménech, A.; Garcia-España, E.; Luis, S. V.; Paoli, P.; Ramirez, J. A. *J. Chem. Soc. Perkin Trans. 2* **1994**, 569-577.
- (76) Marecek, J. F.; Fischer, P. A.; Burrows, C. J. *Tetrahedron Lett.* **1988**, *29*, 6231-6234.
- (77) Hosseini, M. W.; Blacker, A. J.; Lehn, J.-M. *J. Am. Chem. Soc.* **1990**, *112*, 3896-3904.
- (78) Dhaenens, M.; Lehn, J.-M.; Vigneron, J.-P. *J. Chem. Soc. Perkin Trans. 2* **1993**, 1379-1381.
- (79) Aguilar, J. A.; Garcia-España, E.; J.A., G.; Luis, S. V.; Llinares, J. M.; Miravet, J. F.; Ramírez, J. A.; Soriano J. *Chem. Soc., Chem. Commun.* **1995**, 2237-2239.
- (80) Schneider, H.-J.; Philippi, K.; Pöhlmann, J. *Angew. Chem. Int. Ed. Engl.* **1984**, *23*, 908-910.
- (81) Schneider, H.-J.; Busch, R. *Angew. Chem. Int. Ed. Engl.* **1984**, *23*, 911-912.
- (82) Schneider, H.-J.; Müller, W.; Güttes, D. *Angew. Chem. Int. Ed. Engl.* **1984**, *23*, 910-911.
- (83) Fernandez-Saiz, M.; Schneider, H.-J.; Sartorius, J.; Wilson, W. D. *J. Am. Chem. Soc.* **1996**, *118*, 4739-4745.
- (84) Schneider, H.-J.; Theis, I. *Angew. Chem. Int. Ed. Engl.* **1989**, *28*, 753-754.
- (85) Schneider, H.-J.; Schiestel, T.; Zimmerman, P. *J. Am. Chem. Soc.* **1992**, *114*, 7698-7703.
- (86) Schneider, H.; Wang, M. *J. Org. Chem.* **1994**, *59*, 7464-7472.
- (87) Schneider, H.-J.; Kramer, R.; Simova, S.; Schneider, U. *J. Am. Chem. Soc.* **1988**, *110*, 6442-6448.
- (88) Murakami, Y.; Kikuchi, J.; Ohno, T.; Hayashida, O.; Kojima, M. *J. Am. Chem. Soc.* **1990**, *112*, 7672-7681.
- (89) Dietrich, B.; Guilhem, J.; Lehn, J.-M.; Pascard, C.; Sonveaux, E. *Helv. Chim. Acta* **1984**, *67*, 91-104.
-

- 
- (90) Lehn, J.-M.; Sonveaux, E.; Willard, A. K. *J. Am. Chem. Soc.* **1978**, *100*, 4914-4916.
- (91) Hosseini, M. W.; Lehn, J.-M. *Helv. Chim. Acta* **1988**, *71*, 749-755.
- (92) Lehn, J.-M.; Méric, R.; Vigneron, J.-P.; Bkouche-Waksman, I.; Pascard, C. *J. Chem. Soc., Chem. Commun.* **1991**, 62-64.
- (93) Worm, K.; Schmidtchen, F. P. *Angew. Chem. Int. Ed. Engl.* **1995**, *34*, 65-66.
- (94) Murakami, Y.; Kikuchi, J.; Hirayama, T. *Chem. Lett.* **1987**, 161-164.
- (95) Hayashida, O.; Matsuura, S.; Murakami, Y. *Tetrahedron* **1994**, *50*, 13601-13616.
- (96) Fan, E.; Van Arman, S. A.; Kincaid, S.; Hamilton, A. D. *J. Am. Chem. Soc.* **1993**, *115*, 369-370.
- (97) Rebek, J., Jr. *Top. Curr. Chem.* **1988**, *149*, 189-210.
- (98) Kral, V.; Andrievsky, A.; Sessler, J. L. *J. Am. Chem. Soc.* **1995**, *117*, 2953-2954.
- (99) Kral, V.; Springs, S. L.; Sessler, J. L. *J. Am. Chem. Soc.* **1995**, *117*, 8881-8882.
- (100) Amabilino, D. B.; Stoddart, J. F. *Pure & Appl. Chem.* **1993**, *65*, 2351-2359.
- (101) Allwood, B. L.; Spencer, N.; Shahriari-Zavareh, H.; Stoddart, J. F.; Williams, D. J. *J. Chem. Soc., Chem. Commun.* **1987**, 1064-1066.
- (102) Odell, B.; Reddington, M. V.; Slawin, A. M. Z.; Spencer, N.; Stoddart, J. F.; Williams, D. J. *Angew. Chem. Int. Ed. Engl.* **1988**, *27*, 1547-1550.
- (103) Hoss, R.; Vögtle, F. *Angew. Chem. Int. Ed. Engl.* **1994**, *33*, 375-384.
- (104) Anelli, P.; Ashton, P.; Ballardini, R.; Balzani, V.; Delgado, M.; Gandolfi, M.; Goodnow, T.; Kaifer, A.; Philp, D.; Pietraszkiewicz, M.; Prodi, L.; Reddington, M.; Slawin, A.; Spencer, N.; Stoddart, J.; Vicent, C.; Williams, D. J. *J. Am. Chem. Soc.* **1992**, *114*, 193-218.
- (105) Ashton, P.; Brown, C.; Chrystal, E.; Goodnow, T.; Kaifer, A.; Parry, K.; Slawin, A.; Spencer, N.; Stoddart, J.; Williams, D. *Angew. Chem. Int. Ed. Engl.* **1991**, *30*, 1039-1042.
- (106) Ashton, P.; Brown, C.; Chrystal, E.; Parry, K.; Pietraszkiewicz, M.; Spencer, N.; Stoddart, J. *Angew. Chem. Int. Ed. Engl.* **1991**, *30*, 1042-1045.
- (107) Amabilino, D. B.; Ashton, P. R.; Reder, A. S.; Spencer, N.; Stoddart, J. F. *Angew. Chem. Int. Ed. Engl.* **1994**, *33*, 433-437.
- (108) Amabilino, D. B.; Ashton, P. R.; Brown, C. L.; Córdova, E.; Godínez, L. A.; Goodnow, T. T.; Kaifer, A. E.; Newton, S. P.; Pietraszkiewicz, M.; Philp, D.; Raymo, F. M.; Reder, A. S.; Rutland, M. T.; Slawin, A. Z.; Spencer, N.; Stoddart, J. F.; Williams, D. J. *J. Am. Chem. Soc.* **1995**, *117*, 1271-1293.
- (109) Amabilino, D. B.; Anelli, P.-L.; Ashton, P. R.; Brown, G. R.; Córdova, E.; Godínez, L. A.; Hayes, W.; Kaifer, A. E.; Philp, D.; Slawin, A. M. Z.; Spencer, N.; Stoddart, J. F.; Tolley, M. S.; Williams, D. J. *J. Am. Chem. Soc.* **1995**, *117*, 11142-11170.
- (110) Ashton, P. R.; Ballardini, R.; Balzani, V.; Credi, A.; Gandolfi, M. T.; Menzer, S.; Pérez-García, L.; Prodi, L.; Stoddart, J. F.; Venturi, M.; White, A. J. P.; Williams, D. J. *J. Am. Chem. Soc.* **1995**, *117*, 11171-11197.
-

- 
- (111) Armspach, D.; Ashton, P. R.; Ballardini, R.; Balzani, V.; Godi, A.; Moore, C. P.; Prodi, L.; Spencer, N.; Stoddart, J. F.; Tolley, M. S.; Wear, T. J.; Williams, D. J. *Chem. Eur. J.* **1995**, *1*, 33-55.
- (112) Anelli, P.; Spencer, N.; Stoddart, J. *J. Am. Chem. Soc.* **1991**, *113*, 5131-5133.
- (113) Bissell, R. A.; Córdova, E.; Kaifer, A. E.; Stoddart, J. F. *Nature* **1994**, *369*, 133-137.
- (114) Córdova, E.; Bissell, R. A.; Kaifer, A. E. *J. Org. Chem.* **1995**, *60*, 1033-1038.
- (115) Lehn, J.-M. *Angew. Chem. Int. Ed. Engl.* **1990**, *29*, 1304-1319.
- (116) Mann, F. G.; Mukherjee, D. P. *J. Chem. Soc.* **1949**, 2298-2302.
- (117) Mann, F. G.; Baker, F. C. *J. Chem. Soc.* **1957**, 1881-1899.
- (118) Abbiss, T. P.; Mann, F. G. *J. Chem. Soc.* **1964**, 2248-2254.
- (119) Alder, R. W. *Acc. Chem. Res.* **1983**, *16*, 321-327.
- (120) Oae, S.; Hovarth, B.; Zalut, C.; Harris, R. *J. Org. Chem.* **1959**, *47*, 578-579.
- (121) Tabushi, I.; Imuta, J.; Seko, N.; Kobuke, Y. *J. Am. Chem. Soc.* **1978**, *100*, 6287-6288.
- (122) Tabushi, I.; Kobuke, Y.; Imuta, J. *J. Am. Chem. Soc.* **1980**, *102*, 1744-1745.
- (123) Tabushi, I.; Kobuke, Y.; Imuta, J. *J. Am. Chem. Soc.* **1981**, *103*, 6152-6157.
- (124) Diederich, F.; Li, T. *J. Org. Chem.* **1992**, *57*, 3449-3454.
- (125) Diederich, F.; Li, T.; Krasne, S.; Persson, B.; Kaback, H. *J. Org. Chem.* **1993**, *58*, 380-384.
- (126) Vögtle, F.; Zuber, M.; Lichtenthaler, R. G. *Chem. Ber.* **1973**, *106*, 717-718.
- (127) Cochrane, W. P.; Pauson, P. L.; Stevens, T. S. *J. Chem. Soc. (C)* **1968**, 630-632.
- (128) Hesse, G.; Rämish, F. *Chem. Ber.* **1954**, *87*, 764-766.
- (129) Fuson, R.; McKeever, C. *J. Am. Chem. Soc.* **1940**, *62*, 2088-2091.
- (130) van der Made, A. W.; van der Made, R. H. *J. Org. Chem.* **1993**, *58*, 1262-1263.
- (131) Ross, S. D.; Bruno, J. J.; Petersen, R. C. *J. Am. Chem. Soc.* **1963**, *85*, 3999-4003.
- (132) Langlois, M.; Meyer, C.; Soulier, J. L. *Synthetic Communications* **1992**, *22*, 1895-1911.
- (133) Mikhlin, E. E.; Rubtsov, M. V. *J. Gen. Chem. USSR (Engl. Transl.)* **1960**, *30*, 174-181.
- (134) Kaiser, A. *Helv. Chem. Acta.* **1947**, *50*, 2170.
- (135) Watters, J. I.; Matsumoto, S. *J. Am. Chem. Soc.* **1964**, *86*, 3961-3964.
- (136) Smith, R. M.; Alberty, R. A. *J. Am. Chem. Soc.* **1956**, *78*, 2376-2380.
- (137) Schmidtchen, F.; Schiessl, P. *J. Org. Chem.* **1994**, *59*, 509-511.
- (138) Heyer, D.; Lehn, J.-M. *Tetrahedron Lett.* **1986**, *27*, 5869-5872.
- (139) Wess, J.; Buhl, T.; Lambrecht, G.; Mutschler, E. In *Comprehensive Medicinal Chemistry*, J. C. Emmett, Ed.; Pergamon: Oxford, 1990; Vol. 3; pp 423-491.
- (140) Alcántar, C. G.; Eliseev, A. V.; Yatsimirsky, A. K. *Bioorg. Med. Chem. Lett.* **1995**, *5*, 2993-2998.
- (141) Menger, F. M.; Catlin, K. K. *Angew. Chem. Int. Ed. Engl.* **1995**, *34*, 2147-2150.
- (142) Brand, G.; Hosseini, M. W.; Ruppert, R.; De Cian, A.; Fischer, J.; Kyritsakas, N. *New J. Chem.* **1995**, *19*, 9-13.
- (143) Huggins, C. M.; Pimentel, G. C.; Shoolery, J. N. *J. Chem. Phys.* **1955**, *23*, 1244-1247.
-

- 
- (144) Connors, K. A. *Binding Constants*; Wiley Interscience: New York, 1987.
- (145) Wilcox, C. S. In *Frontiers in Supramolecular Chemistry and Photochemistry*, H.-J. Schneider and H. Dürr, Ed.; VCH: Weinheim, 1991; pp 123-143.
- (146) Creswell, C. J.; Allred, A. L. *J. Phys. Chem.* **1962**, *66*, 1469-1472.
- (147) Macomber, R. S. *J. Chem. Educ.* **1992**, *69*, 375-378.
- (148) Job, P. *Ann. Chim., (Paris) (Serie 10)* **1928**, *9*, 113-203.
- (149) Gil, V. M. S.; Oliveira, N. C. *J. Chem. Educ.* **1990**, *67*, 473-478.
- (150) Weber, G. In *Molecular Biophysics*; B. Pullman and M. Weissbluth, Ed.; Academic Press: New York, 1965; pp 369-397.
- (151) Stödeman, M.; Wadsö, I. *Pure & Appl. Chem.* **1995**, *67*, 1059-1068.
- (152) Briggner, L. E.; Wadsö, I. *J. Chem. Thermodynamics* **1990**, *22*, 1067-1074.
- (153) Gómez-Orellana, I.; Hallén, D.; Stödeman, M. *J. Chem. Soc. Faraday Trans.* **1994**, *90*, 3397-3400.
- (154) Hallén, D.; Schön, A.; Shehatta, I.; Wadsö, I. *J. Chem. Soc. Faraday Trans.* **1992**, *88*, 2859-2863.
- (155) Inoue, Y.; Hakushi, T.; Liu, Y.; Tong, L.-H.; Shen, B.-J.; Jin, D.-S. *J. Am. Chem. Soc.* **1993**, *115*, 475-481.
- (156) Rekharsky, M. V.; Schwarz, F. P.; Tewari, Y. B.; Goldberg, R. N. *J. Phys. Chem.* **1994**, *98*, 10282-10288.
- (157) Liu, Y.; Lu, T.-B.; Tan, M.-Y.; Hakushi, T.; Inoue, Y. *J. Phys. Chem.* **1993**, *97*, 4548-4551.
- (158) Buschmann, H.-J. *Inorg. Chim. Acta* **1992**, *195*, 51-60.
- (159) Danil de Namor, A. F. *Pure & Appl. Chem.* **1994**, *66*, 435-440.
- (160) Ladbury, J. E.; Chowdhry, B. Z. *Chem. & Biol.* **1996**, *3*, 791-801.
- (161) Wiseman, T.; Williston, S.; Brandts, J. F.; Lin, L.-N. *Anal. Biochem.* **1989**, *179*, 131-137.
- (162) Young, W. G.; Winstein, S.; Goering, H. L. *J. Am. Chem. Soc.* **1951**, *73*, 1958-1963.
- (163) Winstein, S.; Klinedinst, P. E.; Clippinger, E. *J. Am. Chem. Soc.* **1961**, *83*, 4986-4989.
- (164) Darr, J. A.; Drake, S. R.; Hursthouse, M. B.; Malik, K. M. A. *Inorg. Chem.* **1993**, *32*, 5704.
- (165) Sheldrick, G. M. *Acta Cryst.* **1990**, *A46*, 467.
- (166) Sheldrick, G. M. *SHELX-93 Program for Crystal Structure Refinement*; University of Gottingen: Gottingen, Germany, 1993.
-

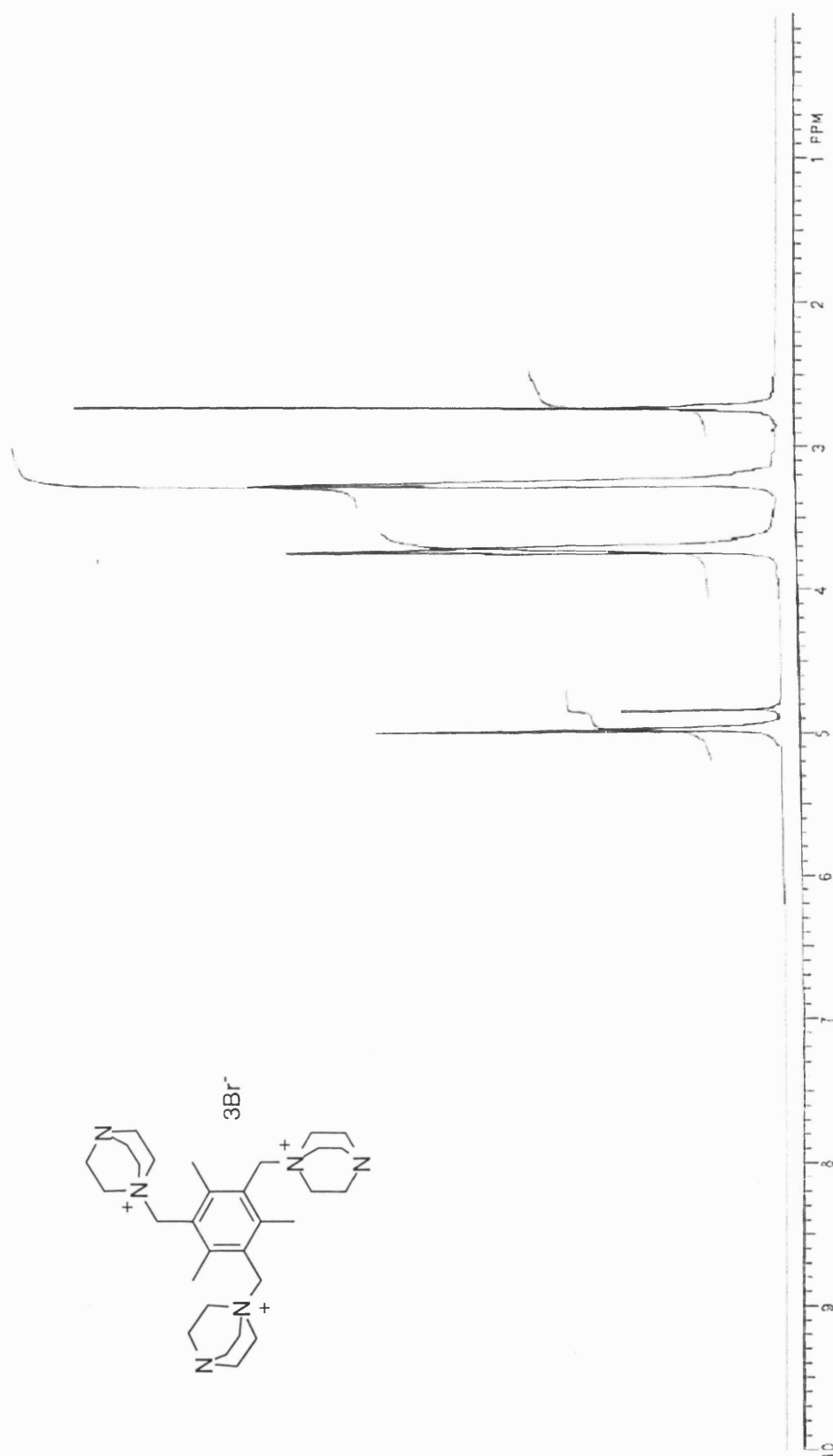
## Appendix 1 - Program Used for the Determination of Association Constants

```

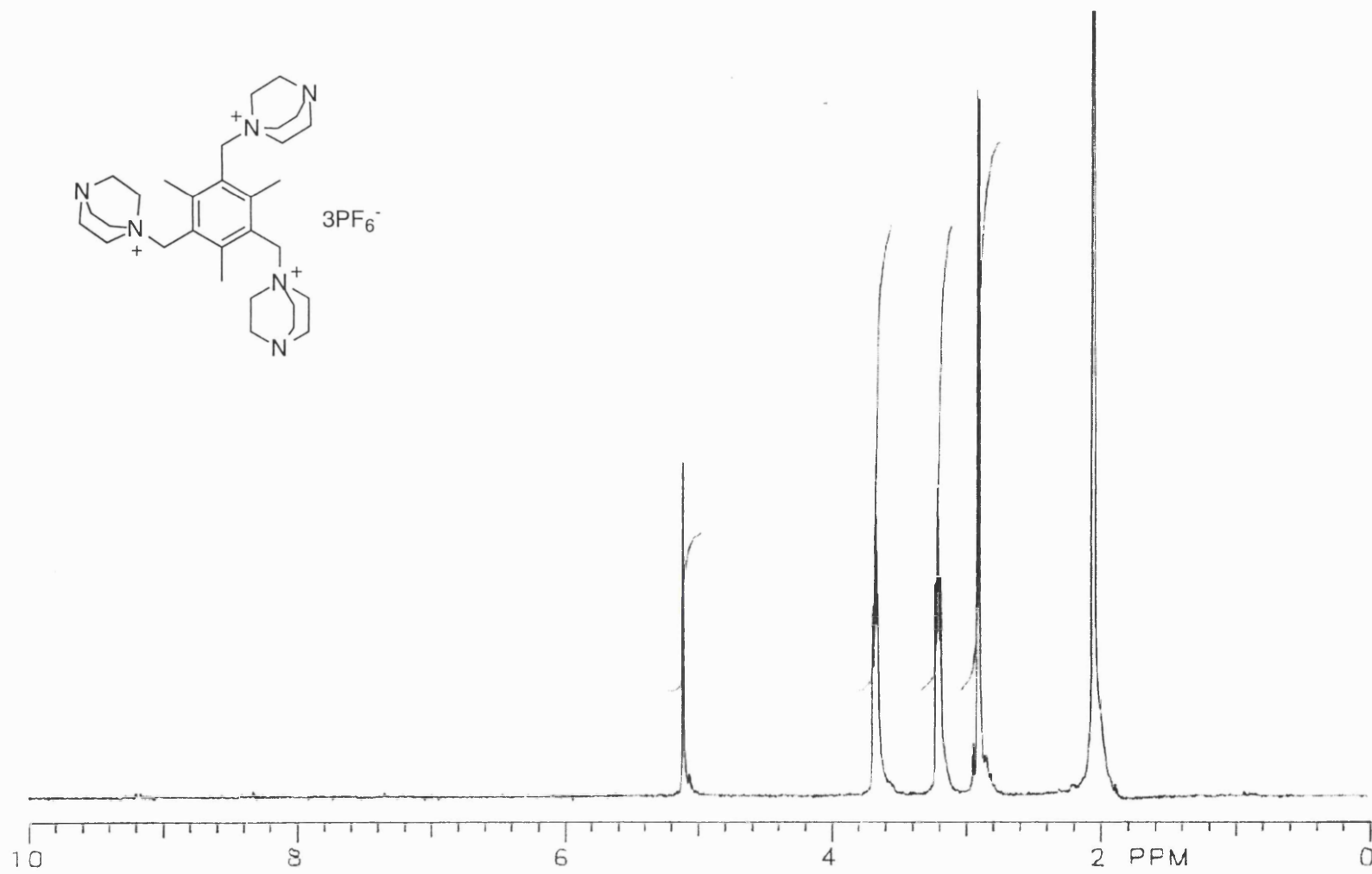
PROGRAM NMR
C Conversion of Basic Program to Fortran
C Based on J. Chem. Ed. 1992, 69, 375-378
  INTEGER I, CN, N, TS, TT
  REAL DH, K, SE
  REAL H(100), G(100), DOBS(100), D(100)
  REAL T(100), B(100), TC(100), BC(100)
  WRITE (*,*) 'ENTER VALUES FOR DH, K, AND N'
  READ *, DH, K, N
  TT=0
  TS=0
  CN=1
  DO 10 I = 1, N
    WRITE (*,*) 'FOR I = ', I
    WRITE (*,*) 'ENTER H(I), G(I) and DO(I)'
    READ *, H(I), G(I), DOBS(I)
10  CONTINUE
    SE=0
    BC(N)=H(N) + G(N) + 1/K
    TC(N) = BC(N) - SQRT(BC(N)*BC(N)-4*H(N)*G(N))
    DC = 2*H(N)*(DOBS(N)-DH)/TC(N) + DH
  C WRITE (*,*) 'THE CURRENT VALUES OF K AND DC ARE', K, DC
    DO 20 I = 1, N
      B(I) = H(I) + G(I) + 1/K
      IF ((B(I)*B(I)-4*H(I)*G(I)).lt.0) GOTO 30
      T(I) = B(I) - SQRT(B(I)*B(I)-4*H(I)*G(I))
      D(I) = DH + (1/(2*H(I)))*T(I)*(DC-DH)
      IF (CN.EQ.999) THEN
        WRITE (*,1) H(I), G(I), DOBS(I), D(I)
1      FORMAT (E9.3,2X,E9.3,2X,F6.3,2X,F6.3)
      ENDIF
30  CONTINUE
      SE=SE+DOBS(I)-D(I)
20  CONTINUE
      TT = TS
  C For negative changes in delta
  C IF (SE.GT.0) THEN
  C For positive changes in delta
    IF (SE.LT.0) THEN
      TS=-1
    ELSE
      TS=1
    ENDIF
50  CONTINUE
    IF (TS*TT.LT.0) THEN
      CN=CN+1
    ENDIF
    K=K*(1+(TS*.5/CN))
    IF (CN.LT.1000) GOTO 10
60  CONTINUE
    WRITE (*,2) K, DC
2  FORMAT ('The current values of K and DC are ',F7.2,1X, F6.3)
    END

```

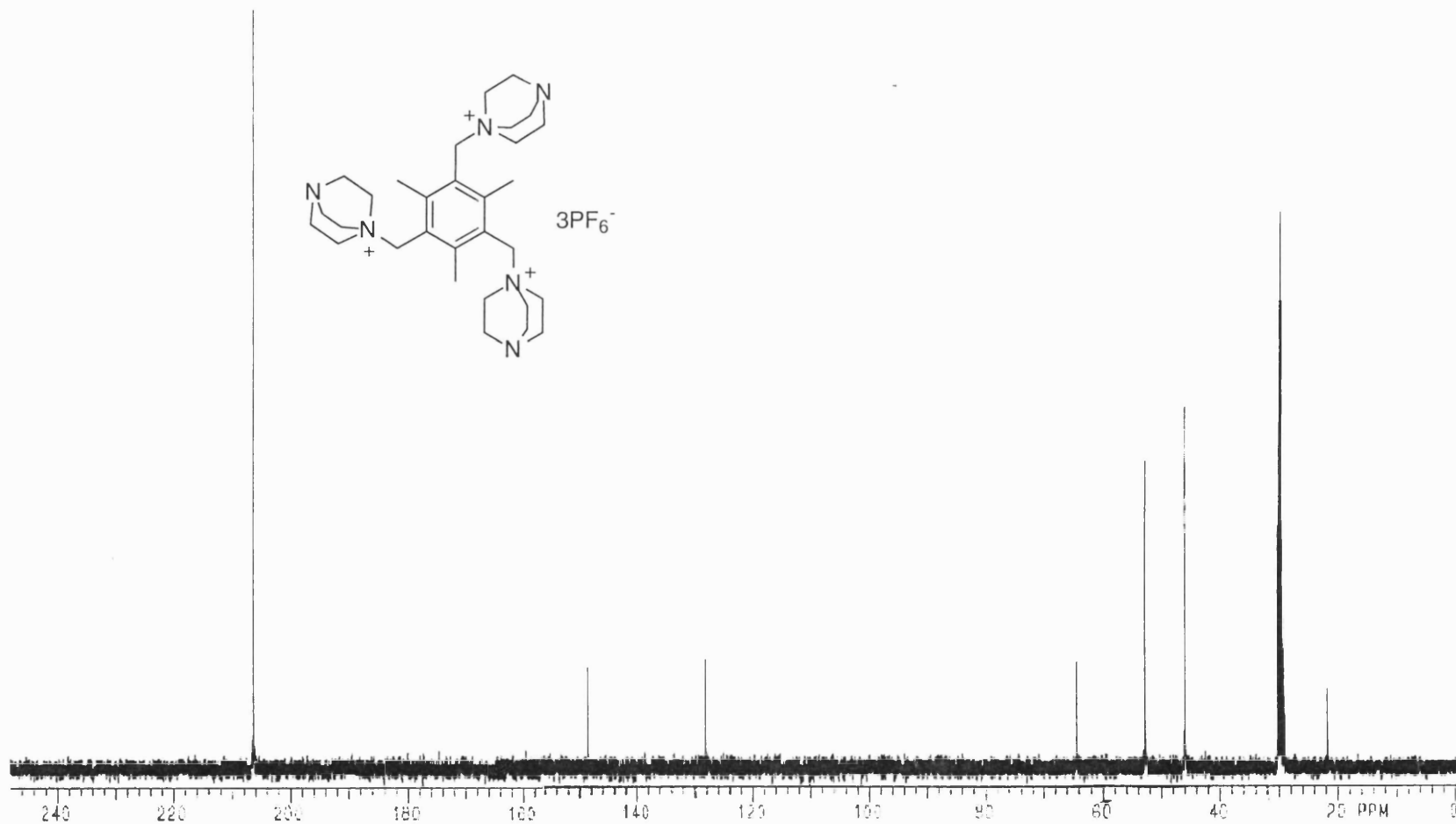
## Appendix 2 - Selected NMR Spectra

 $^1\text{H}$  NMR Spectrum (400 MHz,  $\text{D}_2\text{O}$ ) of 2,4,6-Tris(DABCO-N-methyl)mesitylene Tribromide 109

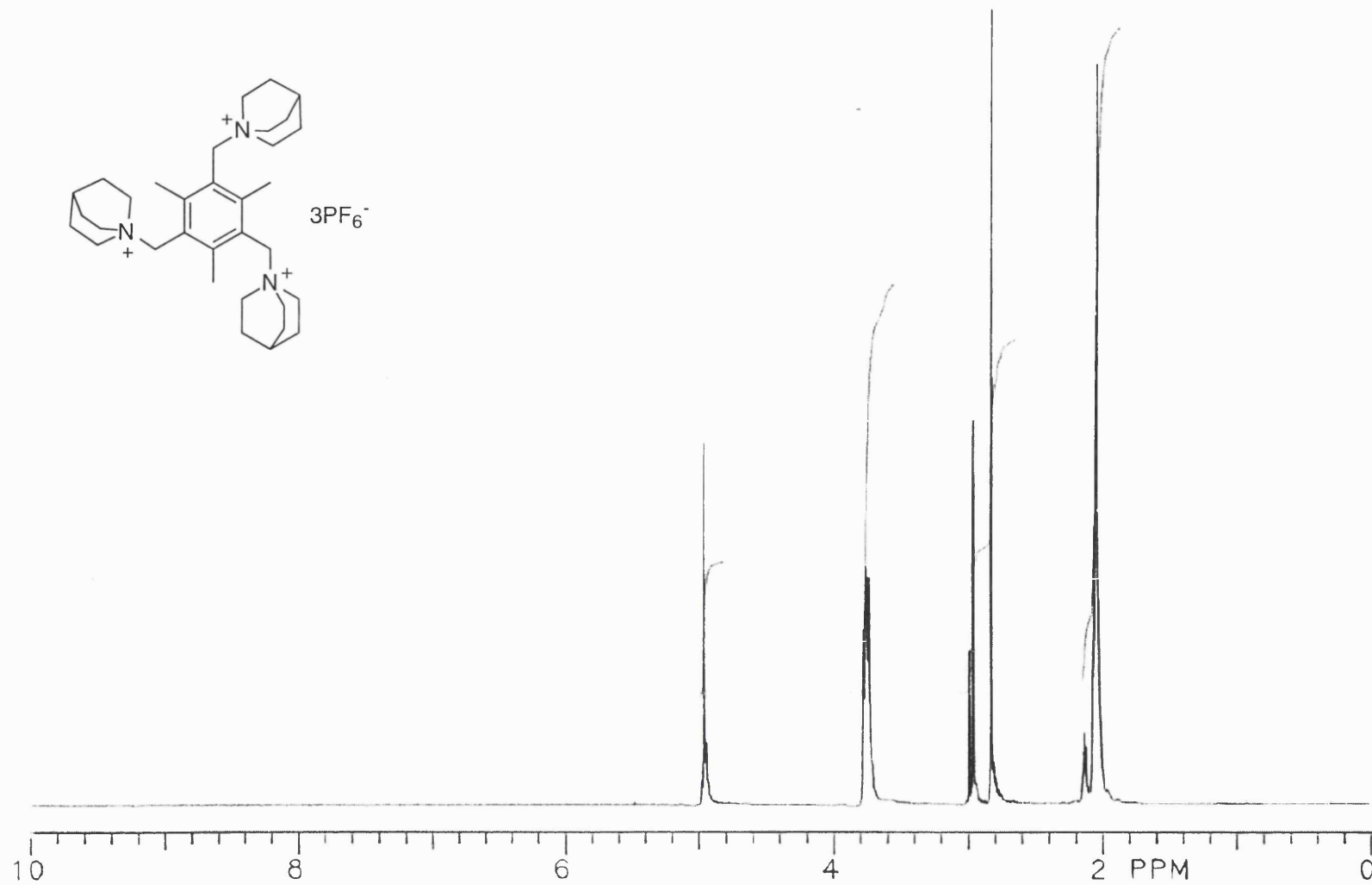




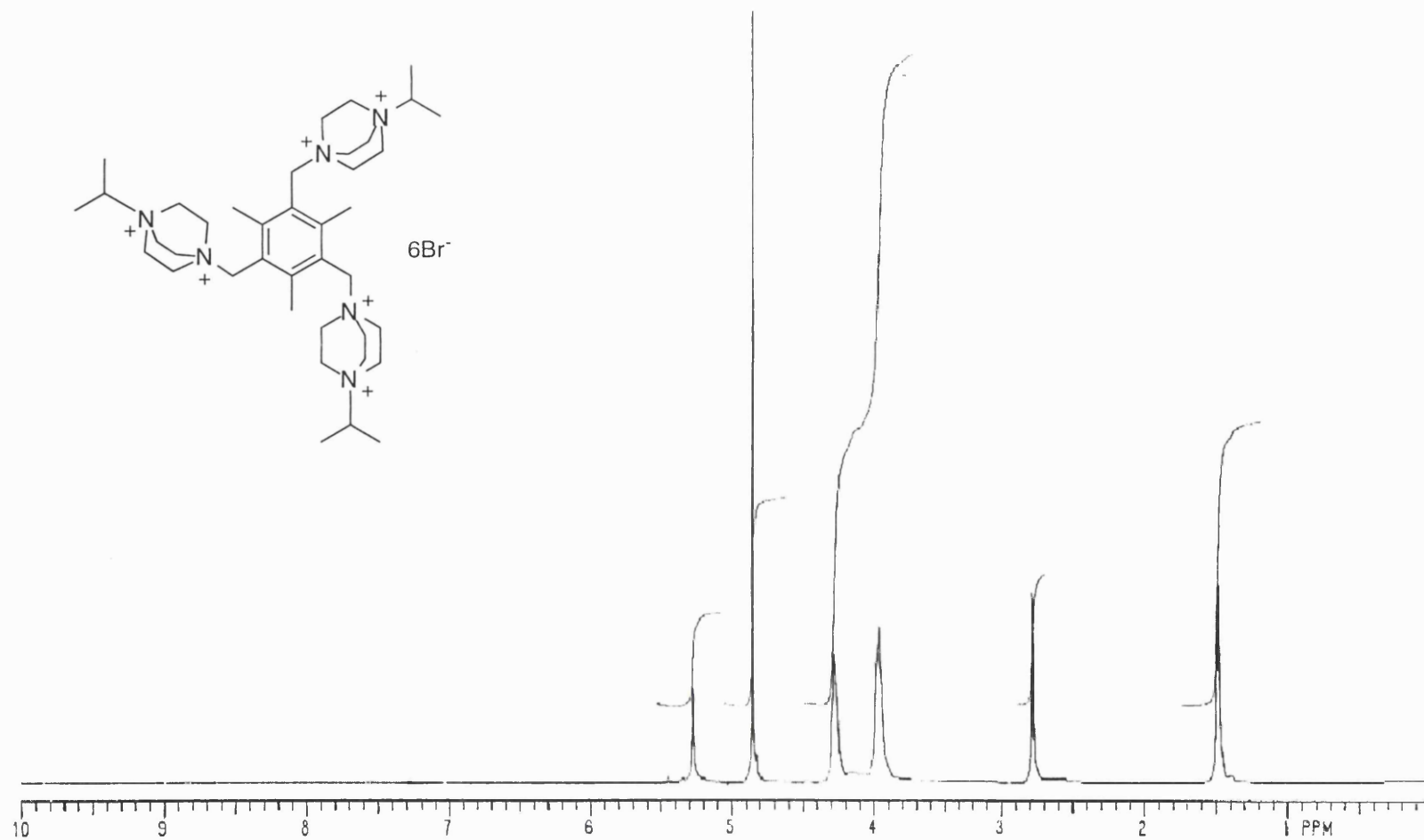
$^1\text{H}$  NMR Spectrum (400 MHz,  $(\text{CD}_3)_2\text{CO}$ ) of 2,4,6-Tris(DABCO-N-methyl)mesitylene Tri(hexafluorophosphate) 112



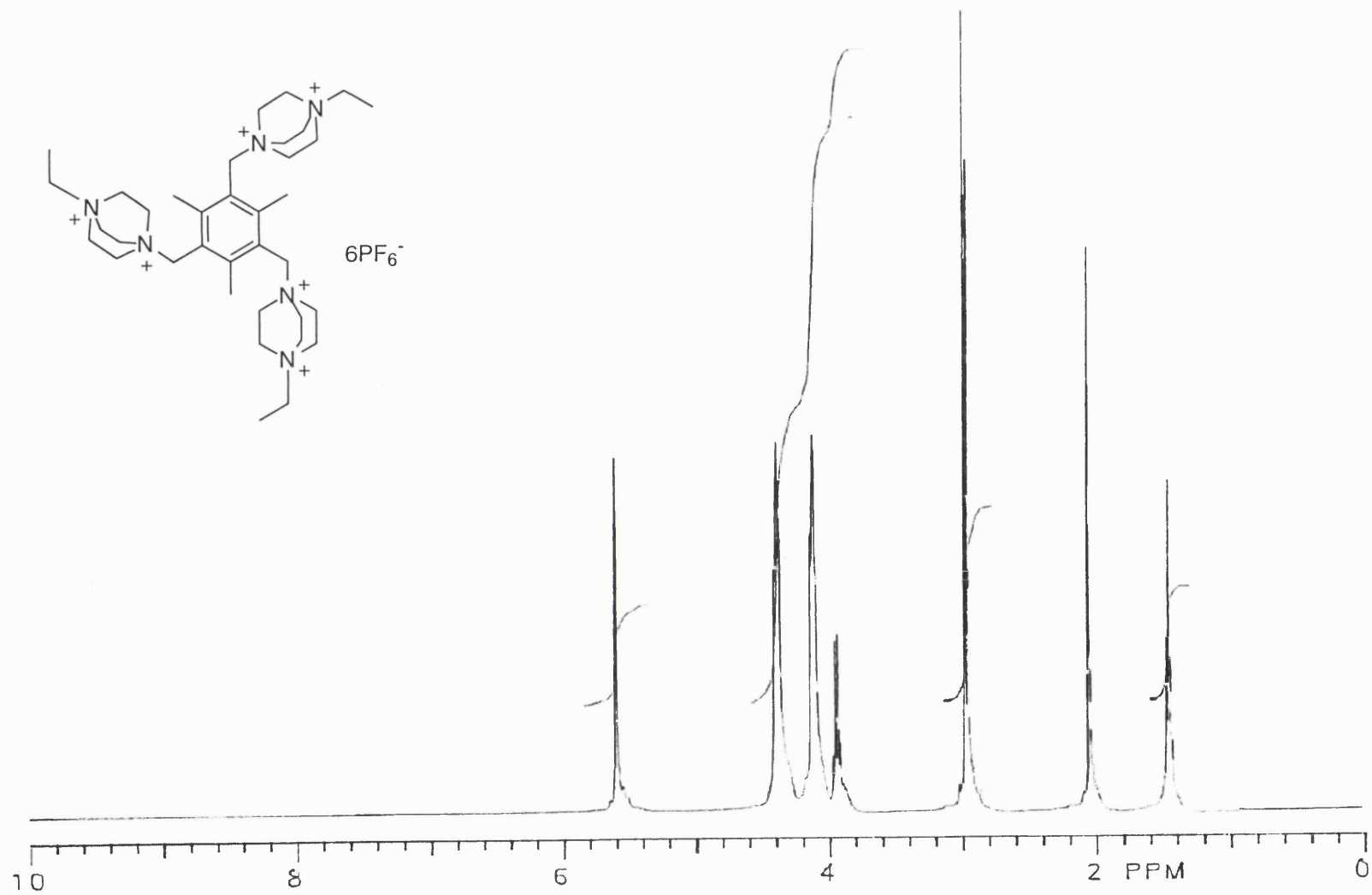
$^{13}\text{C}$  NMR Spectrum (100 MHz,  $(\text{CD}_3)_2\text{CO}$ ) of 2,4,6-Tris(DABCO-N-methyl)mesitylene Tri(hexafluorophosphate) 112



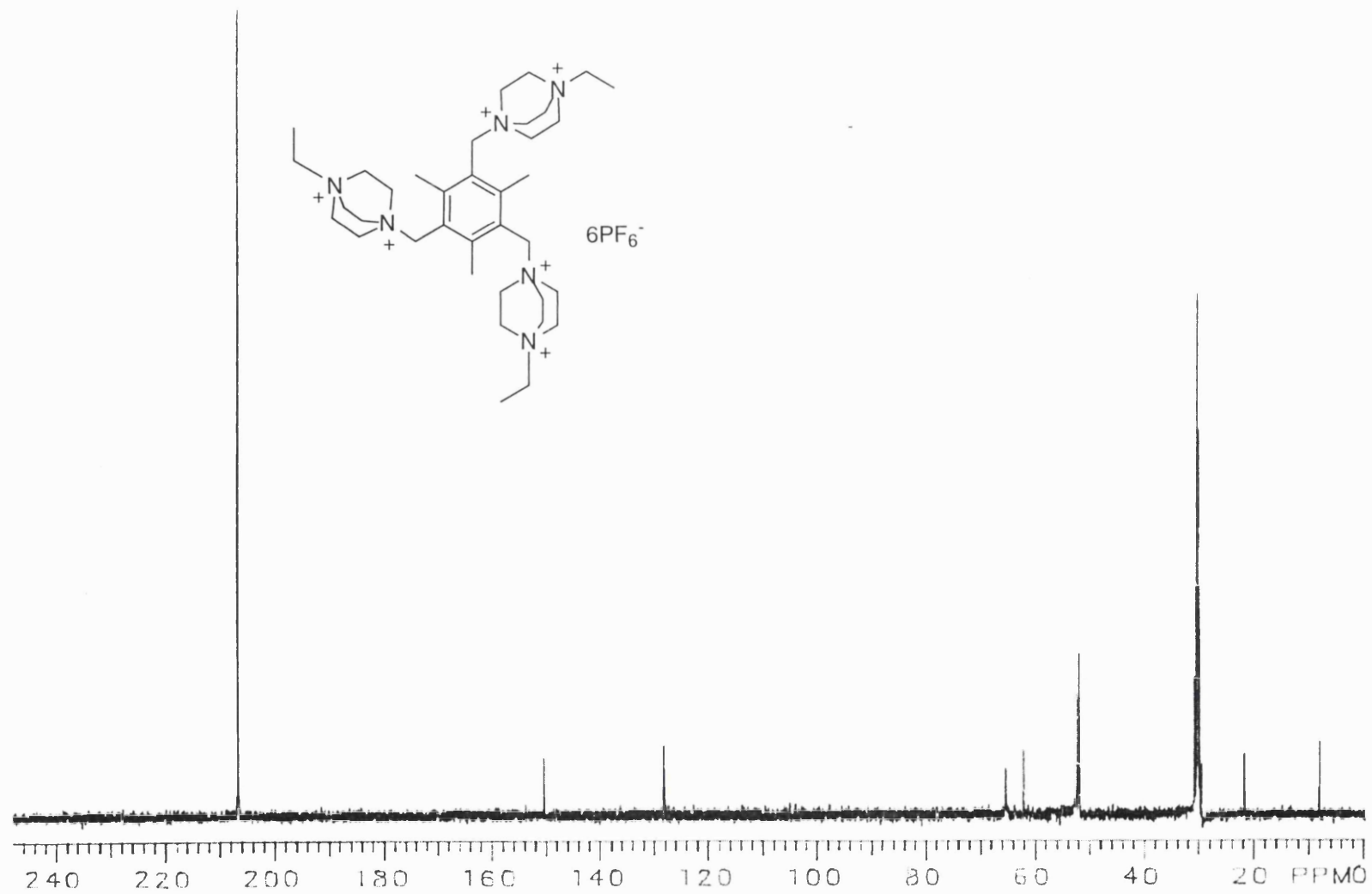
$^1\text{H}$  NMR Spectrum (400 MHz,  $(\text{CD}_3)_2\text{CO}$ ) of 2,4,6-Tris(quinuclidine-N-methyl)mesitylene Tri(hexafluorophosphate) 149



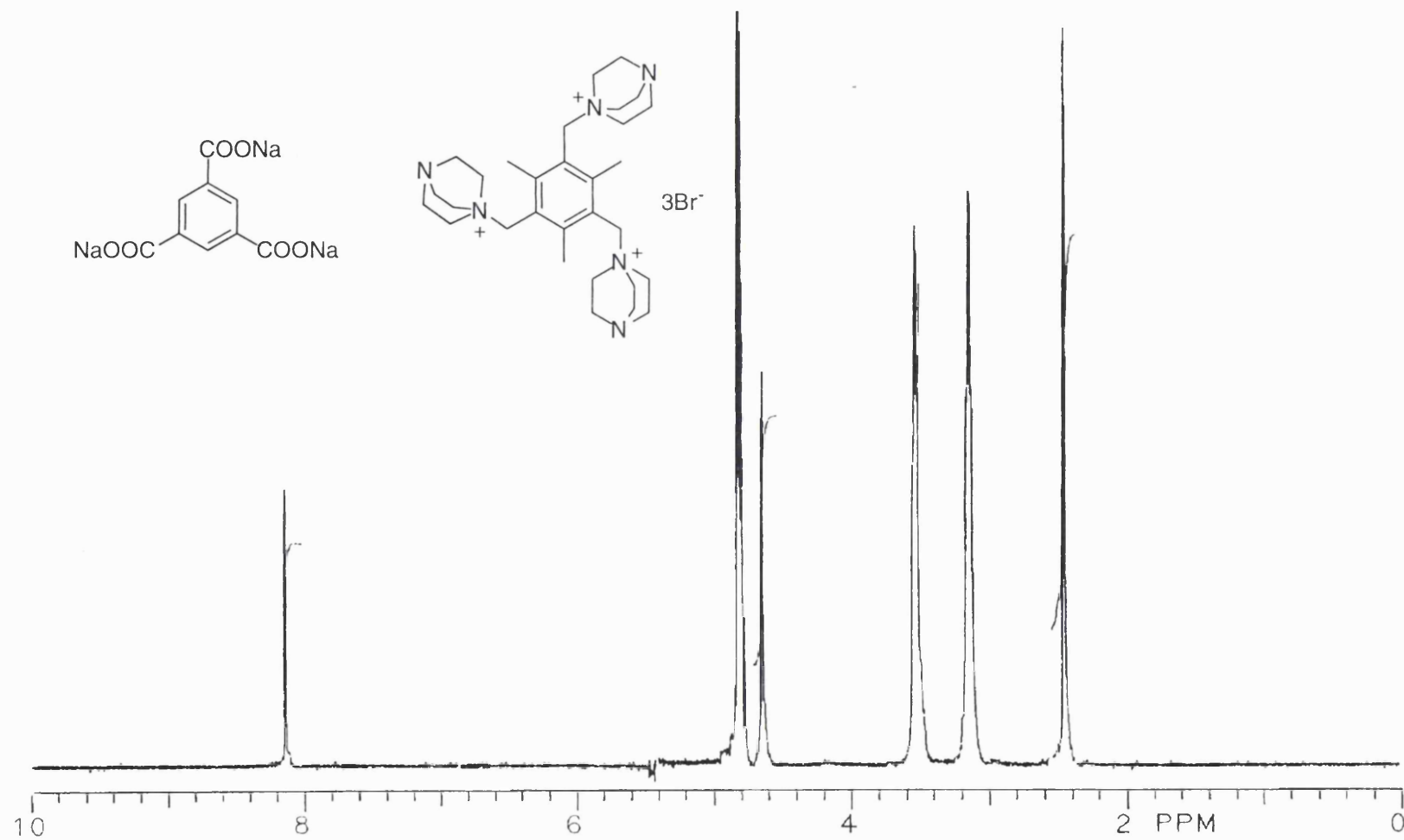
<sup>1</sup>H NMR Spectrum (400 MHz, D<sub>2</sub>O) of 2,4,6-Tris(N'-2-propyl-DABCO-N-methyl)mesitylene Hexabromide 130



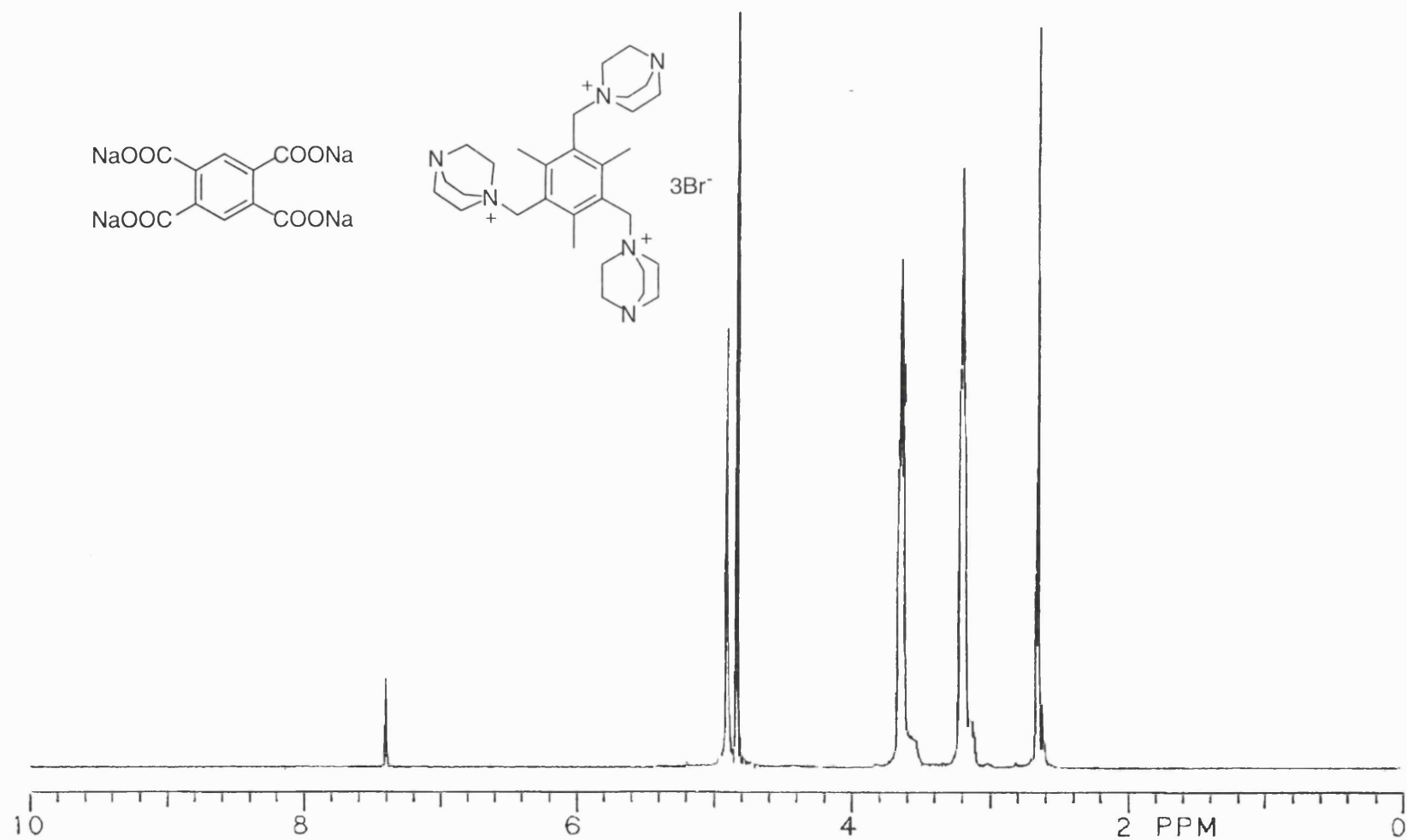
$^1\text{H}$  NMR Spectrum (400 MHz,  $(\text{CD}_3)_2\text{CO}$ ) of 2,4,6-Tris(N'-ethyl-DABCO-N-methyl)mesitylene Hexa(hexafluorophosphate) 138



$^{13}\text{C}$  NMR Spectrum (100 MHz,  $(\text{CD}_3)_2\text{CO}$ ) of 2,4,6-Tris(N'-ethyl-DABCO-N-methyl)mesitylene Hexa(hexafluorophosphate) 138

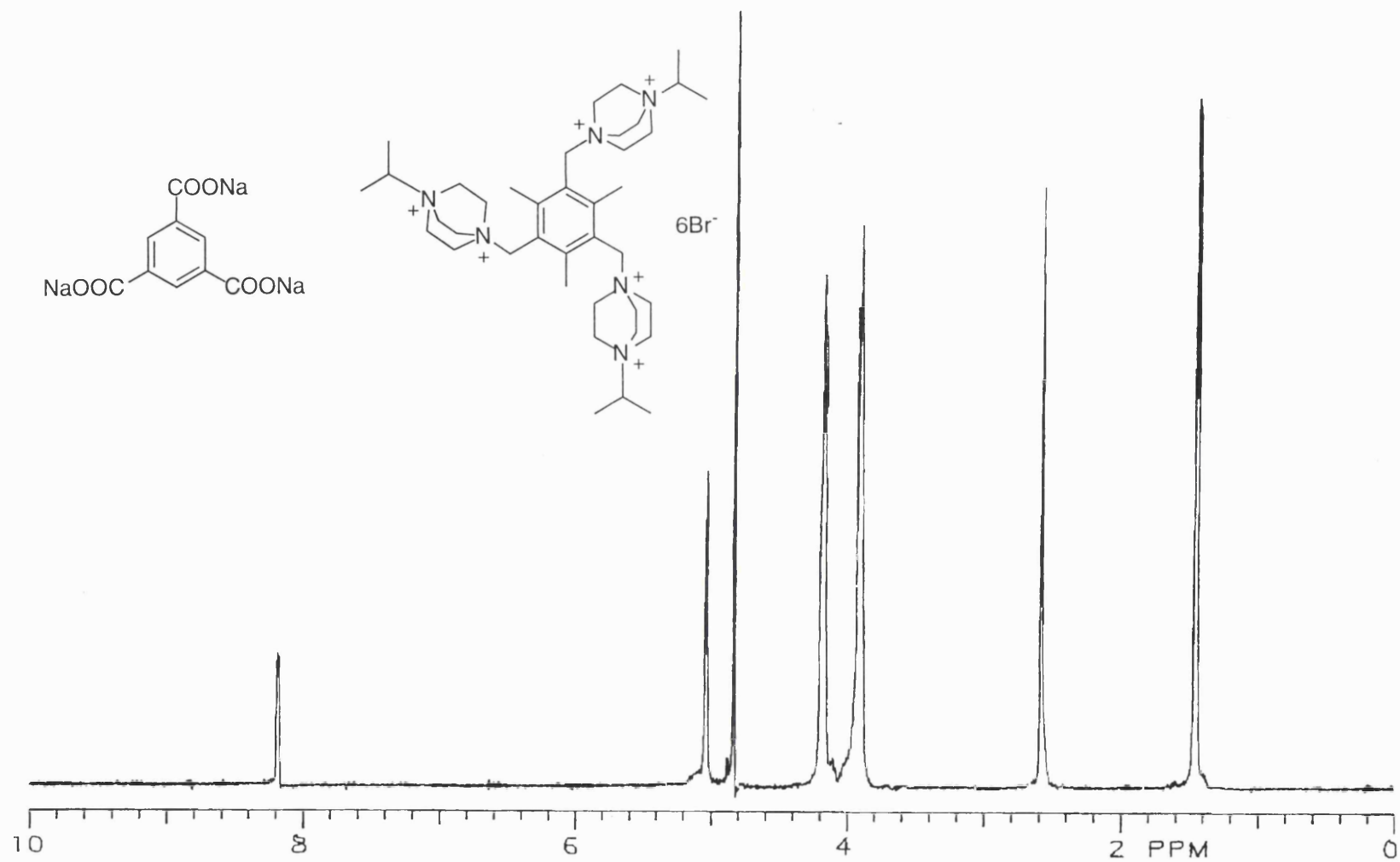


$^1\text{H}$  NMR Spectrum (400 MHz,  $\text{D}_2\text{O}$ ) of 2,4,6-Tris(DABCO-N-methyl)mesitylene Tribromide 109 and Trisodium Benzene-1,3,5-tricarboxylate 186 (1:1)



$^1\text{H}$  NMR Spectrum (400 MHz,  $\text{D}_2\text{O}$ ) of 2,4,6-Tris(DABCO-N-methyl)mesitylene Tribromide 109 and Tetrasodium Benzene-1,2,4,5-tetracarboxylate 189 (1.6:1)





$^1\text{H}$  NMR Spectrum (400 MHz,  $\text{D}_2\text{O}$ ) of 2,4,6-Tris(N'-2-propyl-DABCO-N-methyl)mesitylene Hexabromide 130 and Trisodium Benzene-1,3,5-tricarboxylate 186 (1:1)

### Appendix 3 - Crystal Structure Analysis for 185

Crystal data for  $[\text{C}_{30}\text{H}_{51}\text{N}_6][\text{Fe}(\text{CN})_6] \cdot 8\text{H}_2\text{O}$ ,  $M_r = 851.87$ , Monoclinic,  $P2_1/n$ ,  $a = 16.436(5)$ ,  $b = 19.551(6)$ ,  $c = 13.111(4)$  Å,  $\beta = 90.80(2)^\circ$ ,  $U = 4213(2)$  Å<sup>3</sup>,  $Z = 4$ ,  $D_c = 1.343$  g cm<sup>-3</sup>,  $\mu(\text{Mo-K}\alpha) = 4.22$  cm<sup>-1</sup>,  $F(000) = 1828$ ,  $T = 140$  K. Crystallographic measurements were made using a FAST area detector diffractometer and Mo-K $\alpha$  radiation ( $\lambda = 0.71069$  Å), following previously described procedures.<sup>164</sup> The structure was solved by direct methods (SHELX-S)<sup>165</sup> and refined on  $F_o^2$  by full-matrix least-squares (SHELXL-93)<sup>166</sup> using all 6291 unique data (632 parameters) to final  $wR$  (on  $F^2$ ) = 0.0927 and  $R$  (on  $F$ ) = 0.0545. The non-hydrogen atoms were anisotropic; the hydrogens on water molecules were all experimentally located and refined with O-H distance constrained at 0.95(1) Å, the -CH<sub>3</sub> and -CH<sub>2</sub>- hydrogens were included in riding model;  $U_{\text{iso}}(\text{H})$  free to refine.

### Structural Coordinates and Thermal Parameters

FE	5	0.35800	0.16326	0.11062	11.00000	0.01445	0.01360
		0.01502	0.00074	-0.00091	0.00024		
N1	3	0.21739	0.26872	0.09053	11.00000	0.02222	0.02513
		0.02572	-0.00309	-0.00189	0.00499		
N2	3	0.48871	0.27667	0.12825	11.00000	0.02645	0.02589
		0.03593	0.00261	-0.00498	-0.00525		
N3	3	0.49967	0.05876	0.12589	11.00000	0.02078	0.01640
		0.02035	0.00067	-0.00071	0.00036		
N4	3	0.24991	0.03375	0.10775	11.00000	0.02410	0.02087
		0.03428	0.00217	-0.00230	-0.00505		
N5	3	0.32796	0.17083	0.34301	11.00000	0.02185	0.02483
		0.01952	-0.00037	0.00108	-0.00628		
N6	3	0.36591	0.16098	-0.12541	11.00000	0.02632	0.02584
		0.01770	0.00081	-0.00031	0.00377		
C1	1	0.26945	0.22890	0.09817	11.00000	0.02056	0.01963
		0.01337	-0.00155	-0.00078	-0.00401		
C2	1	0.43828	0.23562	0.12004	11.00000	0.02136	0.01848
		0.01678	0.00289	-0.00163	0.00367		
C3	1	0.44673	0.09773	0.12119	11.00000	0.02002	0.01629
		0.01151	-0.00010	-0.00047	-0.00672		
C4	1	0.28772	0.08348	0.10797	11.00000	0.01620	0.02248
		0.01648	0.00104	-0.00127	0.00853		
C5	1	0.34128	0.16702	0.25673	11.00000	0.01179	0.01295
		0.02392	0.00167	-0.00362	-0.00091		
C6	1	0.36453	0.16178	-0.03727	11.00000	0.01041	0.01243
		0.02531	0.00071	-0.00098	0.00119		
N7	3	0.02258	0.19779	-0.05884	11.00000	0.01406	0.01379
		0.01706	-0.00126	-0.00176	-0.00026		
N8	3	0.08504	0.07761	-0.03891	11.00000	0.02140	0.01539
		0.02382	-0.00067	-0.00096	-0.00073		
N9	3	0.09205	0.37532	0.30459	11.00000	0.01311	0.01187
		0.01426	-0.00150	0.00110	-0.00007		
N10	3	0.19145	0.31654	0.42921	11.00000	0.01965	0.01613
		0.02126	-0.00105	0.00033	0.00277		
N11	3	0.26725	0.44222	-0.08675	11.00000	0.01737	0.01411
		0.01634	0.00097	0.00246	-0.00186		
N12	3	0.41906	0.40926	-0.08845	11.00000	0.02153	0.02270
		0.02381	0.00186	0.00481	-0.00235		
C7	1	0.02282	0.32785	-0.02506	11.00000	0.01084	0.01025
		0.01768	-0.00079	-0.00255	0.00345		
C8	1	0.00129	0.34616	0.07464	11.00000	0.01438	0.01081

		0.01764	0.00314	-0.00170	0.00113		
C9	1	0.04295	0.40007	0.12440	11.00000	0.01302	0.01388
		0.01513	-0.00116	0.00013	0.00278		
C10	1	0.09634	0.44227	0.06783	11.00000	0.01335	0.01163
		0.01950	-0.00099	-0.00369	0.00253		
C11	1	0.11766	0.42371	-0.03267	11.00000	0.01330	0.01292
		0.01637	0.00338	-0.00066	0.00287		
C12	1	0.07957	0.36742	-0.08106	11.00000	0.01529	0.01352
		0.01616	0.00108	-0.00320	0.00572		
C13	1	-0.07248	0.31523	0.12772	11.00000	0.01669	0.02311
		0.02257	-0.00542	0.00268	-0.00335		
H13A	2	-0.10295	0.35095	0.15984	11.00000	0.02357	
H13B	2	-0.05433	0.28298	0.17835	11.00000	0.03654	
H13C	2	-0.10642	0.29236	0.07826	11.00000	0.04006	
C14	1	0.12361	0.51049	0.11134	11.00000	0.02293	0.01648
		0.01988	-0.00320	0.00368	-0.00226		
H14A	2	0.17955	0.50745	0.13291	11.00000	0.02807	
H14B	2	0.09060	0.52199	0.16869	11.00000	0.03549	
H14C	2	0.11796	0.54523	0.05999	11.00000	0.03460	
C15	1	0.09269	0.35352	-0.19321	11.00000	0.02351	0.01938
		0.01680	0.00360	-0.00108	-0.00602		
H15A	2	0.11303	0.39407	-0.22535	11.00000	0.02714	
H15B	2	0.04199	0.34056	-0.22491	11.00000	0.02720	
H15C	2	0.13137	0.31712	-0.20050	11.00000	0.03170	
C16	1	-0.01856	0.26692	-0.07540	11.00000	0.01441	0.01331
		0.01666	0.00049	-0.00251	0.00246		
H16A	2	-0.02221	0.27546	-0.14820	11.00000	0.02753	
H16B	2	-0.07369	0.26399	-0.05029	11.00000	0.00570	
C17	1	0.02874	0.17887	0.05177	11.00000	0.01997	0.01961
		0.01208	0.00117	-0.00021	0.00064		
H17A	2	-0.02468	0.18056	0.08219	11.00000	0.03842	
H17B	2	0.06381	0.21104	0.08760	11.00000	0.01769	
C18	1	0.06390	0.10626	0.06111	11.00000	0.03808	0.02095
		0.02460	0.00287	0.00589	0.00604		
H18A	2	0.11219	0.10739	0.10446	11.00000	0.03918	
H18B	2	0.02429	0.07679	0.09325	11.00000	0.05449	
C19	1	0.10654	0.19545	-0.10536	11.00000	0.01498	0.01998
		0.01715	-0.00208	0.00396	-0.00142		
H19A	2	0.14128	0.22970	-0.07363	11.00000	0.02853	
H19B	2	0.10267	0.20524	-0.17780	11.00000	0.01993	
C20	1	0.14289	0.12441	-0.08871	11.00000	0.02379	0.02107
		0.02579	0.00389	0.00338	0.00338		
H20A	2	0.15827	0.10537	-0.15398	11.00000	0.03968	
H20B	2	0.19170	0.12828	-0.04666	11.00000	0.03240	
C21	1	-0.02953	0.14488	-0.11225	11.00000	0.01645	0.01733
		0.02341	-0.00536	-0.00636	-0.00419		
H21A	2	-0.03549	0.15637	-0.18394	11.00000	0.01615	
H21B	2	-0.08322	0.14395	-0.08250	11.00000	0.01515	
C22	1	0.01092	0.07462	-0.10085	11.00000	0.02820	0.01924
		0.04489	-0.00767	-0.01187	0.00053		
H22A	2	-0.02703	0.04318	-0.06970	11.00000	0.03609	
H22B	2	0.02379	0.05706	-0.16792	11.00000	0.04691	
C23	1	0.02990	0.41182	0.23676	11.00000	0.01367	0.01388
		0.01985	-0.00145	-0.00081	0.00121		
H23A	2	-0.02416	0.39615	0.25412	11.00000	0.02313	
H23B	2	0.03251	0.46053	0.25049	11.00000	0.01424	
C24	1	0.07715	0.39920	0.41302	11.00000	0.02223	0.02037
		0.01506	-0.00387	0.00103	0.00571		
H24A	2	0.08677	0.44804	0.41822	11.00000	0.03202	
H24B	2	0.02113	0.39029	0.43115	11.00000	0.02108	
C25	1	0.13424	0.36115	0.48517	11.00000	0.02574	0.02969
		0.01689	-0.00397	-0.00158	0.00845		
H25A	2	0.16499	0.39394	0.52567	11.00000	0.03783	

H25B	2	0.10252	0.33343	0.53136	11.00000	0.03100	
C26	1	0.17859	0.39144	0.27586	11.00000	0.01221	0.02315
		0.01840	0.00162	0.00321	-0.00166		
H26A	2	0.18692	0.44056	0.27542	11.00000	0.02138	
H26B	2	0.18950	0.37399	0.20816	11.00000	0.01707	
C27	1	0.23595	0.35799	0.35388	11.00000	0.01674	0.02744
		0.02441	0.00375	-0.00019	0.00102		
H27A	2	0.27425	0.32898	0.31854	11.00000	0.04147	
H27B	2	0.26670	0.39327	0.38933	11.00000	0.03160	
C28	1	0.08149	0.29873	0.30198	11.00000	0.02225	0.01174
		0.02540	-0.00241	-0.00025	-0.00098		
H28A	2	0.08936	0.28208	0.23313	11.00000	0.02200	
H28B	2	0.02675	0.28690	0.32235	11.00000	0.01845	
C29	1	0.14325	0.26521	0.37430	11.00000	0.02743	0.01651
		0.02853	0.00175	-0.00543	0.00094		
H29A	2	0.11485	0.23680	0.42292	11.00000	0.04175	
H29B	2	0.17919	0.23601	0.33558	11.00000	0.04416	
C30	1	0.17851	0.46712	-0.08998	11.00000	0.01771	0.01326
		0.01584	0.00234	-0.00100	0.00185		
H30A	2	0.17696	0.51313	-0.06243	11.00000	0.00434	
H30B	2	0.16090	0.46972	-0.16080	11.00000	0.01806	
C31	1	0.31611	0.49262	-0.14924	11.00000	0.02167	0.01657
		0.01901	0.00397	0.00529	-0.00560		
H31A	2	0.31441	0.53748	-0.11777	11.00000	0.03013	
H31B	2	0.29277	0.49621	-0.21739	11.00000	0.02449	
C32	1	0.40422	0.46804	-0.15516	11.00000	0.02678	0.03655
		0.04165	0.01813	0.00024	-0.00569		
H32A	2	0.41609	0.45546	-0.22495	11.00000	0.06457	
H32B	2	0.44047	0.50506	-0.13553	11.00000	0.04836	
C33	1	0.27909	0.37233	-0.13259	11.00000	0.02531	0.01351
		0.02466	-0.00493	0.00343	-0.00072		
H33A	2	0.26206	0.37273	-0.20372	11.00000	0.01547	
H33B	2	0.24616	0.33910	-0.09693	11.00000	0.01728	
C34	1	0.36903	0.35249	-0.12388	11.00000	0.02193	0.03122
		0.04689	-0.01175	0.00636	-0.00080		
H34A	2	0.37495	0.31451	-0.07677	11.00000	0.04523	
H34B	2	0.38787	0.33753	-0.19002	11.00000	0.04897	
C35	1	0.30028	0.44079	0.02038	11.00000	0.02509	0.02146
		0.01358	0.00161	-0.00115	-0.00123		
H35A	2	0.27385	0.40506	0.05915	11.00000	0.02190	
H35B	2	0.29054	0.48427	0.05368	11.00000	0.01132	
C36	1	0.39270	0.42678	0.01458	11.00000	0.02264	0.04733
		0.02592	-0.00077	-0.00094	0.00704		
H36A	2	0.42205	0.46708	0.03767	11.00000	0.06082	
H36B	2	0.40659	0.38949	0.06042	11.00000	0.06108	
O1	4	0.64098	0.34373	0.13829	11.00000	0.02430	0.03144
		0.02988	0.00490	0.00089	-0.00819		
O2	4	0.31530	0.45806	0.59852	11.00000	0.03054	0.02149
		0.02839	0.00393	-0.00365	-0.00026		
O3	4	0.31262	0.31670	0.58268	11.00000	0.02359	0.02179
		0.02960	0.00391	-0.00559	0.00501		
O4	4	0.25296	0.23593	-0.25691	11.00000	0.02052	0.03030
		0.02592	0.00177	0.00218	0.00461		
O5	4	0.21001	0.10756	0.46388	11.00000	0.03548	0.02133
		0.03504	0.00262	0.01545	0.00313		
O6	4	0.34410	0.00535	-0.15337	11.00000	0.02164	0.02213
		0.03149	-0.00337	-0.00208	0.00326		
O7	4	0.13364	-0.02885	0.24838	11.00000	0.03969	0.03871
		0.03206	0.00352	0.00327	-0.00460		
O8	4	0.07913	0.09886	0.32822	11.00000	0.03023	0.06587
		0.04979	-0.02247	0.01276	-0.00932		
H1A	2	0.59145	0.31938	0.13227	11.00000	0.07305	
H1B	2	0.68028	0.31529	0.17171	11.00000	0.09601	

---

H2A	2	0.34234	0.48998	0.55605	11.00000	0.07831
H2B	2	0.26021	0.47336	0.60528	11.00000	0.04833
H3A	2	0.31480	0.36445	0.59300	11.00000	0.02660
H3B	2	0.27151	0.30869	0.53223	11.00000	0.05847
H4A	2	0.28041	0.25808	-0.31142	11.00000	0.06401
H4B	2	0.29072	0.21005	-0.21714	11.00000	0.04586
H5A	2	0.19015	0.13554	0.51739	11.00000	0.07817
H5B	2	0.25084	0.13428	0.43099	11.00000	0.05334
H6A	2	0.34051	0.05286	-0.14096	11.00000	0.04953
H6B	2	0.39468	-0.01377	-0.13520	11.00000	0.06595
H7A	2	0.16820	-0.01259	0.19553	11.00000	0.07594
H7B	2	0.11419	0.01002	0.28463	11.00000	0.08884
H8A	2	0.12207	0.10537	0.37795	11.00000	0.13589
H8B	2	0.03225	0.10398	0.37015	11.00000	0.08817

---